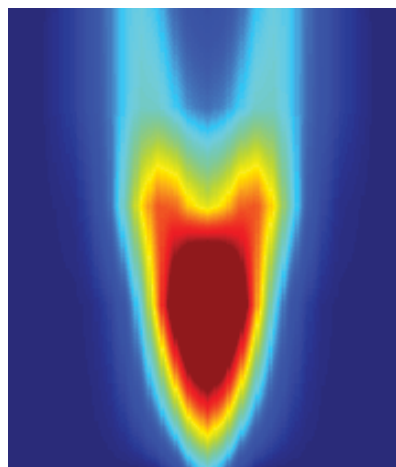
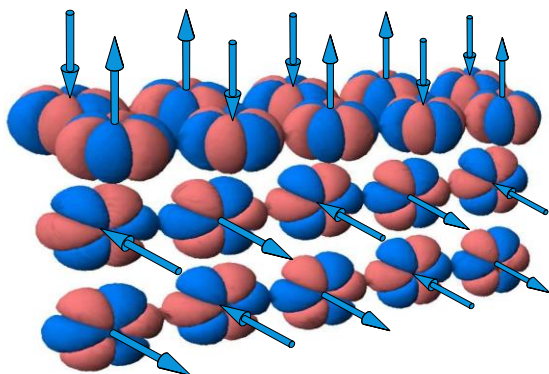
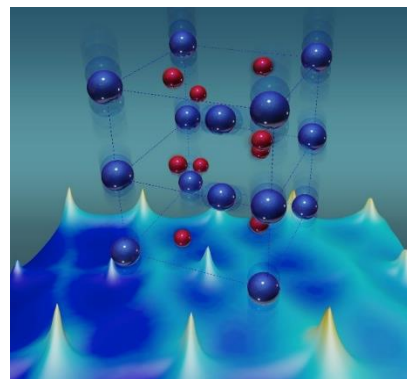
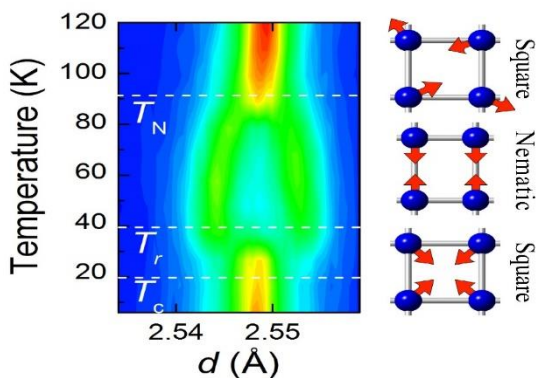


Neutron Scattering Principal Investigators' Meeting

December 19–21, 2016

Hilton Washington DC North/Gaithersburg

Gaithersburg, Maryland



Office of Basic Energy Sciences
Division of Materials Sciences and Engineering



U.S. DEPARTMENT OF
ENERGY

Office of
Science

On the Cover

- Top Left: Neutron diffraction of barium iron arsenide with sodium ions doped onto 24% of the barium sites showing evidence for the new magnetic phase in iron-based superconductors. Left; Nematic order sets in below 90 K but a four-fold symmetry is restored below 40 K. Right; Atomic and magnetic structures for the three states (high temperature disordered – Top Right; magnetic nematic – Middle Right; magnetic four-fold phase – Bottom Right), in which the blue spheres represent iron atoms and the red arrows show the direction of their magnetic moments (Cover Image from Avci et al. *Nature Comm.* 5, 3845, 2014).
- Top Middle: Frozen-in ferroelectric vortices in ErMnO_3 that follow the predictions of the Kibble–Zurek model for cosmological strings formed in the early Universe (Cover Image from Lin et al. *Nature Physics* 10, 970, 2014).
- Top Right: Neutron and X-ray scattering measurements and first principles calculations reveal anomalously large atomic vibrations (phonons) that drive the insulator-to-metal phase transition in vanadium dioxide. Blue atoms are vanadium and red are oxygen. (Cover Image from J.D. Budai et al. *Nature* 515, 535–539, 2014).
- Bottom Left: Cartoon showing the arrangement of ytterbium (Yb) atoms in the crystalline compound made of ytterbium, platinum and lead ($\text{Yb}_2\text{Pt}_2\text{Pb}$). The red and blue “pin cushions” denote the atomic orbitals associated with the large magnetic moments of Yb with the arrows showing the direction of the magnetic moments. Magnetic coupling (through electron hopping) occurs only where lobes of neighboring orbitals point towards one another and share the same color, a condition satisfied only along horizontal chains. (Cover Image from Wu et al. *Science* 352, 1206, 2016).
- Bottom Right: Ce/Yb atoms in $\text{Ce}_{1-x}\text{Yb}_x\text{CoIn}_5$ form a quasi-2D square lattice similar to cuprates. The superconducting order parameter also has d-wave symmetry similar to the cuprates. The neutron spin resonance mode display clear upward dispersion, unlike in the cuprates. (Cover Image from Song et al. *Nature Comm.* 7, 12774, 2016).

This document was produced under contract number DE-SC0014664 between the U.S. Department of Energy and Oak Ridge Associated Universities.

The research grants and contracts described in this document are supported by the U.S. DOE Office of Science, Office of Basic Energy Sciences, Materials Sciences and Engineering Division.

Foreword

This volume comprises the scientific content of the 2016 Neutron Scattering Principal Investigators' (PI) Meeting sponsored by the Division of Materials Sciences and Engineering (MSED) in the Office of Basic Energy Sciences (BES) of the U.S. Department of Energy (DOE). This meeting on December 19–21, 2016, Hilton Washington DC North/Gaithersburg, Maryland, is the fifth in the series, covering the projects funded by the Neutron Scattering Program. BES MSED has a long tradition of supporting a comprehensive neutron scattering program in recognition of the high impact neutron scattering and spectroscopy tools have in discovery and use-inspired research.

The MSED Neutron Scattering Core Research Activity (CRA) supports basic research on the fundamental interactions of neutrons with matter to achieve an understanding of the atomic, electronic, and magnetic structures and excitations of materials and their relationship to materials' properties. Major emphasis is on the application of neutron scattering and spectroscopy for materials research, primarily at BES-supported user facilities. Development of next-generation instrumentation concepts, innovative optics for time-of-flight instruments and application of polarized neutrons are distinct aspects of this activity. The increasing complexity of DOE mission-relevant materials for various energy applications requires sophisticated scattering and computational tools to investigate the structure and dynamics at relevant length and time scales. Additionally, neutrons allow access to the behavior of matter in extreme environments such as high temperature, pressure and magnetic field. A continuing theme of this program is the integration of material synthesis, neutron scattering measurements and computational modeling as this is vital to obtain controlled samples for experiments and modeling for an in-depth understanding of the structure and dynamics of materials and their relationship to macroscopic properties.

The purpose of the BES biennial principal investigators' meetings is to bring together all of the researchers funded by the Neutron Scattering Program at BES-MSED on a periodic basis to facilitate the discussion of new results and research highlights by PIs, to nucleate new ideas and collaborations among participants, and to identify new research opportunities. The meetings also serve MSED to assess the state of the program, to chart new research directions and to identify programmatic needs.

We thank all the meeting participants for their active contributions in sharing their ideas and research accomplishments. Sincere thanks are also due to the speakers from other BES programs involved with neutron scattering in multidisciplinary research. We wish to thank Teresa Crockett in MSED and Linda Severs at the Oak Ridge Institute for Science and Education (ORISE) for their outstanding work in all aspects of the meeting organization.

Thiyaga P. Thiyagarajan and Helen Kerch
MSED, BES, Office of Science
U.S. Department of Energy

Table of Contents

Agenda	vii
---------------------	-----

Abstracts

Institute for Quantum Matter

<i>C. Broholm, N. P. Armitage, R. J. Cava, T. M. McQueen, O. Tchernyshyov, and A. Turner</i>	3
--	---

The Rise of Quantum Materials: Scientific Challenges and Technological Opportunities – Invited Talk

<i>Collin Broholm</i>	13
-----------------------------	----

Impact of Dynamic Instabilities and Microstructure on Energy Materials

<i>J. D. Budai, M. E. Manley, R. P. Hermann, and O. Delaire</i>	14
---	----

Understanding the Mechanism of Lithiation and Delithiation of Si and Mg Electrodes through Neutron Diffraction by In Situ Electrochemical Cell and Neutron Imaging

<i>K. S. Ravi Chandran</i>	21
----------------------------------	----

Multiphasic Soft Colloids: From Fundamentals to Application of Energy Sustainability

<i>Wei-Ren Chen</i>	26
---------------------------	----

Magnetoelastic Coupling and Nonreciprocal Effects in Polar, Chiral, and Ferroaxial Magnets: Neutron and Optical Studies

<i>S.-W. Cheong, V. Kiryukhin, and A. Sirenko</i>	31
---	----

Using Neutron as a Probe to Study Magnetic Excitations in Strongly Correlated Electron Materials

<i>Pengcheng Dai</i>	38
----------------------------	----

Quasiparticle Couplings in Transport of Heat, Charge, and Spin for Novel Energy Materials

<i>Olivier Delaire</i>	44
------------------------------	----

Status and Developments at the NIST Center for Neutron Research – Invited Talk

<i>Robert Dimeo</i>	50
---------------------------	----

LaCNS: Building Neutron Scattering Infrastructure in Louisiana for Advanced Materials

<i>J. F. DiTusa, D. Zhang, J. Zhang, W. A. Shelton, J. C. Garno, R. Jin, V. T. John, R. Kumar, Y. M. Lvov, Z. Mao, E. Nesterov, E. W. Plummer, S. W. Rick, G. J. Schneider, D. P. Young, P. T. Sprunger, L. G. Butler, and M. Khonsari</i>	51
--	----

Vortex Lattices Studies in Type II Superconductors <i>Morten R. Eskildsen</i>	59
Neutron and X-ray Studies of Spin and Charge Manipulation in Magnetic Nanostructures <i>Eric E. Fullerton and Sunil Sinha</i>	64
Vibrational Thermodynamics of Materials <i>Brent Fultz</i>	69
New Insight into the Physics of the Cuprates from Neutron, X-ray and Transport Measurements of $\text{HgBa}_2\text{CuO}_{4+\delta}$ <i>Martin Greven</i>	75
Single Crystal Growth and Superconductivity of $(\text{La}_{1-x}\text{Ca}_x)_2\text{CaCu}_2\text{O}_{6+d}$ <i>G. D. Gu, Igor A. Zaliznyak, and J. M. Tranquada</i>	79
Neutron Scattering Instrumentation Research and Development for High Spatial and Temporal Resolution Imaging at Oak Ridge National Laboratory <i>Jason P. Hayward</i>	83
Rheo-structural Spectroscopy: Fingerprinting the In Situ Response of Fluids to Arbitrary Flow Fields <i>Matthew E. Helgeson</i>	88
Complex Electronic Materials: Neutron Spectroscopy Studies of CeRhIn_5 <i>Marc Janoschek and David Fobes</i>	92
Neutron Sciences at the Oak Ridge National Laboratory – Invited Talk <i>Paul Langan</i>	94
Role of Organic Cations in Organic-Inorganic Perovskite Solar Cells <i>Seung-Hun Lee and Joshua Choi</i>	95
Scattering and Spectroscopic Studies of Quantum Materials <i>Young Lee and Hongchen Jiang</i>	97
Neutron Scattering Studies of Complex Oxides and Alloys <i>Chris Leighton</i>	100
Local Complexity and the Mechanics of Phase Transitions in Novel Materials <i>Despina Louca</i>	105
Sample Environment Capabilities at ORNL – Invited Talk <i>Gary W. Lynn, Harish K. Agrawal, Mark J. Loguillo, and Chris M. Redmon</i>	109

Superionic Conduction using Ion Aggregates <i>Maranas, Janna</i>	110
Correlations and Competition between the Lattice, Electrons, and Magnetism <i>R. J. McQueeney, A. I. Goldman, A. Kreyssig, and D. Vaknin</i>	111
Measurement and Modeling of Structure and Dynamics in Doped Organic Semiconductors <i>Adam J. Moule</i>	119
Interactions Governing the Self-Assembly of Protein-Polymer Conjugates <i>Bradley D. Olsen</i>	125
Neutron Scattering Investigation of the Relationship between Molecular Structure, Morphology and Dynamics in Conjugated Polymers <i>Lilo D. Pozzo</i>	130
Status and Future Plans on Analysis and Modeling Software Capabilities for Neutron Scattering Research at the ORNL Neutron Scattering Facilities – Invited Talk <i>Thomas Proffen</i>	134
Inelastic Neutron and X-ray Scattering Investigation of Electron-Phonon Effects in Quantum Materials <i>Dmitry Reznik</i>	138
The Next Ferroic Order: Synthesis and Neutron Scattering of Ferrotoroidic Materials <i>Efrain E. Rodriguez</i>	143
Complex Electronic Materials <i>Filip Ronning, Eric Bauer, Marc Janoschek, John Joyce, Roman Movshovich, Priscila Rosa, and Joe Thompson</i>	147
Complex Electronic Materials: New Physics Through New Materials <i>Priscila Rosa and Eric Bauer</i>	159
Neutron and X-ray Scattering Studies of Complex Phenomena in Bulk Materials and Heterostructures of Strongly Correlated Systems <i>S. Rosenkranz, O. Chmaissem, R. Osborn, D. Phelan, and S. G. E. te Velthuis</i>	163
Exploration of Novel Magnetic Phenomena in Two Dimensional Nanoengineered Materials <i>Deepak K. Singh</i>	170
National School on Neutron and X-ray Scattering <i>Suzanne G. E. te Velthuis, Bryan C. Chakoumakos, Jonathan C. Lang, Brian H. Toby, and John D. Budai</i>	174

Neutron Scattering Studies of High-Temperature Superconductors <i>J. M. Tranquada, G. D. Gu, and I. A. Zaliznyak</i>	177
Polymer Conformations and Chain Dynamics under 1D and 2D Rigid Confinement <i>Karen I. Winey and Robert A. Riggelman</i>	188
Unpolarized and Polarized Neutron Scattering Studies of Fe-based Superconductors: Magnetism, Electron Itinerancy and Orbital Hybridization <i>I. A. Zaliznyak, G. D. Gu, and J. M. Tranquada</i>	192
Searching for the Universality of Liquid Dynamics At and Out of Equilibrium <i>Yang Zhang</i>	196
Author Index	203
Participant List	207

AGENDA

DOE BES DMSE Neutron Scattering Principal Investigators' Meeting Hilton Gaithersburg MD December 19–21, 2016

Monday

- 7:00 – 8:20** **Breakfast** (also poster set-up, presentation loading on DOE computer, all presentations for Monday need to be loaded onto the DOE laptop and Posters for Monday should be set up under the corresponding Session label, both prior to the start of the meeting on Monday.)
- 8:20 – 8:30** BES Welcome and Discussion of the Meeting Format
• Thiyaga Thiyagarajan, BES, Neutron Scattering Program Manager
- 8:30 – 9:40** **Session I (70 mins)**
• Collin Broholm, Johns Hopkins U, **project lead**, *Institute for Quantum Matter at Johns Hopkins University (30 mins, ensemble presentation)*, Tyrel McQueen, Peter Armitage, Oleg Tchernyshyov, Robert Cava (Princeton)
• Morten Eskildsen, U Notre Dame, *Vortex Lattices Studies in Type II Superconductors (10 mins)*
• Sunil Sinha, UCSD, **project lead**, *Neutron and X-Ray Studies of Spin and Charge Manipulation in Magnetic Nanostructures (10 mins)*, Eric Fullerton
• Karen Winey, U Penn, **project Lead**, *Polymer Conformations and Chain Dynamics under 1D and 2D Rigid Confinement (10 mins)*, Rob Riggelman
• Seunghun Lee, UVa, **project lead**, *Role of Organic Cations in Organic-Inorganic Perovskite Solar Cells (10 mins)*, Joshua Choi
- 9:40 – 10:50** **General questions followed by small group discussions at each Session I-related posters.**
- 10:50 – 11:50** **Session II (60 mins)**
• Paul Langan, ORNL, *Current Capabilities and Future Plans for the Neutron Scattering Facilities at ORNL (Invited talk) (30 mins)*
• Rob McQueeney, Ameslab, **project lead**, *Correlations and Competition between the Lattice, Electrons, and Magnetism (30 mins, ensemble presentation)*, Alan Goldman, Andreas Kreyssig, David Vaknin, Yong Liu, Yongbin Lee
- 11:50 – 12:30** **General questions followed by small group discussions at each Session II-related posters.**
- 12:30 – 2:00** **Working lunch with continued discussions, Introduction by Helen Kerch, Team Lead, Scattering and Instrumentation Sciences, DMSE, BES**

- 2:00 – 3:10** **Session III (70 mins)**
- Rob Dimeo, NIST, *Status and Developments at the NIST Center for Neutron Research (Invited talk) (30 mins)*
 - John Tranquada, BNL, **project lead**, *Neutron Scattering (30 mins, ensemble presentation)*, Igor Zaliznyak, Genda Gu
 - Brad Olsen, MIT, *Thermodynamics of Self-Assembly in Globular Protein-Polymer Conjugates (10 mins)*
- 3:10 – 4:00** **General questions followed by small group discussions at each Session III-related posters.**
- 4:00 – 5:10** **Session IV (70 mins)**
- Collin Broholm, Johns Hopkins U, *The Rise of Quantum Materials: Scientific Challenges and Technological Opportunities (Invited talk) (30 mins)*
 - Matt Helgeson, UCSB (Early Career), *Rheo-structural Spectroscopy: Fingerprinting the In Situ Response of Fluids to Arbitrary Flow Fields (10 mins)*
 - Efrain Rodriguez, UMD, *The Next Ferroic Order: Synthesis and Neutron Scattering of Ferrotoroidic Materials (10 mins)*
 - Olivier Delaire, Duke (Early Career), *Quasiparticle Couplings in Transport of Heat, Charge, and Spin for Novel Energy Materials (10 min)*
 - Suzanne te Velthuis, ANL, **project lead**, *National School for Neutron and X-ray Scattering (10 mins)*, Jonathan Lang, Bryan C. Chakoumakos (ORNL), John Budai
- 5:10 – 6:10** **General questions followed by small group discussions at each Session IV-related posters.**
- 6:10 – 7:30** **Working Dinner: End of day remarks, general discussion. Evening: small group meetings, collaborative exchanges.**

Tuesday

- 7:00 – 8:00** **Breakfast** (also poster set-up, presentation loading on DOE computer, all presentations for Tuesday need to be loaded onto the DOE laptop and Posters for Tuesday should be set up under the corresponding Session label, both prior to the start of the meeting on Tuesday.)
- 8:00 – 9:00** **Session V (60 mins)**
- Sang-Wook Cheong, Rutgers, **project lead**, *Non-reciprocal Effects in Polar/Chiral/Ferroaxial Magnets: Neutron and Optical Studies (10 mins)*, Valery Kiryukhin, Andrei Sirenko (New Jersey Institute of Technology)
 - John Budai, ORNL, **project lead**, *Impact of Dynamic Instabilities and Microstructure on Energy Materials (30 minute ensemble presentation)*, Mike Manley, Raphael Hermann, Olivier Delaire (Duke and ORNL)
 - Wei-Ren Chen, ORNL (Early Career), *Multiphase Soft Colloids: From Fundamentals to Application of Energy Sustainability (10 mins)*

- Despina Louca, U Va, *Emergent Phenomena in Novel Materials and Functionality Control: Characterization at Multiple Length and Time Scales* (**Student Presentation – Junjie Yang**) (5 mins)
- Ravi Chandran, U Utah, *Application of In Situ Neutron Diffraction to Understand the Mechanism of Phase Transitions During Electrochemical Cycling of High Capacity Mg/Si* (**Student Presentation – Bhaskar Vadlamani**) (5 mins)

9:00 – 10:00 **General questions followed by small group discussions at each Session V-related posters.**

10:00 – 11:10 **Session VI (70 mins)**

- Stephan Rosenkranz, ANL, **project lead**, *Neutron and X-ray Scattering* (**30 minute ensemble presentation**), Ray Osborn, Suzanne te Velthuis, Daniel Phelan, Omar Chmaissem (Northern Illinois U)
- Yang Zhang, UIUC, *Atomic-Scale Dynamics of Glass-Forming Metallic Liquids – An Integrated Quasi-Elastic/Inelastic Neutron Scattering and Computational Study* (**10 mins**)
- Thomas Proffen, ORNL, *Status and Future Plans on Analysis and Modeling Software Capabilities for Neutron Scattering Research at ORNL* (**Invited talk**) (**30 mins**)

11:10 – 12:00 **General questions followed by small group discussions at each Session VI-related posters.**

12:00 – 1:30 **Working Lunch with continued discussions on Analysis and Modeling software for neutron scattering at ORNL**

1:30 – 2:30 **Session VII (60 min)**

- Martin Greven, UMN, **project lead**, *University of Minnesota Center for Quantum Materials* (**30 min, ensemble presentation**), Chris Leighton, Bharat Jalan, Rafael Fernandes, Andrey Chubukov
- Brent Fultz, Caltech, *Vibrational Thermodynamics of Materials at High Temperatures* (**10 min**)
- Pengcheng Dai, Rice University, *Using Neutron as a Probe to Study Magnetic Excitations in Strongly Correlated Electron Materials* (**10 min**)
- Adam Moule, University of California –Davis, *Engineering and Doping Profiles in Organic Semiconductor Materials* (**10 min**)

2:30 – 3:30 **General questions followed by small group discussions at each Session VII-related posters.**

3:30 – 4:40 **Session VIII (70 min)**

- Filip Ronning, LANL, **project lead**, *Complex Electronic Materials* (**30 min, ensemble presentation**), Joe Thompson, Eric Bauer, Marc Janoschek, John Joyce, Priscila Rosa, Roman Movshovich
- Deepak Singh, U Missouri, *Exploration of Novel Magnetic Phenomena in Two-Dimensional Nanoengineered Material* (**10 mins**)
- Lilo Pozzo, University of Washington (Early Career), *Neutron Scattering Investigation of the Relationship between Molecular Structure, Morphology and Dynamics in Conjugated Polymers* (**10 min**)

- Gary Lynn, ORNL, *Sample Environment Capabilities at ORNL (Invited talk) (20 mins)*

4:40 – 6:00 **General questions followed by small group discussions at each Session VIII-related posters.**

6:00 – 7:00 **Working Dinner: General discussion on new opportunities, collaborative exchanges.**

Wednesday

7:00 – 8:00 **Breakfast** (also poster set-up, presentation loading on DOE computer, all presentations for Wednesday need to be loaded onto the DOE laptop and Posters for Wednesday should be set up under the corresponding Session label, both prior to the start of the meeting on Wednesday.)

8:00 – 9:00 **Session IX (60 mins)**

- Young Lee, SLAC, **project lead**, *Scattering and Spectroscopic Studies of Quantum Materials (25 min, ensemble presentation)*, Hong Chen Jiang
- Dmitry Reznik, University of Colorado, Boulder, *Inelastic Neutron and X-ray Scattering Investigations of Electron-Phonon Effects in Quantum Materials (10 mins)*
- John DiTusa, LSU, **Project Lead – EPSCoR**, *Building Neutron Scattering Infrastructure in Louisiana for Advanced Materials (15 mins)*
- Jason Hayward, UTK (Early Career), *Neutron Scattering Instrumentation Research and Development for High Spatial and Temporal Resolution Imaging at Oak Ridge National Laboratory (10 mins)*

9:00 – 10:00 **General questions followed by small group discussions at each Session IX-related posters.**

10:00 – 10:30 End of Meeting Wrap-up.

Abstracts

Institute for Quantum Matter

C. Broholm^{1,2,3,6}, N.P. Armitage¹, R.J. Cava⁴, T.M. McQueen^{1,5,6}, O. Tchernyshyov¹ & A. Turner¹

¹Department of Physics and Astronomy, Johns Hopkins University, Baltimore, MD 21218

²NIST Center for Neutron Research, NIST, Gaithersburg, MD 20899

³Quantum Condensed Matter Division, ORNL, Oak Ridge, TN 37831

⁴Department of Chemistry, Princeton University, Princeton, NJ 08544

⁵Department of Chemistry, Johns Hopkins University, Baltimore, MD 21218

⁶Department of Materials Science and Engineering, Johns Hopkins University, Baltimore, MD 21218

Program Scope

The Institute for Quantum Matter brings together expertise in materials synthesis, theory, and spectroscopy with neutrons and THz photons to discover, understand, and control materials dominated by collective quantum physics. Areas of interest include quantum spin liquids in frustrated magnets, superconductivity near magnetism, and topological semimetals and insulators. IQM is also develops new instrumentation and methods to probe quantum materials.

Recent Progress

Topological Materials: Despite its simple cubic structure, the strongly interacting and putative topological insulator SmB₆ presents fundamental challenges that IQM is well suited to address. High quality floating-zone crystals were synthesized and subjected to detailed structural and electronic characterization. We showed the surface and bulk properties of SmB₆ can be controlled chemically[14]. Neutron[56] and Raman[19] scattering provided evidence for a collective exciton that was interpreted using a perturbation theory built on top of a mean field condensate of slave bosons[60]. While the bulk of SmB₆ does not support a DC current, THz conductivity measurements show the material displays significant three-dimensional bulk conduction originating within the Kondo gap[12]. THz conductivity measurements were also used to provide evidence for massless Kane electrons rather than symmetry-protected 3D Dirac particles in Cd₃As₂[11]. Neutron diffraction and optical measurements were also performed on the Weyl semi-metal candidate YbMnBi₂ giving insight into the nature of its electronic structure.

We examined theoretically the neutron scattering cross section for Weyl semimetals. Neutron scattering should be able to expose the Weyl dispersion relation and spin-momentum locking. Indeed the coupling between neutrons and Weyl fermions can be much larger than the vacuum coupling between neutrons and electrons. Experiments are under way to exploit this to probe Weyl electrons.

Quantum Magnetism: Inelastic neutron scattering reveals a broad continuum of excitations in $\text{Pr}_2\text{Zr}_2\text{O}_7$, the temperature and magnetic field dependence of which indicate a continuous distribution of quenched transverse fields (Δ) acting on the non-Kramers Pr^{3+} crystal field ground state doublets. Spin-ice correlations are apparent within 0.2 meV of the Zeeman energy. A random phase approximation provides an excellent account of the data and allows for a determination of the transverse field distribution. Established during high temperature synthesis due to an underlying structural instability, it appears disorder in $\text{Pr}_2\text{Zr}_2\text{O}_7$ actually induces a quantum spin liquid[5].

The synthesis and characterization of compounds in the $\text{RE}_3\text{Sb}_3\text{Zn}_2\text{O}_{14}$ family (RE=La, Pr, Nd, Sm, Eu, Gd) was reported[13]. These are rhombohedral pyrochlore derivatives with rare earth ions on an ideal two-dimensional Kagome lattice. The structure displayed is similar to the cubic $\text{A}_2\text{B}_2\text{O}_7$ pyrochlore structure, but has rare earth ions fully ordered on an ideal Kagome lattice with Zn: RE in the A sites and Zn:Sb in the B sites in the ratio 1:3 (Figure 1), in strict contrast to rare earth pyrochlores, which have magnetic ions connecting Kagome planes.

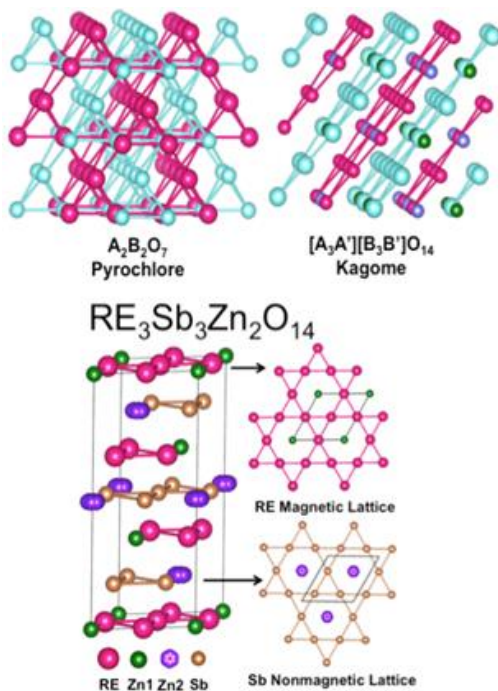


Figure 1 (Upper panel): A (cyan) and B (pink) networks of tetrahedra in the $\text{A}_2\text{B}_2\text{O}_7$ pyrochlore structure. The right panel portrays the $[\text{A}_3\text{A}'][\text{B}_3\text{B}']\text{O}_{14}$ Kagome structure, where the substitution of A' (purple) and B' (green) cations enables the formation of discrete Kagome planes. (Lower panel): Schematic of $\text{RE}_3\text{Sb}_3\text{Zn}_2\text{O}_{14}$

characterization through magnetic susceptibility measurements indicates these compounds display dominantly antiferromagnetic interactions, and the Nd-based material made with Mg in place of Zn was found to magnetically order at temperatures near 0.5 K. The magnetic structure of $\text{Nd}_3\text{Sb}_3\text{Mg}_2\text{O}_{14}$ was determined by low temperature powder neutron diffraction[23]. A corresponding neodymium pyrochlore ($\text{Nd}_2\text{ScNbO}_7$) was synthesized and analyzed for comparison, and shows magnetic ordering at 0.35 K. We also successfully synthesized many other materials of this type with Mg in place of Zn. The synthesized materials are so far in polycrystalline form but melt tests designed to explore the feasibility of crystal growth by the floating zone method will be described.

An exciting perspective in work on quantum magnetism is the possibility of anomalous electronic properties under charge doping. We report the topochemical synthesis of electron-doped herbertsmithite with chemical formula $\text{ZnLi}_x\text{Cu}_3(\text{OH})_6\text{Cl}_2$ from $x = 0$ to $x = 1.8$ (3/5 per Cu^{2+}). While no metallicity or superconductivity is induced, a systematic suppression of magnetism

occurs across the phase diagram[10].

In theoretical work on quantum magnetism, we showed Majorana zero modes (anyons with non-Abelian quantum statistics) can be created in Kitaev's honeycomb spin liquid at certain lattice defects, e.g., dislocations [58,68]. The physical properties of domain walls in antiferromagnets were examined and ways to manipulate them proposed [17,46]. A long-standing paradox concerning the definition of conserved momenta for topological solitons in ferromagnets was resolved [41]. The physical properties of skyrmions in chiral ferromagnets and topological insulators was also studied [45,51,52] and will guide experimental efforts to change transport properties by manipulating magnetic structures and domain walls in putative Weyl semimetals such as Mn_3Sn and Mn_3Ge .

Of the hexagonal rare-earth manganites h-HoMnO_3 (HMO) is of particular interest as Ho ions possess a large rare-earth magnetic moment and the low symmetry of the crystal structure permits an array of magnetic exchange interactions between Ho and Mn moments, resulting in a complex phase diagram of all the hexagonal manganites. Using THz spectroscopy we have found an divergence of the Mn g-factors at the Ho ordering transition, showing evidence for a heretofore unrealized coupling between different magnetic species.

Heavy fermion systems: We discovered that a magnetic field along the tetragonal axis of heavy fermion CeAuSb_2 induces a first order transition from a multi-domain striped structure to a checkered structure with similar wavelengths. We uncovered the magnetic ordered states of near quantum critical $\text{CeNiAs}_{1-x}\text{P}_x\text{O}$ and $\text{YbAl}_{1-x}\text{Fe}_x\text{B}_4$ and determined their crystal field schemes.

Future Plans

A significant future direction is that of discovering and exploiting quantum magnets at the verge of metallization. Not only is this a crucial basic science direction identified in the BRN report on Quantum Materials, but it is an area where materials synthesis and discovery is critical. This line of research builds upon recent synthetic advances a IQM that have allowed, eg., charge to be doped into a canonical strong spin orbit coupled magnet, Na_2IrO_3 , the cluster magnets pioneered by IQM, and the prototype quantum spin liquid Herbertsmithite. Control over quantum magnetic states is crucial for device applications, and builds on the substantial crystal growth expertise developed at IQM.

Transport properties of Weyl semimetals will be explored theoretically and experimentally. One mechanism for getting non-linear I-V relationships from surface states of Weyl semimetals has to do with electrons making quantum jumps from the surface states to the bulk states, and the other has to do with diverging lifetimes for electrons at the end-points of the surface Fermi arcs. These phenomena are easy to understand, but work remains to describe how they contribute to resistivity of the surface and how they compete with bulk resistivity.

We shall pursue manifestations of quantum entanglement and anyon quasiparticles in quantum spin liquids and seek materials capable of producing quantum spin liquids. A particularly important question is how to positively identify a quantum spin liquid short of having an exactly solvable model. A promising direction is to study the properties of lattice defects and edge states, which may harbor anyons. A second major direction will be a study of topological defects in antiferromagnets with complex order parameters, e.g., the 120° order on triangular lattices and non-coplanar orders on pyrochlore lattices.

Publications

- 1 “Anomalous exchange between RE^{+3} - Mn^{+3} moments in h- $HoMnO_3$,” N. J. Laurita, Rongwei Hu, Meixia Wu, S. W. Cheong, and N. P. Armitage. To be submitted in December 2016.
- 2 “THz magneto-optics and spontaneous magnon decay in the skyrmion insulator Cu_2OSeO_3 ,” N. J. Laurita, G. G. Marcus, B. A. Trump, T. M. McQueen, C. L. Broholm, and N. P. Armitage. To be submitted in December 2016.
- 3 “An optical investigation of the magnetic strong spin-orbitally coupled semimetal $YbMnBi_2$,” Dipanjan Chaudhuri, Bing Cheng, Alexander Yaresko, Quinn D. Gibson, R. J. Cava, and N. P. Armitage. To be submitted in December 2016.
- 4 “ $NaSrMn_2F_7$, $NaCaFe_2F_7$, and $NaSrFe_2F_7$: novel single crystal pyrochlore antiferromagnets,” M.B. Sanders, J.W. Krizan, K.W. Plumb, T.M. McQueen, and R.J. Cava, [arXiv:1608.02907](https://arxiv.org/abs/1608.02907).
- 5 “A disordered route to the Coulomb quantum spin liquid: Random transverse fields on spin ice in $Pr_2Zr_2O_7$,” J.-J. Wen, S. M. Koohpayeh, K. A. Ross, B. A. Trump, T. M. McQueen, K. Kimura, S. Nakatsuji, Y. Qiu, D. M. Pajerowski, J. R. D. Copley, and C. L. Broholm, Phys. Rev. Lett. (submitted); [arXiv:1609.08551](https://arxiv.org/abs/1609.08551).
- 6 “Systematic search and a new family of skyrmion materials,” W. Li and J. Zang, [arXiv:1502.03818](https://arxiv.org/abs/1502.03818).
- 7 “Universal ratio of intrinsic resistivities of spin helix in B20 (Fe-Co)Si magnets,” S. X. Huang, J. Kang, F. Chen, J. Zang, G.J. Shu, F.C. Chou, S.V. Grigoriev, V.A. Dyadkin, and C.L. Chien, [arXiv:1409.7869](https://arxiv.org/abs/1409.7869).
- 8 “Quadrupolar singlet ground state of praseodymium in a modulated pyrochlore,” J. van Duijn, K. H. Kim, N. Hur, D. T. Adroja, F. Bridges, A. Daoud-Aladine, F. Fernandez-Alonso, R. Ruiz-Bustos, J. Wen, V. Kearney, Q. Z. Huang, S.-W. Cheong, S. Nakatsuji, C. Broholm, and T. G. Perring, [arXiv:1407.0661](https://arxiv.org/abs/1407.0661).

- 9 “Antiferromagnetic and orbital ordering on a diamond lattice near quantum criticality,” K. W. Plumb, Jennifer Morey, J. A. Rodriguez-Rivera, Hui Wu, A. A. Podlesnyak, T. M. McQueen, and C. L. Broholm, [arXiv:1603.08033](https://arxiv.org/abs/1603.08033). Accepted for publication in Phys. Rev. X (2016).
- 10 Electron Doping a Kagome Spin Liquid Z.A. Kelly, M.J. Gallagher, and T.M. McQueen, [Phys. Rev. X **6**, 041007 \(2016\)](https://doi.org/10.1103/PhysRevX.6.041007).
- 11 “Magneto-Optical Signature of Massless Kane Electrons in Cd₃As₂,” A. Akrap, M. Haki, S. Tchoumakov, I. Crassee, J. Kuba, M. O. Goerbig, C. C. Homes, O. Caha, J. Novák, F. Teppe, W. Desrat, S. Koohpayeh, L. Wu, N. P. Armitage, A. Nateprov, E. Arushanov, Q. D. Gibson, R. J. Cava, D. van der Marel, B. A. Piot, C. Faugeras, G. Martinez, M. Potemski, and M. Orlita, [Phys. Rev. Lett. **117**, 136401 \(2016\)](https://doi.org/10.1103/PhysRevLett.117.136401).
- 12 “Anomalous 3D bulk AC conduction within the Kondo gap of SmB₆ single crystals,” N. J. Laurita, C. M. Morris, S. M. Koohpayeh, P. F. S. Rosa, W. A. Phelan, Z. Fisk, T. M. McQueen, and N. P. Armitage, [Phys. Rev. B **94**, 165154 \(2016\)](https://doi.org/10.1103/PhysRevB.94.165154).
- 13 “Synthesis, crystal structure, and magnetic properties of novel 2D kagome materials RE₃Sb₃Mg₂O₁₄ (RE = La, Pr, Sm, Eu, Tb, Ho): Comparison to RE₃Sb₃Zn₂O₁₄ family,” M. B. Sanders, K. M. Baroudi, J. W. Krizan, O. A. Mukadam, and R. J. Cava, [Phys. Stat. Sol. \(b\) **253**, 2056 \(2016\)](https://doi.org/10.1063/1.4962533).
- 14 “Growth and characterization of iron scandium sulfide (FeSc₂S₄),” J.R. Morey, K.W. Plumb, C.M. Pasco, B.A. Trump, T.M. McQueen, S.M. Koohpayeh, [J. Cryst. Growth **454**, 128 \(2016\)](https://doi.org/10.1016/j.jcrysgro.2016.05.012).
- 15 “Correlation between bulk thermodynamic measurements and the low-temperature-resistance plateau in SmB₆,” W. A. Phelan, S. M. Koohpayeh, P. Cottingham, J. W. Freeland, J. C. Leiner, C. L. Broholm, and T. M. McQueen, [Phys. Rev. X **4**, 031012 \(2016\)](https://doi.org/10.1103/PhysRevX.4.031012).
- 16 “Modulated magnetism and anomalous electronic transport in Ce₃Cu₄As₄O₂,” Jiakui K. Wang, Shan Wu, Yiming Qiu, Jose A. Rodriguez-Rivera, Qingzhen Huang, C. Broholm, and E. Morosan, [arXiv:1606.04937](https://arxiv.org/abs/1606.04937); [Phys. Rev. B **94**, 064430 \(2016\)](https://doi.org/10.1103/PhysRevB.94.064430).
- 17 “Magnetolectric domain wall dynamics and its implications for magnetolectric memory,” K. D. Belashchenko, O. Tchernyshyov, Alexey A. Kovalev, O. A. Tretiakov, [arXiv:1601.02471](https://arxiv.org/abs/1601.02471); [Appl. Phys. Lett. **108**, 132403 \(2016\)](https://doi.org/10.1063/1.4962533).
- 18 “Correlated impurities and intrinsic spin-liquid physics in the kagome material herbertsmithite,” T.-H. Han, M. R. Norman, J.-J. Wen, J. A. Rodriguez-Rivera, J. S. Helton, C. Broholm, and Y. S. Lee, [Phys. Rev. B **94**, 060409\(R\) \(2016\)](https://doi.org/10.1103/PhysRevB.94.060409).

- 19 “Breakdown of the Kondo insulating state in SmB_6 by introducing Sm vacancies,” M.E. Valentine, S. Koohpayeh, W.A. Phelan, T.M. McQueen, P.F.S. Rosa, Z. Fisk, and N. Drichko, [arXiv:1601.02694](#); [Phys. Rev. B 94, 075102 \(2016\)](#).
- 20 “Unusual magnetoresistance in cubic B20 chiral magnets,” S. X. Huang, F. Chen, J. Kang, J. Zang, G.J. Shu, F.C. Chou, and C. L. Chien, [arXiv:1409.7867](#); [New J. Phys. 18, 065010 \(2016\)](#).
- 21 “Single crystal growth by the traveling solvent technique: A review,” S.M. Koohpayeh, [Prog. Cryst. Growth Charact. Mater. doi:10.1016/j.pcrysgrow.2016.03.001](#) (in press).
- 22 “Collective vs. local Jahn-Teller distortion in $\text{Ba}_3\text{CuSb}_2\text{O}_9$: Raman scattering study,” N. Drichko, C. Broholm, K. Kimura, R. Ishii, S. and Nakasutji, [Phys. Rev. B 93, 184425 \(2016\)](#).
- 23 “Effective spin-1/2 scalar chiral order on kagome lattices in $\text{Nd}_3\text{Sb}_3\text{Mg}_2\text{O}_{14}$,” A. Scheie, M. Sanders, J. Krizan, Y. Qiu, R. J. Cava, and C. Broholm, [Phys. Rev. B 93, 180407 \(2016\)](#).
- 24 “A measure of monopole inertia in the quantum spin ice $\text{Yb}_2\text{Ti}_2\text{O}_7$,” L.D. Pan, N.J. Laurita, K.A. Ross, E. Kermarrec, B.D. Gaulin, and N.P. Armitage, [arXiv:1501.05638](#); [Nat. Phys. 12, 361 \(2016\)](#).
- 25 “On the chemistry and physical properties of flux and floating zone grown SmB_6 single crystals,” W. A. Phelan, S. M. Koohpayeh, P. Cottingham, J. A. Tutmaher, J. C. Leiner, M. D. Lumsden, C. M. Lavelle, X. P. Wang, C. Hoffmann, M. A. Siegler, and T. M. McQueen, [Sci. Rep. 6, 20860 \(2016\)](#); [arXiv:1510.07612](#).
- 26 “ $\text{RE}_3\text{Sb}_3\text{Zn}_2\text{O}_{14}$ (RE = La, Pr, Nd, Sm, Eu, Gd): a new family of pyrochlore derivatives with rare earth ions on a 2D Kagome lattice,” M. B. Sanders, J.W. Krizan, and R.J. Cava, [J. Mater. Chem. C 4, 541-550 \(2016\)](#).
- 27 “Static and dynamic XY-like short-range order in a frustrated magnet with exchange disorder,” K. A. Ross, J. W. Krizan, J. A. Rodriguez-Rivera, R. J. Cava, and C. L. Broholm, [Phys. Rev. B 93, 014433 \(2016\)](#).
- 28 “Experimental observation of magnetoelectricity in spin ice $\text{Dy}_2\text{Ti}_2\text{O}_7$,” L. Lin, Y.L. Xie, J.-J. Wen, S. Dong, Z.B. Yan, and J.-M. Liu, [New J. Phys. 17 123018 \(2015\)](#).
- 29 “New honeycomb iridium (V) oxides: NaIrO_3 and $\text{Sr}_3\text{CaIr}_2\text{O}_9$,” D.C. Wallace and T.M. McQueen, [Dalton Trans. 44, 20344-20351 \(2015\)](#).
- 30 “Magnetic order dynamics in optically excited multiferroic TbMnO_3 ,” J. A. Johnson, T. Kubacka, M. C. Hoffmann, C. Vicario, S. de Jong, P. Beaud, S. Grübel, S.-W. Huang, L.

- Huber, Y. W. Windsor, E. M. Bothschafter, L. Rettig, M. Ramakrishnan, A. Alberca, L. Patthey, Y.-D. Chuang, J. J. Turner, G. L. Dakovski, W.-S. Lee, M. P. Minitti, W. Schlotter, R. G. Moore, C. P. Hauri, S. M. Koochpayeh, V. Scagnoli, G. Ingold, S. L. Johnson, and U. Staub, [Phys. Rev. B 92, 184429 \(2015\)](#).
- 31 “U(1) symmetry of the spin-orbit coupled Hubbard model on the kagome lattice,” S.K. Kim and J.D. Zang, [arXiv:1507.03963](#), [Phys. Rev. B 92, 205106 \(2015\)](#).
- 32 “Antiferromagnetic fluctuations in a quasi-two-dimensional organic superconductor detected by Raman spectroscopy,” N. Drichko, R. Hackl, and J.A. Schlueter, [arXiv:1507.07178](#), [Phys. Rev. B 92, 161112 \(2015\)](#).
- 33 “Cr-doped TiSe₂ – a layered dichalcogenide spin glass,” Huixia Luo, Jason W. Krizan, Elizabeth M. Seibel, Weiwei Xie, Girija S. Sahasrabudhe, Susanna L. Bergman, Brendan F. Phelan, Jing Tao, Zhen Wang, Jiandi Zhang, and R. J. Cava, [Chem. Mater. 27, 6810–6817 \(2015\)](#).
- 34 “Representational analysis of extended disorder in atomistic ensembles derived from total scattering data,” J.R. Neilson and T.M. McQueen, [arXiv:1501.04889](#), [J. Appl. Cryst. 48, 1560–1572 \(2015\)](#).
- 35 “Absence of Jahn–Teller transition in the hexagonal Ba₃CuSb₂O₉ single crystal,” N. Katayama, K. Kimura, Y. Han, J. Nasue, N. Drichko, Y. Nakanishi, M. Halim, Y. Ishiguro, R. Satake, E. Nishibori, M. Yoshizawa, T. Nakano, Y. Nozue, Y. Wakabayashi, S. Ishihara, M. Hagiwara, H. Sawa, and S. Nakatsuji, [PNAS 112, 9305-9309 \(2015\)](#).
- 36 “NaSrCo₂F₇, a Co²⁺ pyrochlore antiferromagnet,” J.W. Krizan and R.J. Cava, [J. Phys.: Condens. Matter 27, 296002 \(2015\)](#).
- 37 “Tuning sodium ion conductivity in the layered honeycomb oxide Na_{3-x}Sn_{2-x}Sb_xNaO₆,” R.W. Smaha, J.H. Roudebush, J.T. Herb, E.M. Seibel, J.W. Krizan, G.M. Fox, Q.Z. Huang, C.B. Arnold, and R.J. Cava, [Inorg. Chem. 54, 7985-7991 \(2015\)](#).
- 38 “Direct assignment of molecular vibrations via normal mode analysis of the neutron dynamic pair distribution function technique,” A. M. Fry-Petit, A. F. Rebola, M. Mourigal, M. Valentine, N. Drichko, J. P. Sheckelton, C. J. Fennie and T. M. McQueen, [J. Chem. Phys. 143, 124201 \(2015\)](#).
- 39 “Spin fluctuations from hertz to terahertz on a triangular lattice,” Y. Nambu, J.S. Gardner, D.E. MacLaughlin, C. Stock, H. Endo, S. Jonas, T.J. Sato, S. Nakatsuji, and C. Broholm, [arXiv:1509.04760](#), [Phys. Rev. Lett. 115, 127202 \(2015\)](#).
- 40 “Unstable spin-ice order in the stuffed metallic pyrochlore Pr_{2+x}Ir_{2-x}O_{7-δ},” D. E. MacLaughlin, O. O. Bernal, L. Shu, J. Ishikawa, Y. Matsumoto, J.-J. Wen, M. Mourigal,

- C. Stock, G. Ehlers, C. L. Broholm, Y. Machida, K. Kimura, S. Nakatsuji, Y. Shimura, and T. Sakakibara, [arXiv:1508.02683](#), *Phys. Rev. B* **92**, 054432 (2015).
- 41 “Conserved momenta of a ferromagnetic soliton,” O. Tchernyshyov, [arXiv:1503.02329](#), *Ann. Phys.* **363**, 98-113 (2015).
- 42 “Quenched crystal-field disorder and magnetic liquid ground states in $\text{Tb}_2\text{Sn}_{2-x}\text{Ti}_x\text{O}_7$,” B. D. Gaulin, E. Kermarrec, M. L. Dahlberg, M. J. Matthews, F. Bert, J. Zhang, P. Mendels, K. Fritsch, G. E. Granroth, P. Jiramongkolchai, A. Amato, C. Baines, R. J. Cava, and P. Schiffer, *Phys. Rev. B* **91**, 245141 (2015).
- 43 “ $\text{NaCaNi}_2\text{F}_7$: A frustrated high-temperature pyrochlore antiferromagnet with $S=1$ Ni^{2+} ,” J.W. Krizan and R.J. Cava, [arXiv:1504.07708](#), *Phys. Rev. B* **92**, 014406 (2015).
- 44 “Block magnetic excitations in the orbitally selective Mott insulator BaFe_2Se_3 ,” M. Mourigal, S. Wu, M.B. Stone, J.R. Neilson, J.M. Caron, T.M. McQueen, and C.L. Broholm, *Phys. Rev. Lett.* **115**, 047401 (2015).
- 45 “Electrical probing of field-driven cascading quantized transitions of skyrmion cluster states in MnSi nanowires,” Haifeng Du, Dong Liang, Chiming Jin, Lingyao Kong, Matthew J. Stolt, Wei Ning, Jiyong Yang, Ying Xing, Jian Wang, Renchao Che, Jiadong Zang, Song Jin, Yuheng Zhang, and Mingliang Tian, *Nat. Comm.* doi:10.1038/ncomms8637 (2015).
- 46 “Thermophoresis of an antiferromagnetic soliton,” S.K. Kim, O. Tchernyshyov, and Y. Tserkovnyak, [arXiv:1503.07854](#), *Phys. Rev. B* **92**, 020402(R) (2015).
- 47 “Singlet-triplet excitations and long-range entanglement in the spin-orbital liquid candidate FeSc_2S_4 ,” N. J. Laurita, J. Deisenhofer, L.D. Pan, C. M. Morris, M. Schmidt, M. Johnsson, V. Tsurkan, A. Loidl, N. P. Armitage, [arXiv:1410.6777](#); *Phys. Rev. Lett.* **114**, 207201 (2015).
- 48 “Rhombohedral polytypes of the layered honeycomb delafossites with optical brilliance in the visible,” J.H. Roudebush, G. Sahasrabudhe, S.L. Bergman, and R.J. Cava, *Inorg. Chem.* **54**, 3203 (2015).
- 49 “Raman study of magnetic excitations and magneto-elastic coupling in $\alpha\text{-SrCr}_2\text{O}_4$,” M. Valentine, S. Koohpayeh, M. Mourigal, T. M. McQueen, C. Broholm, N. Drichko, S. Dutton, R. J. Cava, T. Birol, H. Das, and C. J. Fennie, [arXiv:1404.0355](#), *Phys. Rev. B* **91**, 144411 (2015).
- 50 “Polytypism, polymorphism, and superconductivity in $\text{TaSe}_{2-x}\text{Te}_x$,” H.X. Luo, W.W. Xie, J. Tao, H. Inoue, A. Gyenis, J.W. Krizan, A. Yazdani, Y.M. Zhu, and R.J. Cava, *PNAS* **112**, E1174 (2015).

- 51 “Transport theory of metallic B20 helimagnets,” J. Kang and J. Zang, [Phys. Rev. B 91, 134401 \(2015\)](#).
- 52 “Charged skyrmions on the surface of a topological insulator,” H.M. Hurst, D.K. Efimkin, J. Zang, and V. Galitski, [Phys. Rev. B 91, 060401 \(2015\)](#).
- 53 “Large thermal Hall conductivity of neutral spin excitations in a frustrated quantum magnet,” M. Hirschberger, J.W. Krizan, R.J. Cava, and N.P. Ong, [Science 348, 106 \(2015\)](#).
- 54 “Electronic tunability of the frustrated triangular-lattice cluster magnet $\text{LiZn}_{2-x}\text{Mo}_3\text{O}_8$,” [Mater. Horiz. 2, 76-80 \(2015\)](#).
- 55 “Disorder from order among anisotropic next-nearest-neighbor Ising spin chains in SrHo_2O_4 ,” J.-J. Wen, W. Tian, V. O. Garlea, S. M. Koohpayeh, T. M. McQueen, H.-F. Li, J.-Q. Yan, J. A. Rodriguez-Rivera, D. Vaknin, and C. L. Broholm, [arXiv:1407.1341](#), [Phys. Rev. B 91, 054424 \(2015\)](#).
- 56 “Interaction driven subgap spin exciton in the Kondo insulator SmB_6 ,” W. T. Fuhrman, J. Leiner, P. Nikolić, G. E. Granroth, M. B. Stone, M. D. Lumsden, L. DeBeer-Schmitt, P. A. Alekseev, J.-M. Mignot, S. M. Koohpayeh, P. Cottingham, W. A. Phelan, L. Schoop, T. M. McQueen, and C. Broholm, [arXiv:1407.2647](#); [Phys. Rev. Lett. 114, 036401 \(2015\)](#).
- 57 “Fractional excitations in the square-lattice quantum antiferromagnet,” B. Dalla Piazza, M. Mourigal, N. B. Christensen, G. J. Nilsen, P. Tregenna-Piggott, T. G. Perring, M. Enderle, D. F. McMorrow, D. A. Ivanov, and H. M. Rønnow, [arXiv:1501.01767](#), [Nat. Phys. 11, 62 \(2015\)](#).
- 58 “Projective symmetry of partons in the Kitaev honeycomb model,” P. Mellado, O. Petrova, and O. Tchernyshyov, [arXiv:1409.7460](#); [Phys. Rev. B 91, 041103 \(2015\)](#).
- 59 “Structure and magnetic properties of the spin-1/2-based honeycomb $\text{NaNi}_2\text{BiO}_{6-\delta}$ and its hydrate $\text{NaNi}_2\text{BiO}_{6-\delta} \cdot 1.7\text{H}_2\text{O}$,” E.M. Seibel, J.H. Roudebush, M.N. Ali, K.A. Ross, and R.J. Cava, [Inorg. Chem. 53, 10989 \(2014\)](#).
- 60 “Two-dimensional heavy fermions on the strongly correlated boundaries of Kondo topological insulators,” P. Nikolić, [arXiv:1407.4482](#); [Phys. Rev. B 90, 235107 \(2014\)](#).
- 61 “In-gap collective mode spectrum of the topological Kondo insulator SmB_6 ,” W. T. Fuhrman and P. Nikolić, [arXiv:1409.3220](#); [Phys. Rev. B 90, 195144 \(2014\)](#).
- 62 “Crystal structure and electronic structure of CePt_2In_7 ,” T. Klimczuk, O. Walter, L. Muehler, J.W. Krizan, F. Kinnart, and R.J. Cava, [J. Phys.: Condens. Matter 26, 402201 \(2014\)](#).

- 63 “NaCaCo₂F₇: A single-crystal high-temperature pyrochlore antiferromagnet,” J. W. Krizan and R. J. Cava, [Phys. Rev. B 89, 214401 \(2014\)](#).
- 64 “Superconductivity on the Brink of Spin-Charge Order in a Doped Honeycomb Bilayer,” O. Vafek, J. M. Murray, and V. Cvetkovic, [arXiv:1309.3123](#), [Phys. Rev. Lett. 112, 147002 \(2014\)](#).
- 65 “Neutron spectroscopic study of crystal field excitations in Tb₂Ti₂O₇ and Tb₂Sn₂O₇,” J. Zhang, K. Fritsch, Z. Hao, B. V. Bagheri, M. J. P. Gingras, G. E. Granroth, P. Jiramongkolchai, R. J. Cava, and B. D. Gaulin, [Phys. Rev. B 89, 134410 \(2014\)](#).
- 66 “Magnons and continua in a magnetized and dimerized spin-1/2 chain,” M. B. Stone, Y. Chen, D. H. Reich, C. Broholm, G. Xu, J. R. D. Copley, and J. C. Cook, [Phys. Rev. B 90, 094419 \(2014\)](#).
- 67 “Weyl fermions induced magnon electrodynamics in a Weyl semimetal,” J.A. Hutasoit, J.D. Zang, R. Roiban, and C.X. Liu [arXiv:1405.0491](#), [Phys. Rev. B 90, 134409 \(2014\)](#).
- 68 “Unpaired Majorana modes on dislocations and string defects in Kitaev’s honeycomb model,” O. Petrova, P. Mellado, and O. Tchernyshyov, [arXiv:1406.6407](#), [Phys. Rev. B 90, 134404 \(2014\)](#).
- 69 “Electric field-induced Skyrmion distortion and giant lattice rotation in the magnetoelectric insulator Cu₂OSeO₃,” J. S. White, K. Prša, P. Huang, A. A. Omrani, I. Živković, M. Bartkowiak, H. Berger, A. Magrez, J. L. Gavilano, G. Nagy, J. Zang, and H. M. Rønnow, [Phys. Rev. Lett. 113, 107203 \(2014\)](#); Editors’ Suggestion.
- 70 “Low-energy electrodynamics of novel spin excitations in the quantum spin ice Yb₂Ti₂O₇,” L.D. Pan, S.K. Kim, A. Ghosh, C.M. Morris, K.A. Ross, E. Kermarrec, B.D. Gaulin, S.M. Koohpayeh, O. Tchernyshyov, and N. P. Armitage, [arXiv:1406.3576](#), [Nat. Commun. 5, 4970 \(2014\)](#).
- 71 “Constraints on Jones transmission matrices from time-reversal invariance and discrete spatial symmetries,” N.P. Armitage, [Phys. Rev. B 90, 035135 \(2014\)](#). Editors’ Suggestion.
- 72 “Quantum dimer model for the spin-1/2 kagome Z₂ spin liquid,” I. Rousochatzakis, Y. Wan, F. Mila, and O. Tchernyshyov, [arXiv:1308.0738](#), [Phys. Rev. B 90, 100406\(R\) \(2014\)](#).

The Rise of Quantum Materials: Scientific Challenges and Technological Opportunities

**Collin Broholm, Institute for Quantum Matter and Department of Physics and Astronomy,
The Johns Hopkins University, Baltimore, MD 21218**

We now have it from a credible source [1]: “Quantum materials are solids with exotic physical properties, arising from the quantum mechanical properties of their constituent electrons.”

An intense world wide effort is underway to explore the science and exploit the technological opportunities of Quantum Materials. After a lively debate that many of you contributed to, the 2016 BES Workshop on Quantum Materials for Energy Relevant Technology identified four Priority Research Directions [1]:

PRD 1: Control and exploit electronic interactions and quantum fluctuations for design of bulk materials with novel functionality

PRD 2: Harness topological states for groundbreaking surface properties

PRD 3: Drive and manipulate quantum effects (coherence, entanglement) in nanostructures for transformative technologies

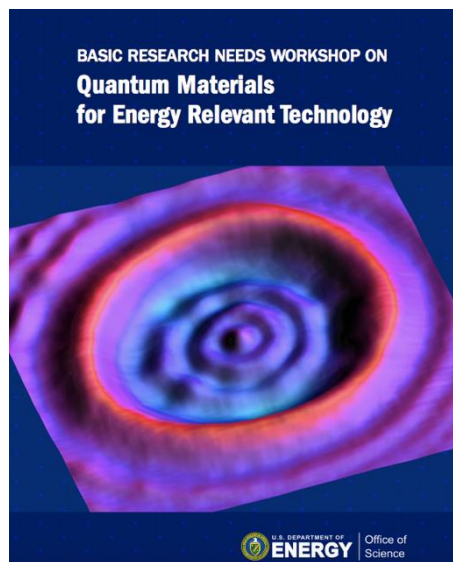
PRD 4: Design revolutionary tools to accelerate discovery and technological deployment of quantum materials

In this talk I will provide more context and information about each of these PRDs with emphasis on the role neutron scattering may play as we explore the fascinating world of quantum materials.

Publications

“Report of the Office of Basic Energy Sciences Workshop on Quantum Materials,”

http://science.energy.gov/bes/community-resources/reports/les/BRNQM_rpt.pdf



Impact of Dynamic Instabilities and Microstructure on Energy Materials

J. D. Budai, M. E. Manley, R. P. Hermann, and O. Delaire*

Materials Science & Technology, Oak Ridge National Laboratory, Oak Ridge, TN

*Mechanical Engineering and Materials Science, Duke University, Durham, NC

Program Scope

Our program focuses on understanding how the interplay of lattice dynamics with atomic and electronic structure control energy transport, phase stability and other functional properties in advanced materials. This research uses DOE neutron and x-ray scattering facilities to assess the full 4-dimensional dynamical structure factor $S(\mathbf{Q}, E)$, and combines the experimental results with first-principles calculations which include finite temperature. We focus on understanding how issues of strong anharmonicity, lattice instabilities and broken local symmetry influence physical behaviors in interrelated model systems. Current research thrusts include investigations of how inhomogeneous nanoregions produce giant piezoelectric response through phonon localization in frustrated ferroics; how atomic bonding modifications control thermal transport and thermoelectric efficiency in skutterudites and phase change materials; and how anharmonic interactions drive lattice instabilities that control phase competition in rutile and perovskite oxides. The long-term research goal in each case is to provide the fundamental knowledge that quantitatively links dynamics and structure with first-principles theories to enable the prediction of enhanced materials properties.

Recent Progress

Ultra-high piezoelectricity enhanced by polar nanoregions. Neutron scattering measurements demonstrate that polar-nanoregion (PNR) vibrations enable the ultra-high piezoelectric response in relaxor-based ferroelectrics [1]. A long-standing challenge has been to understand how this high performance occurs when polar atomic displacements underlying the response are partially broken into PNRs. Our results show that PNR vibrational modes enable the ultra-high piezoelectric response by softening the underlying macro-domain polarization rotations. The mechanism involves the collective motion of the PNRs with transverse acoustic phonons and results in two hybrid modes, one softer and one stiffer than a bare acoustic phonon. The softer mode is the origin of the macroscopic shear softening. In addition, it is found that the PNR modes align in an electric field (Fig. 1) and this enhances the shear softening further (soft shear mode indicated in Fig. 1). This tuning ability of the PNRs suggests a way to optimize the ultra-high piezoelectric response.

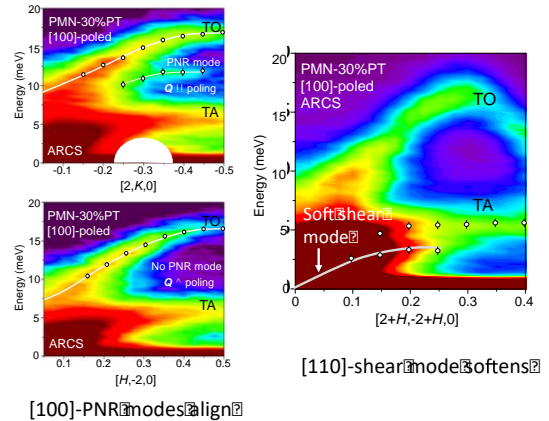


Fig. 1. Alignment of polar nanoregion (PNR) modes (left panels) enhances shear softening (right panel), enabling ultra-high piezoelectric response of PMN-30%PT relaxor-based ferroelectric.

Glassy soft phonon heralds strain glass state in a shape memory alloy. Strain glasses are a class of crystalline materials that contain nanoscale strain domains and exhibit slow relaxation

dynamics [2]. It is possible to change a NiCoMnIn Heusler alloy from a martensitic-transforming shape memory alloy to a non-transforming strain glass via furnace annealing [3]. However, TEM images show no significant change in short- or long-range structure, making the source of the strain glass state a mystery. Our results show that the non-ergodicity associated with the strain glass state extends to dynamics in the phonon (THz) spectrum and to atomic length scales. The transverse acoustic phonon that matches the shape memory transition displacements behaves normally in the shape memory alloy, whilst becoming over-damped across all wavevectors both above and below the strain glass transition temperature. Electronic band structure calculations show that the Fermi nesting vector that drives the displacive shape memory transition can become smeared across wavevectors by chemical disorder, acting to spread the instability across length scales. The existence of the glassy phonon reflects this length-scale distributed instability and portends the low temperature strain glass state.

Bonding modifications drive lattice instabilities We have investigated how bonding modifications influence lattice instabilities and dynamics in thermoelectric and phase change materials with low thermal conductivity. Major progress has been achieved in understanding the behavior of caged atoms, so-called “rattlers”, in thermoelectric skutterudites. First, we have shown how, as the cage shrinks under high applied pressure and becomes too small to allow for large amplitudes of motion, the rattling guest locks in and behaves in line with the host structure [4]. This transition, visible in the density of phonon states and in the pressure dependence of the lattice constants, can be understood as a removal of an avoided crossing by tuning the bonding forces. Second, we have shown a new unique “rattling” scenario in skutterudites filled with anionic guests. Here, neutron diffraction indicates that host atoms get drawn toward the sulphur filler and form a probably transient covalent bond instead of the usual ionic bond [5]. Hence, a rigid diatomic unit is formed. This “rattling” dimer strongly disrupts phonon transport, resulting in state of the art thermoelectric efficiency, at a much lower materials cost than with rare-earth fillers. Further progress concerns the understanding of how pressure can drive the bonding from covalent to resonant in group V elements, such as antimony and arsenic. The softening of select modes in antimony dispersion relations under high pressure indicates a bonding modification. First evidence for force constant modification upon strain doping, that is application of negative pressure by helium implantation, has also been obtained in thin films by nuclear resonance scattering. The Mössbauer spectroscopy laboratory has been setup and data acquisition can now start. This facility will play an important role notably in studying magnetic and lattice properties in ferroic and strain doped films.

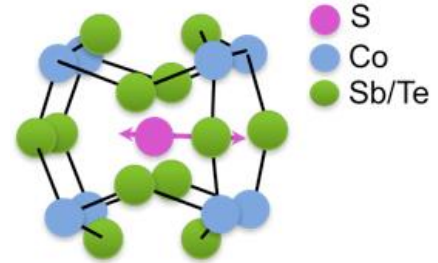


Fig 2. Anionic S guests in $\text{Co}(\text{Sb},\text{Te})_3$ attract a host Sb and deform the host cage. The new rattling behavior of rigid S-Sb units improves thermoelectric performance.

Anharmonic lattice dynamics and phase stability in metal oxides Rutile oxides (MO_2) are model systems for understanding phase stability in transition metal oxides; they have a relatively simple structure, but exhibit complex emergent physical behaviors such as metal-insulator transitions (MITs). Our early studies of phonons in VO_2 showed that the vibrational entropy of soft, strongly anharmonic phonons stabilize the metallic rutile phase above the MIT [6]. First-principles calculations showed that orbitally-driven dimerization stabilizes the insulating low T ground state. Assessing the generality of these mechanisms, we have investigated temperature-

dependent lattice dynamics in other rutile oxides and related metal oxides. In TiO_2 , although the rutile phase is thermodynamically stable, approximately 10 different metastable polymorphs can be formed by controlling nucleation, particle size or pressure. Our scattering studies have identified anomalous phonon softening upon cooling for essentially all low-energy modes in rutile TiO_2 (Fig 3), indicating instabilities over a wide range of symmetries. In contrast, TiO_2 exhibits “normal” temperature dependent elastic properties, i.e. stiffening with cooling. We resolved this apparent contradiction using measurements of long-wavelength phonons at very small Q near zone centers. They reveal normal temperature dependence, explaining how conventional macroscopic elastic properties coexist with short-length-scale instabilities. We have also initiated studies of lattice dynamics in V_2O_3 aimed at understanding how this MIT compares with VO_2 . In contrast to the VO_2 MIT which is driven by large vibrational entropy, we find a much smaller change in vibrational entropy in V_2O_3 , consistent with a Mott MIT dominated by electronic correlations.

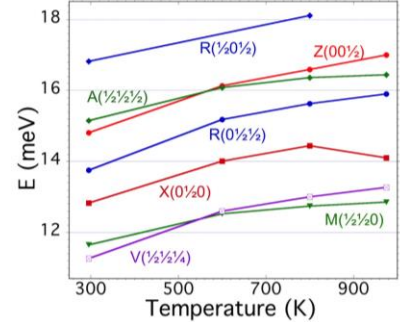


Fig 3 Anomalous softening of low energy TiO_2 phonons upon cooling.

Anharmonic phonon coupling in perovskite oxides Perovskite materials such as SrTiO_3 , EuTiO_3 and $\text{KTa}_{1-x}\text{Nb}_x\text{O}_3$ represent an important related class of oxides where functional properties are often controlled by competing lattice instabilities such as incipient ion off-centering or rotation and tilts of oxygen octahedra. In SrTiO_3 , we have we have identified an electric field dependence of the transverse optic (TO) mode to externally applied E-fields in the quantum paraelectric regime, and we have explained from first-principles the finite-temperature stabilization of the paraelectric phase by anharmonic renormalization of ferroelectric and antiferrodistortive soft-modes, matching the $S(\mathbf{Q},E)$ from inelastic neutron scattering (INS).

Future Plans

Intrinsic and disorder-induced localized modes in functional materials. We will extend ongoing work and initiate new studies of intrinsic and disorder-induced local modes in functional materials. In the relaxor-based ferroelectric PMN-PT, we will investigate electric-field poling effects in order to understand how the interplay between local structure and dynamics can be used to enhance piezoelectric properties. In new studies, our collaborators at Caltech (Minnich group) have used ab-initio molecular dynamics calculations to observe the presence of an intrinsic localized mode (ILM) in the acoustic frequencies of PbSe [7], a chalcogenide of interest for its exceptional thermoelectric properties and strong anharmonicity. This mode is not expected according to the classic definition of an ILM, where the modes appear in spectral gaps [8]. Additional calculations show that this ILM reflects exceptionally strong scattering between the transverse optic and longitudinal acoustic branches that nearly completely annihilates the contribution of the LA branch in the vicinity of the ILM to thermal conductivity. The observation of this ILM experimentally would confirm that these crystals can indeed exhibit sufficient anharmonicity to localize vibrations and thus would pave the way for an exciting scientific investigation of lattice dynamics in highly anharmonic crystals.

Impact of bonding modifications on lattice instabilities We will investigate how lattice dynamics are tied to bonding modifications by extending the program, notably to functional thin films. We will study dynamics in skutterudites with anionic fillers using inelastic neutron scattering to obtain direct evidence for the rigid unit dynamics scenario, a needed confirmation for the so-far

structural insights. This confirmation will enable new lattice dynamics tailoring. The high-pressure inelastic x-ray scattering (IXS) data for antimony will be combined with neutron scattering data and IXS on arsenic as it transitions from a covalently bonded rhombohedral to a resonantly bonded simple cubic structure at 27 GPa. In this combination, we hope to provide the simplest and clearest example so far of resonance bonding in solids. With the Functional Oxides group at ORNL, we will utilize Mössbauer and nuclear inelastic scattering spectroscopies to characterize the structure and magnetism in ferroic films strained by epitaxy and helium implantation. Ultimately we aim to reach atomic layer resolution for vibrational spectroscopy and Mössbauer magnetometry. Unique insights in how lattice dynamics and magnetism evolve away from the film-to-substrate interface are expected.

Anharmonic lattice dynamics in rutile oxides at high pressure We will use pressure- and strain-dependent inelastic scattering to study the role of anharmonicity in controlling phase stability and properties in rutile oxides, e.g. TiO_2 and SnO_2 . Understanding pressure/strain effects is essential for thin-film applications as well as in geophysical models. In a simple quasiharmonic material, the dynamic effect of increasing pressure mimics decreasing temperature, as atoms move closer together. However, anharmonic interactions can lead to behaviors that are quite different, and there is strong interest in using pressure vs. temperature contrast to elucidate anharmonic interactions. In TiO_2 , competing theoretical models give conflicting predictions for softening of vibrational modes and different predictions for external strains that may stabilize ferroelectricity [9]; our experimental measurements will address this controversy. We will contrast the temperature- and pressure- dependence, and combine results with first-principles calculations in order to understand how to accurately incorporate anharmonicity at finite temperature in predictive modeling.

Anharmonic phonon coupling in perovskite oxides Extending our work on SrTiO_3 , we will investigate the coupling between anharmonic soft-modes and magnetic ordering in the multiferroic EuTiO_3 , whose antiferroelectric behavior is closely related to SrTiO_3 . Preliminary INS measurements were performed on an isotopically enriched $^{153}\text{EuTiO}_3$ crystal, mapping both magnetic and nuclear excitation, across the Néel temperature, T_N , and the antiferrodistortive transition at T_{AFD} . These results suggest a strong spin-phonon coupling, in agreement with our first-principles simulations. Model Hamiltonian calculations have predicted that strong spin-phonon coupling can lead to the formation of hybrid excitations, and we will test this prediction by performing polarized neutron scattering.

References

- [1] M. E. Manley, *et al.*, *Science Advances* **16**, e1501814 (2016).
- [2] S. Sarkar, X. Ren and K. Otsuka, *Phys. Rev. Lett.* **95**, 205702 (2005).
- [3] J. A. Monroe, *et al.*, *Acta Materialia* **101**, 107 (2015).
- [4] I. Sergueev, *et al.*, *Phys. Rev. B* **91**, 224304 (2015).
- [5] B. Duan, *et al.*, *Energy & Environmental Science* **9**, no. 6, 2090 (2016).
- [6] J. D. Budai, *et al.*, *Nature* **515**, 535 (2014).
- [7] N. Shulumba, O. Hellman, A. J. Minnich, *arXiv:1609.08254* [cond-mat.mtrl-sci] (2016).
- [8] M. E. Manley, *et al.*, *Scientific Reports* **1**:4 (2011).
- [9] A. Grunebohm, *et al.*, *Phys. Rev. B* **88**, 136102 (2013).

Publications

1. M. E. Manley, D. L. Abernathy, R. Sahul, D. E. Parshall, J. W. Lynn, A. D. Christianson, P. J. Stonaha, E. D. Specht, and J. D. Budai, "Giant electromechanical coupling of relaxor ferroelectrics controlled by polar nanoregion vibrations," *Science Advances* **2**, e1501814 (2016).
2. B. Klobes, M. Y. Hu, M. Beekman, D. C. Johnson, and R. P. Hermann, "Confined lattice dynamics of single and quadruple SnSe bilayers in $[(\text{SnSe})_{1.04}]_m[\text{MoSe}_2]_n$ ferecrystals," *Nanoscale* **8**, 856-861 (2016).
3. M. E. Manley, D. L. Abernathy, R. Sahul, P. J. Stonaha, and J. D. Budai, "Three-mode coupling interference patterns in the dynamic structure factor of a relaxor ferroelectric," *Physical Review B* **94**, 104304 (2016).
4. M. Herlitschke, B. Klobes, I. Sergueev, P. Hering, J. Perßon, and R. P. Hermann, "Elasticity and magnetocaloric effect in MnFe_4Si_3 ," *Physical Review B* **93**, 904304 (2016).
5. B. Duan, J. Yang, J. R. Salvador, Y. He, B. Zhao, S. Wang, P. Wei, F. S. Ohuchi, W. Zhang, R. P. Hermann, O. Gourdon, S. X. Mao, Y. Cheng, C. Wang, J. Liu, P. Zhai, X. Tang, Q. Zhang, and J. Yang, "Electronegative Guests in CoSb_3 ," *Energy & Environmental Science* **9**, no. 6, 2090-2098 (2016).
6. C. Beekman, W. Siemons, M. Chi, N. Balke, J. Y. Howe, T. Z. Ward, P. Maksymovych, J. D. Budai, J. Z. Tischler, R. Xu, W. Liu, and H. M. Christen, "Ferroelectric Self-Poling, Switching, and Monoclinic Domain Configuration in BiFeO_3 Thin Films," *Advanced Functional Materials* **26**, 5166 (2016).
7. V. E. Asadchikov, A. V. Butashin, A. V. Buzmakov, A. N. Deryabin, V. M. Kanevsky, I. A. Prokhorov, B. S. Roshchin, Y. O. Volkov, D. A. Zolotov, A. Jafari, P. Alexeev, A. Cecilia, T. Baumbach, D. Bessas, A. N. Danilewsky, I. Sergueev, H.-C. Wille, and R. P. Hermann, "Single-crystal sapphire microstructure for high-resolution synchrotron X-ray monochromators." *Crystal Research and Technology* **51**, no. 4, 290-298 (2016). (front journal cover)
8. Sesselman, B. Klobes, T. Dasgupta, O. Gourdon, R. P. Hermann, and E. Müller, "Neutron Diffraction and Thermoelectric Properties of Indium Filled $\text{In}_x\text{Co}_4\text{Sb}_{12}$ ($x = 0.05, 0.2$) and Indium Cerium Filled $\text{Ce}_{0.05}\text{In}_{0.1}\text{Co}_4\text{Sb}_{12}$ Skutterudites," *physica status solidi (a)* **213**, 766-773 (2016).
9. F. Tietz, I. A. Raj, Q. Ma, S. Baumann, A. Mahmoud and R. P. Hermann, "Material properties of perovskites in the quasi-ternary system LaFeO_3 - LaCoO_3 - LaNiO_3 ," *Journal of Solid State Chemistry* **237**, 183-191 (2016).
10. M. T. Sougrati, A. Darwiche, X. Liu, A. Mahmoud, R. P. Hermann, S. Jouen, L. Monconduit, R. Dronskowski and L. Stievano "Transition-Metal Carbodiimides as Molecular Negative Electrode Materials for Lithium- and Sodium-Ion Batteries with Excellent Cycling Properties," *Angewandte Chemie International Edition* **55**, 5090-5095 (2016).

11. T. Claudio, N. Stein, N. Petermann, D. G. Stroppa, M. M. Koza, H. Wiggers, B. Klobes, G. Schierning, and R. P. Hermann, "Lattice dynamics and thermoelectric properties of nanocrystalline silicon-germanium alloys," *physica status solidi (a)* **213**, 515-523 (2016).
12. D. Bessas, M. Winkler, I. Sergueev, J. D. König, H. Böttner, and R. P. Hermann, "Lattice dynamics in elemental modulated Sb_2Te_3 films," *physica status solidi (a)* **213**, 694-698 (2016).
13. E. Wetterskog, A. Klapper, S. Disch, E. Josten, R. P. Hermann, U. Rücker, T. Brückel, L. Bergström, and G. Salazar-Alvarez, "Tuning the structure and habit of iron oxide mesocrystals," *Nanoscale* **8**, 15571 (2016).
14. P. J. Stonaha, M. E. Manley, N. M. Bruno, I. Karaman, R. Arroyave, N. Singh, D. L. Abernathy, and S. Chi, "Lattice vibrations boost demagnetization entropy in a shape-memory alloy," *Physical Review B* **92**, 120406(R) (2015).
15. X. Li, J. D. Budai, F. Liu, Y. S. Chen, J. Y. Howe, C. Sun, J. Z. Tischler, R. S. Meltzer and Z. W. Pan, "Crystal structures and optical properties of new quaternary strontium europium aluminate luminescent nanoribbons," *Journal of Materials Chemistry C* **3**, 778 (2015).
16. G. E. Ice and J. D. Budai, "X-Ray Microscopy: Beyond Ensemble Averages," *Nature Materials* **14**, 657 (2015).
17. O. Delaire, I. I. Al-Qasir, A. F. May, C. W. Li, B. C. Sales, J. L. Niedziela, J. Ma, M. Matsuda, D. L. Abernathy, and T. Berlijn, "Heavy-impurity resonance, hybridization, and phonon spectral functions in $\text{Fe}_{1-x}\text{M}_x\text{Si}$ (M= Ir, Os)," *Physical Review B* **91**, 094307 (2015).
18. E. D. Specht, J. Ma, O. Delaire, J. D. Budai, A. F. May, and E. A. Karapetrova, "Nanoscale Structure in AgSbTe_2 Determined by Diffuse Elastic Neutron Scattering," *Journal of Electronic Materials* **44**, 1536 (2015).
19. N. P. Butch, M. E. Manley, J. R. Jeffries, M. Janoschek, K. Huang, M. B. Maple, A. H. Said, B. M. Leu, and J. W. Lynn, "Symmetry and correlations underlying hidden order in URu_2Si_2 ," *Physical Review B* **91**, 035128 (2015).
20. H. Guo, S. Dong, P. D. Rack, J. D. Budai, C. Beekman, Z. Gai, W. Siemons, C. M. Gonzalez, R. Timilsina, A. T. Wong, A. Herklotz, P. C. Snijders, E. Dagotto, and T. Z. Ward, "Strain doping: Reversible single axis control of a complex oxide lattice via helium implantation," *Physical Review Letters* **114**, 256801 (2015).
21. I. Sergueev, K. Glazyrin, I. Kantor, M. A. McGuire, A. I. Chumakov, B. Klobes, B. C. Sales, and R. P. Hermann, "Quenching rattling modes in skutterudites with pressure," *Physical Review B* **91**, 224304 (2015).
22. J. D. Budai, J. W. Hong, M. E. Manley, E. D. Specht, C. W. Li, J. Z. Tischler, D. L. Abernathy, A. H. Said, B. M. Leu, L. A. Boatner, R. J. McQueeney, O. Delaire, "Metallization of vanadium dioxide driven by large phonon entropy," *Nature* **515**, 535 (2014).
23. F. Liu, R.S. Meltzer, X. Li, J.D. Budai, and Z.W. Pan, "New Localized/Delocalized Emitting State of Eu^{2+} in Orange-Emitting Hexagonal EuAl_2O_4 ," *Scientific Reports* **4**, srep07101 (2014).

24. J. Ma, O. Delaire, E. D. Specht, A.F. May, O. Gourdon, J. D. Budai, M. McGuire, T. Hong, D.L. Abernathy, G. Ehlers, and E. Karapetrova, "Phonon Scattering Rates and Atomic Ordering in $\text{Ag}_{1-x}\text{Sb}_{1+x}\text{Te}_{2+x}$ ($x = 0, 0.1, 0.2$) Investigated with Inelastic Neutron Scattering and Synchrotron Diffraction," *Physical Review B* **90**, 134303 (2014).
25. C. W. Li, J. Ma, H. B. Cao, A. F. May, D. L. Abernathy, G. Ehlers, C. Hoffmann, X. Wang, T. Hong, A. Huq, O. Gourdon, and O. Delaire, "Anharmonicity and atomic distribution of SnTe and PbTe thermoelectrics," *Physical Review B* **90**, 214303 (2014).
26. P. Alexeev, V. Asadchikov, D. Bessas, A. Butashin, A. Deryabin, F.-U. Dill, A. Ehnes, M. Herlitschke, R. P. Hermann, A. Jafari, I. Prokhorov, B. Roshin, R. Röhlberger, K. Schlage, I. Sergueev, A. Siemens, and H.-C. Wille, "The sapphire backscattering monochromator at the Dynamics beamline P01 of PETRA III," *Hyperfine Interactions* **237**, 59 (2016).
27. K. Lasri, A. Mahmoud, I. Saadoun, M. T. Sougrati, L. Stievano, P. E. Lippens, R. P. Hermann, and H. Ehrenberg, "Toward understanding the lithiation/delithiation process in $\text{Fe}_{0.5}\text{TiOPO}_4/\text{C}$ electrode material for lithium-ion batteries," *Solar Energy Materials & Solar Cells* **148**, 11 (2016).
28. D. O. Ojwang, J. Grins, D. Wardecki, M. Valvo, V. Renman, L. Häggström, T. Ericsson, T. Gustafsson, A. Mahmoud, R. P. Hermann, and G. Svensson, "Structure Characterization and Properties of K-Containing Copper Hexacyanoferrate," *Inorganic Chemistry* **55**, 5924 (2016).
29. W. Paschinger, G. Rogl, A. Grytsiv, H. Michor, P. R. Heinrich, H. Müller, S. Puchegger, B. Klobes, R. P. Hermann, M. Reinecker, Ch. Eisenmenger-Sitter, P. Broz, E. Bauer, G. Giester, M. Zehetbauer, and P. F. Rogl, "Ba-filled Ni–Sb–Sn based skutterudites with anomalously high lattice thermal conductivity," *Dalton Transactions* **45**, 11071 (2016).
30. N. Peranio, O. Eibl, S. Bäßler, K. Nielsch, B. Klobes, R. P. Hermann, M. Daniel, M. Albrecht,^[1]_{SEP} H. Görlitz, V. Pacheco, N. Bedoya-Martínez, A. Hashibon, and C. Elsässer,^[1]_{SEP} "From thermoelectric bulk to nanomaterials: current progress for Bi_2Te_3 and CoSb_3 ," *physica status solidi (a)* **213**, 739-749 (2016).
31. V. Potapkin, L. Dubrovinsky, I. Sergueev, M. Ekholm, I. Kantor, D. Bessas, E. Bykova, V. Prakapenka, R. P. Hermann, R. Ruffer, V. Cerantola, H. J. M. Jonsson, W. Olovsson, S. Mankovsky, H. Ebert and I. A. Abrikosov, "Magnetic interactions in NiO at ultra-high pressure," *Physical Review B* **93**, 201110(R) (2016).
32. S. Lemal, N. Nguyen, J. de Boor, P. Ghosez, J. Varignon, B. Klobes, R. P. Hermann and M. J. Verstraete, "Thermoelectric properties of the unfilled skutterudite FeSb_3 from first principles and Seebeck local probes," *Physical Review B* **92**, 205204 (2015).

Understanding the Mechanism of Lithiation & Delithiation of Si and Mg Electrodes through Neutron Diffraction by *in situ* Electrochemical Cell and Neutron Imaging

K. S. Ravi Chandran

Department of Metallurgical Engineering, University of Utah, SLC, UT 84112

Program Scope

The performance of Li-ion battery is determined by the kinetics of the phase transitions occurring in bulk of electrodes. The nature of phase transitions governs the battery performance metrics such as electrode structural stability, maximum charge capacity and degree of capacity fading during cycling. The effectiveness of purely electrochemical techniques in understanding bulk phase transitions is very limited, although they give information about the reactions occurring at the electrode surface. The phase transitions in the bulk electrodes can be more appropriately investigated using neutron diffraction (ND) techniques, but an *in-situ* cell, capable of using small volume electrodes, has been lacking so far. Specific objectives of this research are

- Study the real time phase transitions in microcolumnar Si (100) electrodes, using specially designed *in-situ* electrochemical cell, employing neutron diffraction technique
- Investigate phase transitions in Mg(Li) alloy electrode that occur under electrochemical lithiation/delithiation conditions and to determine aspects of phase transition that enable/limit the energy storage capacity
- Study the spatial distribution of Li in V₂O₅ electrodes and to broadly facilitate the qualitative/quantitative imaging of Li distribution in electrodes using computed neutron tomography

Parts of this research are done in collaboration with ORNL using neutron diffraction (Dr. Ke An) and neutron imaging (Dr. H. Bilheux).

Recent Progress

I. Study of phase transitions in microcolumnar Si (100) electrode using ND experiments

Recently, we designed and validated an *in-situ* electrochemical cell¹ that enables capturing of Rietveld-refinable neutron diffraction patterns in VULCAN neutron diffractometer at SNS, to study the phase transitions in battery electrode materials. The cell was successfully used to track the phase transitions from small volume electrodes in LiCoO₂/graphite, LiMn₂O₄/graphite cells. In the current work, the cell (Figure 1a & 1b) is used to study the phase transitions in microcolumnar Si (100) electrodes. The cell containing microcolumnar Si (100) electrodes to be diffracted, is oriented at 45° (Figure 1c) to the VULCAN beam. This is to enable Si (400) and Si (440)/(220) Bragg reflections to appear in the reflection bank and the transmission bank respectively. The real time ND patterns collected during lithiation of Si are shown in Figure 2. The intensities of Si (400), (440), (220) can be seen to be increasing continuously, whereas that of Cu (200) remains the same. The intensity development in ND is in contrast to XRD, which showed combined peak broadening and intensity decrease due to amorphization of Si.

We are currently investigating if the increase in Si (hkl) intensity is due to mosaicity induced in Si (100) during lithiation. During lithiation, as Li diffuses in Si (100) along $\langle 110 \rangle$ direction, the Si-Si bonds across {111} planes will be broken². As a result, micro-cracks could form parallel to {111} planes, causing the collapse of {111} planes, possibly resulting in mosaicity.

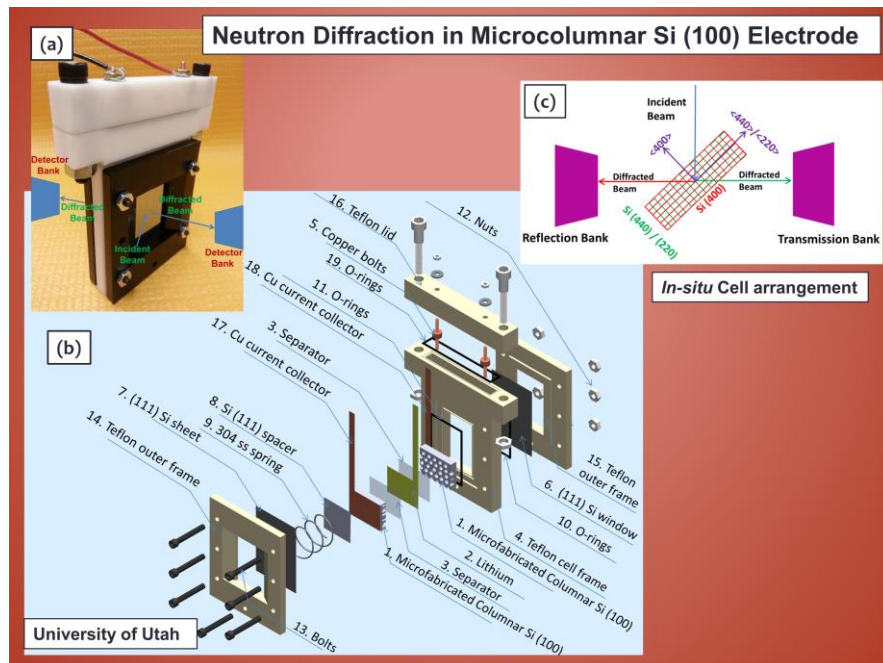


Figure 1(a) Photograph of the *in-situ* cell in the assembled form, (b) exploded view of the designed *in-situ* electrochemical cell, with Si (111) as casing, for ND studies with microcolumnar Si (100) electrodes and (c) *in-situ* cell at VULCAN diffractometer in Spallation Neutron Source, ORNL.

Figure 2. ND patterns obtained in VULCAN using the *in-situ* cell during discharging of microcolumnar Si (100) electrodes. The intensity of Si (400), (440), (220) reflections increases whereas that of Cu (200) remains the same.

II. Neutron tomographic imaging of lithiation and delithiation processes in Li-battery electrodes

In Li(Mg) alloy electrodes actual Li distributions in the bulk govern the charge/discharge rates³ and the reversibility of cell performance and/or electrode utilization during the electrochemical insertion/removal of lithium. To investigate this, neutron tomographic imaging technique has been used for mapping bulk Li distribution in Mg-70 wt.% Li alloy electrodes (Figure 3a). Neutron CT scan was performed at CG-1D Neutron Imaging Prototype Station at High Flux Isotope Reactor (HFIR), ORNL.

In the recent progress, the Li concentration profiles along thickness direction have been determined by neutron imaging. A rigorous analytical model to quantify the diffusion-controlled delithiation, accompanied by phase transition and boundary movement, has also been developed to explain the delithiation mechanism. The analytical modeling scheme successfully predicted the Li concentration profiles which agreed well with the experimental data (Figure 3b&3c). It is demonstrated that during discharge Li is removed by diffusion through the solid solution Li-Mg phase and this proceeds with $\beta \rightarrow \alpha$ phase transition and the associated phase boundary movement through the thickness of the electrode.

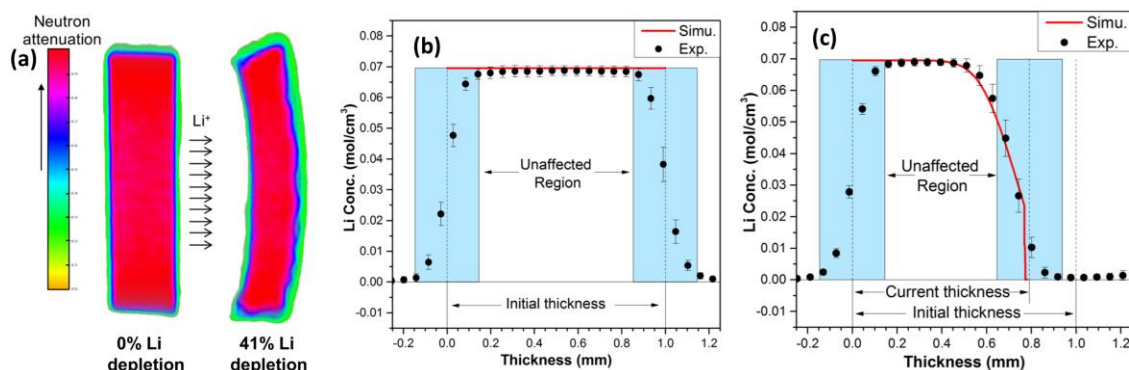


Figure 3 (a) Cross-sectional views of 3D reconstructed pseudo-color images of Mg-70 wt.% Li (~89 at.%) alloy at fresh and 41% Li depleted and (b,c) simulated versus experimental data for delithiation of Mg-70 wt.% Li (~89 at.%) alloy of fresh, 41% Li depletion.

III. Study of spatial distribution of Li in V₂O₅ electrode during lithiation

The distribution of Li in V₂O₅, one of the most commonly used cathodes in Li-ion batteries, was imaged using neutron tomography. Specifically, the effect of cycling rates (C/10, C/5) on the Li spatial distribution inside V₂O₅ cathode was investigated (Figure 4). A relatively higher cycling rate resulted in lesser Li insertion and the Li concentration in bulk is lower than that at lower C-rate. It was found that Li distribution inside V₂O₅ is not homogeneous. The piling up of Li occurred at the active surface during lithiation (Figure 4a & 4b) and in the inner bulk during delithiation (Figure 4c & 4d). Further, the Li distribution under C/10 is more homogeneous (Figure 4b) than that under C/5 (Figure 4a). The non-homogeneous distribution of Li in V₂O₅ could be due to lower diffusivity (10^{-12} - 10^{-13} cm²s⁻¹) of Li in V₂O₅. Our work established that neutron tomography is a powerful technique to study the spatial distribution of Li in energy storage materials.

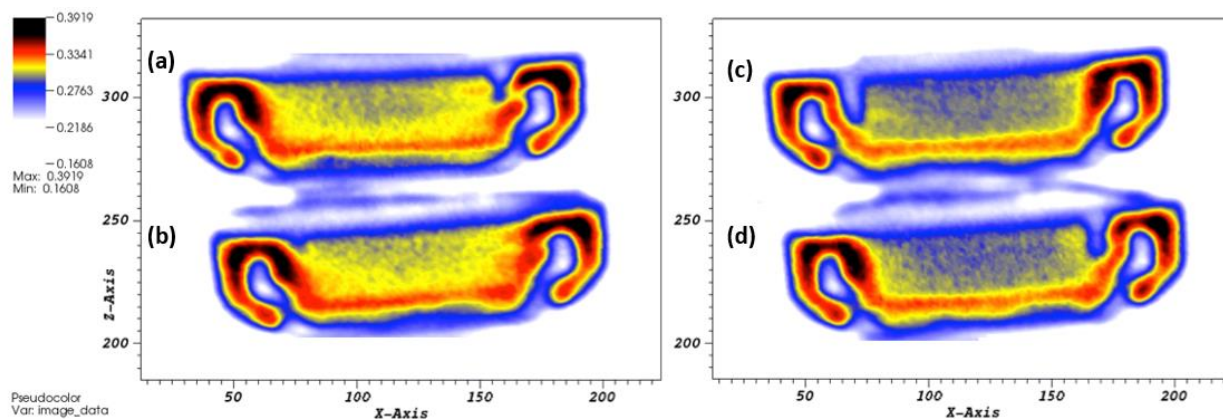


Figure 4. Cross-sectional pseudo-color plots obtained at the center of Li- V_2O_5 cell. (a) Lithiated V_2O_5 at C/5, (b) lithiated V_2O_5 at C/10, (c) delithiated V_2O_5 at C/5 and (d) delithiated V_2O_5 at C/10.

Future Plans

Mosaicity evolution during microcolumnar Si (100) electrode lithiation: The presence of mosaicity in crystal structure will be investigated in detail by studying the transmitted beam using additional detector. Specifically, the question of whether the reversibility in capacity is due to the reversibility in mosaicity will be resolved. Additionally, the effect of various pore morphologies on the performance of Li-ion batteries will be investigated. Electron microscopy of lithiated and delithiated microcolumnar Si (100) electrodes will be performed.

Bulk Li Distribution Study of Delithiated Mg(Li) Alloy Using Neutron Imaging: We have started to design a new *in-situ* electrochemical cell to study real time phase transitions in porous Mg(Li) alloys electrodes by neutron imaging using VENUS at SNS, ORNL. The higher flux at SNS would enable study of phase transitions at high C-rates. Additionally, Li distribution inside Mg(Li) electrodes can be extracted from the 3-D maps constructed due to the higher spatial resolution offered by VENUS. Specifically, the question of how diffusion of Li in Mg(Li) electrode affects cycleability will be addressed. The ultimate objective is to understand how the structure of Mg(Li) electrode affects phase transitions, so that high capacity electrodes, which can cycle for large number of cycles, can be designed.

References

1. B. Vadlamani, K. An, M. Jagannathan, K.S.Ravi Chandran, "A Novel In-situ Electrochemical Cell for Neutron Diffraction Studies of Phase Transitions in Small Volume Electrodes of Li-ion Batteries," *J. Electrochem. Soc.*, 161, A1731 (2014)
2. S.W. Lee, M.T. McDowell, J.W. Choi, Y. Cui, Anomalous shape changes of silicon nanopillars by electrochemical lithiation. *Nano Lett.* 11, 3034–3039 (2011)
3. M. Jagannathan and K. S. Ravi Chandran, "Electrochemical Charge/Discharge Behavior and Phase Transitions during Cell Cycling of Li(Mg) Alloy Anodes," *J. Electrochem. Soc.* 160 (10), pp. A1922-A1926, 2013

Publications from this Project

1. B. Vadlamani, K. An, M. Jagannathan, K.S.Ravi Chandran, "A Novel In-situ Electrochemical Cell for Neutron Diffraction Studies of Phase Transitions in Small Volume Electrodes of Li-ion Batteries," *J. Electrochem. Soc.*, 161, A1731 (2014)
2. M. Jagannathan and K. S. Ravi Chandran, "Analytical modeling and simulation of electrochemical charge/discharge behavior of Si electrodes in Li ion cells," *J. Power Sources*, Vol. 247, 2014, pp. 667-675
3. Y. Zhang, K. S. Ravi Chandran , M. Jagannathan, H. Z. Bilheux, J. C. Bilheux, "The Nature of Electrochemical Delithiation of Li-Mg Alloy Electrodes: Neutron Computed Tomography and Analytical Modeling of Li Diffusion and Delithiation Phenomenon", *J. Electrochem. Soc.* (Accepted for publication, 2016)
4. B. Vadlamani, K. S. Ravi Chandran, "High performance microporous Si (100) as electrode material for on-chip micro Li-ion batteries", *Nature* (manuscript in preparation)
5. Y. Zhang, K. S. Ravi Chandran , M. Jagannathan, H. Z. Bilheux, J. C. Bilheux, "Study of the Li Spatial Distribution inside V₂O₅ Cathode under Different Cycling Rates by Neutron Computed Tomography", *J. Electrochem. Soc.* (manuscript in preparation)
6. M. Jagannathan, B. Vadlamani and K. S. Ravi Chandran, "Energy Storage Capacity and Electrochemical Cyclability of Si Porous/Columnar Structures as Anodes for Li-ion Batteries", *J. Power Sources* (manuscript in preparation)

Multiphasic soft colloids: From fundamentals to application of energy sustainability

Wei-Ren Chen, *Oak Ridge National Laboratory, Oak Ridge, TN 37831*

Program Scope

Neutron scattering is an important component in the research projects supported by DOE-BES, *Multiphasic soft colloids: From fundamentals to application of energy sustainability* (ERKCSNJ). In this project neutron scattering is used in the study of the structure and dynamics of soft colloids to reveal the relationship between the dynamical processes, the structural evolution, and the molecular solvation of soft colloids. We develop new rigorous data analysis methods for neutron scattering experiments to characterize and understand these physical phenomena precisely. Neutron scattering experiments will also be compared with computer simulation results and theoretical predictions on novel materials such as Janus colloids and yolk-shell nanoparticles. Neutron scattering is the critical and major methodology in this project.

Recent Progress

1. Origin of Rheology in Interacting Colloidal Suspensions

Colloidal suspensions represent an important class of complex fluids commonly encountered in our daily lives. There has been much interest in understanding the flow behavior of colloids due to their crucial role in the transport of materials in a wide variety of biological phenomena and industrial applications. While the profound consequence of inter-particle interaction on rheological properties has been widely recognized, the microstructural basis through which the potential characteristics influence the macroscopic deformation behaviors has yet to be explored. Using small angle neutron scattering (SANS)

complemented by computer simulation and rheological measurements, we demonstrate that the rate-dependent flow behavior of a charge-stabilized colloidal suspension is a consequence of localized elastic response generated by particle interactions [1]. Based on the spherical harmonic

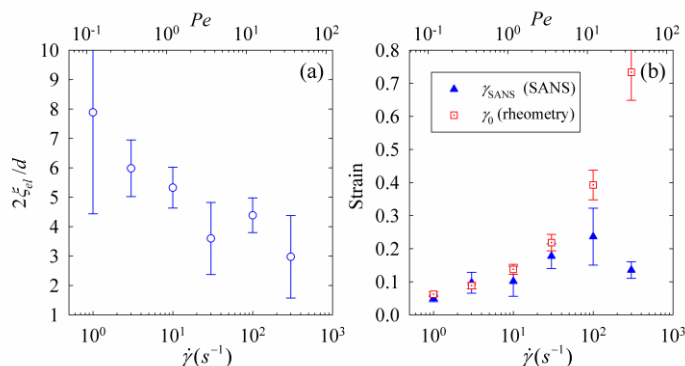


Fig. 1 Size of the time-averaged TEZ, $2\xi_{el}$, determined by the full width at half maximum (FWHM) of the TEZ. (b) The comparison between the strain at the scale of the microstructure revealed by SANS, γ_{SANS} , and macroscopic strain determined by rheological measurement of γ_0 . The fact that the macroscopically determined γ_0 is essentially identical to the microscopically determined γ_{SANS} again demonstrates the local elastic deformation indeed is the principal mechanism controlling the nonlinear rheology of charged colloidal suspensions.

expansion analysis of the 2D anisotropic scattering spectra, we show that these colloids under shear behave like an elastic solid at short distances but like a fluid at long distances. The short-lived, localized elastic region, the *transient elastic zone* (TEZ; Fig 1a), plays a crucial role in determining the observed rheological behaviors. This finding sheds new light on understanding the nature of nonlinear rheology of soft matters with strong interactions.

2. Fingerprinting Molecular Deformation of Entangled Polymers in Fast Flow

During the last several decades, the study of the dynamics of entangled polymers has been focusing on the application of the tube model. Despite the tremendous success of this theoretical

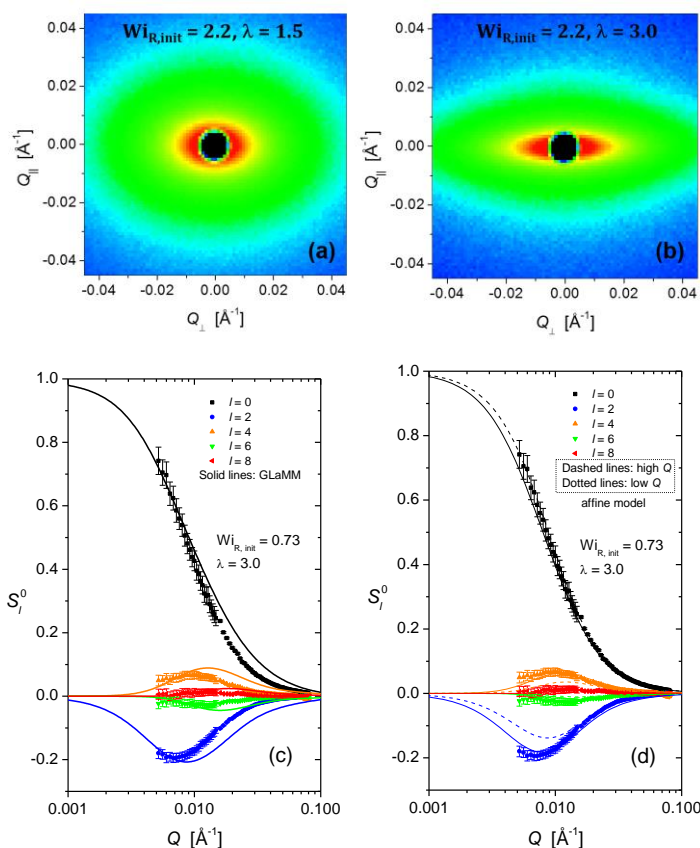


Figure 2. Representative 2D scattering pattern of uniaxially stretched PS melts: (a) $Wi_{R,init} = 2.2$ and $\lambda = 1.5$. (b) $Wi_{R,init} = 2.2$ and $\lambda = 3.0$. (c) and (d): experimental spherical harmonic expansion coefficients for $Wi_{R,init} = 0.73$ and $\lambda = 3.0$ and comparison with theoretical predictions.

approach, a key hypothesis of the tube model concerning nonlinear viscoelasticity has not been fully validated by experiments. Doi and Edwards proposed a unique elastic deformation mechanism to account for the nonlinear rheological behavior of entangled polymers [2]. This mechanism asserts that the external deformation acts on the tube, instead of the polymer chain. A direct consequence of this assumption is that the evolution of chain conformation of an entangled polymer in flow is *non-affine* beyond the Rouse time, with entanglement strands being oriented but hardly stretched. This hypothesis, being a keystone of the tube model, stands in stark contrast to the elastic deformation mechanisms of other alternative theoretical approaches where the *affine* deformation mechanism is adopted. We have recently developed a new approach based on spherical harmonic expansion of

the 2D anisotropic scattering pattern [Fig. 2(a) and 2(b)] to elucidate the molecular deformation mechanism of entangled polymers by SANS [3]. This development makes it possible to unambiguously examine the deformation mechanism predicted by statistical and molecular models of entangled polymers at the microscopic level. Our SANS measurements on uniaxially stretched polystyrene melts show that neither the tube model nor the affine model could provide

a satisfactory description of the Q -dependent spherical harmonic expansion coefficients determined from experiments. The tube model significantly overestimates the deformation anisotropy (Fig. 2c). The failure of the tube model is a direct consequence of its non-affine deformation hypothesis: Rouse retraction within an affinely-deformed tube. On the other hand, the affine model only works in a limited Q range, and there is a gradual loss of “affineness” going from large to small length scales.

3. Development of New Universal Rheo-SANS Shear Cell for Multiple-Plane Measurement

The Couette cells with concentric cylinders have been developed for generating steady shear for *in-situ* rheo-SANS structural investigations. However, the experimental implementation is compounded by the intrinsic limitations of the cells. For example, it has been recognized that the microstructure projected in the flow-velocity gradient (1-2) plane is most

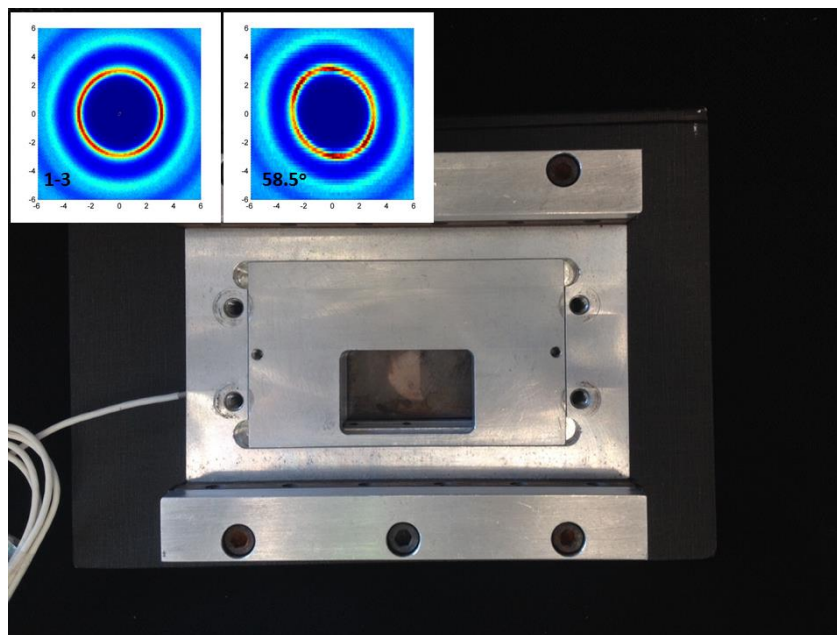


Fig. 3 The shear cell based on the parallel plate geometry. The insets give the simulated spectra on 1-3 plane and the plane with tilt angle of 58.3° relative to the flow direction. Given the spectra of 1-3 plane as a reference, the structural information from 1-2 plane can certainly be extracted from the spectra of the tilted plane.

relevant for understanding the connection between shear and time-dependent viscosity. To minimize the effect of non-flowing regions or “dead zones” on this plane, the path length of the neutrons along the incident direction of vorticity (3) is designed to be at least 5 mm. To avoid coherent multiple scattering, the scattering length density of the solvent has to be nearly identical to that of the suspending colloids and polymers. Inevitably, the coherent scattering power is severely reduced by this adjustment of contrast. As a result so far only the D22 SANS diffractometer at ILL can provide sufficient flux allowing for quantitative structural investigation of soft matter subject to steady shear. We have developed a parallel plate shear cell (Fig. 3) to bypass this constraint. The incident neutron beam is perpendicular to the flow-vorticity (1-3) plane with a path length of 1 mm. The plates can be tilted around the flow direction, therefore allowing this design to investigate the structural distortion projected on the 1-2 plane. Because the path length is 1 mm, the contrast between the solvent and the particles can be greatly enhanced. We have also developed the theoretical framework to compartmentalize the structural information of 1-2 and 1-3 planes from the collected information from the tilted plane [4]. Its feasibility has been demonstrated by analyzing the data of nonequilibrium simulations (insets of

Fig. 3) [4]. The availability of this cell will greatly facilitate the relevant studies with satisfactory signal-to-noise ratios using the currently available neutron scattering facilities in the US.

Future Plans

Having established the theoretical basis for structural analysis of nonequilibrium materials and demonstrated its viability by elucidating the microscopic deformation mechanism of sheared colloids and stretched polymers synergistically using scattering, statistical mechanics, and simulation, we plan to proceed further to address the critical connections between the macroscopic rheological behaviors and structural and dynamical evolutions at the microscopic level in flowing soft matter based on the methodology developed in the past two years. We will extend the current structural study to the dynamical regime. From the anisotropy of the elastic and inelastic scattering spectra collected from the mechanically perturbed soft materials, we will address this crucial link through the following three key aspects:

- [1] *The affineness problem*: How can one distinguish affine and non-affine deformation at the particle/molecular level?
- [2] *The symmetry problem*: how can one distinguish different molecular relaxation/deformation mechanisms based on their symmetry in spherical harmonic expansion analysis?
- [3] *The heterogeneity problem*: how can one identify the “*heterogeneity*” in structure, elasticity, and dynamics in particle/molecular deformation?

This approach directly addresses the rheological behavior of flowing soft materials from the micromechanical perspective and will provide new theoretical ingredients for the development of first-principle constitutive equations for general soft matter systems.

References

1. W.-R. Chen, T. Iwashita, L. Porcar, Z. Wang, Y. Wang, Y. Liu, L. E. Sánchez-Díaz, W. A. Hamilton and T. Egami, “Origin of Nonlinear Rheology in Interacting Colloidal Suspensions”, *Science Advances* (2016) Under Review. Manuscript available from arXiv:1611.03135 [cond-mat.soft].
2. M. Doi and S. F. Edwards, “The Theory of Polymer Dynamics” Oxford University Press, 1986.
3. Y. Wang, W.-R. Chen, L. Porcar, Z. Wang and Y. Liu, “Molecular Deformation Mechanism of Entangled Polymers in Fast Flow as Revealed by Small-Angle Neutron Scattering”, *Phys. Rev. Lett.* (2016) Under Review.
4. B. Wu, Y. Wang, Z. Wang and W.-R. Chen, “Mathematical Basis for the Analysis of Shear-Induced Anisotropic Small Angle Scattering Spectra of Soft Matter Subject to Steady Shear”, *J. Appl. Cryst.* (2016) Under Review.

Publications [FY14 (July)-16 (December)]

- P1. *A Scattering Function from Star Polymers Including Excluded Volume Effects*, X. Li, C. Do, Y. Liu, L. E. Sánchez-Díaz, K. Hong, G. S. Smith, and W.-R. Chen, *J. Appl. Cryst.* **47**,1901-1905 (2014).
- P2. *Dynamical Threshold of Diluteness of Soft Colloids*, X. Li, L. E. Sánchez-Díaz, B. Wu, W. A. Hamilton, L. Porcar, P. Falus, Y. Liu, C. Do, G. S. Smith, T. Egami, and W.-R. Chen, *ACS Macro Lett.* **3** 1271-1275 (2014).
- P3. *Phase behavior under a non- centrosymmetric interaction: shifted charge colloids investigated by Monte Carlo Simulation*, L. E. Sánchez-Díaz, C.-Y. Shew, X. Li, B. Wu, G. S. Smith, and W.-R. Chen, *J. Phys. Chem. B* 2014, **118** 6963–6971.
- P4. *Scattering from Colloid-Polymer Conjugates with Excluded Volume Effect* X. Li, C. N. Lam, L. E. Sánchez-Díaz, G. S. Smith, B. D. Olsen, and W.-R. Chen, *ACS Macro Lett.* **4** 165-170 (2015).
- P5. *The Shape of Protein-Polymer Conjugates in Dilute Solution* C. N. Lam, D. Chang, M. Wang, W.-R. Chen and B. D. Olsen, *J. Polym. Sci. A Polym. Chem.* **2** 292-302 2015.
- P6. *Origin of Nonlinear Rheology in Interacting Colloidal Suspensions* W.-R. Chen, T. Iwashita, L. Porcar, Z. Wang, Y. Wang, Y. Liu, L. E. Sánchez-Díaz, W. A. Hamilton and T. Egami, *Science Advances* (2016) Under Review. Manuscript available from arXiv:1611.03135 [cond-mat.soft].
- P7. *Molecular Deformation Mechanism of Entangled Polymers in Fast Flow as Revealed by Small-Angle Neutron Scattering* Y. Wang, W.-R. Chen, L. Porcar, Z. Wang and Y. Liu, *Phys. Rev. Lett.* (2016) Under Review
- P8. *Mathematical Basis for the Analysis of Shear-Induced Anisotropic Small Angle Scattering Spectra of Soft Matter Subject to Steady Shear* B. Wu, Y. Wang, Z. Wang and W.-R. Chen, *J. Appl. Cryst.* (2016) Under Review.

Magnetoelastic coupling and nonreciprocal effects in polar, chiral, and ferroaxial magnets: neutron and optical studies

S.-W. Cheong (Rutgers Univ.), V. Kiryukhin (Rutgers Univ.), and A. Sirenko (NJIT)

Program Scope

Physical systems with reduced symmetry often exhibit richer physics than their high-symmetry counterparts. In this project, non-reciprocal and nontrivial magnetoelastic effects are investigated in low-symmetry magnetic compounds utilizing inelastic neutron scattering, advanced crystal growth, and Muller matrix spectroscopic ellipsometry. The focus is on studies of polar magnets, magnets with structural chirality, and ferroaxial magnets, such as polar $(\text{Fe,Mn,Co,Ni})_2\text{Mo}_3\text{O}_8$, chiral Fe langasite, polar & chiral Ni_3TeO_6 , and polar & chiral MnSb_2O_6 . In these systems, combination of absent inversion, time-reversal, and mirror symmetries leads to non-reciprocal effects revealed, for example, in non-equivalent magnon/electromagnon spectra for $+Q$ and $-Q$, and as directional dichroism in the far-IR optical spectra. Magnons, electromagnons, crystal field transitions, and optical phonons provide the main contributions to the expected non-reciprocal effects, as well as to dynamic magnetoelectricity. Growth of high-quality monodomain single crystals is crucial for studies of nonreciprocal and magnetoelectric effects. Combined neutron and optical studies are utilized to reveal the physical mechanisms of the magnetoelectric or magnetoelastic coupling in low-symmetry magnets. The goals of the project include understanding the exotic nonreciprocal properties of such systems, and identification of prospective magnets for novel device concepts.

Recent Progress

High-quality single crystals of several low-symmetry magnets, including MnSb_2O_6 , $(\text{Fe,Mn,Co,Ni})_2\text{Mo}_3\text{O}_8$, $\text{Ba}_3\text{NbFe}_3\text{Si}_2\text{O}_{14}$ (iron langasite), BiFeO_3 , and Cu_2OSeO_3 were grown using various methods, including the new laser-diode-heated floating zone technique. The prospective functional properties of these compounds have been identified using laboratory probes, neutron scattering, and optical spectroscopy. In particular we demonstrated: non-trivial magnetoelectric effect in monodomain Fe-langasite single crystals [1], giant non-hysteretic magnetoelectricity in $\text{Fe}_2\text{Mo}_3\text{O}_8$ [2],

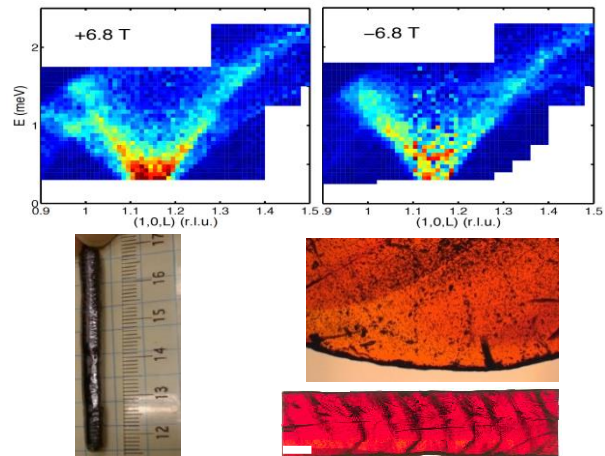


FIG. 1 Top: INS spectra of nonreciprocal magnons in iron langasite in an applied magnetic field: $S(H) \neq S(-H)$. Bottom: langasite single crystal, with the cross sections indicating high crystal quality.

nonreciprocal optical diode effect of spin waves in BiFeO_3 at room temperature [3], and the complex non-collinear magnetic structure in the polar magnet MnSb_2O_6 with the chiral lattice structure [4]. These observations open various opportunities for the discovery and study of nonreciprocal spin-wave effects using inelastic neutron scattering (INS) and spectroscopic ellipsometry. As an example, our very recent INS investigations have identified such effects in the iron langasite, in which spin wave spectra look very different in magnetic fields of the same magnitude, but applied in the opposite directions along the chiral axis of the crystal structure, see Fig 1. Further neutron and optical studies of low-symmetry magnets are currently in progress.

Reduced lattice symmetry often gives rise to new pathways for coupling magnetism to the crystal lattice, resulting in enhanced magnetoelectric (ME) effects. In our studies, we have concentrated on two questions: whether new physical effects could be realized in the low-symmetry systems, and how the largest possible ME responses could be achieved. Several compound families were studied. Hexagonal ABO_3 (A is rare earth, B is transition metal) combine ferroelectricity with two triangular lattices of magnetic ions. The complex interplay between these subsystems could result in enhanced functional properties. These properties are often mediated by the dynamic ME coupling realized, for instance, in the form of hybrid ME excitations (electromagnons). We have studied several compound families with strong electromagnon modes. In addition to the hexagonal ABO_3 systems, orthorhombic ferrites RFeO_3 (R is rare earth) turned out to be another interesting compound exhibiting emergent phenomena due to a significant interplay between two R-Fe magnetic subsystems.

We have stabilized the hexagonal phase of LuFeO_3 by Mn and Sc doping, and studied its magnetic and ME properties by neutron diffraction and magnetometry [5]. We have found that this compound is a rare example of a ferroelectric with weak ferromagnetism, in which the net magnetic moment is potentially controllable by an electric field at temperatures as high as 172 K.

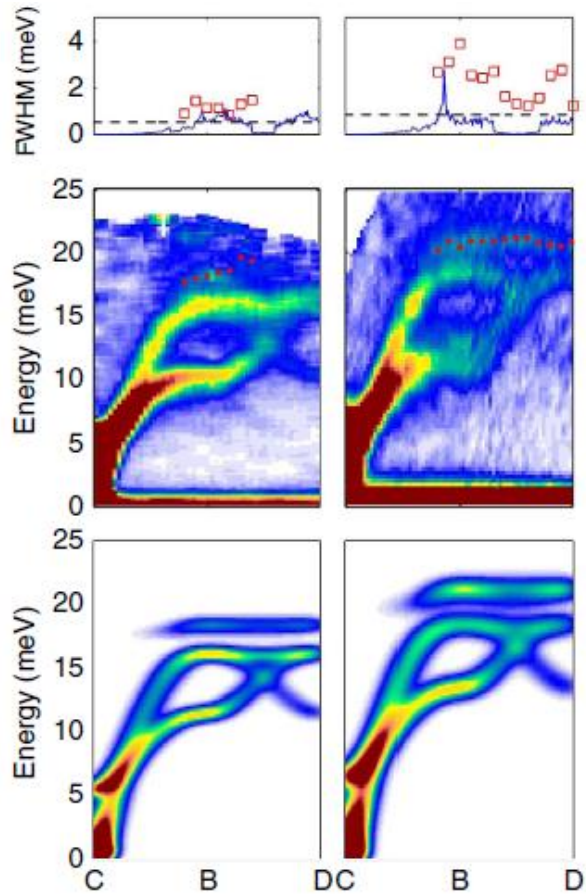


FIG. 2 Neutron-scattering data along the CBD direction (middle) and the calculated dynamical structure factor within the linear spin wave theory (bottom). Observed linewidth broadening of the top mode (square) together with the calculated result from the $1/S$ approximation (line) and the experimental resolution (dashed line) (top) for YMnO_3 (left) and LuMnO_3 (right) [7].

Based on these results, we proposed a mechanism by which room-temperature multiferroicity could be achieved in this compound class.

Previously, we have demonstrated that even though the spin wave picture is generally accepted to hold for high-spin Heisenberg systems, it fails for triangular magnetic lattices, such as that in LuMnO_3 [6]. Magnons and phonons are fundamental quasiparticles in a solid and can be coupled together to form a hybrid quasi-particle. However, detailed experimental studies on the underlying Hamiltonian of this particle are rare for actual materials. Moreover, the anharmonicity of such magnetoelastic excitations remains largely unexplored. We have shown that in non-collinear antiferromagnets, a strong magnon–phonon coupling can significantly enhance the anharmonicity, resulting in the creation of magnetoelastic excitations and their spontaneous decay. By measuring the spin waves over the full Brillouin zone using INS, and carrying out anharmonic spin wave calculations using a Hamiltonian with an explicit magnon–phonon coupling, we have identified a hybrid magnetoelastic mode in $(\text{Y,Lu})\text{MnO}_3$ and quantified its anomalous decay rate and the exchange-striction coupling term required to produce it, see Fig 2 [7].

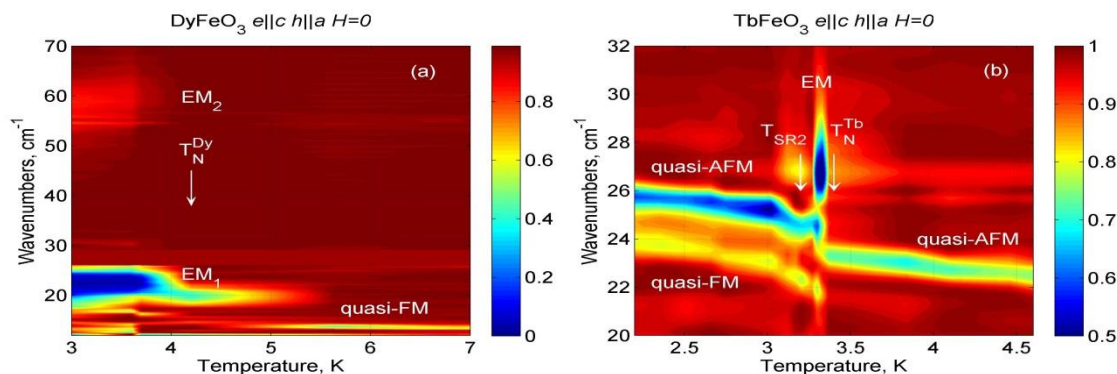


FIG. 3 Spectra of magnetic excitations in (a) DyFeO_3 and (b) TbFeO_3 . The absorption lines correspond to quasi-AFM, quasi-FM and electromagnon (EM) modes. Spin order and reorientation transitions are marked with arrows.

Inelastic neutron experiments are typically time-consuming. To complement neutron experiments by studying fundamental excitations in a larger number of compounds, we used our Mueller matrix ellipsometry and optical transition polarimetry at Brookhaven National Lab. Optical properties of multiferroic orthoferrites $R\text{FeO}_3$ ($R=\text{Tb}$ and Dy) were studied using synchrotron radiation in the far-IR range (10 to 2000 cm^{-1}) and low temperatures (1.5 K to 300 K) [8]. Magnetic properties of $R\text{FeO}_3$ are due to interplay of two magnetic subsystems: R^{3+} and Fe^{3+} . Spectra of quasi-AFM and quasi-FM magnons, electromagnons, and optical phonons have been investigated and described in terms of the temperature and field dependencies of their frequency, damping, and oscillator strength. Below the magnetic ordering of R^{3+} spins $T_N(R^{3+})$, which is at about 4 K in $R\text{FeO}_3$, we observed hardening of the magnon frequencies and modification of the selection rules for quasi-AFM and quasi-FM magnons, which change according to the modified magnetic symmetry of the $R^{3+}\text{--Fe}^{3+}$ system. In TbFeO_3 , the quasi-AFM magnon gains electric-dipole activity below $T_N(\text{Tb})$ and behaves as a hybrid, i.e. both electro- and magnetic-dipole active, mode. In addition to quasi-AFM and quasi-FM magnons in $R\text{FeO}_3$, we discovered electromagnons

which are electric-dipole active along the c -axis, see Fig 3. The oscillator strength of electromagnon in DyFeO₃ at 20 cm⁻¹ provides a significant contribution of about 50% to the static magnetodielectric effect $\Delta\epsilon(H)$. In contrast, the electromagnon in TbFeO₃ at 27 cm⁻¹ has a much weaker strength. Remarkably, it appears only in a very narrow temperature range of 2.7 – 3.3 K at $H=0$ and in a narrow range of magnetic fields of 2.4 – 2.7 T along the b -axis at $T=1.5$ K. These investigations identify the hybrid excitations for the future inelastic neutron scattering studies in the full range of the wave vector transfer.

Future Plans

Inelastic neutron scattering studies of the reduced-symmetry compounds with expected non-reciprocal spin-wave effects: Ba₃NbFe₃Si₂O₁₄ (continuation), MnSb₂O₆, BiFeO₃, and Cu₂OSeO₃. Continuing sample-growth optimization. Quick monitoring of the most promising excitations for the INS studies by optical spectroscopy for the maximum project efficiency. Investigation of the observed nonreciprocal spin waves using optical techniques. Determination of the possible role of the spin-lattice coupling (hybrid nature) in these excitations using polarized neutron scattering, and Muller matrix spectroscopic ellipsometry.

References

- [1] Nara Lee, et al., “*Magnetic control of ferroelectric polarization in a self-formed single magnetoelectric domain of multiferroic Ba₃NbFe₃Si₂O₁₄*”, Appl. Phys. Lett. **104**, 072904 (2014).
- [2] Yazhong Wang, et al., “*Unveiling hidden ferrimagnetism and giant magnetoelectricity in polar magnet Fe₂Mo₃O₈*”, Sci. Rep. **5**, 12268 (2015).
- [3] I. Kézsmárki, et al., “*Optical Diode Effect at Spin-Wave Excitations of the Room-Temperature Multiferroic BiFeO₃*”, Phys. Rev. Lett. **115**, 127203 (2015).
- [4] R. D. Johnson, et al., *MnSb₂O₆: “A Polar Magnet with a Chiral Crystal Structure”*, Phys. Rev. Lett. **111**, 017202 (2013).
- [5] Steven M. Disseler, et al., “*Multiferroicity in doped hexagonal LuFeO₃*”, Phys. Rev. B **92**, 054435 (2015).
- [6] Joosung Oh, et al., “*Magnon Breakdown in a Two Dimensional Triangular Lattice Heisenberg Antiferromagnet of Multiferroic LuMnO₃*”, Phys. Rev. Lett. **111**, 257202 (2013).
- [7] Joosung Oh et al., “*Spontaneous decays of magneto-elastic excitations in non-collinear antiferromagnet (Y,Lu)MnO₃*”, Nature Commun. **7**, 13146, doi: 10.1038/ncomms13146 (2016).
- [8] T. N. Stanislavchuk, et al., “*Magnon and electromagnon excitations in multiferroic DyFeO₃*”, Phys. Rev. B **93**, 094403 (2016).

Publications

- [1] Barbour, A., Alatas, A., Liu, Y., Zhu, C., Leu, B. M., Zhang, X., Sandy, A., Pierce, M. S., Wang, X., Cheong, S.-W. & You, H., “*Partial glass isosymmetry transition in multiferroic hexagonal $ErMnO_3$* ”. Phys. Rev. B 93, 054113 (2016)
- [2] Senn, M. S., Murray, C. A., Luo, X., Wang, L.H., Huang, F.-T., Cheong, S.-W., Bombardi, A., Ablitt, C., Mostofi, A. A. & Bristowe, N. C., “*Symmetry switching of negative thermal expansion by chemical control*”. J. Am. Soc. Chem. 138, 5479 (2016)
- [3] Stock, C., Rodriguez, E. E., Lee, N., Green, M. A., Demmel, F., Ewings, R. A., Fouquet, P., Laver, M., Niedermayer, C., Su, Y., Nemkovski, K., Rodriguez-Rivera, J. A. & Cheong, S.-W. “*Solitary magnons in the $S=5/2$ antiferromagnet $CaFe_2O_4$* .” Phys. Rev. Lett. 117, 017201 (2016)
- [4] Oh, J., Le, M. D., Nahm, H. H., Sim, H., Jeong, J., Perring, T. G. Woo, H., Nakajima, K., Ohira-Kawamura, S., Yamani, Z., Yoshida, Y., Eisaki, H., Cheong, S.-W., Chernyshev, A. L. & Park, J. G. “*Spontaneous decays of magneto-elastic excitations in non-collinear antiferromagnet $(Y,Lu)MnO_3$* ”. Nature Commun. 7, 13146 (2016)
- [5] Stanislavchuk, T. N., Wang, Y., Janssen, Y., Carr, G. L., Cheong, S.-W. & Sirenko, A. A. “*Magnon and electromagnon excitations in multiferroic $DyFeO_3$* ”. Phys. Rev. B 93, 094403 (2016).
- [6] W. Ratcliff, J.W. Lynn, V. Kiryukhin, P. Jain, M.R. Fitzsimmons, “*Magnetic structures and dynamics of multiferroic systems obtained with neutron scattering*”, npj Quantum Materials **1**, 16003 (2016), doi:10.138/npjquantmats.2016.3
- [7] Yazhong Wang, Gheorghe L. Pascut, Bin Gao, Trevor A. Tyson, Kristjan Haule, Valery Kiryukhin & Sang-Wook Cheong, “*Unveiling hidden ferrimagnetism and giant magnetoelectricity in polar magnet $Fe_2Mo_3O_8$* ”, Sci. Rep. **5**, 12268 (2015).
- [8] Xiang-Bai Chen, Nguyen Thi Minh Hien, Kiok Han, Ji-Yeon Nam, Nguyen Thi Huyen, Seong-II Shin, Xueyun Wang, S. W. Cheong, D. Lee, T. W. Noh, N. H. Sung, B. K. Cho & In-Sang Yang, “*Study of spin-ordering and spin-reorientation transitions in hexagonal manganites through Raman spectroscopy*”, Sci. Rep. **5**, 13366 (2015).
- [9] J. Lee, S. A. Trugman, C. L. Zhang, D. Talbayev, X. S. Xu, S.-W. Cheong, D. A. Yarotski, A. J. Taylor, and R. P. Prasankumar, “*The influence of charge and magnetic order on polaron and acoustic phonon dynamics in $LuFe_2O_4$* ”, Appl. Phys. Lett. **107**, 042906 (2015).
- [10] M. S. Senn, A. Bombardi, C. A. Murray, C. Vecchini, A. Scherillo, X. Luo, and S. W. Cheong, “*Negative Thermal Expansion in Hybrid Improper Ferroelectric Ruddlesden-Popper Perovskites by Symmetry Trapping*” Phys. Rev. Lett. **114**, 035701 (2015).

- [11] I. Kézsmárki, U. Nagel, S. Bordács, R. S. Fishman, J. H. Lee, Hee Taek Yi, S.-W. Cheong, and T. Rõdm, “*Optical Diode Effect at Spin-Wave Excitations of the Room-Temperature Multiferroic BiFeO₃*”, Phys. Rev. Lett. **115**, 127203 (2015).
- [12] P. Chen, B. S. Holinsworth, K. R. O’Neal, T. V. Brinzari, D. Mazumdar, C. V. Topping, X. Luo, S.-W. Cheong, J. Singleton, S. McGill, and J. L. Musfeldt, “*Magnetochromic effect in multiferroic RIn_{1-x}Mn_xO₃ (R = Tb, Dy)*”, Phys. Rev. B **91**, 205130 (2015).
- [13] D. Talbayev, Jinho Lee, S. A. Trugman, C. L. Zhang, S.-W. Cheong, R. D. Averitt, A. J. Taylor, and R. P. Prasankumar, “*Spin-dependent polaron formation dynamics in Eu_{0.75}Y_{0.25}MnO₃ probed by femtosecond pump-probe spectroscopy*”, Phys. Rev. B **91**, 064420 (2015).
- [14] Steven M. Disseler, Xuan Luo, Bin Gao, Yoon Seok Oh, Rongwei Hu, Yazhong Wang, Dylan Quintana, Alexander Zhang, Qingzhen Huang, June Lau, Rick Paul, Jeffrey W. Lynn, Sang-Wook Cheong, and William Ratchiff II, “*Multiferroicity in doped hexagonal LuFeO₃*”, Phys. Rev. B **92**, 054435 (2015).
- [15] T. N. Stanislavchuk, A. P. Litvinchuk, Rongwei Hu, Young Hun Jeon, Sung Dae Ji, S.-W. Cheong, and A. A. Sirenko, “*Optical properties, lattice dynamics, and structural phase transition in hexagonal 2H-BaMnO₃ single crystals*,” Phys. Rev. B **92**, 134308 (2015).
- [16] M. N. Popova, K. N. Boldyrev, S. A. Klimin, T. N. Stanislavchuk, A. A. Sirenko, and L. N. Bezmaternykh, “*Spectral signatures of spin–phonon and electron–phonon interactions in multiferroic iron borates*”, Journal of Magnetism and Magnetic Materials **383**, 250–254 (2015).
- [17] S.-Z. Lin, X. Wang, Y. Kamiya, G.-W. Chern, F. Fan, D. Fan, B. Casas, Y. Liu, V. Kiryukhin, W.H. Zurek, C.D. Batista, S.-W. Cheong, “*Topological defects as relics of emergent continuous symmetry and Higgs condensation of disorder in ferroelectrics*”, Nature Physics **10**, 970 (2014).
- [18] J. W. Kim, S. Khim, S. H. Chun, Y. Jo, L. Balicas, H. T. Yi, S.-W. Cheong, N. Harrison, C. D. Batista, J. H. Han and K. H. Kim, “*Manifestation of magnetic quantum fluctuations in the dielectric properties of a multiferroic*”, Nature Communication **5**, 4419 (2014).
- [19] Q.-C. Sun, Xiaoxiang Xi, X. Wang, N. Lee, D. Mazumdar, R. J. Smith, G. L. Carr, S.-W. Cheong, and J. L. Musfeldt, “*Spectroscopic signatures of domain walls in hexagonal ErMnO₃*”, Phys. Rev. B **90**, 121303 (2014).
- [20] J. Jeong, M. Duc Le, P. Bourges, S. Petit, S. Furukawa, S.-A. Kim, S. Lee, S-W. Cheong, and J.-G. Park, “*Temperature-dependent interplay of Dzyaloshinskii-Moriya interaction and single-ion anisotropy in multiferroic BiFeO₃*”, Phys. Rev. Lett. **113**, 107202 (2014).
- [21] A. B. Sushkov, Ch. Kant, M. Schiebl, A. M. Shuvaev, Anna Pimenov, Andrei Pimenov, Bernd Lorenz, S. Park, S.-W. Cheong, Maxim Mostovoy, and H. D. Drew, “*Spectral origin of the colossal magnetodielectric effect in multiferroic DyMn₂O₅*”, Phys. Rev. B **90**, 054417 (2014).

[22] K. N. Boldyrev, T. N. Stanislavchuk, A. A. Sirenko, L. N. Bezmaternykh, and M. N. Popova, "*Coupling between phonon and crystal-field excitations in multiferroic $\text{PrFe}_3(\text{BO}_3)_4$* ", Phys. Rev. B **90**, 121101(R) (2014).

[23] R. Basistyy, T. N. Stanislavchuk, A. A. Sirenko, A. P. Litvinchuk, M. Kotelyanskii, G. L. Carr, N. Lee, X. Wang, and S.-W. Cheong, "*Infrared-active optical phonons and magnetic excitations in the hexagonal manganites RMnO_3 ($R = \text{Ho, Er, Tm, Yb, and Lu}$)*", Phys. Rev. B **90**, 024307 (2014).

USING NEUTRON AS A PROBE TO STUDY MAGNETIC EXCITATIONS IN STRONGLY CORRELATED ELECTRON MATERIALS

Pengcheng Dai

Department of Physics and Astronomy

Rice University

Houston, Texas 77005

Program Scope

This DOE project addresses the fundamental physical processes that give rise to novel collective phenomena such as high-transition temperature superconductivity. The materials known to exhibit these collective phenomena are the strongly correlated electron materials. The understanding of these phenomena will not only enhance our knowledge of basic science, but also gives us the ability to design materials with novel and predictable properties. Specifically, the experimental program integrates neutron scattering experiments with lab based materials efforts, aimed at the fundamental understanding of the spin excitations in NaFeAs family of iron based superconductors. The objective of the program is to explore and understand the microscopic origins of various phases of iron-based high- T_c superconductors using neutron as a probe. Neutron scattering experiments will be performed mostly at the high-flux isotope reactor (HFIR) and Spallation Neutron Source (SNS) at the Oak Ridge National Laboratory. However, the project will also utilize other world-class facilities in the U.S. and Europe when similar capabilities are unavailable at HFIR and SNS. The impact of this research program will include the training of the next generation of neutron scatterers and elucidating the nature of the exotic properties of the correlated electron materials.

Recent Progress

Our primary research efforts are divided into two parts: (1) a strong materials synthesis program focusing on growing large single crystals of known materials; and (2) a neutron scattering program utilizing the most innovative and sophisticated neutron scattering facilities around the world to study the interplay between magnetism and superconductivity in iron-based and heavy Fermion superconductors.

For current DOE supported neutron scattering program, we focus on studying the interplay between magnetism and superconductivity in Co-doped NaFeAs/LiFeAs (see our publication record) and hole-doped $\text{Ba}_{1-x}\text{K}_x\text{Fe}_2\text{As}_2$. Our work has established the basic experimental facts concerning the evolution of spin excitations in the electron-doped NaFeAs, LiFeAs, $\text{BaFe}_{2-x}\text{Ni}_x\text{As}_2$ and hole-doped $\text{Ba}_{1-x}\text{K}_x\text{Fe}_2\text{As}_2$ iron pinictides, and has made significant impact in the condensed matter physics community as summarized in the review article (1). Here we choose three recent work to highlight the progress we made over the past two years.

Highlight #1: Antiferromagnetic order and spin dynamics in iron-based superconductors:

High-transition temperature (high- T_c) superconductivity in the iron pnictides or chalcogenides emerges from the suppression of the static antiferromagnetic order in their parent compounds, similar to copper oxide superconductors. This raises a fundamental question concerning the role of magnetism in the superconductivity of these materials. Neutron scattering, a powerful probe to study the magnetic order and spin dynamics, plays an essential role in determining the relationship between magnetism and superconductivity in high- T_c superconductors. The rapid development of modern neutron time-of-flight spectrometers allows a direct determination of the spin dynamical properties of iron-based superconductors throughout the entire Brillouin zone. In this paper, an overview is presented of the neutron scattering results on iron-based superconductors, focusing on the evolution of spin-excitation spectra as a function of electron and hole doping and isoelectronic substitution. Spin dynamical properties of iron-based superconductors are compared with those of copper oxide and heavy fermion superconductors and the common features of spin excitations in these three families of unconventional superconductors and their relationship with superconductivity are discussed (1).

Highlight #2: Robust upward dispersion of the neutron spin resonance in the heavy Fermion superconductor $Ce_{1-x}Yb_xCoIn_5$: The neutron spin resonance is a collective magnetic excitation that appears in the unconventional copper oxide, iron pnictide and heavy fermion superconductors. Although the resonance is commonly associated with a spin-exciton due to the d (s_{\pm})-wave

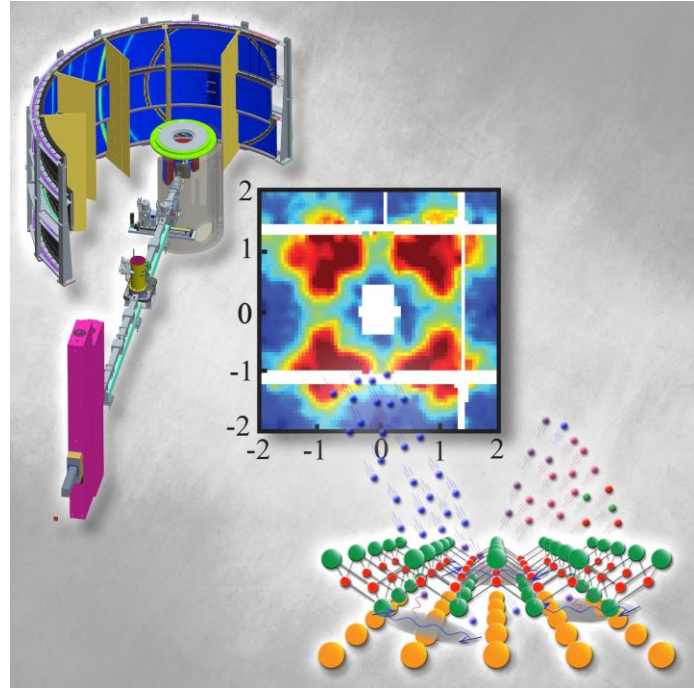


Fig. 1 Schematic diagrams of neutron scattering geometry using spallation neutron source, neutron scattering data from NaFeAs, and real lattice picture.

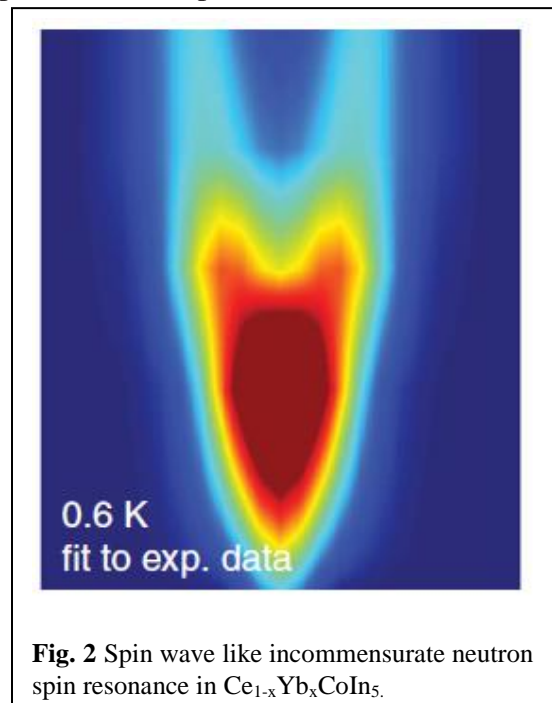


Fig. 2 Spin wave like incommensurate neutron spin resonance in $Ce_{1-x}Yb_xCoIn_5$.

symmetry of the superconducting order parameter, it has also been proposed to be a magnon-like excitation appearing in the superconducting state. Here we use INS to demonstrate that the resonance in the heavy fermion superconductor $\text{Ce}_{1-x}\text{Yb}_x\text{CoIn}_5$ with $x = 0, 0.05$ and 0.3 has a ring-like upward dispersion that is robust against Yb-doping. By comparing our experimental data with a random phase approximation calculation using the electronic structure and the momentum dependence of the $d_{x^2-y^2}$ -wave superconducting gap determined from scanning tunnelling microscopy (STM) for CeCoIn_5 , we conclude that the robust upward-dispersing resonance mode in $\text{Ce}_{1-x}\text{Yb}_x\text{CoIn}_5$ is inconsistent with the downward dispersion predicted within the spin-exciton scenario (Fig. 2) (2).

Highlight #3: A Mott insulator continuously connected to iron pnictide superconductors:

Iron-based superconductivity develops near an AF order and out of a bad metal normal state, which has been interpreted as originating from a proximate Mott transition. Whether an actual Mott insulator can be realized in the phase diagram of the iron pnictides remains an open question. Clarifying it is important to the understanding of whether superconductivity arises from strong electron correlations or originates from a nesting of Fermi surfaces. Here we use transport, transmission electron microscopy, X-ray absorption spectroscopy, and neutron scattering to demonstrate that $\text{NaFe}_{1-x}\text{Cu}_x\text{As}$ near $x \sim 0.5$ exhibits real space Fe and Cu ordering, and are AF insulators with the insulating behavior that persists above the Néel temperature, indicative of a Mott insulator. Further, when x approaches 0.5, we find strong evidence of Cu being in a non-magnetic $3d^{10}$ state while Fe configuration moves toward $3d^5$. Upon decreasing x from 0.5, the AF ordered moment continuously decreases, yielding to superconductivity around $x = 0.05$. Our discovery of a Mott insulating state in $\text{NaFe}_{1-x}\text{Cu}_x\text{As}$ thus makes it the only known Fe-based material in which superconductivity can be smoothly connected to the Mott insulating state, highlighting the important role of electron correlations in the high- T_c superconductivity (Fig. 3) (3).

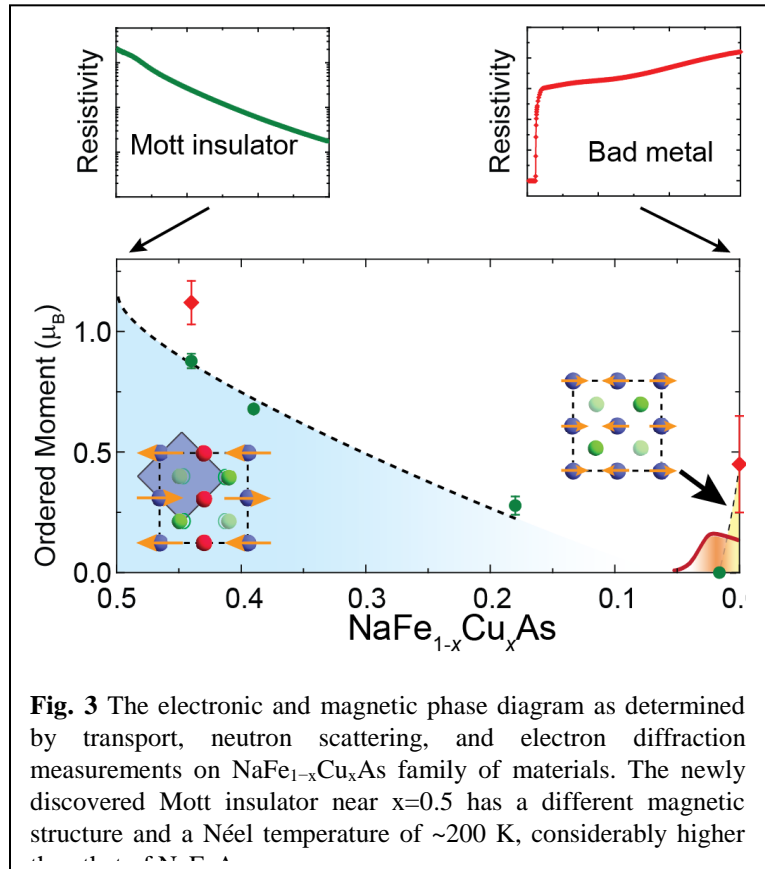


Fig. 3 The electronic and magnetic phase diagram as determined by transport, neutron scattering, and electron diffraction measurements on $\text{NaFe}_{1-x}\text{Cu}_x\text{As}$ family of materials. The newly discovered Mott insulator near $x=0.5$ has a different magnetic structure and a Néel temperature of ~ 200 K, considerably higher

Future Plans

In the coming years, we plan to map out the electron-doping evolution of the spin excitations spectra in the $\text{NaFe}_{1-x}\text{Co}_x\text{As}$, $\text{NaFe}_{1-x}\text{Ni}_x\text{As}$, and $\text{BaFe}_2(\text{As}_{1-x}\text{P}_x)_2$ class of materials, and compare them with electron-doped $\text{BaFe}_{2-x}\text{Ni}_x\text{As}_2$ family of materials. In addition, we plan systematically investigate the uniaxial pressure on spin excitations of $\text{NaFe}_{1-x}\text{Ni}_x\text{As}$ and $\text{BaFe}_2\text{As}_{2-x}\text{P}_x$ class of materials (4).

We can also envision electron, hole, and isovalent doping to Mott insulating $\text{NaFe}_{0.5}\text{Cu}_{0.5}\text{As}$ by making Co, Zn, As substituted samples, respectively, to search for new superconductors. The magnetic properties of these new materials can also be studied by neutron scattering and compared with those of $\text{NaFe}_{1-x}\text{Co}_x\text{As}$. In addition, we can study what happens in $\text{LiFe}_{1-x}\text{Cu}_x\text{As}$, $\text{Fe}_{1-x}\text{Cu}_x\text{Te}$, and $\text{Fe}_{1-x}\text{Cu}_x\text{Se}$. Recent neutron scattering experiments on lightly Cu-doped $\text{FeTe}_{0.5}\text{Se}_{0.5}$ superconductors reveal anomalous enhancement of low-energy spin excitations similar to Cu-doped NaFeAs (5). A systematic investigation in Cu-doped pnictides and chalcogenides will open an entirely new avenue of research and offer exciting prospects of discovering new states of matter.

References

1. Dai P. "Antiferromagnetic order and spin dynamics in iron-based superconductors." *Reviews of Modern Physics*. 2015;87(3):855-96.
2. Song Y, Van Dyke J, Lum IK, White BD, Jang S, Yazici D, Shu L, Schneidewind A, Cermak P, Qiu Y, Maple MB, Morr DK, Dai PC. "Robust upward dispersion of the neutron spin resonance in the heavy fermion superconductor $\text{Ce}_{1-x}\text{Yb}_x\text{CoIn}_5$." *Nature communications*. 2016;7:10. doi: 10.1038/ncomms12774.
3. Song Y, Yamani Z, Cao C, Li Y, Zhang CL, Chen JS, Huang Q, Wu H, Tao J, Zhu YM, Tian W, Chi S, Cao H, Huang YB, Dantz M, Schmitt T, Yu R, Nevidomskyy AH, Morosan E, Si Q, Dai PC. "A Mott insulator continuously connected to iron pnictide superconductors." *Nat Commun*. 2016;in the press.
4. Lu X, Park JT, Zhang R, Luo H, Nevidomskyy AH, Si Q, Dai P. "Nematic spin correlations in the tetragonal state of uniaxial-strained $\text{BaFe}_{2-x}\text{Ni}_x\text{As}_2$." *Science*. 2014;345(6197):657-60. doi: 10.1126/science.1251853.
5. Wen JS, Li SC, Xu ZJ, Zhang C, Matsuda M, Sobolev O, Park JT, Christianson AD, Bourret-Courchesne E, Li Q, Gu GD, Lee DH, Tranquada JM, Xu GY, Birgeneau RJ. "Enhanced low-energy magnetic excitations via suppression of the itinerancy in $\text{Fe}_{0.98-z}\text{Cu}_z\text{Te}_{0.5}\text{Se}_{0.5}$." *PhysRevB*. 2013;88(14):5. doi: 10.1103/PhysRevB.88.144509.

Publications

1. “Study of vortex dynamics in single crystalline $\text{Ba}_{0.54}\text{K}_{0.46}\text{Fe}_2\text{As}_2$ superconductor using dc and ac magnetization”, D. Paladhi, C. Zhang, Gutai Tang, P. Dai, T. K. Nath, *J. Alloys and Compounds* **686**, 938-945 (2016).
2. “Robust upward dispersion of the neutron spin resonance in the heavy fermion superconductor $\text{Ce}_{1-x}\text{Yb}_x\text{CoIn}_5$ ”, Y. Song, J. Van Dyke, I. K. Lum, B. D. White, S. Jang, D. Yazici, L. Shu, A. Schneidewind, P. Cermak, Y. Qiu, M. B. Maple, D. Morr, and Pengcheng Dai, *Nat. Comm.* **7**, 12447 (2016).
3. “Iron-based high transition temperature superconductors”, Xianhui Chen, Pengcheng Dai, Donglai Feng, Tao Xiang, and Fu-Chun Zhang, *National Science Review* **1**, 371 (2014).
4. “Evolution of London penetration depth with scattering in single crystals of $\text{K}_{1-x}\text{Na}_x\text{Fe}_2\text{As}_2$ ”, H. Kim, M. A. Tanatar, Y. Liu, Z. Sims, C. Zhang, Pengcheng Dai, T. A. Lograsso, and R. Prozorov, *Phys. Rev. B* **89**, 174519 (2014).
5. “Long-range two-dimensional superstructure in the superconducting electron-doped cuprate $\text{Pr}_{0.88}\text{LaCe}_{0.12}\text{CuO}_4$ ”, B. J. Campbell, S. Rosenkranz, H. J. Kang, H. T. Stokes, P. J. Chupas, S. Komiya, Y. Ando, S. Li, and Pengcheng Dai, *Phys. Rev. B* **92**, 014118 (2015).
6. “Mott localization in a pure stripe antiferromagnet $\text{Rb}_{1.8}\text{Fe}_{1.5}\text{S}_2$ ”, M. Wang, M. Yi, H. Cao, C. de la Cruz, S. K. Mo, Q. Z. Huang, E. Bourret-Courchesne, Pengcheng Dai, D. H. Lee, Z. X. Shen, and R. J. Birgeneau, *Phys. Rev. B* **92**, 121101 (2015).
7. “Electron doping evolution of the magnetic excitations in $\text{NaFe}_{1-x}\text{Co}_x\text{As}$ ”, S. V. Carr, C. Zhang, Y. Song, G. Tan, D. L. Abernathy, M. B. Stone, G. E. Granroth, T. G. Perring, and Pengcheng Dai, *Phys. Rev. B* **93**, 214506 (2016).
8. “Two spatially separated phases in semiconducting $\text{Rb}_{0.8}\text{Fe}_{1.5}\text{S}_2$ ”, M. Wang, W. Tian, P. Valdivia, S. Chi, E. Bourret-Courchesne, Pengcheng Dai, and R. J. Birgeneau, *Phys. Rev. B* **90**, 125148 (2014).
9. “Anisotropic neutron spin resonance in underdoped superconducting $\text{NaFe}_{1-x}\text{Co}_x\text{As}$ ”, Chenglin Zhang, Y. Song, L. P. Regnault, Y. Su, M. Enderle, J. Kulda, G. Tan, Z. Sims, T. Egami, Q. Si, and Pengcheng Dai, *Phys. Rev. B* **90**, 140502(R) (2014).
10. “Phase separation, competition, and volume-fraction control in $\text{NaFe}_{1-x}\text{Co}_x\text{As}$ ”, L. Ma, J. Dai, P. S. Wang, Y. Song, C. Zhang, G. T. Tan, Pengcheng Dai, D. Hu, S. Li, B. Borman, and W. Yu, *Phys. Rev. B* **90**, 144502 (2014).
11. “Chemical tuning of electrical transport in $\text{Ti}_{1-x}\text{Pt}_x\text{Se}_{2-y}$ ”, J. S. Chen, J. Wang, S. Carr, S. Vogel, O. Gourdon, Pengcheng Dai, and E. Morosan, *Phys. Rev. B* **91**, 045125 (2015).
12. “Neutron spin resonance as a probe of superconducting gap anisotropy in partially detwinned electron underdoped $\text{NaFe}_{0.985}\text{Co}_{0.015}\text{As}$ ”, Chenglin Zhang, J. T. Park, Xingye Lu, Rong Yu, Yu Li, Wenliang Zhang, Yang Zhao, J. W. Lynn, Qimiao Si, and Pengcheng Dai, *Phys. Rev. B* **91**, 104520 (2015).
13. “Spin waves and spatially anisotropic exchange interactions in the $S = 2$ stripe antiferromagnet $\text{Rb}_{0.8}\text{Fe}_{1.5}\text{S}_2$ ”, Meng Wang, P. Valdivia, Ming Yi, J. X. Chen, W. L. Zhang, R. A. Ewings, T. G. Perring, Yang Zhao, L. W. Harriger, J. W. Lynn, E. Bourret-Courchesne, Pengcheng Dai, D. H. Lee, D. X. Yao, and R. J. Birgeneau, *Phys. Rev. B* **92**, 041109(R) (2015).

14. “Critical quadrupole fluctuations and collective modes in iron pnictide superconductors”, V. K. Thorsmølle, M. Khodas, Z. P. Yin, Chenglin Zhang, S. V. Carr, Pengcheng Dai, and G. Blumberg *Phys. Rev. B* **93**, 054515 (2016).
15. “Electron doping evolution of structural and antiferromagnetic phase transitions in $\text{NaFe}_{1-x}\text{Co}_x\text{As}$ iron pnictides”, Guotai Tan, Yu Song, Chenglin Zhang, Lifang Lin, Zhuang Xu, Tingting Hou, Wei Tian, Huibo Cao, Shiliang Li, Shiping Feng, and Pengcheng Dai, *Phys. Rev. B* **94**, 014509 (2016).
16. “Spin excitations in optimally P-doped $\text{BaFe}_2(\text{As}_{0.7}\text{P}_{0.3})_2$ superconductor”, Ding Hu, Zhiping Yin, Wenliang Zhang, R. A. Ewings, Kazuhiko Ikeuchi, Mitsutaka Nakamura, Bertrand Roessli, Yuan Wei, Lingxiao Zhao, Genfu Chen, Shiliang Li, Huiqian Luo, Kristjan Haule, Gabriel Kotliar, and Pengcheng Dai, *Phys. Rev. B* **94**, 094504 (2016).
17. “Electron doping evolution of the neutron spin resonance in $\text{NaFe}_{1-x}\text{Co}_x\text{As}$ ”, Chenglin Zhang, Weicheng Lv, Guotai Tan, Yu Song, Scott V. Carr, Songxue Chi, M. Matsuda, A. D. Christianson, J. A. Fernandez-Baca, L. W. Harriger, and Pengcheng Dai, *Phys. Rev. B* **93**, 174533 (2016).
18. “Effect of Pnictogen Height on Spin Waves in Iron Pnictides”, Chenglin Zhang, Leland W. Harriger, Zhiping Yin, Weicheng Lv, Miaoyin Wang, Guotai Tan, Yu Song, D. L. Abernathy, Wei Tian, Takeshi Egami, Kristjan Haule, Gabriel Kotliar, and Pengcheng Dai, *Phys. Rev. Lett* **112**, 217202 (2014).
19. “Orbital Selective Spin Excitations and their Impact on Superconductivity of $\text{LiFe}_{1-x}\text{Co}_x\text{As}$ ”, Yu Li, Zhiping Yin, Xiancheng Wang, David W. Tam, D. L. Abernathy, A. Podlesnyak, Chenglin Zhang, Meng Wang, Lingyi Xing, Changqing Jin, Kristjan Haule, Gabriel Kotliar, Thomas A. Maier, and Pengcheng Dai, *Phys. Rev. Lett* **116**, 247001 (2016).
20. “ $\text{NaFe}_{0.56}\text{Cu}_{0.44}\text{As}$: A Pnictide Insulating Phase Induced by On-Site Coulomb Interaction”, C. E. Matt, N. Xu, Baiqing Lv, Junzhang Ma, F. Bisti, J. Park, T. Shang, Chongde Cao, Yu Song, Andriy H. Nevidomskyy, Pengcheng Dai, L. Patthey, N. C. Plumb, M. Radovic, J. Mesot, and M. Shi, *Phys. Rev. Lett* **117**, 097001 (2016).
21. “Observation of Momentum-Confined In-Gap Impurity State in $\text{Ba}_{0.6}\text{K}_{0.4}\text{Fe}_2\text{As}_2$: Evidence for Antiphase s_{\pm} Pairing”, P. Zhang, P. Richard, T. Qian, X. Shi, J. Ma, L.-K. Zeng, X.-P. Wang, E. Rienks, C.-L. Zhang, Pengcheng Dai, Y.-Z. You, Z.-Y. Weng, X.-X. Wu, J. P. Hu, and H. Ding, *Phys. Rev. X* **4**, 031001 (2014).
22. “Antiferromagnetic order and spin dynamics in iron-based superconductors”, Pengcheng Dai, *Rev. Mod. Phys.* **87**, 855 (2015).
23. “Photoemission study of the electronic structure and charge density waves of $\text{Na}_2\text{Ti}_2\text{Sb}_2\text{O}$ ”, S. Y. Tan, J. Jiang, Z. R. Ye, X. H. Niu, Y. Song, C. L. Zhang, P. C. Dai, B. P. Xie, X. C. Lai, D. L. Feng, *Scientific Reports* **5**, 9515 (2015).
24. “A Mott insulator continuously connected to iron pnictide superconductors”, Yu Song, Zahra Yamani, Chongde Cao, Yu Li, Chenglin Zhang, Justin Chen, Qingzhen Huang, Hui Wu, Jing Tao, Yimei Zhu, Wei Tian, Songxue Chi, Huibo Cao, Yao-Bo Huang, Marcus Dantz, Thorsten Schmitt, Rong Yu, Andriy H. Nevidomskyy, Emilia Morosan, Qimiao Si, and Pengcheng Dai, *Nat. Comm. (in the press)* [arXiv:1504.05116](https://arxiv.org/abs/1504.05116).
25. “High-Temperature Superconductors”, Yu Song and Pengcheng Dai, *Book Chapter in "Neutron Scattering-Magnetic and Quantum Phenomena" Edited by Felix Fernandez-Alonso and David L. Price, Volume 48 in Experimental Methods in the Physical Sciences (ISBN: 978-0-12-802049-4 ISSN: 1079-4042), pages 145-201 (2015).*

Quasiparticle Couplings in Transport of Heat, Charge, and Spin for Novel Energy Materials

Olivier Delaire

Mechanical Engineering and Materials Science & Physics, Duke University, Durham, NC
Joint Faculty Affiliate, Oak Ridge National Laboratory, Oak Ridge, TN 37831

Program Scope:

This program focuses on elucidating the couplings between microscopic degrees-of-freedom of atomic vibrations, spins, and electrons, which underpin heat, charge, and spin transport in novel energy materials. Understanding the microscopic processes involved in the transport and conversion of energy from the atomic-scale to the meso-scale is critical for the development of next-generation materials for energy sustainability. At a microscopic level, these couplings result from anharmonic phonon-phonon interactions, and interaction of phonons with electrons or spin degrees of freedom, which can lead to hybrid excitations. This project investigates these quasiparticle interactions, how hybrid quasiparticles form or break down, and their consequences on transport properties. We use state-of-the-art neutron and x-ray scattering techniques, optical spectroscopy, synthesis and transport measurements, and first-principles computer simulations.

Recent Progress:

Giant phonon anharmonicity in rocksalt chalcogenides PbX, SnX:

Our INS measurements and modeling of the phonon-phonon interaction in single-crystalline PbTe (see Fig. 1) revealed the source of the low thermal conductivity in this important thermoelectric material [1-3]. We have shown that a strong anharmonic coupling between the ferroelectric transverse-optic (TO) mode and the acoustic modes results in increased scattering rates for heat-carrying acoustic modes, and a large suppression of phonon mean-free-paths and thermal conductivity [1-3]. The harmonic phonon theory is both elegant and convenient, but new physics arise from large anharmonic coupling terms between quasiparticles, which can lead to new hybrid excitations or fluctuations. Our full first-principles simulations of the phonon self-energy and spectral functions in the rocksalts PbTe, SnTe have detailed the origin of the anomalous splitting of the TO mode [3-4, p1], and our new results explained the anomalous shape of the pair-distribution function [p1] (Fig. 2). Further, we recently used ultrafast time-resolved x-ray diffuse scattering at LCLS to

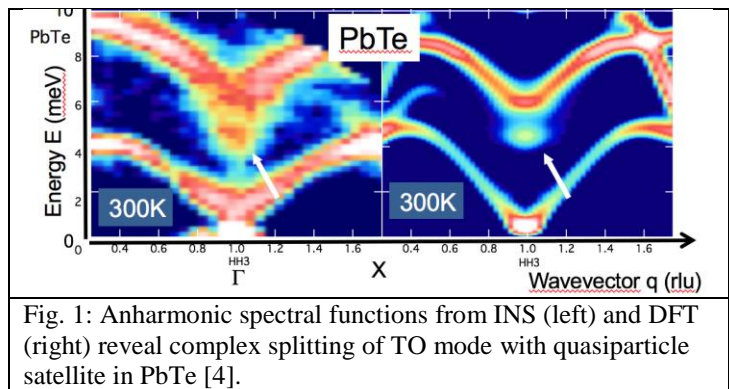


Fig. 1: Anharmonic spectral functions from INS (left) and DFT (right) reveal complex splitting of TO mode with quasiparticle satellite in PbTe [4].

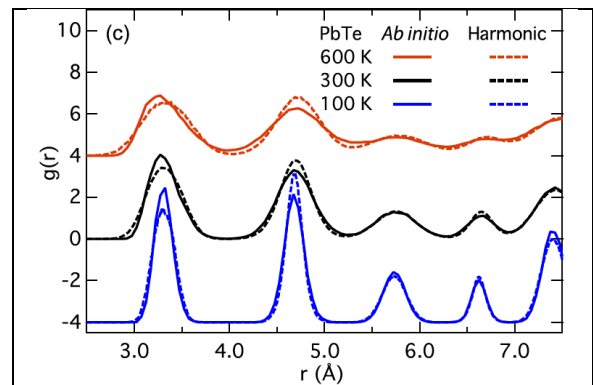


Fig. 2: Pair-distribution function of PbTe from AIMD simulations, showing anharmonic asymmetry of peaks.

complement our INS measurements, and showed that the strong anharmonicity is sensitive to the states at the top of the valence band and is tuned with photoexcitation. The photoexcitation destabilizes the resonant bonding and thus favors the paraelectric phase. In addition, no time-averaged diffuse scattering is seen beyond thermal diffuse scattering, ruling out off-centering of atoms [p9].

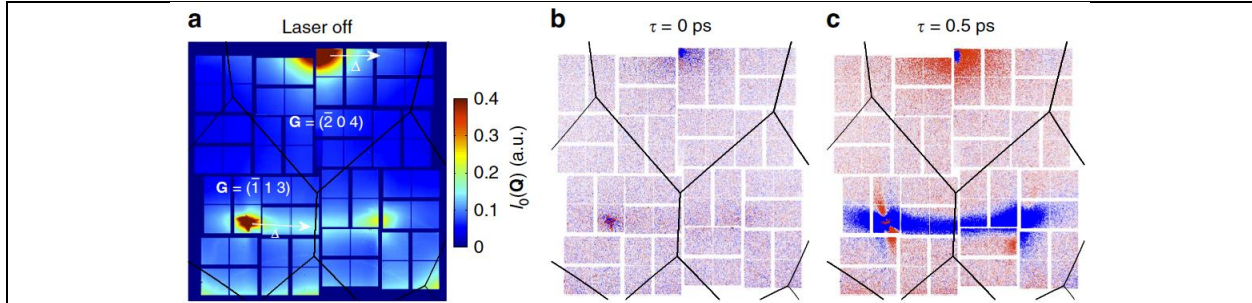


Fig. 3: Static (a) and femtosecond x-ray diffuse scattering from PbTe (b,c). [Jiang2016, p9]

[Publications 1,9]

Electron-phonon coupling and thermal transport in Mo₃Sb₇:

The compound Mo₃Sb₇ has attracted much interest for its favorable thermoelectric properties (~0.8 at 1050K), as well as evidence of strong electron-phonon coupling [6,7]. Prior studies also reported superconductivity, spin fluctuations, and unusual magnetism at low T [6-10]. Substituting Te for Sb (up to 1.8 Te per formula unit) induces a strong decrease in carrier concentration, which considerably improves thermoelectric properties [6,7]. Our DFT simulations show that the electronic effect of Te alloying can be understood in a rigid-band picture, with the Fermi level shifting past a peak, as it moves toward the top of the valence band.

Thus, Te alloying strongly suppresses the electronic density at the Fermi level, $N(E_F)$, and correspondingly we observe a drastic stiffening of the phonon spectrum with Te alloying [p3]. The average phonon energy increases by a very large +7% from Mo₃Sb₇ to Mo₃Sb_{5.4}Te_{1.6}, dwarfing the quasiharmonic effect of lattice contraction (+0.1%). We explain the phonon stiffening from the suppression in electronic screening, as we previously observed in vanadium-A15 compounds and in thermoelectrics La_{3-x}Te₄ and doped FeSi [p4]. The significance of electron-phonon coupling was also observed in our analysis of thermal transport, as Te alloying counter-intuitively increases the lattice thermal conductivity, via the suppressed electron-phonon scattering.

[Publications: 2,3]

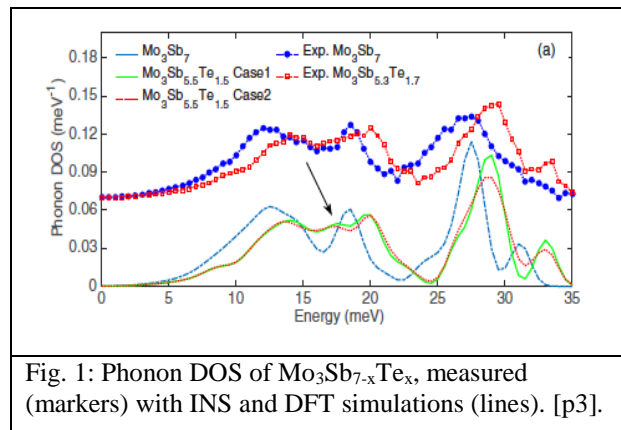


Fig. 1: Phonon DOS of Mo₃Sb_{7-x}Te_x, measured (markers) with INS and DFT simulations (lines). [p3].

Investigation of thermal transport in complex quasi-1D crystal structures:

Quasi-1D crystal structures yield distinctive electronic, spintronic, optical and thermoelectric properties. They also exhibit unusual and interesting lattice and spin dynamics at a fundamental

level. In the quasi-1D spin-ladder compound $\text{Sr}_{14}\text{Cu}_{24}\text{O}_{41}$, magnetic fluctuations are strong and the magnon thermal conductivity reaches $\sim 75\text{W/m/K}$ at 150K [14-20]. In addition, the structure is aperiodic, with two nearly-commensurate sublattices along the c axis – CuO_2 chains and Cu_2O_3 two-leg spin ladders. We have performed INS measurements of the phonons and magnons (ARCS at SNS and CTAX at HFIR, crystals from Profs L. Shi and J. Zhou at UT Austin). Our measurements revealed very steep magnons responsible for the large magnetic thermal conduction, as well as intricate phonon dispersions. In particular, the phonons in $\text{Sr}_{14}\text{Cu}_{24}\text{O}_{41}$ showed unusual pseudo-acoustic modes with small gaps, revealing the sliding motions of incommensurate sublattices in the structure.

So-called higher manganese silicide, $\text{Mn}_{27}\text{Si}_{47}$, is another quasi-1D compound. It adopts a Nowotny chimney ladder structure, consisting of a tetragonal Mn chimney sublattice based on the beta-Sn structure and a Si ladder sublattice with coupled helices. Our INS measurements (ARCS at SNS and HB1 at HFIR) on single crystals revealed numerous low-energy optical modes, including unusually low frequency twisting motions of the Si ladders inside the Mn chimneys, which provide a large phase space for scattering acoustic phonons, resulting in the low thermal conductivity.

[Publications: 4,8]

Modeling of INS data with first-principles simulations and lattice dynamics:

We have developed the modeling of phonon $S(\mathbf{Q},E)$ for neutron and x-ray scattering measurements, including the optimization of force-constants obtained from first-principles simulations. Our simulations are working on massively parallel computers at ORNL (Titan), using algorithms we have developed for efficient optimization over large parameter space. In addition, we have developed models of anharmonicity and alloy disorder on the phonon self-energy and spectral functions from first-principles.

[Publications: 1,2,6,7]

Future Plans:

Hybrid quasiparticles and spectral function satellites in strongly anharmonic materials:

We will use INS to map the phonon dynamical structure $S(\mathbf{Q},E)$ in single-crystals of strongly anharmonic materials PbX , SnX , GeX ($X=\text{S,Se,Te}$), to identify deviations of spectral functions from the usual Lorentzian or damped-harmonic oscillator profiles. Our first-principles anharmonic modeling of the phonon self-energy and spectral functions (method previously reported in [4]) enable us to predict and identify anharmonic self-energy effects leading to satellite peaks, corresponding to new emergent quasiparticles. These emergent hybrid quasiparticles can be dispersive or localized, short or long-lived, and we will investigate the process of their formation and their dependence on temperature and disorder. We have shown how systems near lattice instabilities, especially soft-mode driven transitions, harbor strong anharmonicity. In particular, we will continue our on-going investigations of rocksalt chalcogenides (PbX , SnX , GeX) near-ferroelectric instabilities, in which we previously discovered strong anharmonic phenomena leading to the satellite feature in the TO mode. Further, we will also investigate anharmonic hybrid quasiparticles in other systems nearby lattice instabilities, in which our preliminary investigations indicate a similar effect. Our studies of these strongly anharmonic quasiparticle couplings will be integrated with our rationalization of thermal transport in complex materials, an integral part of this Early Career project.

Spin-phonon coupling, multiferroicity, and effects on thermal transport:

Coupling between lattice and magnetic degrees of freedom is central to multiferroics and spin-caloritronics, and leads to unusual and poorly understood thermal transport properties. We will continue our investigations of quasiparticle couplings in magnetic systems using a combination of inelastic neutron and x-ray scattering measurements, transport measurements, and theoretical modeling. In particular, we will perform new investigations of the phonon dispersions and linewidths across reciprocal space in CrSb₂, CuCrO₂, yttrium-iron garnet (YIG), and FeS, in which our preliminary experimental and simulation data show interesting effects. These will be correlated with transport measurements and first-principles simulations.

Finite-temperature electron-phonon coupling and thermal transport:

Building on our previous INS/IXS investigations of electron-phonon interaction (EPI) and thermal transport [12,13, p2,p3], we will investigate materials with strong EPI leading to phonon instabilities such as Kohn anomalies (Nb) and charge-density waves (BaPt₂As₂). In these materials, extended phonon anomalies can be observed in reciprocal space, and we will track the temperature dependence of both phonon dispersions and linewidths, and compare the measurements with DFT simulations. The EPI often leads to interesting transport properties, and our phonon investigations will be complemented with measurements and modeling of thermal transport.

References

- [1] O. Delaire *et al.*, Nature Materials **10**, 614 (2011).
- [2] T. Shiga, J. Shiomi, J. Ma, O. Delaire, *et al.* “Microscopic mechanism of low thermal conductivity in lead telluride”, Physical Review B **85**, 155203 (2012).
- [3] T. Shiga, T. Murakami, T. Hori, O. Delaire, and J. Shiomi, “Origin of anomalous anharmonic lattice dynamics of lead telluride”, Appl. Phys. Express **7**, 041801 (2014).
- [4] C. Li, *et al.* “Phonon self-energy and origin of anomalous neutron scattering spectra in SnTe and PbTe thermoelectrics”, Phys. Rev. Letters **112**, 175501 (2014).
- [5] C. Li, *et al.* “Anharmonicity and Atomic Distribution of SnTe and PbTe Thermoelectrics”, Phys. Rev. B **90**, 214303 (2014).
- [6] C. Candolfi, B. Lenoir, A. Dauscher, *et al.* Phys. Rev. B **84**, 224306 (2011)
- [7] X. Shi, Y. Pei, G. J. Snyder and L. Chen, Energy Environ. Sci. **4**, 4086 (2011).
- [8] C. Candolfi, B. Lenoir, A. Dauscher, *et al.* Phys. Rev. Lett. **99**, 037006 (2007).
- [9] V. H. Tran, W. Müller, Z. Bukowski, Phys. Rev. Lett. **100**, 137004 (2008).
- [10] T. Koyama, H. Yamashita, Y. Takahashi, *et al.* Phys Rev Lett **101**, 126404 (2008).
- [11] J.-Q. Yan, M.A. McGuire, A.F. May *et al.*, Phys. Rev. B **87**, 104515 (2013).
- [12] O. Delaire, *et al.* Physical Review Letters **101**, 105504 (2008).
- [13] O. Delaire, *et al.*, Phys. Rev. B **80**, 184302 (2009).
- [14] Sologubenko, *et al.*. Physical Review Letters **84**, 2714-2717 (2000).
- [15] Uehara, M. *et al.* Journal of the Physical Society of Japan **65**, 2764-2767 (1996).
- [16] Regnault, L. P. *et al.* Physical Review B **59**, 1055-1059 (1999).
- [17] Eccleston, R. S. *et al.* Physical Review Letters **81**, 1702-1705 (1998).
- [18] Hess, C. European Physical Journal-Special Topics **151**, 73-83 (2007).

Publications resulting from work supported by the DOE grant over the previous 2.5 years:

Refereed publications in archival journals:

[p11] (submitted) J. Hong and O. Delaire “Electronic Instability and Anharmonicity in SnSe”, (arXiv:1604.07077v2)

[p10] Dipanshu Bansal, Jiawang Hong, Chen W. Li, Andrew F. May, Wallace Porter, Michael Y. Hu, Douglas L. Abernathy, and Olivier Delaire, “Phonon anharmonicity and negative thermal expansion in SnSe”, *Phys. Rev. B* **94**, 054307 (2016).

[p9] M.P. Jiang, M. Trigo, S. Fahy, É.D. Murray, I. Savić, C. Bray, J. Clark, T. Henighan, M. Kozina, M. Chollet, J.M. Glowina, M. Hoffmann, D. Zhu, O. Delaire, A.F. May, B.C. Sales, A.M. Lindenberg, P. Zalden, T. Sato, R. Merlin, and D.A Reis “The origin of incipient ferroelectricity in lead telluride”, *Nature Communications* **7**, 12291 (2016).

[p8] Xi Chen, Dipanshu Bansal, Sean Sullivan, Douglas L. Abernathy, Adam A. Aczel, Jianshi Zhou, Olivier Delaire, and Li Shi, “Weak coupling of pseudoacoustic phonons and magnon dynamics in the incommensurate spin-ladder compound $\text{Sr}_{14}\text{Cu}_{24}\text{O}_{41}$ ”, *Phys. Rev. B* **94**, 134309 (2016).

[p7] Feng Bao, Richard Archibald, Jennifer Niedziela, Dipanshu Bansal and Olivier Delaire, “Complex optimization for big computational and experimental neutron datasets”, *Nanotechnology* **27**, 484002 (2016).

[p6] Feng Bao, Rick Archibald, Dipanshu Bansal, Olivier Delaire, “Hierarchical Optimization for Neutron Scattering Problems”, *Journal of Computational Physics* **315**, 39-51, (2016)

[p5] Dipanshu Bansal, Amjad Aref, Gary Dargush, Olivier Delaire, “Modeling non-harmonic behavior of materials from experimental inelastic neutron scattering and thermal expansion measurements”, *Journal of Physics: Condensed Matter* **28**, 385201 (2016).

[p4] Xi Chen, Annie Weathers, Jesús Carrete, Saikat Mukhopadhyay, Olivier Delaire, Derek A. Stewart, Natalio Mingo, Steven N. Girard, Jie Ma, Doug L. Abernathy, Jiaqiang Yan, Raman Sheshka, Daniel P. Sellan, Fei Meng, Song Jin, Jianshi Zhou, Li Shi, “Twisting Phonons in Complex Crystals with Quasi-One-Dimensional Substructures”, *Nature Communications* **6**, 6723 (2015).

[p3] Dipanshu Bansal, Chen W. Li, Ayman H. Said, Douglas L. Abernathy, Jiaqiang Yan, and Olivier Delaire, “Electron-phonon coupling and thermal transport in the thermoelectric compound $\text{Mo}_3\text{Sb}_{7-x}\text{Te}_x$ ”, *Physical Review B* **92**, 214301 (2015).

[p2] O. Delaire, I. I. Al-Qasir, A. F. May, C. W. Li, B. C. Sales, J. L. Niedziela, J. Ma, M. Matsuda, D. L. Abernathy, T. Berlijn, “Heavy-impurity resonance, hybridization, and phonon spectral functions in $\text{Fe}_{1-x}\text{M}_x\text{Si}$, $\text{M}=\text{Ir,Os}$ ”, *Phys. Rev. B* **91**, 094307 (2015).

[p1] C.W. Li, J. Ma, H.B. Cao, A.F. May, D.L. Abernathy, G. Ehlers, C. Hoffmann, X. Wang, T. Hong, A. Huq, O. Gourdon, and O. Delaire, “Anharmonicity and Atomic Distribution of SnTe and PbTe Thermoelectrics”, *Phys. Rev. B* **90**, 214303 (2014).

Title:

Status and Developments at the NIST Center for Neutron Research

Presenter:

**Dr. Robert Dimeo, Director
NIST Center for Neutron Research**

Abstract:

The NIST Center for Neutron Research is a national user facility operated by the Department of Commerce. In this presentation, an update on the latest facility and instrument developments will be presented.

Rob Dimeo, Director

NIST Center for Neutron Research

301.975.6210

www.ncnr.nist.gov

LaCNS: Building Neutron Scattering Infrastructure in Louisiana for Advanced Materials

J. F. DiTusa¹ (ditusa@phys.lsu.edu), D. Zhang², J. Zhang¹, W. A. Shelton³, J. C. Garno², R. Jin¹, V. T. John⁴, R. Kumar², Y. M. Lvov⁵, Z. Mao⁶, E. Nesterov², E. W. Plummer¹, S. W. Rick⁷, G. J. Schneider², D. P. Young¹, P. T. Sprunger¹, L. G. Butler², M. Khonsari⁸

¹*Department of Physics and Astronomy, Louisiana State University, Baton Rouge, LA 70803*

²*Department of Chemistry, Louisiana State University, Baton Rouge, LA 70803*

³*Department of Chemical Engineering, Louisiana State University, Baton Rouge, LA 70803*

⁴*Dept. of Chem. and Biomolecular Engineering, Tulane University, New Orleans, LA 70118*

⁵*Institute for Micromanufacturing, Louisiana Tech University, Ruston, LA 71272*

⁶*Department of Physics and Engineering Physics, Tulane University, New Orleans, LA 70118*

⁷*Department of Chemistry, University of New Orleans, New Orleans, LA 70148*

⁸*Louisiana Board of Regents, Baton Rouge, LA 70821*

Program Scope: This DOE EPSCoR / LA Board of Regents program aims to build neutron scattering infrastructure capable of treating both soft and hard materials. Our objectives include: discovery of the coupling of degrees of freedom that determine the emergent properties of complex materials, training of talented students in synthesis and neutron scattering techniques who will become the next generation of neutron users; and building a base of users of SNS and HFIR.

The scientific focus of this program is to understand the role of coupling in emergent complex materials and its impact on structure/property relationships, and to explore how this information can be applied in the guided-design of materials. Our goal is to tune dominant couplings to enhance critical properties in order to derive new functionality. In the hard materials we focus on transition metal oxides where electronic, magnetic, phononic, and orbital degrees of freedom are all important to describing these materials with their couplings leading to novel behaviors, non-centrosymmetric structured materials where the Dzyaloshinskii-Moriya interaction leads to interesting magnetic structures and spin textures, and Dirac systems where magnetic ordering likely leads to the formation of Weyl semimetal states. In the soft materials we explore the role of secondary interactions in determining the structural and dynamic properties of polymeric systems.

Recent Progress

I include here two examples of projects that demonstrate the progress we have achieved over the initial 2 years of funding. These include investigations of the evolution of the helical and Skyrmion lattice (SkL) states of MnSi with chemical substitution and the investigation of tunable charged soft colloids where we make use of peptoid amphiphiles as a model system.

In 2009, small angle neutron scattering in a small pocket of the (H,T)-phase diagram (so-called A phase) of the prototypical non-centrosymmetric itinerant magnet MnSi resulted in the discovery

of a bulk SkL phase[1]. Since then, control of the size and helicity of magnetic Skyrmions is at the heart of an intense research activity worldwide. These countable magnetic defects, carrying a quantum of electromagnetic flux, are indeed envisioned as potential building blocks for next-generation electronics [2].

Previously, it has been shown that the magnetic properties of MnSi can be tuned by chemical substitution of Mn by Fe or Co [3], or by application of hydrostatic[4] or uniaxial[5] pressure. Quite generally, doping and hydrostatic pressure leads to a suppression of magnetic order and hence the disappearance of the SkL. On the other hand, uniaxial pressure was found to stabilize these over a larger portion of the (H,T) -space. The uniaxial pressure, which emulates lateral strains inherent to thin films, implies a contraction in one direction with an expansion in the orthogonal direction. It thus remains unclear which is the driving force leading to the extension of the SkL.

Here, instead of the traditional substitution of the magnetic Mn ions, Si is replaced by a small amount of Al or Ga. As shown in [6], slight substitution of Si by Al (3.8 %) appears to dramatically increase the critical temperature (+30%) and ordered magnetic moment (+20%). It is remarkable that such a small change in the material structure, a small increase of the unit cell volume by $\approx 0.5\%$, induces such drastic improvements of its magnetic properties despite enhanced chemical disorder. In turn, the lattice expansion is homogeneous and its effect can be studied in a transparent way. Most importantly, we have shown that such a negative pressure leads to an extension of the so-called A phase as well as a temperature-induced reversal of the sign of anomalous Hall effect (AHE, Fig. 1c,d)[6]. These features imply (i) a drastically enhanced stability of the SkL and (ii) the unique possibility to choose the chirality of the magnetic structure – hence of the SkL- by a simple temperature change. This would open a completely new and unexpected avenue in the field of Skyrmionics.

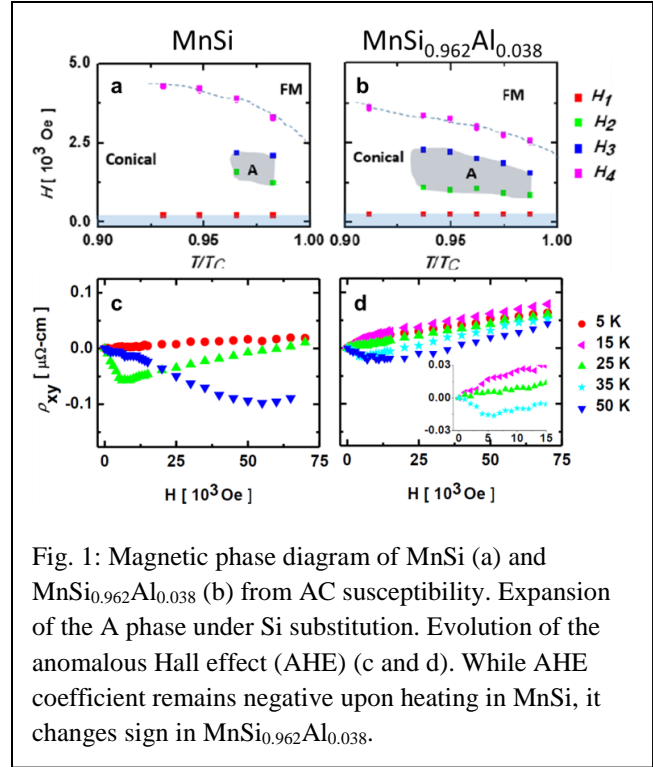


Fig. 1: Magnetic phase diagram of MnSi (a) and MnSi_{0.962}Al_{0.038} (b) from AC susceptibility. Expansion of the A phase under Si substitution. Evolution of the anomalous Hall effect (AHE) (c and d). While AHE coefficient remains negative upon heating in MnSi, it changes sign in MnSi_{0.962}Al_{0.038}.

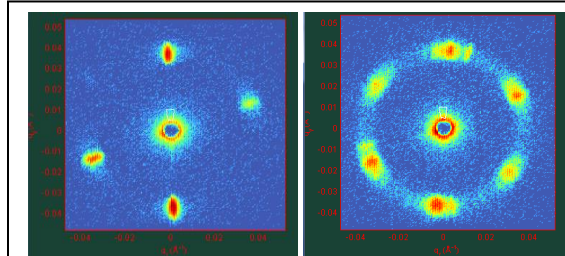


Fig. 2: Small angle neutron scattering from MnSi_{0.992}Ga_{0.008} in the zero field helical state (a) and in the skyrmion lattice phase at 0.15 T (b) at 32.5 K.

Our SANS experiments, Fig. 2, have confirmed the increased stability of the SkL while indicating no strong dependence of the helical wavelength with Al or Ga substitutions.

Soft colloids are employed in a wide range of applications from simple dispersions in surface coatings to complex fluids for oil recovery. Understanding of the principles governing their nanoscopic structure, central to their behavior as well as their macroscopic dynamics, is prerequisite to discovery of next generation soft materials crucial to the development of new technologies. We introduce a new tunable di-block copolymer as a model system for polyelectrolyte micelles based on newly synthesized polypeptoid amphiphiles. This di-block copolymer forms in a star-like spherical micellar core-shell morphology [7]. We have performed SANS (Fig. 3) to explore the structure of the micelles that form. The corresponding form factor was modelled using a compact hard-sphere core and star-like density profile for the shell. For the first time we are able to successfully tune the number of arms attached to the central core, a.k.a. the aggregation number, simply by placing a charged monomer at different positions along the corona segment. Such a high degree of accuracy is made possible by precision synthesis of the amphiphilic peptoids. The modular nature and synthetic control of the solid state sub-monomer technique [8] offers atomic level control over the sequence and charge placement of the resulting peptoids. Their self-assembly allows fine tuning of the charge quantity and location inside the micellar corona. As illustrated in Fig. 4, three special cases where there is isotropic charge distribution (green) in 3-dimensions, inside the outer (case 1), middle (case 2) and inner (case 3) layer of the micellar corona were investigated. It also depicts the blob picture of micellar corona [9]. In this unique class of polyelectrolyte micelles, we have defined an intra-molecular interaction length i.e. the distance of the charge from the core-shell interface as the single most important parameter that determines the architecture of micellar morphology - the size and the aggregation number.

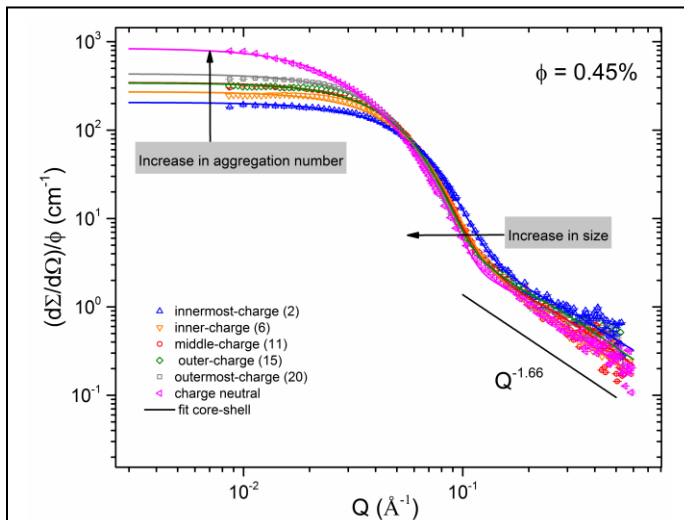


Fig. 3: SANS scattering intensity - cross section normalized by the volume fraction vs. Q . Legend refers to the charge position from innermost (case 3 in Fig.4, monomer 2 is charged) to outermost (case 1, monomer 20 is charged) from the core-shell interface. Lines are fits using modified core-shell model designed for star-like micellar systems [1].

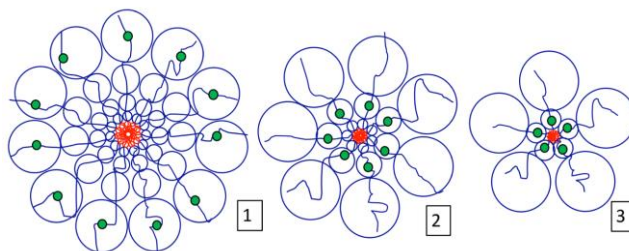


Fig. 4: Schematic core-shell micellar structure (blob picture) for (1) outer, (2) middle and (3) inner charge distribution of charged polypeptoid based block copolymer micelles.

Such a high degree of accuracy is made possible by precision synthesis of the amphiphilic peptoids. The modular nature and synthetic control of the solid state sub-monomer technique [8] offers atomic level control over the sequence and charge placement of the resulting peptoids. Their self-assembly allows fine tuning of the charge quantity and location inside the micellar corona. As illustrated in Fig. 4, three special cases where there is isotropic charge distribution (green) in 3-dimensions, inside the outer (case 1), middle (case 2) and inner (case 3) layer of the micellar corona were investigated. It also depicts the blob picture of micellar corona [9]. In this unique class of polyelectrolyte micelles, we have defined an intra-molecular interaction length i.e. the distance of the charge from the core-shell interface as the single most important parameter that determines the architecture of micellar morphology - the size and the aggregation number.

Future Plans

We will continue to develop a neutron-centric program in Louisiana in hard and soft materials as well as in the understanding of catalytic systems. For the research themes highlighted here, we plan to leverage our success thus far to open new areas of exploration. In MnSi, short term plans include the determination of the helicity (handedness) of the magnetic structure in $\text{MnSi}_{1-x}\text{Al}_x$ to investigate whether the reversal of the Berry curvature evident in AHE with cooling is reflected in the magnetic ordering. This would evidence the close coupling of electronic and magnetic degrees of freedom suggested in theoretical work[10]. In addition, we will continue to search for spin texture effects in other weak itinerant non-centrosymmetric magnetic materials, including ScFeGe which forms in the Fe_2P structure (hexagonal) and where we have recently demonstrated a helical magnetic order. For the polypeptoid research, we will be developing methods for the investigation of polymer synthesis at the neutron beam line; Lab-on-an Instrument. That is, we will work to create a chemistry lab on the neutron instruments to investigate reaction-driven self-assembly in complex fluids. The goal is to explore the structural and dynamic evolution of hierarchical self-assembly resulting from the complex interplay between secondary (non-covalent) interactions and primary (covalent) interactions in a reactive system. The complex nature of the multi-length-scale experimental system requires a combined approach: synthesis of well-characterized model systems, neutron scattering to identify the structural features, and simulations to suggest which interactions determine the morphology.

References

- [1] S. Mühlbauer, B. Binz, F. Jonietz, C. Pfleiderer, A. Rosch, A. Neubauer, R. Georgii, and P. Böni, *Science* **323**, 915 (2009).
- [2] A. Fert, V. Cros, and J. Sampaio, *Nature Nanotechnology* **8**, 152 (2013).
- [3] A. Bauer, A. Neubauer, C. Franz, W. Munzer, M. Garst, and C. Pfleiderer, *Phys. Rev. B* **82**, 064404 (2010).
- [4] C. Pfleiderer, D. Reznik, L. Pintschovious, H. v. Lohneysen, M. Garst, and A. Rosch, *Nature* **427**, 227 (2004) and references therein.
- [5] Y. Nii, T. Nakajima, A. Kikkawa, Y. Yamasaki, K. Ohishi, J. Suzuki, Y. Taguchi, T. Arima, Y. Tokura, and Y. Iwasa, *Nature Communications* **6**, 8539 (2015).
- [6] C. Dhital, M. A. Khan, M. Saghayezhian, W. A. Phelan, D. P. Young, R. Y. Jin, and J. F. DiTusa, arXiv:1609.08181 (2016).
- [7] S. Gupta, M. Camargo, J. Stellbrink, J. Allgaier, A. Radulescu, P. Lindner, E. Zaccarelli, C. N. Likos, and D. Richter, *Nanoscale* **7**, 13924 (2015).
- [8] G. M. Figliozzi, R. Goldsmith, S. C. Ng, S. C. Banville, and R. N. Zuckermann, *Methods Enzymol* **267**, 437 (1996).
- [9] M. Daoud, and J. P. Cotton, *J. Physique* **43**, 531 (1982).
- [10] F. Freimuth, R. Bamler, Y. Mokrousov, and A. Rosch, *Phys. Rev. B* **88**, 214409 (2014).

Publications

- 1) Arai K, Sagawa N, Shikata T, Sternhagen, GL, Li X, Guo L, Do C, and Zhang D. Pronounced dielectric and hydration/dehydration behaviors of monopolar poly(n-alkyl glycine)s in aqueous solution. *J Phys Chem B* **120**(37):9978-9986 (2016).
<http://pubs.acs.org/doi/abs/10.1021/acs.jpcc.6b05379>
- 2) Feng J, Tan A, Wagner S, Liu J, Mao Z, Ke X, and Zhang P. Charge modulation and structural transformation in TaTe₂ studied by scanning tunneling microscopy/spectroscopy. *Appl Phys Lett* **109**:021901 (2016).
<http://scitation.aip.org/content/aip/journal/apl/109/2/10.1063/1.4958616>
- 3) Liu J, Hu J, Cao H, Zhu Y, Chuang A, Graf D, Adams DJ, Radmanesh SMA, Spinu L, Chiorescu I, and Mao Z. Nearly massless Dirac fermions hosted by Sb square net in BaMnSb₂. *Scien Rep (Nature Publ)* **6**:30525 (2016). www.nature.com/articles/srep30525
- 4) Zou T, Cao H, Liu GQ, Peng J, Gottschalk M, Zhu M, Zhao Y, Leao JB, Tian W, Mao ZQ, and Ke X. Pressure-induced electronic and magnetic phase transitions in a Mott insulator: Ti-doped Ca₃Ru₂O₇ bilayer ruthenate. *Phys Rev B* **94**:041115 (R) (2016).
<http://journals.aps.org/prb/abstract/10.1103/PhysRevB.94.041115>
- 5) Bhaskaran-Nair K, Kowalski K, and Shelton, WA. Coupled cluster Green function: Model involving single and double excitations. *J Chem Phys* **144**:144101 (2016).
<http://scitation.aip.org/content/aip/journal/jcp/144/14/10.1063/1.494496>
- 6) Carrillo J-MY, Siebers Z, Kumar R, Matheson MA, Ankner JF, Goswami M, Bhaskaran-Nair K, Shelton WA, Sumpter BG, and Kilbey SM. Petascale simulations of the morphology and the molecular interface of bulk heterojunctions. *ACS Nano* **10**:7008-7022 (2016).
<http://pubs.acs.org/doi/full/10.1021/acsnano.6b03009>
- 7) Dionisi C, Hanafy N, Nobile C, De Giorgi ML, Rinaldi R, Casciaro S, Lvov Y, and Leporatti S. Halloysite clay nanotubes as carriers for curcumin: Characterization and application. *IEEE Transactions on Nanotechnology* **15**(5):720-724 (2016).
https://www.researchgate.net/publication/293010472_Halloysite_Clay_Nanotubes_as_Carriers_for_Curcumin_Characterization_and_Application
- 8) Hu J, Liu JY, Graf D, Radmanesh SMA, Adams DJ, Chuang A, Wang Y, Chiorescu I, Wei J, Spinu L, and Mao ZQ. π Berry phase and Zeeman splitting of Weyl semimetal TaP. *Scien Rep (Nature Publ)* **6**:18674 (2016). <http://www.nature.com/articles/srep18674>
- 9) Li A, Lu L, Li X, He LL, Do C, Garno JC, and Zhang D. Amidine-mediated Zwitterionic ring-opening polymerization of n-alkyl n-carboxyanhydride: Mechanism, kinetics, and architecture elucidation. *Macromolecules* **49**(4):1163-1171 (2016).
<http://pubs.acs.org/doi/full/10.1021/acs.macromol.5b02611>

- 10) Lvov Y, DeVilliers M, and Fakhrullin R. The application of halloysite tubule nanoclay in drug delivery. *Expert Opinion Drug Delivery* **13**(7):977-986 (2016).
<https://www.ncbi.nlm.nih.gov/pubmed/27027933>
- 11) Lvov Y, Wang WC, Zhang LQ, and Fakhrullin RF. Halloysite clay nanotubes for loading and sustained release of functional compounds. *Adv Mater* **28**(6):1227-1250 (2016).
<http://onlinelibrary.wiley.com/doi/10.1002/adma.201502341/full>
- 12) Peng J, Hu J, Gu XM, Zhou GT, Liu JY, Zhang FM, Wu XS, and Mao ZQ. Normal and inverse bulk spin valve effects in single-crystal ruthenates. *Appl Phys Lett* **108**:162402 (2016).
<http://scitation.aip.org/content/aip/journal/apl/108/16/10.1063/1.4947489>
- 13) Rivero P, Meunier V, and Shelton WA. Electronic, structural, and magnetic properties of LaMnO₃ phase transition at high temperature. *Phys Rev B* **93**:024111 (2016).
<http://journals.aps.org/prb/abstract/10.1103/PhysRevB.93.024111#fulltext>
- 14) Rivero P, Meunier V, and Shelton WA. Uniaxial pressure-induced half-metallic ferromagnetic phase transition in LaMnO₃. *Phys Rev B* **93**:094409 (2016).
<http://journals.aps.org/prb/abstract/10.1103/PhysRevB.93.094409#fulltext>
- 15) Rivero P, Meunier V, and Shelton WA. Surface properties of hydrogenated diamond in the presence of adsorbates: a hybrid functional DFT study. *Carbon* **110**:469-479 (2016).
<http://www.sciencedirect.com/science/article/pii/S0008622316308107>
- 16) Tully J, Yendluri R, and Lvov Y. Halloysite clay nanotubes for enzyme immobilization. *Biomacromolecules* **17**(2):615-621 (2016).
<http://pubs.acs.org/doi/full/10.1021/acs.biomac.5b01542>
- 17) Xuan ST, Lee CU, Chen C, Doyle AB, Zhang YH, Guo L, John VT, Hayes D, and Zhang D. Thermoreversible and injectable ABC polypeptoid hydrogels: Controlling the hydrogel properties through molecular design. *Chem Mat* **28**(3):727-737 (2016).
<http://pubs.acs.org/doi/full/10.1021/acs.chemmater.5b03528>
- 18) Youm SG, Hwang E, Chavez CA, Li X, Chatterjee S, Lusker KL, Lu L, Strzalka J, Ankner JF, Losovyj Y, Garno JC, and Nesterov EE. Polythiophene thin films by surface-initiated polymerization: Mechanistic and structural studies. *Chem Mat* **28**(13):4787-4805 (2016).
<http://pubs.acs.org/doi/full/10.1021/acs.chemmater.6b01957>
- 19) Bhaskaran-Nair K, Kowalski K, Jarrell M, Moreno J, and Shelton WA. Equation of motion coupled cluster methods for electron attachment and ionization potential in polyacenes. *Chem Phys Lett* **641**:146-152 (2015).
<http://www.sciencedirect.com/science/article/pii/S0009261415008349>

- 20) Bhaskaran-Nair K, Valiev M, Deng SHM, Shelton WA, Kowalski K, and Wang XB. Probing microhydration effect on the electronic structure of the GFP chromophore anion: Photoelectron spectroscopy and theoretical investigations. *J Chem Phys* **143**:224301 (2015). <http://scitation.aip.org/content/aip/journal/jcp/143/22/10.1063/1.4936252>
- 21) Dzamukova MR, Naumenko EA, Lvov YM, and Fakhrullin RF. Enzyme-activated intracellular drug delivery with tubule clay nanoformulation. *Scien Rep (Nature Publ)* **5**:10560 (2015). <https://www.ncbi.nlm.nih.gov/pmc/articles/PMC4432568/>
- 22) Qian B, Hu J, Liu J, Han Z, Zhang P, Guo L, Jiang X, Zou T, Zhu M, Dela Cruz CR, Ke X and Mao ZQ. Weak ferromagnetism of $\text{Cu}_x\text{Fe}_{1+y}\text{As}$ and its evolution with Co doping. *Phys Rev B* **91**:014504 (2015). <http://journals.aps.org/prb/pdf/10.1103/PhysRevB.91.014504>
- 23) Wang H, Lou W, Luo J, Wei J, Liu Y, Ortmann JE, and Mao ZQ. Enhanced superconductivity at the interface of W/Sr₂RuO₄ point contacts. *Phys Rev B* **91**:184514 (2015). <http://journals.aps.org/prb/pdf/10.1103/PhysRevB.91.184514>

Papers Recently Submitted:

- 1) Dhital C, Khan MA, Saghayezhian M, Phelan WA, Young DP, Jin RY, and DiTusa JF. Effect of negative chemical pressure on the prototypical itinerant magnet MnSi (submitted 2016).
- 2) Du P, Li A, Li X, Zhang Y, Do C, He L, Rick S, John VT, Kumar R, and Zhang DH. Aggregation of cyclic polypeptoids bearing Zwitterionic end-groups with attractive dipole-dipole and solvophobic interactions: A study by small-angle neutron scattering and molecular dynamics simulation (submitted).
- 3) Liu JY, Hu J, Zhang Q, Graf D, Cao HB, Radmanesh SMA, Adams DJ, Zhu YL, Cheng GF, Liu X, Phelan WA, Wei J, Jaime M, Balakirev F, Tennant DA, DiTusa JF, Chiorescu I, Spinu L, and Mao ZQ. Discovery of a magnetic topological semimetal $\text{Sr}_{1-y}\text{Mn}_{1-z}\text{Sb}_2$ ($y, z < 0.10$). *Nat. Mat.* (submitted).
- 4) Owoseni O, Zhang Y, He J, Li X, Lal J, Raghavan S, Bose A, and John V. Nanostructured amphiphile mesophases as buoyant gel dispersants (submitted 2016).
- 5) Owoseni O, Omarova M, Zhang Y, McPherson GL, Zhang DH, and John VT. Emulsion stabilization mechanisms and effectiveness of buoyant gel dispersants in oil spill treatment (submitted).
- 6) Xuan S, Lee CH, Chen C, Doyle AB, Zhang Y, Li G, John VT, Hayes D, and Zhang D. Design, synthesis and characterization of polypeptoid thermogels and investigation of stem cell and protein encapsulation. *J Am Chem Soc* (submitted 2015).

- 7) Ying YA, Zakrzewski BM, Cai X, Mills S, Yan X, Staley NE, Wang Z, Sun WF, Mao ZQ, and Liu Y. Sensitive Josephson junction detection of chiral edge currents in Sr_2RuO_4 . *Appl Phys Lett* (submitted 2016).
- 8) Cai X, Ying YA, Ortmann JE, Sun WF, Mao ZQ, and Liu Y. Magnetoresistance oscillations and the half-flux-quantum state in spin triplet superconductor Sr_2RuO_4 (submitted).
- 9) Hanke T, Singh UR, Cornils L, Manna S, Kamlapure A, Bremholm M, Hedegaard EMJ, Iversen BB, Hofmann P, Hu J, Wiebe J, Mao Z, and Wiesendanger R. Reorientation of the bicollinear antiferromagnetic structure at the surface of Fe_{1+y}Te bulk and thin films. *Nat Comm* (submitted).
- 10) Liu JY, Hu J, Graf D, Zou T, Zhu M, Shi Y, Che S, Radmanesh SMA, Lau CN, Spinu L, Chiorescu I, Cao H, Ke X, and Mao ZQ. Unusual interlayer quantum transport behavior caused by the zeoth Landau level in YbMnBi_2 . *Nat Comm* (submitted).
- 11) Wang H, Luo J, Lou W, Wei J, Ortmann JE, Mao ZQ, and Liu Y. Probing chiral superconductivity in Sr_2RuO_4 underneath the surface by point contact measurements. *New J of Phys* (submitted).

Vortex Lattices Studies in Type-II Superconductors

M. R. Eskildsen, Department of Physics, University of Notre Dame

Program Scope

The main thrust of the program has been on using small-angle neutron scattering (SANS) to vortices and the vortex lattice (VL) in type-II superconductors. These studies had a dual focus: (a) Properties of vortex matter, with an emphasis on the kinematic and structural properties of metastable VL phases. The metastable phases constitute an entirely new kind of collective vortex behavior, and in a broader context falls in the category of out-of-equilibrium phenomena. (b) Using the VL as a probe of the superconducting state in unconventional (exotic) and/or novel superconductors. This has included materials that exhibit triplet pairing, member of the pnictide and chalcogenide superconductors and more recently topological superconductors. Moving forward, there is an effort to extend the scope to include other long-range magnetic structures (skyrmions).

Recent Progress

Kinematic and structural properties of metastable vortex lattice phases in MgB₂. The metastable VL phases observed in MgB₂ are not due to pinning, but constitute an entirely novel kind of collective vortex behavior.¹ We have used a stop-motion technique, imaging the VL between successive applications of AC magnetic field cycles, which allow us to perform a detailed study of how the metastable VL is driven back to the ground state. Our results show a dichotomy in the behavior for the metastable configurations induced by crossing the equilibrium, second order phase transition in different directions. For a metastable state induced by super heating, the VL returns to the ground state through a continuous domain rotation, Fig. 1(a). In contrast, in the super cooled case, the transition to the ground state takes on a first order nature with VL ground state domains that nucleate and grow at their final orientation, Fig. 1(b). In the latter case the metastable VL volume fraction may be determined, and is found to follow a power law as shown in Fig. 1(c). Here the exponent increase with increasing AC field amplitude. Both metastable and ground state configurations show correlations along the field (vortex) direction that are comparable to the sample thickness. Finally, spatially resolved measurements (scanning-SANS) shows a spatial variation in the VL domain population on length scales of the order 100 μm , Fig. 1(d).

Superconducting order parameter in UPt₃. With three different mixed (vortex) phases the heavy-fermion material UPt₃ is a paradigm for unconventional superconductivity, and definitive understanding of the superconducting state in this material has remained elusive.² The order

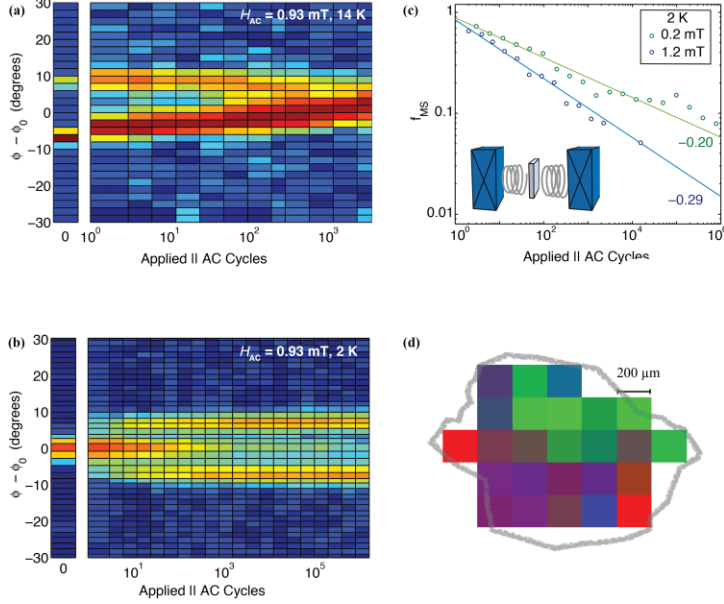


Fig. 1 VL metastability in MgB₂. Evolution of respectively a super heated (a) and super cooled (b) VL, from the metastable configuration (left) to the ground state (right) as a function of applied AC field cycles. In the super cooled case the metastable volume fraction (f_{MS}) follows a power law (c). Spatially resolved SANS measurements (d) show variation in the VL domain population, indicated by a RGB color coding.

an order parameter chirality that is in the same/opposite sense as the VL supercurrent circulation. Our results provide direct, bulk evidence for broken time reversal symmetry in the B-phase of UPt₃ in non-zero fields.

Superconducting anisotropy and multiband superconductivity in Sr₂RuO₄ and KFe₂As₂.

Triplet pairing has also been suggested for Sr₂RuO₄, but like in the case for UPt₃ experiments to determine the detailed structure of the order parameter leads to seemingly contradictory results. One open question is which of the three Fermi surface sheets are the one(s) primarily responsible

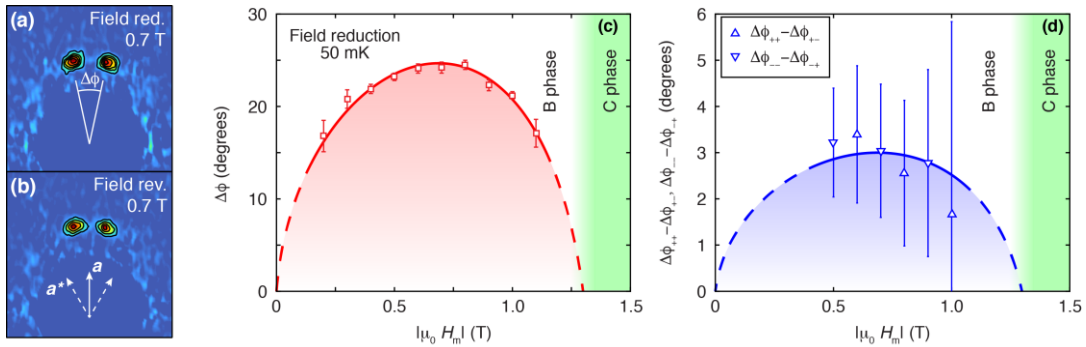


Fig. 2 VL rotation in the B phase of UPt₃. Panels (a) and (b) show diffraction patterns following respectively a field reduction and field reversal, with the splitting angle defined in (b). The VL rotation for both field histories has a maximum at ~ 0.7 T and extrapolates to zero at 0 T and in the vicinity of the B-to-C transition, shown in (c) for the field reduction case. The VL rotation differs for the field reduction and field reversal (d).

parameter structure that is consistent with a number of experiments is an odd-parity, f -wave orbital state. This order parameter is chiral, and breaks time reversal symmetry in the low-temperature B phase. We have focused on SANS measurements with $\mathbf{H} \parallel \mathbf{c}$, where the VL configuration is most sensitive to small changes in the superconducting properties. We discovered a previously unknown field-induced VL rotation in the B phase, Fig. 2(a-c). Furthermore, the magnitude of the VL rotation show a subtle magnetic field history dependence; VLS prepared with the field parallel or anti-parallel with respect to initial direction with which one enters the B phase are rotated by different amounts, Fig. 2(d). This indicates an intrinsic degree of freedom for the vortex cores, possibly related to

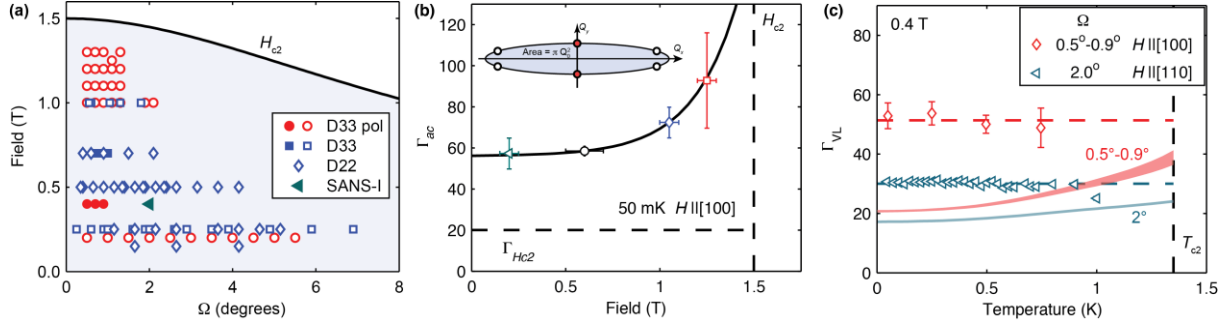


Fig. 3 Superconducting anisotropy in Sr_2RuO_4 . Extensive measurements were performed in the H - Ω phase diagram (a) as well as a function of temperature (solid symbols). The superconducting anisotropy (Γ_{ac}) increases with field, indicating multiband effects (b). The insert in (b) shows how the VL anisotropy (Γ_{VL}) is determined from the position of the Bragg peaks. No temperature dependence of Γ_{VL} (and by extension (Γ_{ac})) was observed (c).

for the unconventional superconductivity in this material. Previously we have shown that the intrinsic superconducting anisotropy (Γ_{ac}) ~ 60 , greatly exceeding the upper critical field anisotropy ~ 20 .³ This suggests Pauli limiting which is difficult to reconcile with triplet pairing. We have extended SANS measurement significantly, to both higher temperatures and fields, Fig. 3(a). Our results show a Γ_{ac} that increases even further with increasing field as seen in Fig. 3(b), indicating that superconductivity on some Fermi surface sheets are suppressed. In contrast, no temperature dependence was observed, Fig. 3(c).

Building on the experience described above, we used SANS to measure the superconducting anisotropy in KFe_2As_2 .⁴ Like for Sr_2RuO_4 , Γ_{ac} was found to be strongly field dependent indicating multi-band superconductivity, and with a value exceeding the upper critical field anisotropy that provide further support for Pauli limiting in KFe_2As_2 for $H \perp c$. In addition, from the ratio of scattered intensities due to the longitudinal and transverse VL field modulation, we were able to determine the effect of Pauli paramagnetism on the unpaired quasiparticles in the vortex cores. This is the first instance where these effects have been^[SEP]observed simultaneously and in a comprehensive manner by a single measurement technique.

Future Plans

Continued studies of the metastable VL phases. We will continue studies of the kinematics involved with the metastable-to-ground state transition, and in particular the power law behavior shown in Fig. 1(c). Emphasis will be put to establish scaling relations between the AC field amplitude, which can be considered as an effective “temperature”, and the number of AC cycles applied (effective “time”). The impact of these studies may ultimately extend beyond the vortex field, providing a model for non-equilibrium matter in general. SANS studies will be combined with molecular dynamics simulations in collaboration with Cynthia and Charles Reichhardt from LANL.

Extending UPT_3 measurements to the C phase. From an experimental point of view the C phase is difficult to access, and techniques that can probe this phase together with the B-to-C

phase transition are very scarce. Indeed, most of the published studies of UPt_3 have been carried out in the zero-field Meissner phase. Extending SANS measurements into the C phase presents a tremendous opportunity, which was recently made possible using the new SANS magnet acquired by ORNL. As discussed above SANS studies of the VL have provided experimental evidence for an internal degree of freedom in the vortex core structure in the mixed state B phase. From a technical perspective this establishes SANS as being sensitive to BTRS phenomena.

Vortices in topological superconductors (TSCs). Topology has recently emerged as a central concept for understanding material properties, UPt_3 and Sr_2RuO_4 . In the case of topological superconductors (TSCs), there is therefore an opportunity to provide a much-needed characterization of the bulk properties of actual candidate materials from which the surface properties are ultimately derived. Currently, the theoretical discussion of TSCs is based on group theoretical arguments, with predictions for gap structures that can be directly tested by SANS measurements.

Topologically stable large-scale magnetic structures (skyrmions). Since the initial discovery of a skyrmion lattice (SkL) in bulk $MnSi$, this has been observed in a range of other conducting, semiconducting and insulating materials, and includes both Bloch- and Néel-type of skyrmions. We will apply our expertise with SANS to begin studies skyrmions and related magnetic structures, with a focus on how these states may be manipulated by dc and ac electric and magnetic fields. This will build on our experience with metastable VL phases.

References

1. P. Das *et al.*, Phys. Rev. Lett. **108**, 167001 (2012); C. Rastovski *et al.*, Phys. Rev. Lett. **111**, 087003 (2013).
2. J.D. Strand *et al.*, Science **328**, 1368 (2010); E.R. Schemm *et al.*, Science **345**, 190 (2014).
3. C. Rastovski *et al.*, Phys. Rev. Lett. **111**, 087003 (2013).
4. S.J. Kuhn *et al.*, Phys. Rev. B **93**, 104527 (2016).

Publications

W.J. Gannon, W.P. Halperin, C. Rastovski, K.J. Schlesinger, J. Hlevyack, M.R. Eskildsen, A.B. Vorontsov, J. Gavilano, U. Gasser, and G. Nagy, “Nodal gap structure and order parameter symmetry of the unconventional superconductor UPt_3 from Small Angle Neutron Scattering,” *New J. Phys.* **17**, 023041 (2015).

M. Marzali Bermúdez, M.R. Eskildsen, M. Bartkowiak, G. Nagy, V. Bekeris, and G. Pasquini, “Dynamic reorganization of vortex matter into partially disordered lattices,” *Phys. Rev. Lett.* **115**, 067001 (2015).

S.J. Kuhn, H. Kawano-Furukawa, E. Jellyman, R. Riyat, E.M. Forgan, M. Ono, K. Kihou, C.H. Lee, F. Hardy, P. Adelman, Th. Wolf, C. Meingast, J. Gavilano, and M.R. Eskildsen, “Simultaneous Evidence for Pauli Paramagnetic Effects and Multiband Superconductivity in KFe_2As_2 by Small-Angle Neutron Scattering Studies of the Vortex Lattice,” *Phys. Rev. B* **93**, 104527 (2016).

S.J. Kuhn, M.K. Kidder, W.M. Chance, C. de la Cruz, M.A. McGuire, D.S. Parker, L. Li, L. Debeer-Schmitt, J. Ermentrout, K. Littrell, M.R. Eskildsen, and A.S. Sefat, “FeS: Structure and Composition Relations to Superconductivity and Magnetism,” arXiv:1603.01598.

Neutron and X-Ray Studies of Spin and Charge Manipulation in Magnetic Nanostructures

Eric E. Fullerton¹ and Sunil Sinha²

¹Departments of Electrical and Computer Engineering and NanoEngineering, University of California, San Diego. La Jolla, CA 92093-0401

²Department of Physics. University of California, San Diego. La Jolla, CA 92093

Program Scope

Electronic and magnetic materials constitute some of the most important and highly tunable materials systems currently being studied, and have been associated with a wide range of new scientific discoveries. Understanding of the dynamics and the fundamental nanoscale physics of these materials is a crucial cornerstone for developing ways in which electronic and magnetic order parameters can be designed, controlled and manipulated. By combining skills in neutron and synchrotron techniques with sample fabrication, magnetic and transport measurements in films, nanostructures and devices we probe fundamental properties of nanoscale magnetic materials. The ongoing research has two major research thrusts:

- Competing, frustrated and disordered magnetic systems.
- Ultrafast structure/magnetism dynamics.

Within these thrusts we have we have ongoing research and future plans in the following areas:

A. Chiral magnetic structure in Fe/Gd thin films where we describe skyrmion formation in this system, the magnetic properties that give rise to chiral structures, their dynamics and their interaction with current.

B. FeRh studies where we probe the nature of the magnetic phase transition at the surface and nanostructured FeRh films and describe upcoming neutron scattering experiments.

C. Study of the Spin Glass Transition using X-ray Photon Correlation Spectroscopy where we highlight recent and promising XPCS measurement of magnetic spin glasses.

D. Ultrafast magnetic-structural interactions describes recently published work on the excitation of phonons by the ultrafast demagnetization of Cr.

E. Coercive Field Enhancement in Ni films on a V₂O₃ substrate at the Metal-Insulator Transition of V₂O₃ describes ongoing neutron scattering measurement of the interplay of magnetic order and the MIT in vanadium oxide/nickel bilayers.

Recent Progress

A. We have used Fe/Gd multilayers as a model system to study chiral nano structures and we have probed them by neutron reflectivity, resonant soft x-ray scattering, resonant soft x-ray imaging, XPCS, Lorentz TEM, ferromagnetic resonance, magneto-transport and modeling. The samples exhibit stripe domain patterns in zero applied field but arrange into a hexagonal skyrmion lattice with modest perpendicular fields as seen in Lorentz TEM (Fig. 1). The skyrmion size is <100 nm and depending on the field cycling we can observe bubbles with winding number ($W=0$), skyrmions ($W=1$) and bi-skyrmions which are the merging of two skyrmions with opposite chirality ($W=2$) In addition to studying the interesting physics of topological spin structure such as resonant properties and interaction with current we are also interested in understanding the magnetic properties that lead to these spin structures. Our results provide a guideline of magnetic properties required to stabilize these spin textures in thin-film ferromagnets and ferrimagnets.

We have used X-ray Photon Correlation Spectroscopy (XPCS) to study the spin fluctuation dynamics of skyrmions in the Fe/Gd systems. Until recently, XPCS has been used to measure relatively slow fluctuations, such as in soft matter or glassy systems. However, recent developments at LCLS XFEL source at SLAC have enabled it to fire two successive pulses at the sample with controlled delays of the order of nanoseconds. This has the consequence that the speckle pattern on the detector will correspond to the sum of the scattered intensities from the sample at time $t = 0$ and $t = \tau$ the delay time. Due to the sample dynamics and corresponding speckle fluctuations, this will result in a decreased contrast in the speckle patterns as a function of τ . The contrast can be obtained by fitting the probabilities of 1, 2, 3,etc. photons per detector pixel as a function of mean photon density per pixel with the formula [1], and the contrast factor β as a function of τ can be used to obtain a function similar to the usual 2-time intensity autocorrelation function $g_2(q, \tau)$ [2]. Two pulses from the source with delays ranging from 1 nsec to 25 nsecs were used to record the speckle patterns from the sample and initial results are shown the first XPCS measurements at these timescales. The contrast factor shows damped oscillatory behavior as a function of τ roughly consistent with the resonant frequency obtained in the ferromagnetic resonance studies.

B. We have studied the heterogeneous nature of the phase transition in FeRh films where results were recently published in Nat. Comm. **7**, 13113 (2016). Unlike bulk single crystals, measurement of thin films across the phase transition gives a continuous smooth transition that is relatively broad (~10K). This is a result of phase-separated domains with different transition temperatures. The broadening of the transition is linked to heterogeneity originating from local structural variations. However when the films were patterned into wires whose lateral dimensions are similar to the characteristic domain size seen in imaging FeRh films, we observe a quantitative change in the transition behavior. When cooling the sample through the FM-AFM transition we observed for 2-4 μm long wires a single jump in the resistance indicating that the reversal becomes largely collective. Conversely when warming, the transition is relatively broad exhibiting many small discrete steps suggesting that here the transition is governed by local nucleation. We understand this behavior as the qualitative difference in interplay between ferromagnetic and antiferromagnetic exchange correlations in the presence of disorder.

C. As discussed in our last renewal proposal, the spin-glass problem was never resolved experimentally, as the neutron scattering experiments (including the classic neutron spin echo experiments of Mezei and Murani [3] could never probe with good enough energy resolution or long enough time scales to resolve whether a transition to an actual static disordered ground state occurred. XPCS using Resonant X-ray Magnetic Scattering offers the ability to probe much longer

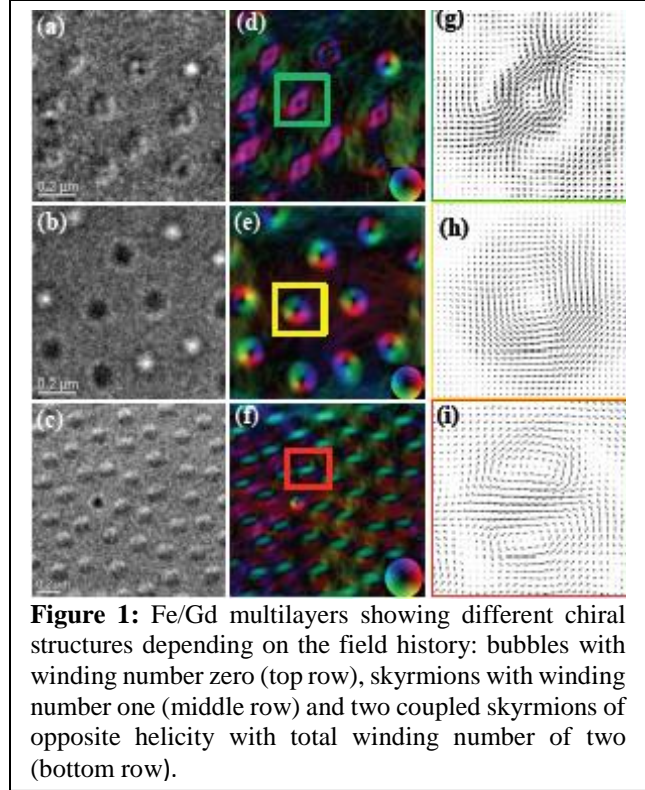


Figure 1: Fe/Gd multilayers showing different chiral structures depending on the field history: bubbles with winding number zero (top row), skyrmions with winding number one (middle row) and two coupled skyrmions of opposite helicity with total winding number of two (bottom row).

time scales for the magnetic fluctuations as the spin glass “freezes”. Accordingly, we have made three runs at the CSX-1 (Soft Coherent X-ray Scattering) beam line at the NSLS II Light Source at Brookhaven National Laboratory to study the classic spin glass alloys $\text{Cu}(1-x)\text{Mn}(x)$. For the first 2 runs (at which we were actually the first outside users of the NSLS II facility), we were plagued by problems associated with the new beamline, detector and associated software problems, as well as considerable synchrotron down time during the run, and unexplained beam-induced surface effects on our thin film samples at grazing incidence in reflection geometry. For the third run (carried out at the time of writing this abstract), we took fresh samples (showing clear spin-glass transitions by magnetometry) made on Silicon Nitride substrates to be used in transmission geometry (as we have to work with soft X-rays at the Mn L3 edge at 636 eV) on a beamline which was much improved and with better data analysis software. We were able to study 16% Mn and 12% Mn samples. We have preliminary indications that we were indeed seeing magnetic x-ray scattering by studying the q-dependence of the small angle scattering from the sample with X-ray photon energies on and off the Mn resonance as well as indications of slow spin fluctuations above the spin glass transition on time scales of ~ 100 seconds or greater.

D. We have continued our investigations on ultrafast magnetic-structural interactions which we have studied in two systems including the charge-density-wave (CDW) order in Cr and the lattice structure in FePt nanoparticles. We find that ultra-fast demagnetization by an optical pulse can drive strong structural excitations. We recently completed our work on the Cr CDW published in *Phys. Rev. Lett.* **117**, 056401 (2016). In this paper we used the unique capabilities now possible with hard x-ray free-electron lasers to directly observe a dramatic enhancement of the CDW amplitude in chromium following photoexcitation: 30% above its maximum value in equilibrium. We identify the ultrafast underlying physical processes by discerning multiple time scales and explain our results by three main processes, referred to as “dynamic electron-phonon interaction”.

E. We are studying via magnetic neutron scattering the magnetic domains induced in a Ni film by coupling via strain to the structural transition in a V_2O_3 film on which it is deposited. Recent magnetization results show a roughly 2-fold increase in the magnetic coercive field as the V_2O_3 was taken below its metal-insulator transition (MIT) at 160K. At the transition the group of Schuller at UCSD observed a peak within a narrow temperature range in the coercivity which was roughly four times the coercivity at higher temperatures. de la Venta et al. [4], attributed the coupling of magnetism with structural phase transformation to interfacial stress. Modeling predicts magnetic domain sizes of 100 nm during magnetization reversal at the MIT, and suggests a relationship between metal-insulating domains (electronic phase separation) in the V_2O_3 film and magnetic domains in the Ni film. In order to look for scattering signatures of these domains, we first undertook an unpolarized small-angle scattering experiment on this system on the SANS spectrometer at the Cold Neutron Research Facility at NIST. The SANS was done in the usual transmission geometry. However, these results did not show an unambiguous signal of magnetic domain scattering. We therefore subsequently obtained beam time on the polarized neutron SANS instrument at NIST and studied these samples again. The results showed magnetic SANS scattering in the vicinity of the transition, but only from relatively large magnetic domains of size microns or greater, which was somewhat beyond the capability of the SANS instrument to determine definitively.

Future Plans

A. We have ongoing neutron scattering, resonant x-ray imaging and resonant x-ray scattering experiments on the Fe/Gd system. We plan to directly probe the dynamics of the skyrmion phase

building the on magnetic resonance experiments and magnetic modeling. To directly probe the magnetic response at these characteristic frequency we designed a wire sample on a SiN membrane with Fe/Gd layer that hosts the skyrmion phase capped with a Au layer. Passing an *a.c.* current that primarily flows in the Au layer puts an *a.c.* magnetic field on the magnetic sample, and we will image the magnetic response as a function of frequency. These results will be combined with follow-up experiments at the LCLS XFEL source at SLAC on XPCS and more detailed theoretical analysis of the data.

We will further explore the direct role of current on the topological nature of the skyrmions. This interaction can come in two forms, either a spin transfer torque (STT) where the current directly flows in the Fe/Gd film and interacts with the skyrmions and spin orbit torques (SOT) where spin currents flow from the Ta capping layer and interact with the chiral Neel character of the wall. Finally, we will complete analysis of the neutron reflectivity measurements at SNS to quantify the depth dependent magnetic properties in the stripe and skyrmion phases.

B. We now have two SNS beamtimes scheduled (one in December 2016 and one in January 2017) to probe the phase transition phenomena in FeRh. The first beamtime will use neutron reflectivity for FeRh films with different structure: continuous films and laterally structured films. The second beamtime (Jan. 2017) will be diffraction results where we will measure the structural and magnetic (both antiferromagnetic and ferromagnetic) correlations as a function of temperature. This will allow us to directly measure and link the antiferromagnetic correlations in the film to switching volumes at the phase transition.

C. We plan to build on the exciting results of seeing magnetic x-ray scattering from a Cu-Mn spin glass samples. We preliminary indications of slow spin fluctuations above the spin glass transition on time scales of ~ 100 seconds or greater await confirmation with more detailed analysis. We further plan to study a range of Mn concentrations.

D. For the charge density wave order of Cr a further interesting question is whether the dynamic electron-phonon interaction can be combined with repeated photoexcitation to maintain the coherent lattice oscillation or to achieve an even higher enhancement of the charge density wave amplitude. Our results also raise fundamental questions regarding the dynamics of the magnetic ordering and the electronic structure of the system. We further will explore the direct photo-excitation of standing phonon modes in thin Cr films and measure their dispersion. We plan to extend these results to other systems where there is strong coupling of the magnetism and structure (i.e. magnetostriction).

E. In order to look for scattering signatures of the domains at the transition, we first undertook an unpolarized small-angle scattering experiment on this system on the SANS spectrometer at the Cold Neutron Research Facility at NIST. However, these results did not show an unambiguous signal of magnetic domain scattering. We have now obtained beam time (November, 2016) on the magnetic reflectometer at SNS to carry out grazing incidence off-specular neutron scattering studies on these samples. In this geometry we are in a position to measure domain sizes of up to several microns, if there is enough intensity in the diffuse scattering. These studies are being carried out in collaboration with M. Fitzsimmons of ORNL.

References

- [1]. Speckle Phenomena in Optics: Theory and Applications, J.W. Goodman (Roberts and Co., Englewood, Colo. 2007).
- [2]. C. Gutt et al., *Optics Express* **17**, 55 (2009)
- [3]. F. Mezei and A.P. Murani, *J. Magn. Magn. Mat.* **14**, 211 (1979)
- [4]. J. de la Venta, et al., *Appl. Phys. Lett.* **104**, 062410 (2014).

Publications

- S. K. Sinha, Z. Jiang, and L. B. Lurio, “X-ray Photon Correlation Spectroscopy Studies of Surfaces and Thin Films.” *Adv. Mater.* **26**, 7764-7785 (2014)
- A.E. Berkowitz, S.K. Sinha, E.E. Fullerton and D.J. Smith, “Exchange bias mediated by interfacial nanoparticles”, *J. Appl. Phys.* **117**, 172607-1-6 (2015).
- M. Urbánek *et al.*, “Dynamics and efficiency of magnetic vortex circulation reversal”, *Phys. Rev. B* **91**, 094415 (2015).
- F. Pressacco, *et al.*, Accessing the magnetic susceptibility of FeRh on a sub-nanosecond time scale, in *Ultrafast Magnetism I*, J.Y. Bigot, et al., Eds. 2015. p. 294-296.
- A. Singer *et al.*, “Condensation of collective charge ordering in chromium” *Phys. Rev. B* **91**, 115134-1-8 (2015).
- T. Fan, et al., “Bright circularly polarized soft X-ray high harmonics for X-ray magnetic circular dichroism” *Proc. Nat. Acad. Sci.* **112**, 14206-14211 (2015).
- J. C. T. Lee, *et al.* “Synthesizing Skyrmion Molecules in Fe-Gd Thin Films”, *Appl. Phys. Lett.*, **109**, 022402 (2016).
- V. Uhlíř, J. A. Arregi and E. E. Fullerton, “Colossal magnetic phase transition asymmetry in mesoscale FeRh stripes”, *Nat. Comm.* **7**, 13113 (2016).
- F. Pressacco, V. Uhlíř, M. Gatti, A. Bendounan, E. E. Fullerton, and F. Sirotti, “Stable room-temperature ferromagnetic phase at the FeRh(100) surface”, *Sci. Rep.* **6**, 22383 (2016).
- A. Singer, *et al.* “Enhancement of charge ordering by dynamic electron-phonon interaction”, *Phys. Rev. Lett.* **117**, 056401 (2016).
- A. Singer, *et al.*, “Phase coexistence and pinning of charge density waves by interfaces in chromium”, *Phys. Rev. B*, in press (2016).
- K. Chesnel, A. Safsten, M. Rytting and E. E. Fullerton, “Shaping nanoscale magnetic domain memory by field cooling” *Nat. Comm.* **7**, 11648-1-8 (2016).
- J. J. Chess, S. A. Montoya, E. E. Fullerton, and B. J. McMorran, “Determination of Domain Wall Chirality Using in situ Lorentz Transmission Electron Microscopy”, *AIP Advances*, in press (2016).

Publications: under review

- S. A. Montoya, et al., “Tailoring magnetic energies to form skyrmions and skyrmion lattices”, *Phys. Rev. X*, under review, arXiv:1608.01368.
- J. J. Chess, *et al.*, “A streamlined approach to mapping the magnetic induction of skyrmionic materials”, *Ultramicroscopy*, under review; arXiv:1608.06000
- H. Reid, *et al.*, “Ultrafast spin-lattice motion of laser-heated L₁₀ FePt nanoparticles”, *Proc. Nat. Acad. Sci.*, under review: arXiv: 1602.04519.

Vibrational Thermodynamics of Materials

**Brent Fultz, Rawn Professor of Materials Science and Applied Physics
California Institute of Technology, W. M. Keck Laboratory, Pasadena CA 91125 USA**

Program Scope

The primary objective is to understand the origin of vibrational entropy, assess its importance to the Gibbs free energies of materials, and assess its effects on phase transformations. The work is designed to address cases where vibrational entropy is expected to be large and interesting, especially at high temperatures where there can be significant effects from anharmonicity and electron-phonon interactions. The work also focuses on the importance of vibrational dynamics for other thermophysical properties such as thermal expansion.

This is primarily an experimental investigation based on inelastic neutron scattering measurements performed at national user facilities, especially the Spallation Neutron Source, ORNL. Inelastic neutron scattering, in conjunction with computation, is the most powerful approach today for understanding the different contributions to vibrational entropy. Much of the work involves experimental determinations of accurate phonon densities of states (DOS). From DOS curves obtained at different temperatures, we obtain the temperature dependences of vibrational entropies of materials. Measurements on single crystals are also performed, and these offer a more detailed understanding of why phonons undergo changes with temperature.

Computational methods such as ab-initio molecular dynamics simulations help elucidate the underlying reasons for differences in entropies. So far, these methods have been able to accommodate large anharmonicities beyond the realm of phonon-phonon perturbation theory. At high temperatures there is a hierarchy of anharmonic effects, and we have methods for separating them into quasiharmonic entropy, anharmonic entropy, and effects of electron-phonon interactions. Negative thermal expansion associated with highly anharmonic behavior is also within the scope of the program.

Recent Progress

Despite the widespread use of silicon in modern technology, its peculiar thermal expansion is still not well understood. The assumption of harmonic vibrations adapted to the specific volume at temperature has become accepted for simulating the thermal expansion, but this "quasiharmonic model" has given ambiguous interpretations for microscopic mechanisms [1-3]. To test the atomistic mechanisms behind the thermal expansion of silicon, we performed inelastic neutron scattering experiments on a single crystal of silicon to measure the changes in lattice dynamics up to 1500 K. Figure 1a is from one temperature of this data set from the ARCS instrument. Figure 1b shows that our state-of-the-art ab initio calculations (sTDEP [4]), which account for phonon anharmonicity, reproduced well the measured shifts of individual phonons

with temperature. In contrast, the quasiharmonic approximation (QH) gave results of the wrong sign. This was true for most of the transverse phonon modes throughout the Brillouin zone. Curiously, the quasiharmonic model was found to predict the correct thermal expansion owing to a surprising cancellation of erroneous contributions from individual phonons [5].

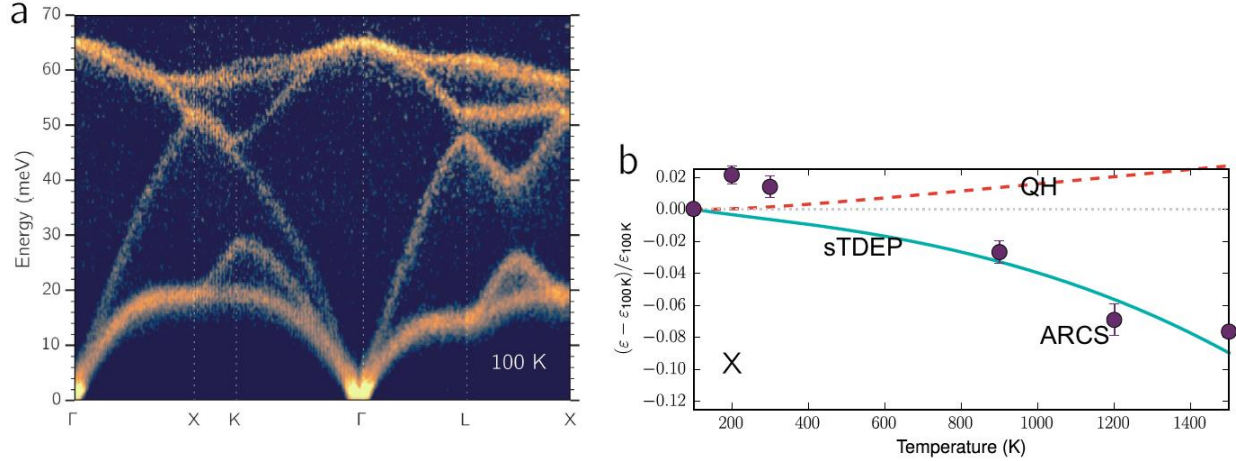


Fig. 1 (a) Experimental phonon dispersions from Si single crystal at 100 K, assembled from multiple Brillouin zones and corrected approximately for thermal factor. (b) Transverse mode at X point versus temperature, showing the incorrect sign of the temperature dependence for the quasiharmonic (QH) calculations, whereas anharmonic calculations (sTDEP) are much more consistent with the experimental trend. From [5].

Inelastic neutron scattering, nuclear resonant inelastic x-ray scattering, with support from ab-initio molecular dynamics simulations, showed an anomalous thermal softening of a transverse phonon at the M point in B2-ordered FeTi [6]. This anomalous temperature dependence could not be explained by the usual phenomena of quasiharmonic softening, phonon-phonon interactions, or electron-phonon interactions calculated at low temperatures. A computational investigation showed that the Fermi surface undergoes a novel thermally-driven electronic topological transition (Fig. 2a) – new features arise at the R point of the Fermi surface at high temperatures. This thermally-induced electronic topological transition causes an increased electronic screening for the atom displacements in the anomalous phonon modes. The spanning vectors from X to R (along [110]) show an excellent match with the mode softenings (Fig. 2b).

This thermally-driven electronic topological transition (ETT) occurs because thermal atom displacements cause a lowering of electron states near the R-point, and temperature allows electrons to occupy states above the Fermi level. The ETT alters the Gibbs free energy of FeTi. It should also couple the processes of electron transport and phonon transport at high temperatures. Thermally-driven electronic topological transitions are not expected to be universal, but they may occur in other materials that have electronic states within tenths of an eV near the Fermi level.

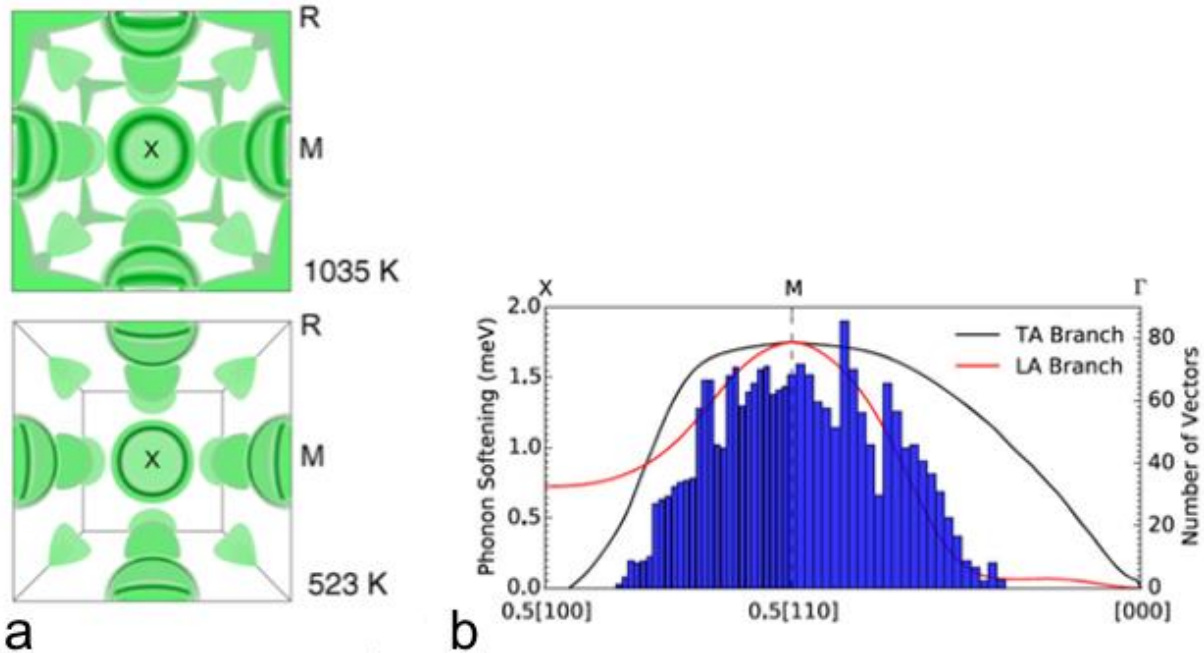


Fig. a (a) Fermi surface of B2 FeTi at 523 K and 1035 K, showing the new features at R points at high temperatures. (b) Distribution of spanning vectors from X to R of the Fermi surface at 1035 K, and thermal shifts of the TA and LA phonons near the M point. From [6].

Future Plans

In earlier work we reported that the thermal softening of phonons in transition metal alloys depended on the electronic density of states at the Fermi level [7-9]. In general, the greater the electronic density of states, the more effective the electronic screening of ion core displacements, and the softer are the phonon frequencies. Such effects were larger in some alloys than others, and we have begun to revisit these cases. We expect that some may originate with thermally-driven electronic topological transitions like the one we found in FeTi [6].

The work on our phonon data set of single-crystal silicon is continuing, with a new emphasis on how individual phonon linewidths change with temperature. This study can check the accuracy of calculations of anharmonicity by density functional theory. It is also relevant to thermal transport behavior because phonon linewidths in silicon are dominated by the same phonon-phonon scatterings that give rise to thermal resistivity. The full analysis of thermal conductivity seems beyond our present abilities, but the phonon lifetime information will be of intense interest for other workers who are developing methods to calculate thermal transport.

We are completing a study of phonons in FeGe₂, for which we have data from both powders and a single crystal. It seems that this material exhibits an average behavior that might be interpreted as quasiharmonic, but the individual phonons seem to show different trends with temperature.

References

- [1] S. Wei, C. Li, and M. Chou, "Ab initio calculation of thermodynamic properties of silicon," *Phys. Rev. B* **50**, 14587 (1994).
- [2] C. Xu, C. Wang, C. Chan and K. Ho, "Theory of the thermal expansion of Si and diamond," *Phys. Rev. B* **43**, 5024 (1991).
- [3] Z.-K. Liu, Y. Wang and S. Shang, "Thermal Expansion Anomaly Regulated by Entropy," *Sci. Rep.* **4**, 7043 (2014).
- [4] This is a stochastic variant on the molecular dynamics approach of: O. Hellman, P. Steneteg, I. Abrikosov and S. Simak, "Temperature dependent effective potential method for accurate free energy calculations of solids," *Phys. Rev. B* **87**, 104111 (2013).
- [5] D.S. Kim, O. Hellman, J. Herriman, H.L. Smith, J.Y.Y. Lin, N. Shulumba, J.L. Niedziela, C.W. Li, D.L. Abernathy, and B. Fultz, "Pure phonon anharmonicity and the anomalous thermal expansion of silicon," *Science*, submitted.
- [6] F.C. Yang, J.A. Muñoz, O. Hellman, L. Mauger, M.S. Lucas, S.J. Tracy, M.B. Stone, D.L. Abernathy, Y-M. Xiao and B. Fultz, "Thermally Driven Electronic Topological Transition in FeTi," *Phys. Rev. Lett.* **117**, 076402 (2016)
- [7] O. Delaire, M.G. Kresch, J.A. Munoz, M.S. Lucas, J.Y.Y. Lin, and B. Fultz, "Electron-Phonon Interactions and High-Temperature Thermodynamics of Vanadium and its Alloys", *Phys. Rev. B*, **77**, 214112 (2008).
- [8] O. Delaire, M.S. Lucas, J.A. Munoz, M. Kresch, and B. Fultz, "Adiabatic Electron-Phonon Interaction and High-Temperature Thermodynamics of the A15 Compounds V_3X ", *Phys. Rev. Lett.* **101**, 105504 (2008).
- [9] J. A. Muñoz, M. S. Lucas, O. Delaire, M. L. Winterrose, L. Mauger, Chen W. Li, A. O. Sheets, M. B. Stone, D. L. Abernathy, Yuming Xiao, Paul Chow, and B. Fultz, "Positive vibrational entropy of chemical ordering in FeV" *Phys. Rev. Lett.* **107**, 115501 (2011).

Publications

M. Palumbo, B. Burton, A. Costa e Silva, B. Fultz, B. Grabowski, G. Grimvall, B. Hallstedt, O. Hellmann, B. Lindahl, A. Schneider, P.E.A. Turchi, and W. Xiong, "Thermodynamic modelling of crystalline unary phases," *Physica Status Solidi B* 251, 14 (2014).

Tian Lan, C.-W. Li, J.L. Niedziela, H. Smith, D.L. Abernathy, G.R. Rossman, and B. Fultz, "Anharmonic lattice dynamics of cuprite Ag_2O studied by inelastic neutron scattering and first principles molecular dynamics simulations," *Phys. Rev. B* 89, 054306 (2014).

Chen W. Li, H. Smith, T. Lan, J.A. Muñoz, J.B. Keith, L. Mauger, D. Abernathy, and B. Fultz, "Phonon anharmonicity of monoclinic zirconia and yttrium-stabilized zirconia at elevated temperatures", *Phys. Rev. B* 91, 144302 (2015).

D.S. Kim, H.L. Smith, J.L. Niedziela, C.W. Li, D.L. Abernathy, and B. Fultz, "Phonon Anharmonicity in Silicon from 100 to 1500 K," *Phys. Rev. B* 91, 014307 (2015).

Tian Lan, C.W. Li, O. Hellman, J. A. Muñoz, H. Smith, D.L. Abernathy, and B. Fultz, "Phonon quarticity induced by changes in phonon-tracked hybridization during lattice expansion, and its stabilization of rutile TiO_2 ", *Phys. Rev. B*, 92, 054304 (2015).

Yang Shen, Chen W. Li, Xiaoli Tang, Hillary L. Smith, and B. Fultz, "Phonon Anharmonicity and Components of the Entropy in Palladium and Platinum," *Phys. Rev. B* 93, 241303 (2016).

F.C. Yang, J.A. Muñoz, O. Hellman, L. Mauger, M.S. Lucas, S.J. Tracy, M.B. Stone, D.L. Abernathy, Y-M. Xiao and B. Fultz, "Thermally Driven Electronic Topological Transition in FeTi," *Phys. Rev. Lett.* 117, 076402 (2016).

H.L. Smith, C.W. Li, A. Hoff, G. Garrett, M. Demetriou, M.B. Stone, D.L. Abernathy, Brent Fultz, "Experimental Determination of Configurational and Vibrational Entropy in Amorphous Copper-Zirconium," *Nature Physics*, submitted.

D.S. Kim, O. Hellman, J. Herriman, H.L. Smith, J.Y.Y. Lin, N. Shulumba, J.L. Niedziela, C.W. Li, D.L. Abernathy, and B. Fultz, "Pure phonon anharmonicity and the anomalous thermal expansion of silicon," *Science*, submitted.

Ph.D. Theses

Tian Lan, "Studies of Phonon Anharmonicity in Solids" Ph.D. in Applied Physics, May 6, 2014.

Hillary L. Smith, "Phase Transformations and Entropy of Non-Equilibrium Materials" Ph.D. in Materials Science, May 29, 2014.

Conference Proceedings

R.I. Barabash, G. Kostorz, B. Fultz and P.K. Liaw, "Neutron and X-ray Studies of Advanced Materials VI: Diffraction Centennial and Beyond Foreword," *Metall. Mater. Trans. A* 45, 72-74 (2014).

Jorge A. Muñoz and Brent Fultz, "Miscibility gap and phonon thermodynamics of Fe-Au alloys studied by inelastic neutron scattering and nuclear-resonant inelastic x-ray scattering," *RADIATION PHYSICS: XI International Symposium on Radiation Physics*, AIP Conference Proceedings 1671, 020001 (2015); doi: 10.1063/1.4927178.

New insight into the physics of the cuprates from neutron, X-ray and transport measurements of $\text{HgBa}_2\text{CuO}_{4+\delta}$

Martin Greven (greven@umn.edu)

Center for Quantum Materials and School of Physics and Astronomy
University of Minnesota, Minneapolis, MN 55455

Program Scope

After three decades of research, the cuprate superconductors continue to pose formidable challenges [1]. Among the well over 100 compounds, arguably the most desirable ones for experimental study are the mercury-based materials $\text{HgBa}_2\text{Ca}_{n-1}\text{Cu}_n\text{O}_{2n+\delta}$, which feature the highest superconducting (SC) transition temperatures (T_c) and relatively simple crystal structures. We are uniquely able to grow sizable, high-quality crystals of $\text{HgBa}_2\text{CuO}_{4+\delta}$ (Hg1201; optimal $T_c=97\text{K}$), the first ($n=1$) and simplest member of this materials family, and have recently begun to explore the sister compound $\text{HgBa}_2\text{CaCu}_2\text{O}_{6+\delta}$ (Hg1212; $n=2$; optimal $T_c=126\text{K}$). This is enabling significant research activities aimed to understand the cuprate phase diagram through our neutron, X-ray, and charge transport experiments, and through an extensive network of collaborations. *In 2017, this grant will be subsumed by the new DOE-BES funded Center for Quantum Materials (CQM) at the University of Minnesota (PIs: A.V. Chubukov, R. Fernandes, M. Greven, B. Jalan, C. Leighton). The program scope will increase to include work on related complex oxides, especially on titanates and cobaltites.*

Recent Progress

Evidence for Fermi-liquid (FL) behavior from transport measurements. As part of our crystal characterization work, we are pursuing charge transport measurements. Our most recent accomplishments in this regard include the demonstration of the validity of Kohler's rule for the magnetoresistance (in the pseudogap (PG) regime, for $T < T^{**} < T^*$), which had long been thought to be violated in the cuprates. This supports our prior evidence for FL charge transport in the PG regime [2]. We also refined prior quantum oscillation work by demonstrating the existence of a sole reconstructed Fermi surface pocket in high magnetic fields in underdoped Hg1201 [3]. Most recently, we uncovered that the transport scattering rate remains quadratic across the PG temperature (T^*), upon entering the strange-metal (SM) state, and that this quantity is doping and compound independent, and hence universal. In other words, the scattering mechanism must be the same as in the well-established FL region at high doping [4] (Fig. 1). This points to the distinct possibility that the pseudogap phenomenon signifies the completion of the gradual localization of one hole per planar CuO_2 unit upon cooling [4].

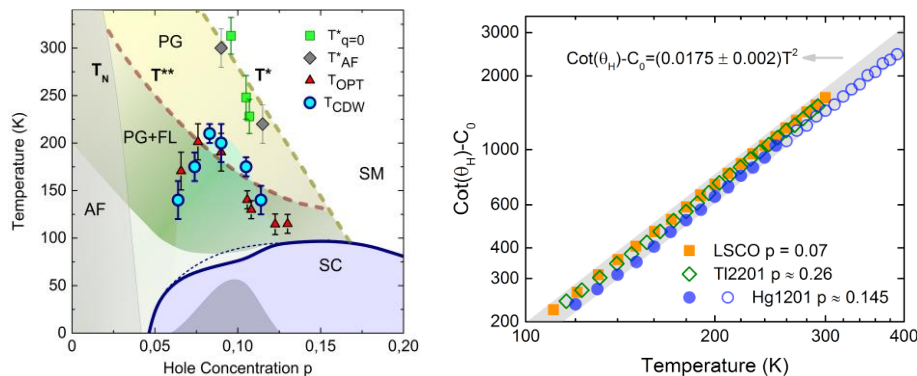


Fig. 1 Left: Hg1201 phase diagram, with SC, SM, PG, and Fermi-liquid (FL+PG) regimes [2,4], charge (T_{cdw} [7,8], T_{opt} [9]) and magnetic (T_{AF} & $T_{q=0}$ [5,6]) characteristic temperatures. **Right:** Analysis of cotangent of Hall angle reveals universal FL transport scattering rate throughout the phase diagram [4].

Pseudogap signatures from inelastic neutron scattering. Similar to our transport results, the study of Hg1201 enables us to reveal the underlying AF response of the quintessential copper-oxygen planes most clearly. Surprisingly, we observed commensurate, gapped correlations associated with the PG formation (Fig. 2) at two distinct doping levels [5,6]. This is contrasted by the incommensurate “hourglass” response typically seen in the normal state and often interpreted in terms of charge-spin stripes in lower- T_c cuprates such as $\text{La}_{2-x}\text{Sr}_x\text{CuO}_4$. Remarkably, AF correlations grow significantly below a characteristic temperature T_{AF} that is indistinguishable from T^* (Fig. 1 & 2). It is a distinct possibility that AF fluctuations drive the unconventional $q=0$ magnetism previously observed below $T_{q=0}$, and the CDW order and superconductivity at lower temperatures. Near optimal doping, Hg1201 develops a resonance and an hourglass dispersion in the SC state [6]. This phenomenology is reminiscent of that exhibited by bilayer cuprates. Irrespective of doping and compound, the resonance spectral weight scales linearly with the binding energy of a putative spin-exciton described by an itinerant-spin formalism [6].

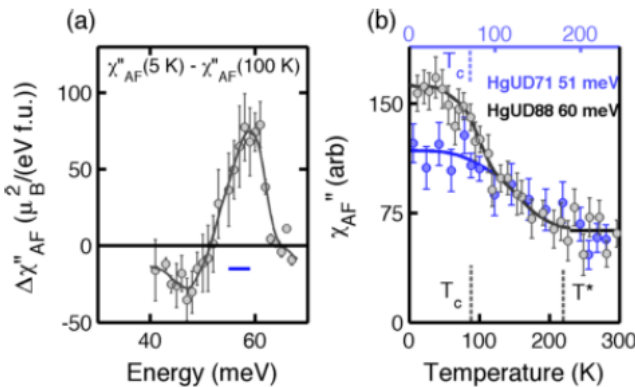


Fig. 2 (a) Evidence for a magnetic resonance in the SC state from the susceptibility difference at the AF wave vector at 5K and 100K for a $T_c=88\text{K}$ Hg1201 sample [6]. (b) Temperature dependence at the respective energies of the susceptibility peak for $T_c=88\text{K}$ [6] and $T_c=71\text{K}$ [5] samples. In both cases, the AF response significantly decreases below T^* , shows no anomaly at T_{CDW} (see also Fig. 1), and shows no evidence of an hourglass dispersion at temperatures above T_c . Only the $T_c=88\text{K}$ sample shows evidence for a resonance below and hourglass dispersion below T_c [5,6].

New insights from synchrotron X-ray experiments. After numerous unsuccessful attempts to observed charge-density-wave (CDW) order with hard X-rays, we eventually found relatively weak, short-range CDW correlations in moderately-doped Hg1201 ($T_c=72\text{K}$) [7]. We furthermore established a simple connection between the reconstructed Fermi surface area and the CDW modulation wave vector. This unifying insight would not have been possible without our prior quantum oscillation results for Hg1201. Since then, we have mapped out the doping-temperature dependence of the CDW phenomenon [8] (Fig. 1). The CDW correlations first appear at a temperature that is in excellent agreement with the emergence of anomalies in the quasiparticle recombination lifetime observed in recent collaborative time-resolved optical measurements [9], but that is distinctly lower than T^* . We find that the CDW correlations do not exceed the typical distance between interstitial oxygen dopants and that they disappear well below optimal doping, once the correlation length is comparable to the CDW modulation wave vector [8]. In other yet unpublished X-ray work, we discovered CDW correlations in the sister compound Hg1212, and we mapped out the doping and temperature dependence of oxygen-chain order in the Hg-O reservoir layer of Hg1201 and investigated the effects of high pressure on this order. Finally, we have been using X-ray absorption spectroscopy (XAS) to establish the exact hole occupancy of the various O and Cu orbitals.

New insight from collaborative work. Our extensive collaborative work on Hg1201 includes new insights from time-resolved optics [9-11], NMR [12], and photoemission [13].

Future Plans

Neutron scattering experiments. The unusual normal-state AF response of Hg1201 and the intriguing connection between AF correlations, the PG phenomenon and $q=0$ magnetism warrants further exploration as a function of doping and temperature. Preliminary results obtained at the SNS indicate that the AF gap extrapolates to zero at the hole doping level of $p \sim 5\%$ at which superconductivity disappears. It is of high interest to establish the nature of this quantum critical point from the superconducting to the non-superconducting state. It also will be important to extend the present measurements to higher energy, and to observe the effects of a magnetic field and of intentionally introduced disorder (e.g., Zn doping) on the $q=0$ order and AF response.

Synchrotron X-ray experiments. We plan to build on our initial observation of CDW order in Hg1212 and to carry out a comparative study with our detailed results for Hg1201. Similarly, we will search for interstitial oxygen order and use XAS to determine orbital occupancy in Hg1212. In both compounds, we wish to investigate the effects of intentionally introduced disorder and of replacing interstitial oxygen with fluorine. We plan to further investigate the effects of high pressures on the chain order to establish a possible (anti)correlation with the known pressure enhancement of the optimal T_c .

Transport experiments. It will be important to extend the quantum oscillation and magneto-resistance experiments to a wide doping range in Hg1201 in order to match the neutron scattering and X-ray work. We also wish to determine the transport properties to very high temperatures in order to better understand how the Fermi-liquid-like state evolves into the strange metal state (Fig. 1a) and to complete initial measurements of the Seebeck effect. The effects of intentionally introduced disorder and of fluorination can be expected to shed new light on how the underlying Fermi-liquid behavior becomes masked by disorder effects. We will furthermore begin to extend these measurements to Hg1212.

Collaborations. The formation of the new Center for Quantum Materials (CQM) at the University of Minnesota will enable new synergistic endeavors and help ensure a far-reaching impact beyond our group's immediate scattering and transport experiments. The CQM's goal is to substantially raise the level of knowledge of the distinct quantum electronic phases of matter exhibited by complex oxides and, critically, of the transitions between these phases that have proven so challenging to understand. To this end, the CQM's PIs (*Chubukov, Fernandes, Jalan, Greven, Leighton*) will initially focus on the experimental and theoretical investigation of three representative families of complex oxides: The cuprates, the cobaltites and the titanates. For example, in collaboration with *Jalan*, who is a world-leader in the growth of titanate films, we will grow single crystals of titanates and pursue complementary scattering and transport experiments in order to achieve a deeper understanding of these doped Mott insulators. In terms of external collaborations, our group will continue to pursue a comprehensive approach through collaborations with experimental experts using complementary experimental tools, including photoemission, Raman scattering, optical spectroscopy and NMR. At present, we have established more than a dozen such collaborations. A significant number of these collaborators are presently supported by DOE-BES.

References

1. B. Keimer *et al.*, Nature **518**, 179 (2015)

Publications

2. M.K. Chan, M.J. Veit, C.J. Dorow, Y. Ge, Y. Li, W. Tabis, Y. Tang, X. Zhao, N. Barišić, and M. Greven. In-plane magnetoresistance obeys Kohler's rule in the pseudogap phase of cuprate superconductors. *Phys. Rev. Lett.* **113**, 177005 (2014).
3. M.K. Chan, N. Harrison, R.D. McDonald, B.J. Ramshaw, K.A. Modic, N. Barišić, and M. Greven. Single reconstructed Fermi-surface pocket in an underdoped single-layer cuprate superconductors. *Nat. Comm.* **7**, 12244 (2016).
4. N. Barišić, M.K. Chan, M.J. Veit, C.J. Dorow, Y. Ge, Y. Tang, W. Tabis, G. Yu, X. Zhao, and M. Greven. Hidden Fermi-liquid behavior throughout the phase diagram of the cuprates. *Phys. Rev. X* (in review); arXiv:1507.07885.
5. M.K. Chan, Y. Tang, C.J. Dorow, L. Mangin-Thro, Y. Ge, M.J. Veit, X. Zhao, A.D. Christianson, J.T. Park, Y. Sidis, P. Steffens, D.L. Abernathy, P. Bourges, and M. Greven. Commensurate antiferromagnetic fluctuations as a signature of the pseudogap formation in a model cuprate. *Nat. Commun.* **7**, 12244 (2016).
6. M.K. Chan, Y. Tang, C.J. Dorow, J. Jeong, L. Mangin-Thro, M.J. Veit, Y. Ge, D. L. Abernathy, Y. Sidis, P. Bourges, and M. Greven. Hourglass dispersion and resonance of magnetic excitations in the superconducting state of the single-layer cuprate $\text{HgBa}_2\text{CuO}_{4+\delta}$. *Phys. Rev. Lett.* (in review); arXiv:1610.01097.
7. W. Tabis, Y. Li, M. Le Tacon, E. Weschke, L. Braicovich, A. Kreyssig, M. Minola, G. Della, A. Goldman, T. Schmitt, G. Ghiringhelli, N. Barišić, M. K. Chan, C. J. Dorow, M. J. Veit, G. Yu, X. Zhao, B. Keimer and M. Greven. Charge order and its connection with Fermi-liquid charge transport in a pristine high-Tc cuprate. *Nat. Commun.* **5**, 5875 (2014).
8. W. Tabis, B. Yu, I. Bialo, M. Bluschke, G. Yu, T. Kolodziej, A. Kozłowski, Y. Tang, E. Weschke, B. Vignolle, M. Hepting, H. Gretarsson, R. Sutarto, M. Le Tacon, N. Barišić, and M. Greven. New insight into cuprate charge from X-ray measurements of $\text{HgBa}_2\text{CuO}_{4+\delta}$. To be submitted to *Phys. Rev. Lett.*
9. J.P. Hinton, E. Thewalt, Z. Alpichshev, F. Mahmood, J.D. Koralek, M.K. Chan, M.J. Veit, C.J. Dorow, N. Barišić, A.F. Kemper, D.A. Bonn, W.N. Hardy, R. Liang, N. Gedik, M. Greven, A. Lanzara, and J. Orenstein. The rate of quasiparticle recombination probes the onset of coherence in cuprate superconductors. *Sci. Rep.* **6**, 23610 (2016).
10. F. Cilento, S. Dal Conte, G. Coslovich, S. Peli, N. Nembrini, S. Mor, F. Banfi, G. Ferrini, H. Eisaki, M. K. Chan, C. J. Dorow, M. J. Veit, M. Greven, D. van der Marel, R. Comin, A. Damascelli, L. Rettig, U. Bovensiepen, M. Capone, C. Giannetti, and F. Parmigiani. Photo-enhanced antinodal conductivity in the pseudogap state of the high-Tc cuprates. *Nat. Commun.* **5**, 4353 (2014).
11. S. Dal Conte, L. Vidmar, D. Golez, M. Mierzejewski, G. Soavi, S. Peli, F. Banfi, G. Ferrini, R. Comin, L. Ludbrook, N. D. Zigaldo, H. Eisaki, M. Greven, S. Lupi, A. Damascelli, D. Brida, M. Capone, J. Bonca, G. Cerullo, and C. Giannetti. Snapshots of the retarded interaction of charge carriers with ultrafast fluctuations in the cuprates. *Nat. Phys.* **11**, 421 (2014).
12. D. Rybicki, J. Kohlrantz, J. Haase, M. Greven, X. Zhao, M.K. Chan, C.J. Dorow, M.J. Veit. Electronic spin susceptibilities and superconductivity in $\text{HgBa}_2\text{CuO}_{4+\delta}$ from nuclear magnetic resonance. *Phys. Rev. B* **92**, 081115 (2015).
13. I. M. Vishik, N. Barišić, M. K. Chan, Y. Li, G. Yu, X. Zhao, D. D. Xia, W. S. Lee, W. Meevasana, T. P. Devereaux, M. Greven, and Z. X. Shen. Angle-resolved photoemission spectroscopy study of $\text{HgBa}_2\text{CuO}_{4+\delta}$. *Phys. Rev. B* **89**, 195141 (2014).

Single Crystal Growth and superconductivity of $(\text{La}_{1-x}\text{Ca}_x)_2\text{CaCu}_2\text{O}_{6+d}$

G. D. Gu (ggu@bnl.gov), Igor A Zaliznyak and J. M. Tranquada

Condensed Matter Physics Department, Brookhaven National Laboratory, Upton, NY 11973-5000, USA

Program Scope

Among the perovskite-related high temperature superconducting (T_c) cuprates with double layers of copper oxide pyramids, the La-2126 compounds of La-Sr-Ca-Cu-O [1] and La-Ca-Cu-O [2] have the simplest crystallographic structure. The La-2126 has neither the additional carrier reservoir layers of the superconducting compounds Bi-2212 and Tl-2212, nor the square planar CuO chain in the superconducting compound YBCO. The simple CuO double layer structure offers a great advantage for studying the cuprate's superconducting properties. By using high oxygen pressure synthesis method, Cava [1] and Kinoshita [2] finally successfully obtained the superconducting $\text{La}_{1.6}\text{Sr}_{0.4}\text{CaCu}_2\text{O}_6$ ($T_c = 60\text{K}$) and $\text{La}_{1.75}\text{Ca}_{1.25}\text{Cu}_2\text{O}_6$ ($T_c = 44.7\text{K}$). A number of experiments have tried to explain the effect of high oxygen pressure synthesis and to determine the relationship between the crystal structure and the superconductivity of these compounds [3]. However, a number of important questions about the superconductivity of La-2126 compounds still remain. One key question is why the highest T_c obtained to date in La-2126 is just 60K, compared to $T_c \sim 90\text{K}$ for double CuO layer YBCO and Bi-2212. Another question is which maximum T_c of La-2126 compounds should be. In order to understand the superconducting properties of the La-2126 compounds, and especially for studies using neutron scattering, the large and high quality single crystals with bulk superconductivity are indispensable.

The project is to grow a number of large size single crystals $(\text{La}_{1-x}\text{Ca}_x)_2\text{CaCu}_2\text{O}_{6+d}$ ($x = 0.0325$ to 0.15) by using the floating zone method. The effects of growth conditions and composition on the crystal growth have been studied. A smooth solid-liquid growth interface of $(\text{La}_{1-x}\text{Ca}_x)_2\text{CaCu}_2\text{O}_{6+d}$ tended to break down into a cellular interface when the growth velocity was higher than 0.5 mm/h. When the solid-liquid interface became cellular, the single crystal size in an as-grown rod decreased abruptly and the as-grown rod was not single phase. Various sized CaO inclusions were found inside the as-grown single crystals of $(\text{La}_{1-x}\text{Ca}_x)_2\text{CaCu}_2\text{O}_{6+d}$ ($x \geq 0.075$). Cubic centimeter size single crystals were successfully grown for composition $(\text{La}_{1-x}\text{Ca}_x)_2\text{CaCu}_2\text{O}_{6+d}$ ($x = 0.0325 \sim 0.075$).

The as-grown single crystals of $(\text{La}_{1-x}\text{Ca}_x)_2\text{CaCu}_2\text{O}_{6+y}$ under 1 bar pressure of oxygen were not superconducting. The superconducting temperature of the $(\text{La}_{1-x}\text{Ca}_x)_2\text{CaCu}_2\text{O}_{6+y}$ crystals grown at 11 bars oxygen is 28K with only 0.01% superconducting volume in the single crystals. The application of high pressure oxygen during crystal growth is an effective method to get the superconductivity in the crystals, but is not enough to get the bulk superconductivity. The superconductivity of the large single crystals can be tuned by using a hot isostatic press furnace with a mixed gas of 20% oxygen and 80%Ar with 7000 bar gas pressure. We are first in the world to successfully obtain large single crystals of $(\text{La}_{1-x}\text{Ca}_x)_2\text{CaCu}_2\text{O}_{6+y}$ with bulk superconductivity, achieving a maximum superconducting temperature of 62 K.

Recent Progress

Figure 1 shows photographs of the single crystals of $(\text{La}_{0.95}\text{Ca}_{0.05})_2\text{CaCu}_2\text{O}_6$. (a) the as-grown single crystal rod in the floating zone machine; (b) the single crystal with $T_c = 56$ K annealed by using a hot isostatic press furnace for neutron experiments.

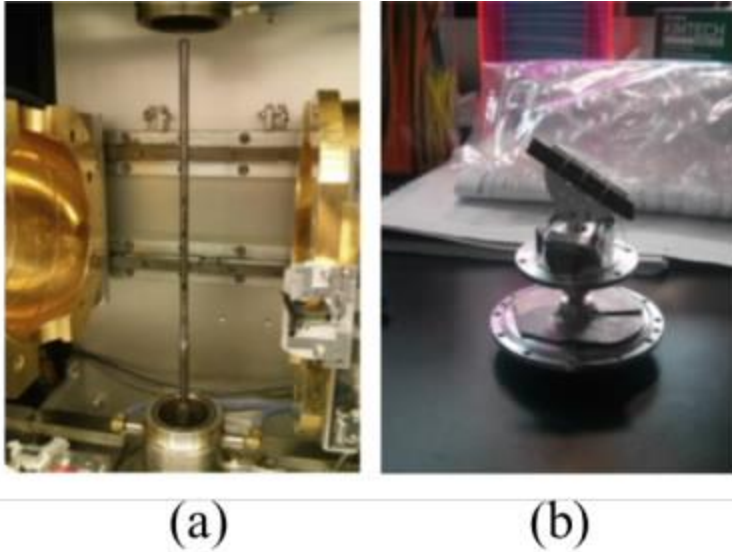


Fig. 1 The photographs of the single crystals $(\text{La}_{0.95}\text{Ca}_{0.05})_2\text{CaCu}_2\text{O}_6$. (a) the as-grown single crystal rod; (b) the single crystal for neutron experiments.

Figure 2 shows the microstructure of the cross section of the as-grown rods under a polarizing microscope. When the velocity is 1 mm/h, the solid-liquid interface of the as-grown rod is a cellular interface, and the as-grown rod consists of small size La-2126 single crystals as matrix and second phases of CaO at the grain boundaries of La-2126 single crystals, shown in (a). When the velocity is 0.35 mm/h, the solid-liquid interface of the as-grown rod of $(\text{La}_{0.95}\text{Ca}_{0.05})_2\text{CaCu}_2\text{O}_{6+d}$ is a smooth growth front, and the as-grown rod consists of single phase of La2126 and has large size single crystals as shown in (b). The smooth solid-liquid growth front of an as-grown rod is indispensable for obtaining the single crystal rod. The low growth velocity (less than 0.5 mm/h) is a key factor in obtaining the single crystal rod of $(\text{La}_{1-x}\text{Ca}_x)_2\text{CaCu}_2\text{O}_{6+d}$ ($x=0.05$ to 0.06).

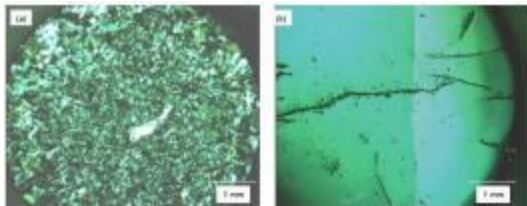


Fig. 2 Effect of the growth velocity on the size of single crystals in the as-grown rod $(\text{La}_{0.95}\text{Ca}_{0.05})_2\text{CaCu}_2\text{O}_{6+d}$ with a velocity of 1 mm/h (a) and a velocity of 0.35 mm/h in pure oxygen flow.

Figure 3 shows the microstructure of the cross section of the as-grown rod of $(\text{La}_{0.925}\text{Ca}_{0.075})_2\text{CaCu}_2\text{O}_{6+d}$ grown in 11 bars oxygen pressure under a polarizing microscope. The as-grown rod consists of a number of single crystal matrix domains of La-2126 phase as shown in (a) and small second phase inclusions of CaO inside the single crystal domains of La-2126 matrix, as shown in (b). The estimated Ca solubility limit of $(\text{La}_{1-x}\text{Ca}_x)_2\text{CaCu}_2\text{O}_{6+d}$ is $x < 0.075$ under 11 bars oxygen pressure. When CaO content $x \geq 0.075$, the as-grown rods consist of La-2126 crystal matrix and CaO second phase. The CaO content $x < 0.075$ is a necessary condition for growth of single crystal rods of $(\text{La}_{1-x}\text{Ca}_x)_2\text{CaCu}_2\text{O}_{6+d}$.

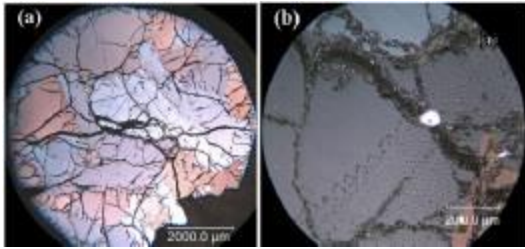


Fig. 3 The microstructure (a) at a magnification of 2.5 times and microstructure (b) at a magnification of 20 times of the cross section of the as-grown rod of $(\text{La}_{0.925}\text{Ca}_{0.075})_2\text{CaCu}_2\text{O}_{6+d}$ under 11 bars oxygen pressure at a velocity of 0.35 mm/h. The long black lines in the photo (a) and (b) are micro-cracks, which are caused by thermal stress. The small size black dots in photo (b) are CaO second phase.

Figure 4 shows different superconducting property of one single crystal $(\text{La}_{0.95}\text{Ca}_{0.05})_2\text{CaCu}_2\text{O}_{6+d}$ after annealing in the hot isostatic press furnace, and then post-annealing at different temperatures in air to study the oxygen order effect in the single crystals.

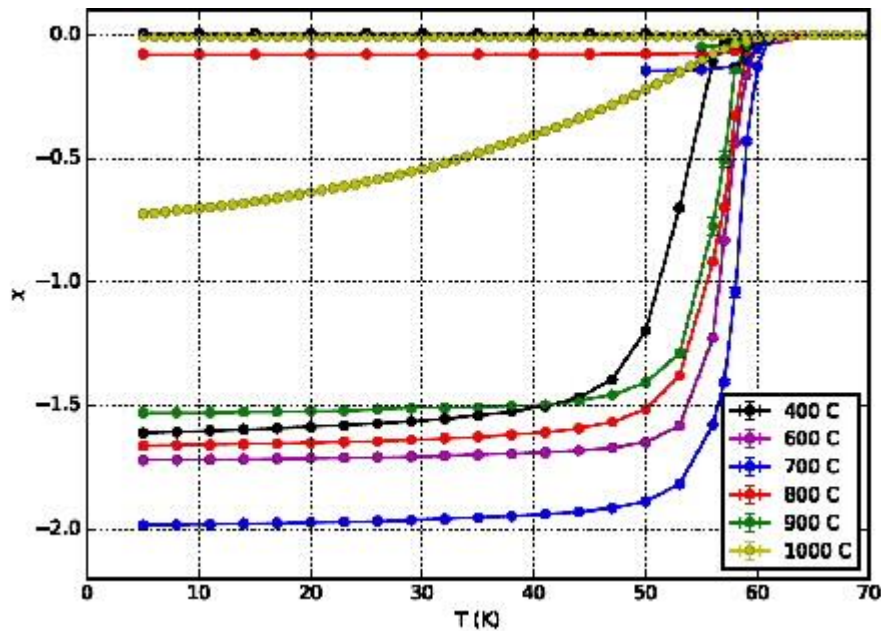


Fig. 4 the FC and ZFC magnetization measurement of one single crystal $(\text{La}_{0.95}\text{Ca}_{0.05})_2\text{CaCu}_2\text{O}_{6+d}$ after annealed by using a hot isostatic press furnace, then annealed

again at different temperature.

We are the first in the world to successfully obtain the large single crystals with highest superconducting temperature 62K ($(\text{La}_{1-x}\text{Ca}_x)_2\text{CaCu}_2\text{O}_{6+y}$) with bulk superconductivity.

Future Plans

We will continue to grow the large $(\text{La}_{1-x}\text{Ca}_x)_2\text{CaCu}_2\text{O}_{6+d}$ ($x=0.05$) single crystal by using a floating-zone machine. We will continue to anneal the single crystals at different annealing condition, such as temperature, time and pressure *etc.* to study the effect of the annealing condition on superconductivity. We will study various physical properties of the single crystals with different superconducting transition temperatures. Initial neutron scattering results are presently being analyzed.

References

- [1] R. J. Cava, B. Batlogg, R. B. Van Dover, J.J. Krajewski, J. V. Waszczak, R. M. Fleming, W. F. Peck Jr, L. W. Rupp Jr, P. Marsh, A. C. P. James & L F Schneemeyer, *Nature* **345**, 602 (1990).
- [2] K. Kinoshita, H. Shibata and T. Yamada, *Physica C* **171**, 523 (1990).
- [3] K. Kinoshita, F. Izumi, T. Yamada and H. Asano, *Phys. Rev. B*, **45**, 5558 (1992).

Publication

- [1] Hefei Hu, Yimei Zhu, Xiaoya Shi, Qiang Li, Ruidan Zhong, John A. Schneeloch, Genda Gu, John M. Tranquada, and Simon J. L. Billinge, *Phys. Rev. B* **90**, 134518 (2014).

Neutron Scattering Instrumentation Research and Development for High Spatial and Temporal Resolution Imaging at Oak Ridge National Laboratory

**Prof. Jason Hayward, Associate Professor and UCOR Fellow
University of Tennessee, Knoxville, TN 37916**

Program Scope

The spatial resolution of current neutron scattering instruments is fundamentally limited by the variance introduced by the charged particle tracks emitted from event to event in neutron absorption. In past work, we used simulation and modeling to investigate an approach to reach spatial resolution down to $\sim 1 \mu\text{m}$ using a scintillating lithium-glass microfiber array (see Fig. 1) in combination with charged particle tracking, in order to determine the interaction site of each individual event [1]. More specifically, highly efficient collection of scintillation light from the alpha and triton tracks is expected to allow us to reconstruct them through the use of the Hough transform. This, in turn, enables a high precision estimate of the neutron absorption location, allowing for micron level spatial resolution [1]. Research and development in the fabrication of such scintillating lithium-glass microfiber arrays and experiments to test these arrays at the ORNL High Flux Isotope Reactor are ongoing.

Fig. 1. When neutrons are absorbed by enriched ${}^6\text{Li}$ -glass microfibers, the resulting reaction emits an alpha and a triton back-to-back. The heavy charged particles produce scintillation light, which is channeled down a waveguide comprised of the ${}^6\text{Li}$ -glass cores surrounded by optical cladding glass, to be collected at an ICCD.

Recent Progress

1. *Optical Microfiber Array Fabrication*

Two generations of the microfiber arrays have been fabricated via optoelectronic methods in collaboration with the Optoelectronics Research Centre (ORC) at the University of Southampton, and a third generation is in process. The second generation fabrication is described next. The multi-core optical fiber was fabricated through stacking unit elements composed by Guardian Glass (NuSAFE Inc., Oak Ridge, TN, USA), a scintillating glass, as the core and a silicate glass as the cladding. The core glass is doped with isotopically enriched ${}^6\text{Li}$ for the detection of neutrons and Ce^{3+} for scintillation. The cladding has a composition similar to the LLF1 glass (Schott AG, Mainz, Germany). The two glasses were chosen because of their similar thermal properties that allow for co-drawing. The core glass, provided in a cylindrical rod with a diameter of 7.5 mm, was inserted into a cladding tube with an external square cross section. The set of core/cladding rod-in-tube was caned to an external diameter of $730 \mu\text{m}$ (see Fig. 2(a)) at which the core had a diameter of $460 \mu\text{m}$. The square cane was then stacked into a square array, as illustrated in Fig. 2(b). The fused array was consolidated in a furnace to produce a monolithic square preform (see Fig. 2(c)) before being drawn into the fiber. The fiber had a width ranging from $126 \mu\text{m}$ to $160 \mu\text{m}$.

Fig. 2(d) shows a cross section of a fabricated multicore fiber, which presents a number of microbubbles, resulting from the cavities left in the preform during consolidation. As already

observed in other scintillating fibers, the presence of small bubbles is not believed to be detrimental to the fiber operation in that it increases the numerical aperture of the fiber cores, thus decreasing the core cross talk. However, uniformity is required for ideal high resolution neutron imaging.

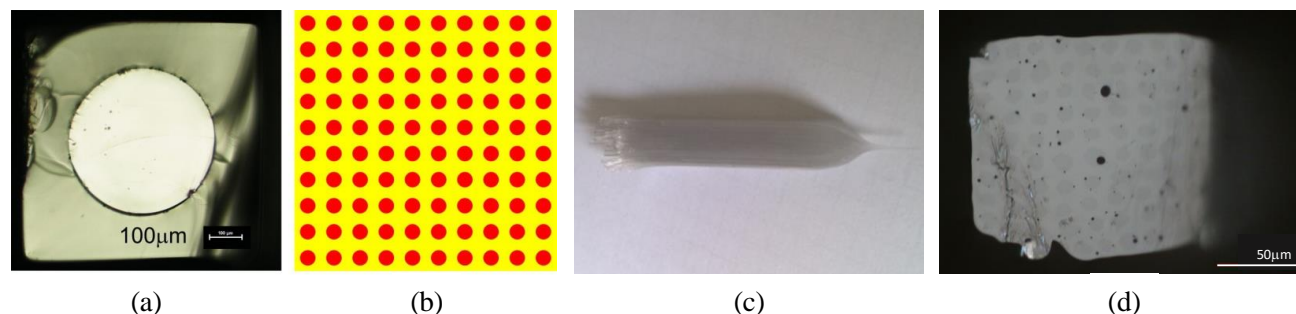


Figure 2. (a) Optical photo of elongated core/cladding square cane. The side length of the cane is $730\ \mu\text{m}$ and the core diameter is $460\ \mu\text{m}$. (b) Schematic of stack of 10×10 canes before final draw. (c) Photograph of the stack. On the right it is possible to see the neckdown region where the preform is pulled into a fiber. (d) Optical photo of ${}^6\text{Li}$ glass multicore fiber. The fiber width is $140\ \mu\text{m}$, while the core diameter is $7\ \mu\text{m}$.

Since a large field-of-view is desired, a proof-of-concept-sized array of scintillating fibers was produced. In order to create an array of the fiber, it was loaded onto a glass plate with a rigid UV curable epoxy for further processing. The glass plate was then cut into two pieces, stacked together, and the top glass plate ground away. After re-assembly, the new two-layer array was then cut in half and re-assembled to produce a four-layer array. This process was repeated to create a 64 by 64 array of the fibers with a thickness of $1.7 \times 1.7\ \text{mm}$. The array was finished by polishing the surface, cutting the array from the glass, and leaving glass sidewalls in place for support.

2. Testing with Neutron Sources

The readout of our proof-of-concept array is illustrated in Figure 1. It employs a microscope objective lens to zoom in on micron-sized scintillator fibers. We have characterized an Intensified CCD coupled to our visible and UV-sensitive optical system, stationed on a negative stiffness vibration isolator, capable of resolving $1\ \mu\text{m}$ features. At 10% of the Modulation Transfer Function (MTF), the resolvable spatial frequency is $\sim 3.3\ \text{cycles}/\mu\text{m}$ with blue light (see Figure 3).

To determine how the drawing process has affected the scintillation performance of the Guardian Glass core and to verify that scintillation light is being efficiently channeled with micron-level architecture, the fiber array was assayed with a cold neutron source. Testing was carried out at the High Flux Isotope Reactor's CG-1D beamline at Oak Ridge National Laboratory, Oak Ridge TN, USA. Initially, a nominal background was observed when a calibrated Hamamatsu photomultiplier tube (PMT) R977 was placed in the beamline without the fiber array. The entire surface of the fiber array was then secured to the PMT window, wrapping it first with Teflon and then black tape. The response of the fiber array to the background

Figure 3. MTF of ICCD micro-setup using USAF 1951 Target with blue light

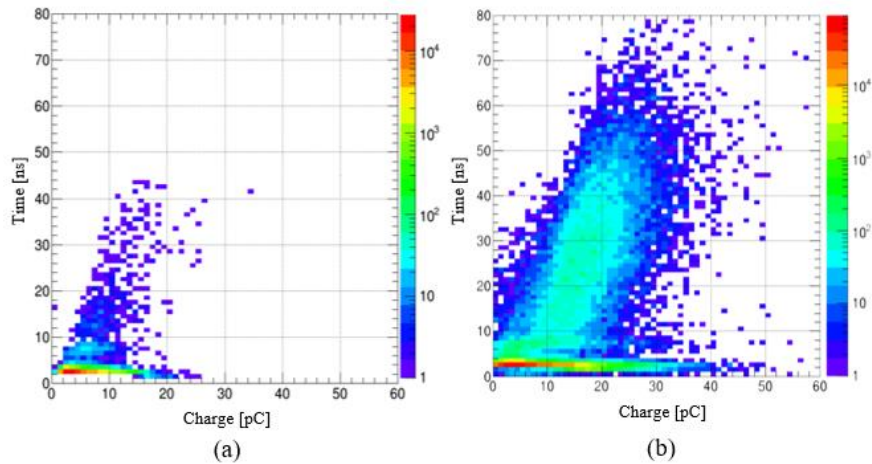
(neutron shutter closed), and to the neutron beam (neutron shutter open) was observed. Scintillation was clearly seen for both cases (see Fig. 4). The response to the neutron beam displays a significant increased integrated charge distribution. Thus, cold neutrons clearly exhibit a higher light output response than the gamma background radiation present in the beamline.

It was found that the PMT had an integrated charge response to a single photon of 122 ± 60 fC under a bias of -1,500 V. The neutron response yields approximately 246 photoelectrons. Previous analysis of a larger monolithic Guardian Glass sample with dimensions of 23.88 mm (diameter) by 2.85 mm (thickness) established that Guardian Glass can be expected to produce $\sim 9,000$ photoelectrons per thermal neutron capture⁸. The difference in light output between the two experiments is a result of the difference in scintillator form—monolithic crystal vs. thin fibers—and the small surface area of the scintillator in contact with the PMT window.

3. Selective Doping

Placing an ICCD directly into a neutron beam line is deleterious, sometimes irreparably, to this photosensor. In order to avoid light loss while preventing damage to our photosensor, we plan to directly couple a bent microfiber array to the photosensor. Because neutron absorptions along the entire length of the bent microfiber array would create confusion regarding neutron interaction location (there would not be a 1-to-1 relationship), we are researching selective doping through controlled diffusion of cerium into the surface of undoped lithium glass.

In our recent publication, we showed that cerium metal can be thermally diffused into one end of an undoped lithium-6 enriched glass sample [2]. After using a sputtering system to coat samples of monolithic, undoped lithium glass with cerium metal, the samples were each heated, and the diffusion profiles of cerium for different heating temperatures (500–600 °C) and durations (1–4 h) were studied using the alpha Rutherford backscattering technique (see Fig. 5). From experimental results, it was



(a) background radiation, in the beamline, and (b) the neutron beam.

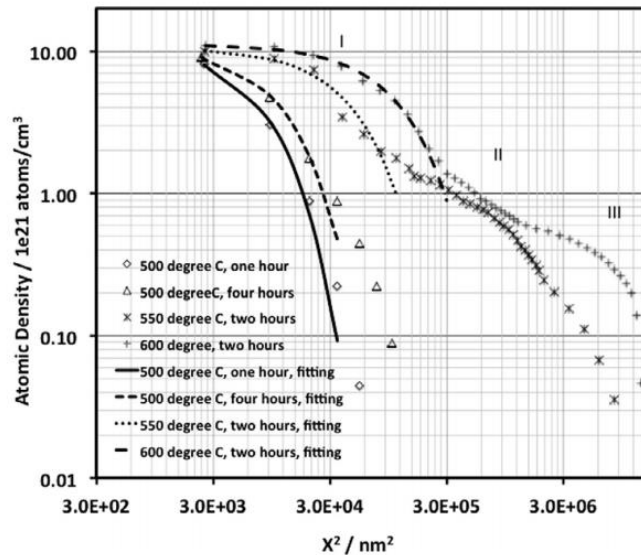


Figure 5. Concentration of cerium as a function of the square of the diffusion depth for samples heated using different temperatures and durations. [2]

observed that longer annealing times and higher annealing temperatures increased diffusion depth. Now this diffusion response is understood.

While sputtering cerium from its metallic form resulted in successful thermal diffusion into the lithium-glass, it does not allow for precise control of the cerium's charge state. Since the 3+ charge state is desired for scintillation, we report on a different wet chemistry approach in this paper. Specifically, cerium acetylacetonate $\text{Ce}(\text{AcAc})_3$, commonly referred to as "cerium AcAc," is attractive because it is unreactive with air, and it is expected to be better capable of maintaining cerium's 3+ charge state throughout diffusion. Since cerium AcAc is not able to be sputtered, doping is accomplished using a liquid solution containing the cerium AcAc. To find a stable solution, the compound was dissolved into several solvents, yielding success with a toluene solvent. This time, we are diffusing for longer times (exceeding 4 h). We are currently studying the data we have collected, including scintillation light output and characteristics vs. heating conditions. We are also authoring a peer-reviewed publication on this work.

Future Plans

Using lessons learned from our measurements of earlier generation microfiber designs at CG-1D, we are working on a new design and improved characterization setup. We are in the process of fabricating a new generation of microfibers with an expected improved packing fraction of cores, ~40%, and a higher NA value of ~0.44. Simulations of the optical setup and expected light output are ongoing. We are also conducting studies on the thermal properties of the NuSAFE Li-glass in collaboration with the ORC.

In December 2016, we expect to take data using new scintillator samples to be provided soon by RMD Inc. (under a nondisclosure agreement). In Spring 2017, we expect that our two 3rd generation microfiber arrays, with core diameters of 10 or 2 μm , will be measured and characterized at CG-1D. We would also like to make our measurements with the neutron microscopy setup at the Swiss Spallation Neutron Source (SINQ) of the Paul Scherrer Institute (PSI); the PI visited PSI this past summer to discuss such collaboration. Furthermore, we will continue said studies on AcAc, including a study of the effect of annealing. Finally, we are also now collaborating with Lanzhou University in similar work to ours, since a UTK faculty member working on our project, Prof. Xiaodong Zhang, recently started his own research group at his alma mater. He is making beamline measurements at CG-1D this week.

We have had some recent publications, but we need to work more on peer-reviewed publications in the short term.

References

- [1] Y. Song, J. Conner, X. Zhang, J. P. Hayward, "Monte Carlo simulation of a very high resolution thermal neutron detector composed of glass scintillator microfibers," *Applied Radiation and Isotopes* 108 (2016) 100-107.
- [2] X. Zhang, M. E. Moore, K.M. Lee, E. D. Lukosi, J. P. Hayward, "Study of cerium diffusion in undoped lithium-6 enriched glass with Rutherford backscattering spectrometry," *NIM B* 378 (2016) 8-11.

Publications

Peer-reviewed publications

1. Y. Song, J. Conner, X. Zhang, and J. P. Hayward, "Monte Carlo simulation of a very high resolution thermal neutron detector composed of glass scintillator microfibers," *Applied Radiation and Isotopes*, vol. 108, pp. 100-107, 2016.
2. X. Zhang, M. E. Moore, K.-M. Lee, E. D. Lukosi, and J. P. Hayward, "Study of cerium diffusion in undoped lithium-6 enriched glass with Rutherford backscattering spectrometry," *Nuclear Instruments and Methods in Physics Research Section B: Beam Interactions with Materials and Atoms*, vol. 378, pp. 8-11, 2016.

Refereed conference presentations

3. X. Zhang, Y. Song, J. Conner, J.P. Hayward, "Monte Carlo simulation of a Very High Resolution Thermal Neutron Detector Composed of Glass Scintillator Microfibers," *IEEE Nuclear Science Symposium*, Seattle, WA, November 2014.
4. X. Zhang, J. Conner, M.E. Moore, H. Bhandari, V. Nagarkar, J.P. Hayward, "Next generation, micron-order spatial resolution thermal/cold neutron imaging detector," *International Conference on Radioanalytical and Nuclear Chemistry*, Budapest, Hungary, April 2016.
5. M.E. Moore and J.P. Hayward, "Development and Experimental Evaluation of Scintillating Microfiber Lithium Glass Array for High Spatial Resolution Neutron Imaging at Neutron Scattering Facilities," *American Conference on Neutron Scattering*, Long Beach, CA, July 2016.
6. H. Qiao, C. Wan, M.E. Moore, J.P. Hayward, L. Jingwen, S.Wang, B. Tang, X. Zhang, "Progress Report on R&D of High Resolution Cold Neutron Microscope," *IEEE Nuclear Science Symposium*, Strasbourg, France, November 2016.
7. M.E. Moore, J. Lousteau, X. Feng, F. Poletti, G. Brambilla, J.P. Hayward, "A multicore compound glass optical fiber for neutron detection," submitted to the 25th *International Conference on Optical Fiber Sensors*, April 2017.

Rheo-structural spectroscopy: fingerprinting the *in situ* response of fluids to arbitrary flow fields

Matthew E. Helgeson, Department of Chemical Engineering, University of California, Santa Barbara

Program Scope

Small angle neutron scattering (SANS) is a powerful tool for understanding the development of morphology during flow processing of complex fluids, such as polymeric liquids and colloidal suspensions, so that they can be engineered for energy materials with controlled properties. Although existing methods for *in situ* neutron scattering during flow have been successful in characterizing structure-processing-property relationships for fluids under shearing deformation, most industrial processes involve more complicated deformations including combinations of shearing, elongation, and rotation. The goal of this research program is to develop new tools for *in situ* SANS measurements under fluid flows involving arbitrary, time-programmable deformation types, and apply these tools to study microstructural transformations in energy-relevant complex fluids including polymeric liquids and nanoparticle suspensions. We will achieve this through three primary objectives to: (1) design and validate a millifluidic four roll mill (mFoRM) device and associated methods that are optimized for SANS and flow velocimetry measurements; (2) combine the mFoRM with modeling to develop and refine microscopically-informed rheological models for complex fluids in complex deformations; (3) understand how deformation type and nanoscale architecture impact a number of flow-induced structural transformations observed during processing of a range of complex fluids.

Recent Progress

In the current 2-year period, we have been successful in optimizing and constructing an mFoRM device for SANS and flow visualization, verifying the ability of this device to impose controlled, uniform and arbitrary 2D deformation types to both Newtonian and viscoelastic fluids, and demonstrating the ability of the device to be used for *in situ* SANS measurements.

Design and optimization of an mFoRM device. The mFoRM design is based on a geometry proposed by Muller and co-workers [1] for hydrodynamic trapping of colloidal objects and subjecting them to arbitrary two-dimensional deformation fields. The device (Fig. 1a) consists of eight hydrodynamically-isolated rectangular channels that converge onto a central stagnation region. Half of these channels are supplied with fluid at a flow rate Q_1 , and the other half with a flow rate Q_2 . The operating principle for achieving controlled, two-dimensional flow types is that variation in the flow rate ratio (Q_1/Q_2) controls the relative flow rates of fluid into the four partitioned entry planes into the stagnation region, which establishes the applied deformation type in the central region. The device can thus be considered as a pressure-driven analog to

Taylor's original drag-driven four roll mill device.[2] The intent of both devices is to generate a nearly uniform, idealized two-dimensional flow, whose velocity gradient tensor is given by

$$\nabla \mathbf{u} = \frac{\Gamma}{2} \begin{bmatrix} (1 + \Lambda) & (1 - \Lambda) \\ -(1 - \Lambda) & -(1 + \Lambda) \end{bmatrix}$$

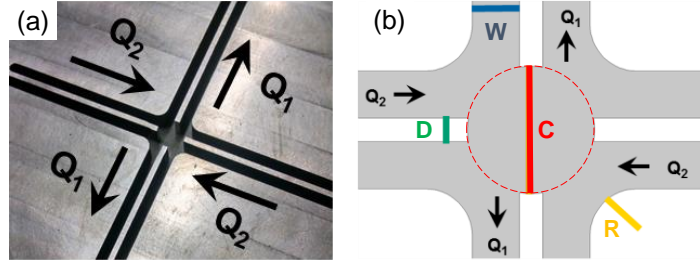


Figure 1. (a) Photograph of the mFoRM device. (b) Schematic diagram indicating geometric parameters used for optimization.

Here, Λ is flow type parameter representing the type of applied deformation, which varies continuously from $\Lambda = 1$ to 0 to -1 as the deformation is varied from pure elongation to pure shear to pure rotation, respectively; Γ indicates the magnitude of the two-dimensional strain rate, which in the mFoRM increases as Q_1 is increased.

We adapted the geometry (Fig. 1b) in order to: (i) have dimensions that are compatible with conventional SANS experiments, both in terms of beam collimation and transmission attenuation; (ii) produce a relatively uniform flow type and deformation rate within a typical SANS scattering volume; (iii) achieve larger deformation rates in the stagnation region relative to the shear rates in the (iii) accommodate non-Newtonian, viscoelastic fluids.

We used computational fluid dynamics (CFD) simulations in COMSOL on a representative shear thinning viscoelastic fluid modeled by the Carreau-Yasuda constitutive equation in order to optimize the various geometrical parameters of the device depicted in Figure 1. The particular objective functions used were to: (a) achieve maximal uniformity of Λ and Γ within a typical collimated beam diameter (1-2 mm), (b) achieve steady state fluid rheology at the stagnation point (i.e. a sufficiently large accumulated strain so that deformation history effects due to the upstream channels is eliminated), and (c) achieve an out-of-plane device thickness that is simultaneously large enough to minimize three-dimensional flows due to the confining walls while small enough to minimize beam attenuation in SANS measurements. The resulting optimized geometry is depicted to scale in Fig. 1b.

Verification of controlled flow type. We constructed the optimized geometry (Fig. 1a) in a stainless steel device, which is sealed with two face plates whose design matches an existing cross-slot flow-SANS device available at the NIST Center for Neutron Research (NCNR).[3] The ability of the design to successfully achieve the design objectives listed above was verified using a combination of flow visualization and velocimetry measurements using particle tracking velocimetry (PTV) and CFD simulations on an aqueous suspension of rod-like cellulose nanocrystals, which is modeled accurately by the Carreau-Yasuda model. For PTV measurements, a LOESS statistical analysis is performed on the resulting velocity field data in order to compute the velocity gradient tensor from local derivatives of the velocity, from which local values of Λ and Γ can be computed throughout the entire flow geometry.

The results of these experiments is summarized in Figure 2. Firstly, we find excellent quantitative agreement between the experiments and simulations with respect to the velocity, flow type parameter and strain rate fields for the full range of applied nominal flow type

parameters (achieved by varying the flow rate ratio Q_1/Q_2 , thereby validating the simulation approach. Furthermore, we find that in all cases the local values of both Λ and Γ are uniform within 10% in a circular region spanning 1-2 mm (including variations in the out-of-plane direction) depending on the applied flow type. These results confirm that the optimized device design achieves the desired objectives of uniform flow within a scattering volume that is commensurate with most collimated neutron beams, and thus enabling SANS measurements under controlled, arbitrary two-dimensional deformations.

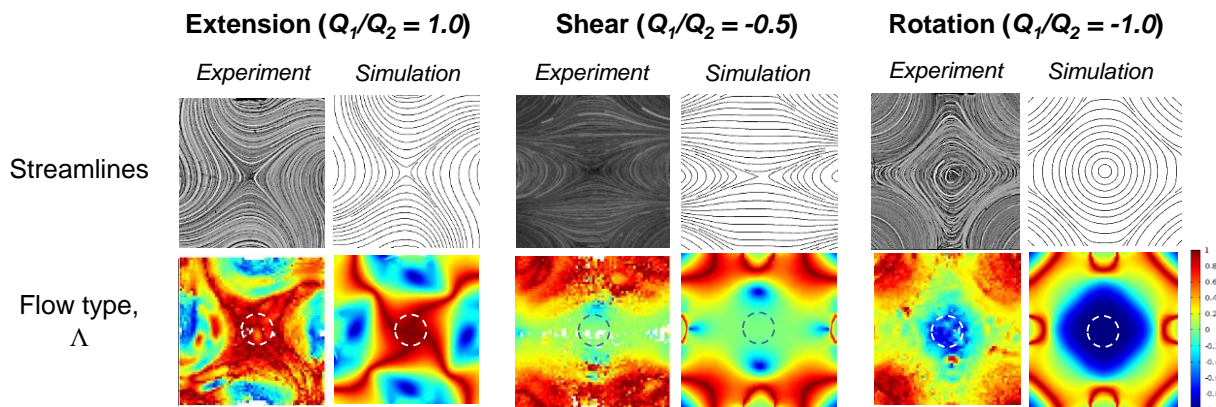


Figure 2. Results of PTV experiments (left panels) and CFD simulations (right panels) in the mFoRM under various nominal applied flow types including pure extensional (left), shearing (center) and rotational (right) deformations. Both tracer streamlines (top panels) and locally computed flow types (bottom panels) are shown. The color scale indicates the magnitude of Λ . Dotted circles indicate the region encompassing a 1 mm beam.

Proof-of-concept SANS experiments. We used the optimized device design of the mFoRM to make the first-ever flow-SANS measurements under arbitrarily varying, steady state two-dimensional deformation. The device was commissioned on the NGB 10 m SANS instrument at the NCNR in October 2016. The same aqueous suspension of cellulose nanocrystals was used as a model system. This fluid and composition were chosen such that the rod-like particles will exhibit preferential orientation along the outflow axis, which rotates as the nominal applied flow type, Λ_{app} , is changed (from nearly 45° when $\Lambda_{app} = 1$ to nearly 30° when $\Lambda_{app} = 0$). In this way, the rods serve as a probe in order to determine whether the expected microstructural orientation and alignment is achieved upon varying the applied flow type.

Results of the mFoRM-SANS experiments are summarized in Figure 3. Specifically, we find that the average orientation of rod-like particles matches well with the expected orientation based on the expected orientation given the orientation of the outflow axis. Given the strong agreement between the two, these experiments verify a number of facets about the design of the mFoRM device. Specifically, it achieves (1) the desired control over the microscopically applied deformation field, (2) sufficiently homogeneous flow within the scattering volume to reproduce the expected structural orientation for a uniform two-dimensional flow, and (3) sufficiently large accumulated strains within the region of homogeneous flow in order to eliminate upstream flow history effects. Therefore, the experiments demonstrate the success of the mFoRM design, and its ability to be used for flow-SANS experiments under arbitrary deformation fields.

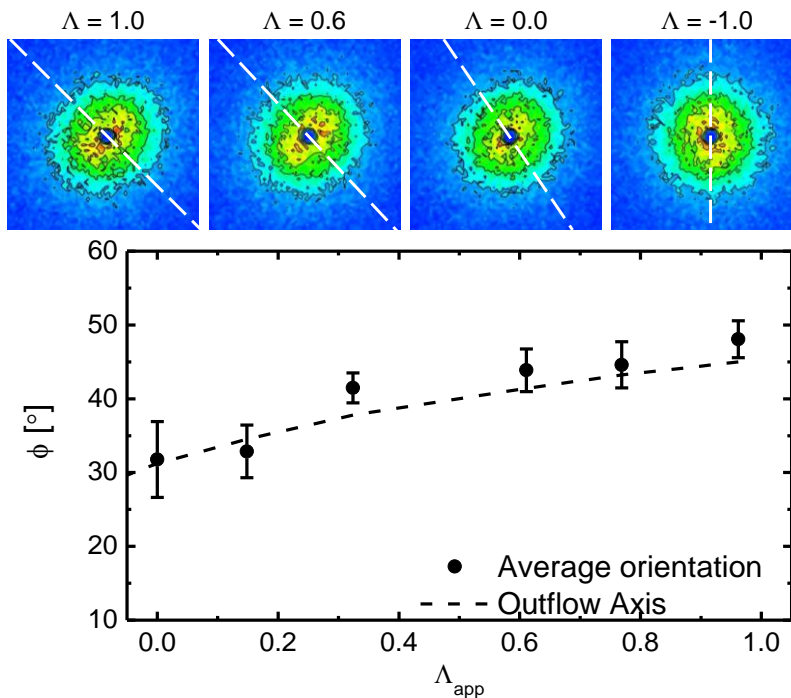


Figure 3. Results of mFoRM-SANS measurements for a semi-dilute aqueous suspension of rod-like cellulose nanocrystals for an applied value of $\Gamma = 10 \text{ s}^{-1}$. (top) Two-dimensional SANS intensity patterns for the indicated values of Λ within the scattering volume. White lines indicate the direction of the outflow axis measured by PTV. (b) Average rod orientation measured by mFoRM-SANS (points), and direction of outflow axis (line).

Future Plans

The mFoRM device and related SANS methods have been validated for a representative shear thinning fluid. To prove the versatility of this new tool, future experiments will involve a range of fluids with non-Newtonian rheology including elastic, shear thickening and yield stress fluids. Furthermore, we will test the ability to use the mFoRM to achieve time-varying flows. This will require the development of more sophisticated CFD simulations involving fully viscoelastic constitutive models in the OpenFOAM computational package.

We also plan to begin using mFoRM-SANS to understand flow-induced structuring in self-assembled polymeric micelles. Specifically, we plan to determine how flow-induced anisotropy and breakage of micelles depends on the type of deformation encountered. This information will be used to develop and validate novel constitutive models for micellar solutions.

References

- [1] J.S. Lee *et al.*, Applied Physics Letters 90, 074103 (2007).
- [2] G.I. Taylor, Proceedings of the Royal Society of London Series A 146, 501-523 (1934).
- [3] R. McAllister and K.M. Weigandt. NCNR Accomplishments and Opportunities: 49 (2015).

Complex Electronic Materials: Neutron Spectroscopy Studies of CeRhIn₅

Marc Janoschek and David Fobes (Los Alamos National Lab)

Program Scope

Complex and collective states that emerge in strongly correlated electron materials pose significant scientific challenges, solutions to which define the frontier of science and enable the energy and defense security of the nation. Research in this project focuses on developing a fundamental understanding of complex electronic materials, with strongly correlated f-electron systems serving as prototypes of classes of problems found broadly in d- and f-electron materials. Slight changes in sample composition, temperature, pressure or magnetic field tune the delicate balance among competing interactions and induce transitions between states of matter. These complex behaviors are most pronounced near magnetic/non-magnetic and metal/insulator boundaries and become particularly poorly understood as these boundaries are tuned to absolute zero temperature, i.e., to a quantum-critical point. A successful program of discovering new physics through new materials requires integration of materials preparation, preferably as single crystals, with complementary programs of materials characterization and in-depth investigations leading to microscopic understanding for which new techniques are developed as necessary. A broad suite of tools, ranging from structural, thermodynamic, magnetic, and transport measurements to spin and charge spectroscopies, in most cases at extremes of temperature (to 20 mK), pressure (to 5.5 GPa) and field (to 100 T), and aided by theoretical calculations, is employed to discover and understand new science that emerges on multiple length and time scales. Our pursuit of new science in complex electronic materials makes extensive use of DOE national facilities and special facilities at Los Alamos and is leveraged through an extensive network of collaborators.

Recent Progress

A unifying theme among various types of quantum matter is the ubiquity of energetically near-degenerate ground states. For example, in strongly-correlated electron systems unconventional superconductivity typically emerges in the vicinity of a magnetic quantum phase transition and competes with electronic-nematic, charge density, and magnetic phases. Alternatively, frustrated magnetic short-range interactions are prone to generate a multitude of degenerate magnetic configurations leading to quantum spin liquid physics. The magnetic Ruderman-Kittel-Kasuya-Yosida (RKKY) interaction that couples neighboring magnetic moments arising from localized electrons via surrounding conduction electrons is involved in both electron localization/delocalization and magnetic frustration. This suggests that the rich landscape of quantum ground states in certain materials may be concurrently controlled by both mechanisms.

Our recent neutron spectroscopy measurements on the prototypical strongly-correlated electron material CeRhIn₅ demonstrated that its zero-magnetic-field antiferromagnetic ground state that arises below 4 K is characterized by frustrated nearest- and next-nearest neighbor interactions [1]. Because CeRhIn₅ can be tuned to a so-called “unconventional” quantum critical point (QCP) via the application of pressure, where the f-electron becomes delocalized at the same pressure where the magnetic order parameter is tuned to zero giving rise to a dome of superconductivity, this makes it an ideal system to study how the interplay of electron localization/delocalization and magnetic frustration controls the emergent properties near the QCP. We have additionally carried out an extensive neutron spectroscopy study as function of magnetic fields up to 9 T, and find that the hybridization of localized f-electrons and conduction electrons results in a field-induced easy-axis anisotropy [2]. In turn, the complex temperature vs. magnetic field phase diagram can be described remarkably accurately via the Axial-Next-Nearest-Neighbor (ANNNI) model— an archetypal framework for describing frustrated magnetic interactions. In addition, our work provides interesting insights in the magnetic properties of CeRhIn₅ near the QCP. For example the frustration results in the generation of energetically almost degenerate magnetic microphases that provide a natural explanation of why the superconducting state in CeRhIn₅ is ‘textured’ in a certain temperature and pressure regime.

In addition, we have developed a strain cell for small angle neutron scattering that was recently tested at the HFIR facility and allows to apply both compressive and tensile strain of about 0.05%. Finally, we are currently working on a design to implement a small transportable focusing guide system for several triple-axis spectrometers at HFIR that will allow to investigate small samples at high pressure.

Future Plans

Our neutron measurements quantitatively determined the magnetic exchange interactions in CeRhIn₅, but also revealed the presence of an unexplained spin gap, which may provide insight into the interplay between Kondo and RKKY interactions. We will investigate the Kondo scale in CeRhIn₅ and related compounds. In particular, for CeRhIn₅ an additional issue is how the observed microphases change as function of pressure. Using a new type of hybrid clamp-type pressure cell with improved signal to noise ratio that we are currently developing in collaboration with James Hamlin (Univ. Florida), we plan to investigate these frustrated magnetic states as function of pressure.

References

[1] P. Das, S.-Z. Lin, N.J. Ghimire, K. Huang, F. Ronning, E.D. Bauer, J.D. Thompson, C.D. Batista, G. Ehlers, and M. Janoschek, “The magnitude of the magnetic exchange interaction in the heavy fermion antiferromagnet CeRhIn₅,” *Phys. Rev. Lett.* **113**, 246403 (2014).

[2] D. Fobes, et al. unpublished.

Neutron Sciences at the Oak Ridge National Laboratory

Paul Langan

Oak Ridge National Laboratory

Program Scope

The vision of Oak Ridge National Laboratory is to operate and develop the Spallation Neutron Source (SNS) and the High Flux Isotope Reactor (HFIR) as world-leading neutron scattering user facilities and centers of scientific excellence, attracting leading researchers to come and work with us to solve outstanding problems that are important to the mission of the U.S. Department of Energy and the nation.

Recent Progress

In this presentation I will discuss recent progress in key activities involved in achieving that vision, including 1) improvements in neutron production at SNS and HFIR, 2) optimization of neutron scattering instrumentation and development of related innovative capabilities and technologies, and 3) continuous engagement with the scientific community to drive the development of a high impact science program.

Future Plans

I will discuss plans to design, build, and commission a Second Target Station at the SNS, supported by a Proton Power Upgrade Project that will double the available proton beam power from 1.4 to 2.8 MW.

Role of Organic Cations in Organic-Inorganic Perovskite Solar Cells

Seung-Hun Lee, Department of Physics, University of Virginia, and Joshua Choi, Department of Chemical Engineering, University of Virginia

Program Scope

Development of solar cells that can produce electrical power at a cheap rate is highly desirable for securing long term prosperity of mankind and mitigating the threat of climate change. Recently, hybrid organic-inorganic perovskites (HOIPs) have shown staggeringly rapid improvement in solar cell efficiency reaching 22.1% power conversion efficiency [1-6]. Despite the impressive progress in device performance, the microscopic mechanism of high solar cell efficiency is still poorly understood.

This DOE program investigates the properties of HOIPs at multiple length scales to achieve a full understanding of the microscopic mechanism of the photovoltaic effect. Specifically, the research is testing the hypothesis that the structure and dynamics of organic cations and their associated electric dipoles cause nanoscale separation of electrons and holes which results in high solar cell efficiency. Different organic cations, including methylammonium, formamidinium, methylformamidinium and guanidinium with different molecular symmetries and electric dipole moments are being studied. Elastic and inelastic neutron scattering techniques are employed to probe molecular and crystal structure and dynamics at the microscopic level. Optical spectroscopy, electrical transport measurements and solar cell fabrication and testing are employed to determine the impact of organic cations on the bulk properties and photovoltaic performance. The first principle calculations are also being performed.

Recent Progress

Using neutron diffraction and first-principles calculations on formamidinium (FA) lead iodide (FAPbI₃), we show that the entropy contribution to the Gibbs free energy caused by isotropic rotations of the FA⁺ cation plays a crucial role in the cubic-to-hexagonal structural phase transition. Furthermore, we observe that the cubic-to-hexagonal phase transition exhibits a large

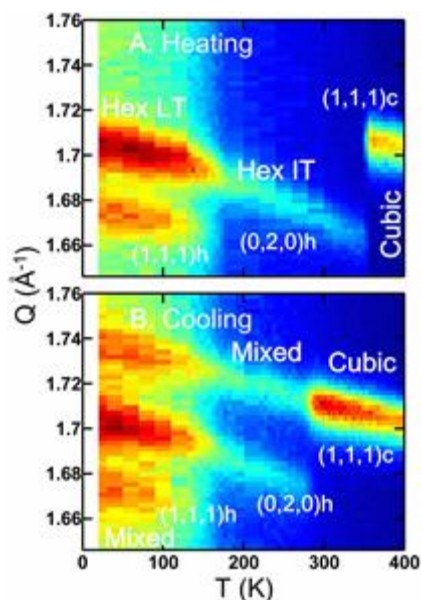


Figure: Elastic neutron scattering data obtained from FAPbI₃ upon heating (A) and upon cooling (B).

thermal hysteresis. Our first-principles calculations confirm the existence of a potential barrier between the cubic and hexagonal structures, which provides an explanation for the observed thermal hysteresis. By exploiting the potential barrier, we demonstrate kinetic trapping of a pseudo-cubic phase, desirable for solar cells.

Future Plans

Different organic cations, including methylammonium, formamidinium, methylformamidinium and guanidinium with different molecular symmetries and electric dipole moments will be studied, using various experimental and computational techniques such as elastic and inelastic neutron scattering techniques, optical spectroscopy, electrical transport measurements and solar cell fabrication and testing are employed to determine the impact of organic cations on the bulk properties and photovoltaic performance.

References

- 1 Brenner, T. M., Egger, D. A., Kronik, L., Hodes, G., Cahen, D. Hybrid organic—inorganic perovskites: low-cost semiconductors with intriguing charge-transport properties. *Nature Reviews Materials* **1**, 15007 (2016).
- 2 Leijtens, T., Eperon, G. E., Noel, N. K., Habisreutinger, S. N., Petrozza, A., Snaith, H. J. Stability of Metal Halide Perovskite Solar Cells. *Adv. Energy Mater.* **5**, 1500963 (2015).
- 3 Park, N.-G. Organometal Perovskite Light Absorbers Toward a 20% Efficiency Low-Cost Solid-State Mesoscopic Solar Cell. *The Journal of Physical Chemistry Letters* **4**, 2423-2429 (2013).
- 4 Park, N.-G., Grätzel, M., Miyasaka, T., Zhu, K., Emery, K. Towards stable and commercially available perovskite solar cells. *Nature Energy* **1**, 16152 (2016).
- 5 Seo, J., Noh, J. H., Seok, S. I. Rational Strategies for Efficient Perovskite Solar Cells. *Acc. Chem. Res.* **49**, 562-572 (2016).
- 6 Stranks, S. D., Snaith, H. J. Metal-halide perovskites for photovoltaic and light-emitting devices. *Nat Nano* **10**, 391-402 (2015).

Publications

T. Chen, B. J. Foley, C. Park, C. M. Brown, L. W. Harriger, J. Lee, J. Ruff, M. Yoon, J. J. Choi, and S.-H. Lee “Entropy Driven Structural Transition and Kinetic Trapping in Formamidinium Lead Iodide Perovskite” *Science Advances*, **2**, e1601650 (2016)

B. J. Foley, J. Girard, B. A. Sorenson, A. Z. Chen, J. S. Niezgoda, M. R. Alpert, A. F. Harper, D.-M. Smilgies, P. Clancy, W. A. Saidi, and J. J. Choi “Controlling Nucleation, Growth, and Orientation of Metal Halide Perovskite Thin Films with Rationally Selected Additives” *Journal of Materials Chemistry A*, DOI: 10.1039/C6TA07671H (2016) (featured as inside front cover)

Scattering and Spectroscopic Studies of Quantum Materials

Young Lee (Stanford University and SLAC National Accelerator Laboratory)

Hongchen Jiang (SLAC National Accelerator Laboratory)

Program Scope

This project focuses on the fundamental physics of quantum materials with a comprehensive effort involving experiment (neutron and x-ray scattering, crystal growth, and thermodynamic measurements) and theory. A long-sought goal in condensed matter physics is finding materials whose ground states exhibit novel types of order, which break the classical paradigm of local order parameters. Several examples have recently been realized, such as the quantum spin liquid. This spin liquid state is relevant to theories of high- T_c superconductivity and has possible applications in quantum information. Our project follows an important path towards improved understanding by performing scattering and spectroscopic studies on crystals of real materials (such as $\text{ZnCu}_3(\text{OH})_6\text{Cl}_2$) and comparing the results with theoretical calculations for these materials. We also study other interesting quantum many-body phenomena such as topological magnon bands (the magnetic analogue of topological insulators) as well as intertwined order in high- T_c superconductors.

Recent Progress

We have been studying the $S=1/2$ kagome material herbertsmithite ($\text{ZnCu}_3(\text{OH})_6\text{Cl}_2$) which is a leading candidate to have a quantum spin liquid (QSL) ground state. Our studies have confirmed that the relevant spin Hamiltonian is the nearest neighbor Heisenberg model to good approximation. This allows for a close comparison with theoretical expectations. In particular, our neutron scattering experiments have shown the presence of fractionalized spinon excitations as the low energy excitations, a hallmark of the QSL. Recent progress has intensely focused on the important question of whether there is a gap in the excitation spectrum. By growing single crystals enriched with ^{17}O , we collaborated with Imai's group (McMaster) to distinguish the magnetic susceptibility associated with the intrinsic kagome spins versus spins near the small fraction of impurities.[1] The intrinsic susceptibility shows evidence for a spin gap in zero applied field. Moreover, we have performed inelastic neutron scattering with high energy resolution in both the (HK0) and (HHL) zones. This allowed us to distinguish correlations associated with the impurities from the intrinsic kagome spins.[2] Our analysis confirmed the presence of a spin gap consistent in magnitude with the NMR results. These results are also in accord with numerical calculations predicting the presence of a small spin gap.

In our project, the PI Jiang has performed density matrix renormalization group (DMRG) calculations of structure factor for the $S=1/2$ kagome Heisenberg model. These calculations are performed on long cylindrical geometries, and include next-nearest neighbor exchange (J_2) and a Dzyaloshinsky-Moriya interaction (D_z) in addition to the nearest neighbor exchange (J_1). By comparing to the neutron scattering intensities in the (HK0) plane, we can provide quantitative limits which show that J_2 and D_z are small perturbations in herbertsmithite.

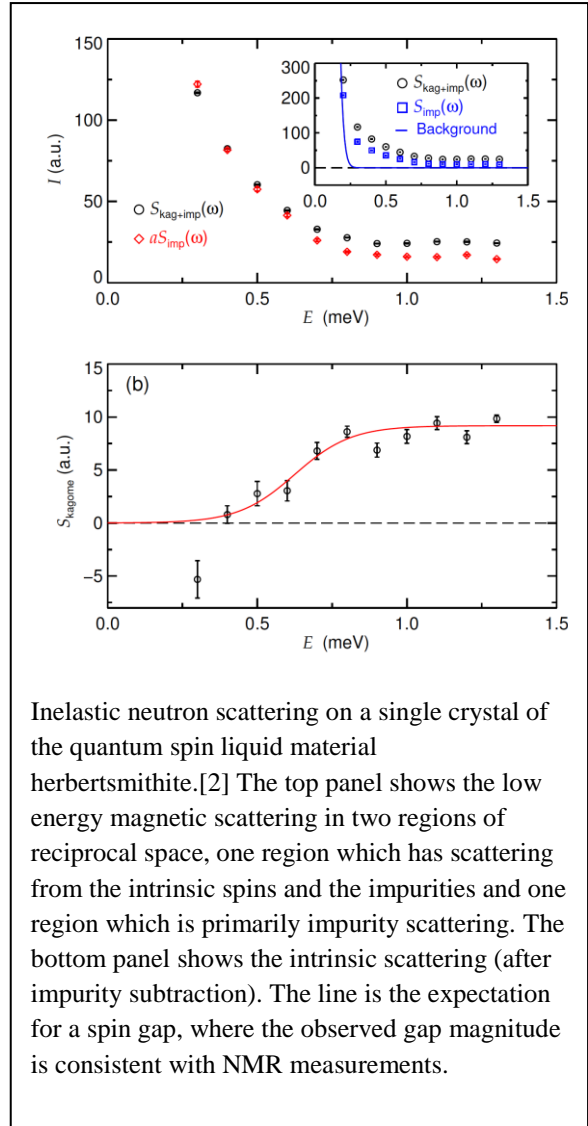
We are also studying other kagome materials which magnetically order. Here, the presence of a Dzyaloshinsky-Moriya interaction gives rise to bulk gaps between the magnon bands. More importantly, this also gives rise to a non-trivial topology for the lowest and highest magnon bands. Interesting physics appears, such as the magnon Hall effect and protected chiral edge states. This kagome material is the first clear example of a "topological magnon insulator." [3]

Using x-ray scattering, we are examining the behavior of charge density wave (CDW) order in the La_2CuO_4 -based superconductors. We have recently performed experiments at the LCLS x-ray free electron laser facility to measure the CDW in high magnetic fields (using pulsed fields). Our results indicate that the field-enhanced CDW remains two-dimensional, in contrast to similar x-ray experiments on YBCO superconductors.

We have also performed x-ray scattering in high pressures and low temperatures on the $S=1/2$ chain compound TiOCl . With increasing pressure, the magnetic exchange interaction also increases, such that at ~ 8 GPa, the material is in the spin-Peierls state even at room temperature. Also, at higher pressures, the system crosses over from an insulating to a more metallic state.

Future Plans

In the future, we plan further studies on herbertsmithite, such as systematic neutron scattering in high fields as the spin-gap closes. We will perform numerical calculations that



include the effect of magnetic field to directly compare with the neutron data. We also plan to understand how disorder affects the CDW in the cuprates, by studying materials with ordered dopants in contrast to randomly substituted dopants. We are continually trying to make new spin liquid materials in single crystalline form, as well as control the degree of disorder. We are also exploring other frustrated systems which may exhibit interesting topological phases.

References

- [1] M. Fu, T. Imai, T.H. Han, and Y.S. Lee, *Evidence for a gapped spin-liquid ground state in a kagome Heisenberg antiferromagnet*, Science 350, 655 (2015).
- [2] Tian-Heng Han, M. R. Norman, J.-J. Wen, Jose A. Rodriguez-Rivera, Joel S. Helton, Collin Broholm, and Young S. Lee, *Correlated impurities and intrinsic spin-liquid physics in the kagome material herbertsmithite*, Phys. Rev. B 94, 060409(R) (2016).
- [3] R. Chisnell, J.S. Helton, D.E. Freedman, D.K. Singh, R.I. Bewley, D.G. Nocera, and Y.S. Lee, *Topological Magnon Bands in a Kagome Lattice Ferromagnet*, Phys. Rev. Lett. 115, 147201 (2015).

Publications

- 9) Takashi Imai and Young S. Lee, *Do quantum spin liquids exist?*, Physics Today 69, 8, 30 (2016).
- 8) Tian-Heng Han, M. R. Norman, J.-J. Wen, Jose A. Rodriguez-Rivera, Joel S. Helton, Collin Broholm, and Young S. Lee, *Correlated impurities and intrinsic spin-liquid physics in the kagome material herbertsmithite*, Phys. Rev. B 94, 060409(R) (2016).
- 7) R. Chisnell, J.S. Helton, D.E. Freedman, D.K. Singh, F. Demmel, C. Stock, D.G. Nocera, and Y.S. Lee, *Magnetic transitions in the topological magnon insulator Cu(1,3-bdc)*, Phys. Rev. B 93, 214403 (2016).
- 6) D.R. Gardner, C.J. Bonnoit, R. Chisnell, A.H. Said, B.M. Leu, T.J. Williams, G.M. Luke, and Y.S. Lee, *Inelastic x-ray scattering measurements of phonon dynamics in URu₂Si₂*, Phys. Rev. B 93, 075123 (2016).
- 5) F. Mahmood, C.-K. Chan, Z. Alpichshev, D. Gardner, Y.S. Lee, P.A. Lee & N. Gedik, *Selective scattering between Floquet–Bloch and Volkov states in a topological insulator*, Nature Physics 12, 306 (2016).
- 4) M. Fu, T. Imai, T.H. Han, and Y.S. Lee, *Evidence for a gapped spin-liquid ground state in a kagome Heisenberg antiferromagnet*, Science 350, 655 (2015).
- 3) R. Chisnell, J.S. Helton, D.E. Freedman, D.K. Singh, R.I. Bewley, D.G. Nocera, and Y.S. Lee, *Topological Magnon Bands in a Kagome Lattice Ferromagnet*, Phys. Rev. Lett. 115, 147201 (2015).
- 2) M. Hirschberger, R. Chisnell, Y.S. Lee, and N.P. Ong, *Thermal Hall Effect of Spin Excitations in a Kagome Magnet*, Phys. Rev. Lett. 115, 106603 (2015).
- 1) T. Asaba, T.-H. Han, B.J. Lawson, F. Yu, C. Tinsman, Z. Xiang, G. Li, Y.S. Lee, and L. Li, *High-field magnetic ground state in S=1/2 kagome lattice antiferromagnet ZnCu₃(OH)₆Cl₂*, Phys. Rev. B 90, 064417 (2014).

Neutron Scattering Studies of Complex Oxides and Alloys

University of Minnesota Center for Quantum Materials

Chris Leighton, Chemical Engineering and Materials Science, University of Minnesota

Program Scope

This program focuses on the study of complex oxide and alloy systems, particularly *via* neutron scattering [SANS (Small-Angle Neutron Scattering), neutron diffraction, and PNR (Polarized Neutron Reflectometry)], transport, magnetic, and thermodynamic probes. This research was originally focused on the magnetism of complex oxides, specifically the problem of electronic and magnetic phase separation, thought to underpin some of their most interesting properties. After establishing the cobaltites as model systems for such studies [see Fig. 1 for a phase diagram of the prototypical $\text{La}_{1-x}\text{Sr}_x\text{CoO}_3$ (LSCO)], the work has now expanded to include other cobaltites, Ti-based perovskites, and other systems with nanoscale magnetic inhomogeneity. The latter include complex alloys that have not previously been examined in this light, but are model systems to study magnetic phase competition. These materials, such as the Heusler-derived $\text{Ni}_{50-x}\text{Co}_x\text{Mn}_{25+y}\text{Sn}_{25-y}$, now form a significant fraction of our effort. Model titanates such as SrTiO_3 make up the remainder of the program. These Ti oxides still pose substantial challenges to our understanding, despite being some of the most extensively studied, and are central to many

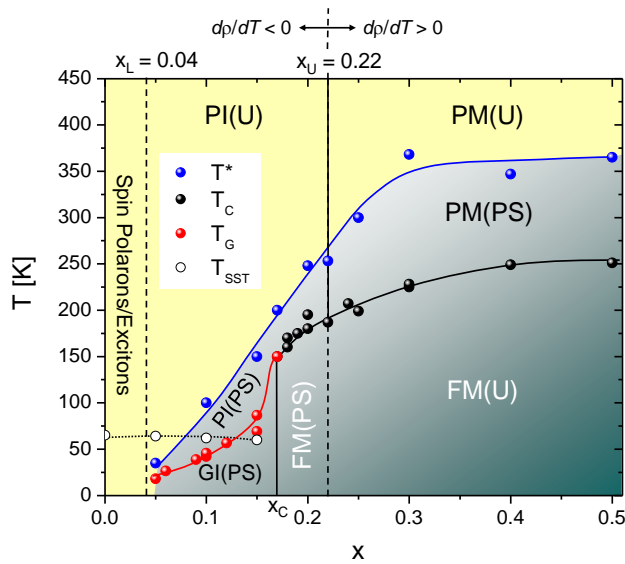


Figure 1: Magnetic/electronic phase diagram of $\text{La}_{1-x}\text{Sr}_x\text{CoO}_3$. x_c is the percolation threshold, and T^* , T_C , T_G , and T_{SST} are the cluster formation, Curie, glass transition, and spin-state transition temperatures. I = Insulator, M = Metal, P = Paramagnet, F = Ferromagnet, and G = Glassy. U and PS denote magnetically uniform and phase-separated.

emerging oxide electronic and energy technologies. Importantly, this research features not only synthesis and measurement of bulk crystals, but also epitaxial films and heterostructures. Growth of the latter is now possible with atomic precision in these oxides, opening up many opportunities in science and technology. This program is thus directly aligned with grand challenges such as controlled synthesis of materials and structures with advanced function, and emergence of novel properties from complex correlations. The research is also highly collaborative, being carried out in conjunction with experimentalists and theorists at multiple US universities and national labs.

As returned to below, beginning in 2017 this award will be gradually subsumed by the BES-funded Center

for Quantum Materials at the U. of MN, with PIs Chubukov, Fernandes, Greven, Jalan and Leighton. The program scope will then expand to include work on other complex oxides.

Recent Progress

Bulk Perovskite Cobaltites. Following from the work encompassed by Fig. 1, we have been investigating arguably the largest remaining mystery in the LSCO phase diagram: the very low x

regime. In this region the interplay between spin-state transitions and magnetic phase separation yields rich physics. We have recently elucidated this by obtaining the first direct, scattering-based evidence for entities known as magnetic excitons in $\text{LaCoO}_{3-\delta}$ crystals [13]. These excitons, which are analogous to spin-state polarons, form when a defect (in this case an oxygen vacancy) locally stabilizes finite spin Co in an $S = 0$ matrix. SANS was shown capable of detecting such excitons (Fig. 2), which were confirmed to collectively order below 60 K. Understanding how this excitonic/polaronic state evolves into the established magnetic cluster state at higher x is an important general problem, which forms a major focus of our current work. By examining carefully-characterized single crystals with AC and DC magnetometry, SANS, magnetotransport and heat capacity, and comparing to extensive calculations and simulations (with R. Fernandes, U. of MN) we have developed a new picture of this crossover, emphasizing the previously ignored role for frustration of magnetic interactions.

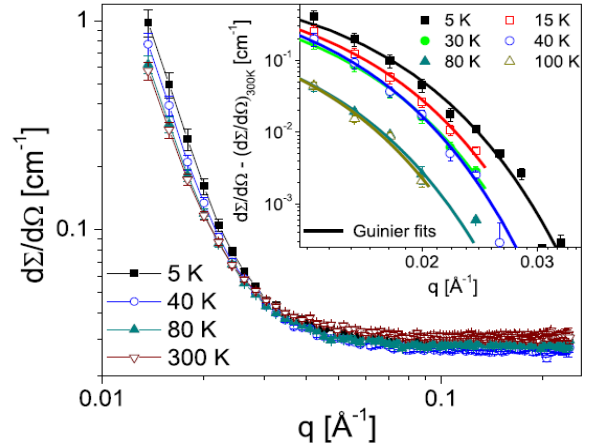


Figure 2: Wavevector dependence of the SANS cross-section in $\text{LaCoO}_{3-\delta}$. The inset shows the magnetic component, which follows a Guinier form, due to scattering from magnetic excitons.

The second frontier in the study of bulk cobaltites is provided by the Pr-based compounds that have generated such excitement by revealing a first-order metal-insulator transition driven by a transition in *Pr valence*. This occurs in systems such as $\text{Pr}_{1-x}\text{Ca}_x\text{CoO}_3$, and can be stabilized up to ~ 160 K by Y-doping. Our work has emphasized the spatial inhomogeneity of this transition [16], in addition to clarifying the fundamental mechanism *via* extensive DFT (Density Functional Theory) calculations with R. Wentzcovitch (U. of MN). The latter highlight the vital role for Pr f electrons near the Fermi level [7]. Beyond this, we recently provided (Fig. 3) not only the first direct observation of the Pr valence transition with atomic resolution [using EELS (Electron Energy Loss Spectroscopy) in a

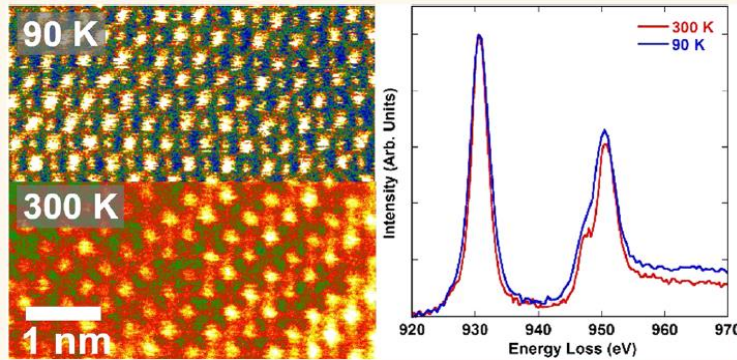


Figure 3: Left: Transition from oxygen vacancy order (300 K) to disorder (90 K) across the $(\text{Pr}_{1-y}\text{Y}_y)_{0.7}\text{Ca}_{0.3}\text{CoO}_{3-\delta}$ valence transition. Right: Associated Pr valence change from Pr EELS.

variable temperature STEM (Scanning Transmission Electron Microscope)], but also the discovery that this can trigger an oxygen vacancy order/disorder transition [8]. Oxygen vacancy ordering is now well-known in cobaltites, but this work shows how a reduction in Co valence (induced by the $\text{Pr}^{3+} \rightarrow \text{Pr}^{4+}$ shift) can stimulate a reversible order/disorder transition of oxygen vacancies, even at the remarkably low temperature of 150 K [8].

Cobaltite Films and Heterostructures. Building on our understanding in the bulk, for a number of years we have been using LSCO films to elucidate fundamental problems in complex oxide heterostructures. A primary example is the “dead layer” effect, where ferromagnetism and

conductivity are gradually degraded in the ultrathin film limit in ferromagnetic complex oxides. Our prior work revealed that this occurs due to an interface-induced form of magnetic phase separation, where LSCO breaks into nanoscopic ferromagnetic clusters in a non-ferromagnetic insulating matrix, explaining the reduced magnetization and conductivity. While prior work deduced this from transport and SANS, we now have real-space imaging of this effect from collaborative scanning tunneling spectroscopy measurements [15]. Most importantly, we understand this interfacial magnetic phase separation to be induced by oxygen vacancy accumulation at the substrate interface, driven by a novel mechanism for lattice mismatch accommodation. In essence these systems undergo oxygen vacancy ordering to modulate the in-plane lattice constants, hence lattice matching the substrate. Epitaxial strain thus controls the oxygen vacancy concentration and ordering, in turn controlling the magnetic and transport properties. We have now completed a full study of this effect, combining STEM/EELS with PNR. Equally interesting is our discovery that this spontaneous superlattice formation due to oxygen vacancy ordering can also lead to surprising property enhancements. For example, for reasons that are not yet fully understood, oxygen vacancy ordering in LSCO leads to both giant anisotropic magnetoresistance and perpendicular magnetic anisotropy, both phenomena that do not typically occur in cobaltites. These effects are currently under active investigation. A number of other features of the magnetism and transport in ultrathin LSCO films have also been elucidated, one noteworthy example being the interplay with the well-known cubic-to-tetragonal phase transition in films grown on SrTiO₃(001). This transition induces transport anomalies around 105 K, which we have confirmed to result from evanescent soft phonons traversing the interface, in addition to strong domain effects due to magnetoelastic coupling.

Complex Alloys. As noted above, our work on systems with nanoscale magnetic inhomogeneity has now expanded beyond perovskites, to complex alloys. The first of these studied was Ni_{50-x}Co_xMn_{25+y}Sn_{25-y}. This system was discovered *via* a program of rational synthesis (by R. James, U. of MN), seeking ferromagnetic shape memory alloys that undergo martensitic transformations with ultra-low thermal hysteresis. Such materials are of interest for applications in actuators and sensors, as well as in energy conversion applications [11,12]. From the basic science perspective, these materials, which are derived from the ferromagnetic full Heusler Ni₂MnSn by deliberate off-stoichiometric substitution, exhibit strong magnetic phase competition. Specifically, the excess Mn (y) generates antiferromagnetic Mn-Mn bonds in the ferromagnetic host, which results in nanoscale magnetic phase separation, much like perovskites. This leads to surprising effects, such as superparamagnetism in a bulk solid, and intrinsic exchange bias [11,12]. Following our SANS study providing the first proof of the existence of nanoscale spin clusters, our recent work in collaboration with M. Hoch (National High Magnetic Field Lab) has applied NMR to resolve important open questions in these systems [3,6,10]. This includes the first understanding of the short-range antiferromagnetic nature of the martensitic matrix, as well as a detailed picture of the dynamics of superparamagnetism and exchange bias. More recent SANS measurements across the entire phase diagram confirm the poorly understood separation of superparamagnetic and exchange bias blocking temperatures at low Co doping, while heat capacity studies have revealed surprisingly large electronic correlations. A doping-fluctuation-based model for this behavior is under development, and other materials are being explored.

Titanates. Ti-based systems are of special importance in perovskites, partly due to the enduring interest in SrTiO₃, the most heavily studied perovskite, and partly due to the intense interest in 2D electron systems at titanate interfaces. Motivated by this, our group has studied various aspects of the physics and chemistry of SrTiO₃. This yielded a detailed understanding of how

quantum para-electricity impacts electronic transport, as well as the discovery of light-induced magnetism in this d^0 system. Recently, we have tackled a different aspect to the behavior of SrTiO₃, namely the widely-known 105 K antiferrodistortive transition from cubic to tetragonal. While this has been understood since the 60's to take place *via* phonon mode softening, one aspect that has *not* yielded to quantitative understanding is the response of the transition temperature, T_a , to chemical substitution. This is illustrated in Fig. 4 (left panel), where T_a

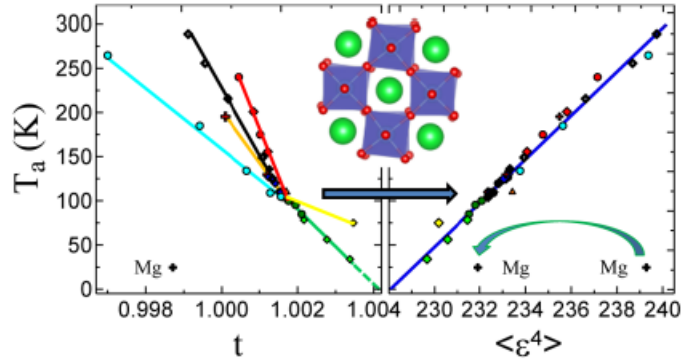


Figure 4: Antiferrodistortive transition temperature vs. tolerance factor (left), and the newly developed parameter $\langle \epsilon^4 \rangle$ (right), for various chemical substitutions in SrTiO₃.

is plotted *vs.* tolerance factor, t , for a range of substituents (Ba, Ca, Gd, Pb, *etc.*). The trends are remarkably complex, and have evaded explanation. Following from heat capacity measurements of T_a in the Nb-substituted system of high interest for transport, we have developed the first quantitative model capable of rationalizing these trends [2]. This is based on bond valence concepts, quantifying not the impact of the *size* mismatch of the substituent ions, but rather their *valence* mismatch. This establishes a new structural parameter, $\langle \epsilon^4 \rangle$, which exhibits a universal linear relationship with T_a for every known substituent in SrTiO₃ (Fig. 4, right panel), providing the first predictive understanding of the response of T_a to substitution [2]. These heat capacity measurements also provide new insight into the lattice dynamics of SrTiO₃, as well as the evolution of the electron effective mass across the Lifshitz transitions in this system.

Future Plans

A number of these results suggest immediate directions for further work, particularly in cobaltite heterostructures, complex alloys, and titanates. Work with LSCO films will continue, particularly x -dependent studies of oxygen vacancy ordering, magnetoresistance, and anisotropy, as well as $x = 0$ films under tensile strain. The latter exhibit ferromagnetism, despite the $S = 0$ bulk ground state, which will be probed with PNR. Transport and PNR will also be used to study ultrathin [LaAlO₃/LSCO] superlattices. This will address an open general question in complex oxide heterostructures, *i.e.*, whether a ground state different to bulk is a general feature under extreme dimensional confinement (as in LaNiO₃, La_{1-x}Sr_xMnO₃, *etc.*). Pr_{1-x}Ca_xCoO₃ films will also be studied, seeking strain control of the Pr valence and metal-insulator transition, potentially even at room temperature. In terms of complex alloys, in addition to completing work on Ni-Co-Mn-Sn, we will also investigate (with Seshadri, UC Santa Barbara) Ru₂Mn_{1-x}Fe_xSn. The end-members in this series are ferromagnetic and antiferromagnetic, the competition at intermediate x leading to nanoscale magnetic phase separation in what is potentially a structurally simple cubic alloy. Finally, the establishment of the MN Center for Quantum Materials will open up a number of future opportunities, one noteworthy example being studies of bulk and heterostructured rare-earth titanates. To this end we will not only extend our work on SrTiO₃ (working with Fernandes and Jalan), but will also commence study of the ferromagnetic to antiferromagnetic crossover in $RTiO_3$ systems, coupled with studies of the Mott insulator-metal transition with doping. This will be done in collaboration with Chubukov, Fernandes and Greven, complementary work on heterostructures being performed with Jalan. Ultimately, a full understanding of the magnetic Mott insulator to correlated metal transition is sought, using titanates as model systems.

Publications (2014 – 2016)

1. “*Static and dynamic interfacial effects in magnetism*”, F. Hellman, A. Hoffmann, Y. Tserkovnyak, G.S.D. Beach, E.E. Fullerton, C. Leighton, A.H. MacDonald, D.C. Ralph, D.A. Arena, H.A. Durr, P. Fischer, J. Grollier, J.P. Heremans, T. Jungwirth, A.V. Kimel, B. Koopmans, I.N. Krivorotov, S.J. May, A.K. Petford-Long, J.M. Rondinelli, N. Samarth, I.K. Schuller, A.N. Slavin, M.D. Stiles, O. Tchernyshyov, A. Thiaville and B.L. Zink, under review, *Rev. Mod. Phys.* (2016).
2. “*A unified view of the substitution-dependent antiferrodistortive phase transition in SrTiO₃*”, E. McCalla, J. Walter and C. Leighton, *Chem. Mater.* **28**, 7973 (2016).
3. “*Magnetic-field-induced changes in superparamagnetic cluster dynamics in the martensitic phase of Ni₄₃Co₇Mn₄₀Sn₁₀*”, P.L. Kuhns, M.J.R. Hoch, S. Yuan, A.P. Reyes, V. Srivastava, R.D. James and C. Leighton, *Appl. Phys. Lett.* **108**, 252403 (2016).
4. “*Defects, stoichiometry, and electronic transport in SrTiO_{3-δ} epilayers: A high pressure oxygen sputter deposition study*”, P. Ambwani, P. Xu, G. Haugstad, J.S. Jeong, R. Deng, A. Mkhoyan, B. Jalan and C. Leighton, *J. Appl. Phys.* **120**, 055704 (2016).
5. “*Electrostatic vs. electrochemical doping and control of ferromagnetism in ion-gel-gated ultrathin La_{0.5}Sr_{0.5}CoO_{3-δ}*”, J. Walter, H. Wang, C.D. Frisbie and C. Leighton, *ACS Nano* **10**, 7799 (2016).
6. “*Phase separation and superparamagnetism in the martensitic phase of Ni_{50-x}Co_xMn₄₀Sn₁₀*”, S. Yuan, P.L. Kuhns, A.P. Reyes, J.S. Brooks, M.J.R. Hoch, V. Srivastava, R.D. James and C. Leighton, *Phys. Rev. B.* **93**, 094425 (2016).
7. “*First principles study of crystal and electronic structure of rare-earth cobaltites*”, M. Topsakal, C. Leighton and R.M. Wentzcovitch, *J. Appl. Phys.* **119**, 244310 (2016).
8. “*Simultaneous first-order valence and oxygen vacancy order/disorder transitions in (Pr_{0.85}Y_{0.15})_{0.7}Ca_{0.3}CoO_{3-δ} via analytical transmission electron microscopy*”, A. Gulec, D.P. Phelan, C. Leighton and R.F. Klie, *ACS Nano* **10**, 938 (2016).
9. “*Determination of the lamellae-to-disorder heat of transition in a diblock copolymer by relaxation calorimetry*”, T.M. Gillard, D.P. Phelan, C. Leighton and F.S. Bates, *Macromolecules*, **48**, 4733 (2015).
10. “*Magnetically nanostructured state in a Ni-Mn-Sn shape memory alloy*”, S. Yuan, P.L. Kuhns, A.P. Reyes, J.S. Brooks, M.J.R. Hoch, V. Srivastava, S. El-Khatib, R.D. James and C. Leighton, *Phys. Rev. B.* **91**, 214421 (2015).
11. “*Magnetic phase competition in off-stoichiometric martensitic Heusler alloys: The Ni_{50-x}Co_xMn₄₀Sn₁₀ system*”, K.P. Bhatti, V. Srivastava, D.P. Phelan, R.D. James and C. Leighton, invited book chapter in *Heusler Alloys*, eds. A. Hirohata and C. Felser, Springer (2015).
12. “*Thermodynamics and energy conversion in Heusler alloys*”, Y. Song, C. Leighton and R.D. James, invited book chapter in *Heusler Alloys*, eds. A. Hirohata and C. Felser, Springer (2015).
13. “*Neutron-scattering-based evidence for interacting magnetic excitons in LaCoO₃*”, S. El-Khatib, D. Phelan, J.G. Barker, H. Zheng, J.F. Mitchell and C. Leighton, *Phys. Rev. B. Rapid Comm.* **92**, 060404(R) (2015).
14. “*Sphericity and symmetry breaking in the formation of Frank-Kasper phases from one component materials*”, S. Lee, C. Leighton and F.S. Bates, *Proc. Nat. Acad. Sci.* **111**, 17723 (2014).
15. “*Direct real space observation of magneto-electronic inhomogeneity in ultra-thin film SrTiO₃(001)/La_{0.5}Sr_{0.5}CoO_{3-δ}*”, S. Kelly, F. Galli, J. Aarts, S. Bose, M. Sharma and C. Leighton, *Appl. Phys. Lett.* **105**, 112909 (2014).
16. “*Magnetically inhomogeneous ground-state below the first order valence transition in (Pr_{1-y}Y_y)_{0.7}Ca_{0.3}CoO_{3-δ}*”, D. Phelan, K.P. Bhatti, M. Taylor, S. Wang and C. Leighton, *Phys. Rev. B.* **89**, 184427 (2014).
17. “*Magnetocaloric effect and critical behavior in Pr_{0.5}Sr_{0.5}MnO₃: An analysis on the validity of the Maxwell relation and the nature of phase transitions*”, R. Caballero-Flores, N.S. Bingham, M.H. Phan, M.A. Torija, C. Leighton, V. Franco, A. Conde and H. Srikanth, *J. Phys.: Cond. Mat.* **26**, 286001 (2014).

Local complexity and the mechanics of phase transitions in novel materials

Despina Louca, University of Virginia

Program Scope

Novel materials of interest today provide unique opportunities to study emergent exotic states of matter that arise from the intricate coupling of the electronic and lattice degrees of freedom, and of their implications in the mechanics of phase transitions. A central theme of this project has been the exploration of distinct features resulting from the coexistence of two (or more) order parameters, the nucleation of different phases in the parent matrix, the formation of spin/charge density waves, and the formation of structural patterns that break the global symmetry. These are key components to our understanding of the evolution across phase boundaries. However, they cannot be readily characterized with traditional means used for probing single electron behavior. This is because their behavior is a collective effect, in response to strong interactions. The goal of the proposed program has been to explore such states of matter that appear to be endemic in oxides, superconductors and intermetallic compounds using scattering techniques.

By combining scattering and synthesis, we have been investigating the underlying mechanisms leading to phase transitions. This has been accomplished by guided sample synthesis and thermodynamic properties characterization, followed by scattering experiments to probe the static and dynamic structures. The measurements have been coupled with modeling that help determine the length- and time-scales of inhomogeneities, be it magnetic or structural. In this program, we have experimentally identified the local microstructure, the distortions invoked by magnetic interactions, the effects of orbital hybridization and crystal phase transitions, local and global distortions and of their role in materials functionality and phase transitions in a number of systems. In addition, we have experimentally identified the nature of spin correlations and of their role in spin-charge and -lattice interactions by varying temperature, magnetic field, pressure and magnetic ion doping, and characterized magnetic incommensurabilities. Furthermore, we have developed an understanding into how different electronic, magnetic and structural order parameters compete and co-exist and how they can lead to phase separation. For the purpose of this abstract, we will focus only on the Fe-based superconductors.

Recent Progress

Much remains unknown of the microscopic origin of superconductivity when it materializes in atomically disordered systems as in amorphous alloys or in crystals riddled with defects. A manifestation of this conundrum is seen in the highly defective iron chalcogenide superconductors. How can superconductivity survive under such crude conditions that call for

strong electron localization and scattering? With vacancies present both at the K and Fe sites in the $K_xFe_{2-y}Se_2$ superconductor, superconductivity is bordering a semi-metallic region below $x \sim 0.7$ and an insulating and antiferromagnetic region above $x \sim 0.85$. While suppression of long-range magnetic order occurs with the onset of superconductivity in many of the Fe-based superconductors, this is not the case in $K_xFe_{2-y}Se_2$ with a T_C of the order of 30 K or so [1]. The intercalated FeSe has a very complex phase diagram where the superconducting phase co-exists with large magnetic moments and a high antiferromagnetic transition, T_N , close to 560 K and is sandwiched between semi-metallic ($x < \sim 0.7$) and insulating ($x > \sim 0.8$) antiferromagnetic states [2]. The crystal system consists of iron vacancies at one of the two possible crystal sites and their ordering gives rise to the $\sqrt{5} \times \sqrt{5} \times 1$ type unit cell with the $I4/m$ crystal symmetry [3-6]. The vacancies go through an order-disorder transition at $T_S \sim 500$ K [7], while in the high temperature disordered state, the symmetry is $I4/mmm$. This system presents an opportunity to investigate the interplay of magnetism, superconductivity and vacancies. It is currently debated whether this system is phase separated or not. In this talk, I will discuss our recent results on the bulk local atomic structure and single crystal work that show striking differences between superconducting and non-superconducting compositions regarding the ordering of the Fe and K sublattices and of the magnetic order.

In a related system, the intercalation of LiFeOH in the tetragonal lattice of $Fe_{1-y}Se$ leads to a great enhancement of the superconducting transition temperature, $T_C \sim 43$ K and possibly to an antiferromagnetic transition at 8.5 K [8]. The crystal structure of $(Li_{1-x}Fe_xOH)_yFeSe$ consists of alternating tetrahedral layers of FeSe and $Li_{1-x}Fe_xOH$. Whether or not the enhancement of T_C is the result of introducing well-ordered spacer layers in the lattice that change the Fermi surface remains an open question. What if the intercalating filling fraction is not uniform? Resolving these issues are not only relevant to understanding how intercalation yields higher T_C , but address a broader issue of how bulk superconductivity survives even in the presence of lattice disorder. Moreover, earlier work suggested that upon cooling below T_C , the superconducting state of $(Li_{1-x}Fe_xOH)_yFeSe$ coexists with antiferromagnetism. A more recent small angle neutron scattering experiment contradicted the presence of the antiferromagnetic component and instead provided evidence for short-range ferromagnetic correlations below 12.5 K with a very small ferromagnetic ordered moment [9]. The origin of the magnetic signal is not understood at present. While the LiFeOH layer acts as a charge reservoir, its Fe ion is thought to be magnetic that may create a magnetic buffer layer. Most recently, we developed a new synthesis method to control the Fe concentration in the intercalating layer as well as the filling ratio of the $(Li_{1-x}Fe_xOH)_yFeSe$ layers. Neutron scattering measurements were carried out on powder samples of $(Li_{1-x}Fe_xOH)_yFeSe$ and the results were compared to Mossbauer measurements on the same samples. With the intercalation, no crystal structural transition from the $P4/nmm$ symmetry occurs but the c-axis lattice constant expands substantially, evidence of the intercalation. Our results indicate that the amount of Fe in the LiFeOH layer has a direct correlation to the transition temperature and evidence will be presented that support the coexistence of superconductivity with magnetism.

Future Plans

This is the final year of this project. A more immediate plan is to complete the work on the Fe-based superconductors and continue in a new direction involving semiconductors.

References

1. J. Guo, S. Jin, G. Wang, S. Wang, K. Zhu, T. Zhou, M. He, and X. Chen, *Phys. Rev. B* **82**, 180520(R) (2010).
2. Y. J. Yan, M. Zhang, A. F. Wang, J. J. Ying, Z. Y. Li, W. Qin, X. G. Luo, J. Q. Li, J. P. Hu and X. H. Chen, *Sci. Rep.* **2**, 00212 (2012).
3. W. Bao, Q.-Z. Huang, G.-F. Chen, M. a. Green, D.-M. Wang, J.-B. He, and Y.-M. Qiu, *Chin. Phys. Lett.* **28**, 086104 (2011).
4. F. Ye, S. Chi, Wei Bao, X. F. Wang, J. J. Ying, X. H. Chen, H. D. Wang, C. H. Dong, and M. H. Fang, *Phys. Rev. Lett.* **107**, 137003 (2011).
5. M.-H. Fang, H.-D. Wang, C.-H. Dong, Z.-J. Li, C.-M. Feng, J. Chen, and H. Q. Yuan, *Europhys. Lett.* **94**, 27009 (2011).
6. Z. Wang, Y. J. Song, H. L. Shi, Z. W. Wang, Z. Chen, H. F. Tian, G. F. Chen, J. G. Guo, H. X. Yang, and J. Q. Li, *Phys. Rev. B* **83**, 140505(R) (2011).
7. W. Bao, G. N. Li, Q. Huang, G. F. Chen, J. B. He, M. A. Green, Y. Qiu, D. M. Wang and J. L. Luo, arXiv:1102.3674 (2011).
8. U. Pachmayr, F. Nitsche, H. Luetkens, S. Kamusella, F. Brückner, R. Sarkar, H.-H. Klauss, D. Johrendt, *Angew. Chem. Int. Ed.* **53** (2014); DOI:10.1002/anie.201407756; arXiv:1409.3982.
9. X. Zhou, C. K. H. Borg, J. W. Lynn, S. R. Saha, J. Paglione, and E. E. Rodriguez, *J. Mater. Chem. C* **4**, 3934 (2016).

Publications

“Compositional dependence of magnetic ordering and dynamics in $\text{La}_{1-x}\text{Sr}_x\text{CoO}_3$: an inelastic neutron scattering study”, D. Phelan, D. Louca, S.-H. Lee, S. N. Ancona, P. J. Chupas, H. Zheng, J. F. Mitchell, J. W. Lynn and S. Rosenkranz, to be submitted (2016).

“An investigation of the lattice and magnetic dynamics in perovskite $\text{Y}_{1-x}\text{La}_x\text{TiO}_3$ ”, B. Li, D. Louca, J. Niedziela, Z. Li, L. Zhang, J. Zhou, J. B. Goodenough, accepted in *Phys. Rev. B* (2016).

“Phonon anomalies in YVO_3 ”, Y. Liang, D. Louca, T. Yildirim, D. L. Abernathy, to be submitted (2016).

- “Evidence of Nematicity in $K_{0.8}Fe_{2-y}Se_2$ ”, C. Duan, J. Yang, F. Ye and D. Louca, *J. Supercond. Nov. Magn.* **29**, 663 (2016).
- “The magnetic and crystal structures of new oxyfluorides $SrFeO_{2-x}F_x$ ”, B. Li, J. Woods, J. Siewenie, D. Louca, , *Chem. Comm.* **52**, 2386 (2016).
- “Magnetic structure of $NiS_{2-x}Se_x$ ”, S. Yano, D. Louca, U. Chatterjee, D. E. Bugaris, D. Y. Chung, and M. G. Kanatzidis, *Phys. Rev. B* **93**, 024409 (2016).
- “Local Jahn-Teller distortions and orbital ordering in $Ba_3Cu_{1+x}Sb_{2-x}O_9$ investigated by neutron scattering”, B. Li, D. Louca, M. Feyngenson, C. M. Brown, J. R. D. Copley, *Phys. Rev. B* **93**, 014423 (2016).
- “The magnetic transitions and dynamics in the multiferroic $Lu_{0.5}Sc_{0.5}FeO_3$ ”, J. Yang, C. Duan, J. R. D. Copley, C. M. Brown and D. Louca, *MRS Advances* DOI: 10.1557/adv.2016.141 (2016).
- “Strong correlations between vacancy and magnetic ordering in the superconducting of $K_{0.8}Fe_{2-y}Se_2$ ”, J. Yang, C. Duan, Q. Huang, C. Brown, J. Neuefeind, and D. Louca, *Phys. Rev. B* **94**, 024503 (2016).
- “Insulating droplet in metallic $LaNiO_3$ ”, B. Li, D. Louca, S. Yano, L. G. Marshall, J. Zhou, and J. B. Goodenough, *Advanced Electronic Materials*, DOI: 10.1002/aelm.201500261 (2015).
- “Suppression of magnetic coupling by in-plane buckling in $SrFeO_2$ ”
K. Horigane, A. Llobet, and D. Louca, *Phys. Rev. Lett.* **112**, 097001 (2014).
- “Structure and composition of the superconducting phase in alkali iron selenide $K_yFe_{1.6+x}Se_2$ ”, S. V. Carr, D. Louca, J. Siewenie, Q. Huang, A. Wang, X. Chen, P. Dai, *Phys. Rev. B* **89**, 134509 (2014).
- “ $La_xY_{1-x}VO_3$: Effects of doping on orbital ordering”, S. Yano, D. Louca, J.-Q. Yan, J. C. Neuefeind, J.-S. Zhou, J. B. Goodenough, *Phys. Rev. B* **90**, 214111 (2014).
- “Dynamic distortions in the $YTiO_3$ ferromagnet”, B. Li, D. Louca, B. Hu, J. Zhou, N. A. Benedek, J. B. Goodenough, *J. Phys. Soc. JPN* **83**, 084601 (2014).
- “Local crystal structure of Mott-insulating Iron Oxychalcogenides $La_2O_2Fe_2OSe_2$ ”, K. Horigane, K. Kawashima, S. Ji, M. Yoshikawa, D. Louca, J. Akimitsu, *JPS Conf. Proc.* **3**, 015039 (2014).
- “Intertwining of frustration with magneto-elastic coupling in the multiferroic $LuMnO_3$ ”, S. Yano, D. Louca, S. Chi, M. Matsuda, Y. Qiu, J. R. D. Copley, S. W. Cheong, *J. Phys. Soc. JPN* **83**, 024601 (2014).
- “Dynamics of local bond correlations in $FeSe_xTe_{1-x}$ by inelastic neutron scattering”, K. Park, J. W. Taylor, and D. Louca, *J. Supercond. Novel Magn.* **27**, 1927 (2014).

Sample Environment Capabilities at ORNL

Gary W. Lynn, Harish K. Agrawal, Mark J. Loguillo, Chris M. Redmon

Neutron Scattering Sciences Directorate

Oak Ridge National Laboratory

With the United States' highest flux reactor-based neutron source for condensed matter research (the High Flux Isotope Reactor) and the world's most intense pulsed accelerator-based neutron source (the Spallation Neutron Source), ORNL is becoming the world's foremost center for neutron science. Research at these facilities encompasses the physical, chemical, materials, biological, and medical sciences and provides opportunities for up to 2000 researchers each year from industry, research facilities, and universities all over the world.

We recognize that sample environment is an integral component to these experiments performed at our facilities. A brief overview of new sample environments and capabilities that we have brought online within the last two years will be presented. Future directions will also be discussed.

Superionic Conduction using Ion Aggregates

Janna Maranas (jmaranas@engr.psu.edu)

The Pennsylvania State University, University Park, PA 16802

(Abstract – Not Submitted)

Correlations and Competition between the Lattice, Electrons, and Magnetism

R. J. McQueeney (mcqueeney@ameslab.gov), A. I. Goldman, A. Kreyssig, D. Vaknin

Ames Laboratory and Iowa State University, Ames, IA 50011

Program Scope

The program strives to broaden our fundamental understanding of the interactions between the lattice, electrons, and magnetism in functional and quantum materials, such as high-temperature superconductors, frustrated magnetic systems, and multiferroics. Neutron and x-ray scattering are powerful techniques that directly probe the structural, electronic, and magnetic aspects of complex ground states, phase transitions, and corresponding excitations. Within this FWP, the varied expertise of the PIs in different scattering methods is employed in a synergistic approach and systems are studied using a wide range of neutron and x-ray techniques. Scattering studies of magnetism, structure and novel electronic phases are performed under a variety of control parameters, such as temperature, chemical composition, magnetic field, and pressure. The experimental program is supported by an effort in *ab initio* band structure calculations, theoretical modeling, and scattering simulations.

Recent Progress

Iron pnictides and chalcogenides: Iron-based superconductors are characterized by balanced interactions between structural, magnetic, and electronic states, leading to interesting and unusual phases, such as spin and electronic nematic phases, in addition to superconductivity. We have used inelastic neutron scattering (INS) to investigate the impact of nematic order on the magnetic spectra of LaFeAsO and Ba(Fe_{0.953}Co_{0.047})₂As₂. These materials are ideal to study the paramagnetic-nematic state, since the nematic order, signaled by the tetragonal-to-orthorhombic transition at T_S, sets in well above the stripe antiferromagnetic (AFM) ordering at T_N. We find that the dynamic susceptibility displays an anomaly at T_S followed by a sharp enhancement in the spin-spin correlation length. Our findings can be described by a model that attributes the nematic transition to magnetic fluctuations, and unveils the key role played by nematic order in promoting the long-range stripe AFM order in iron pnictides.[P7]

The picture that places importance on nematic phases driven by spin degrees-of-freedom has been confounded by recent investigations of FeSe where the nematic and magnetic transitions appear to be decoupled. We used high-energy x-ray diffraction and time-domain Mössbauer spectroscopy under applied pressure to show that nematicity and magnetism in FeSe are indeed strongly coupled. Distinct structural and magnetic transitions are observed for pressures between 1.0 and 1.7 GPa and merge into a single first-order transition for pressures ≥ 1.7 GPa, reminiscent of what has been found for the evolution of these transitions in the prototypical system Ba(Fe_{1-x}Co_x)₂As₂. Our results are again consistent with a spin-driven mechanism for nematic order in FeSe and provide an important step towards a universal description of the normal state properties of the iron-based superconductors.[P21]

The possibility of ionic ordering in AFe₂As₂ system with chemical substitutions on the A-site would allow for the study of superconducting materials without site disorder. CaKFe₄As₄ (or 1144) is a member of a new structural class of superconducting materials where A-site ions are ordered in alternating layers. Other than superconductivity, there is no indication of any other phase transition for $1.8 \text{ K} \leq T \leq 300 \text{ K}$. The thermodynamic and transport data reveal striking

similarities to those found for optimally doped and site-disordered $(\text{Ba}_{1-x}\text{K}_x)\text{Fe}_2\text{As}_2$, suggesting that stoichiometric $\text{CaKFe}_4\text{As}_4$ is intrinsically close to what is referred to as “optimal-doped” on a generalized, Fe-based superconductor, phase diagram. [P19]

Manganese and cobalt arsenides: Cobalt arsenides share some similarities and differences with their superconducting iron arsenide cousins. While SrCo_2As_2 displays no magnetic order in the ambient pressure Tet phase, it has fluctuating stripe AFM spin fluctuations.[5] On the other hand, CaCo_2As_2 adopts a collapsed-tetragonal (cT) structure at ambient pressure along with A-type AFM order (with 2D ferromagnetism (FM) in the Co square lattice). Whereas the Tet and cT phases in iron arsenides adopt magnetic and non-magnetic ground states respectively, both states appear to be magnetic in the cobalt arsenides. We studied the Tet-cT transition in SrCo_2As_2 under applied pressure using high-energy x-ray diffraction up to 29 GPa and discovered the Tet-cT transition above 6 GPa at 7 K. In addition, neutron diffraction measurements have been performed up to 1.1 GPa, but no magnetic order has been found, whereas spin-polarized total-energy calculations indicate that the cT phase of SrCo_2As_2 should manifest either A-type AFM or FM order.[P15]

We also found evidence for extreme magnetic frustration leading to one-dimensional spin fluctuations in CaCo_2As_2 . In the J_1 - J_2 magnetic exchange model for these materials, J_1 is FM and the AFM J_2 introduces frustration. When $|2J_2/J_1| < 1$, 2D FM occurs whereas stripe order is adopted for $|2J_2/J_1| > 1$. We find that $|2J_2/J_1|$ is close to 1 for CaCo_2As_2 , suggesting that it sits near a quantum critical point where spin liquid and other exotic phases are possible.[P29]

We have been trying to tune towards perfect magnetic frustration in the CaCo_2As_2 system by using chemical substitution. Our magnetization, neutron diffraction, and high-energy x-ray diffraction results for $\text{Ca}(\text{Co}_{1-x}\text{Fe}_x)_y\text{As}_2$, $0 \leq x \leq 1$, $1.86 \leq y \leq 2$, reveal that A-type AFM order persists up to $x \sim 0.125$, and that the ordered moment and T_N linearly decrease with increasing x . A smooth evolution occurs from the cT phase of $\text{CaCo}_{1.86}\text{As}_2$ to the Tet phase of CaFe_2As_2 . [P27]

BaMn_2As_2 is a Néel AFM insulator that undergoes a metal-insulator transition with hole doping. Néel AFM order is hardly affected by this transition, but surprisingly FM order develops at low temperatures and coexists with AFM order. X-ray magnetic circular dichroism (XMCD) measurements on $\text{Ba}_{0.6}\text{K}_{0.4}\text{Mn}_2\text{As}_2$ show that FM below $T_C \approx 100$ K arises in the As 4p conduction band, and that no XMCD signal is observed at the Mn x-ray absorption edges. These results show that distinct local-moment AFM and itinerant FM coexist in this compound. [P8]

It is important to confirm that this unusual behavior also occurs in the Mn-based structural classes, such as the RMnPnO (1111) materials. Neutron powder diffraction reveals Néel-type AFM order below $T_N = 347$ K for CeMnAsO , 255 K for LaMnSbO , and 240 K for CeMnSbO , all much lower than BaMn_2As_2 ($T_N = 618$ K). The ordered moments are somewhat smaller than those expected for Mn^{2+} ($S=5/2$), but large enough to suggest that these compounds are local-moment AFM. The lower T_N found in the 1111 compounds, as compared to the 122, could indicate more 2D-like interactions or increased frustration from AFM NNN interactions. Within the 1111 compounds, the Mn- Pn hybridization that mediates the Mn- Pn -Mn superexchange is weaker for the Sb-based compounds. A sharp Mn spin-reorientation transition and Ce ordering is observed at $T_{\text{SR}}=34$ K for CeMnAsO and 4.5 K for CeMnSbO . [P11,P17]

Heavy fermions: X-ray and neutron diffraction have been used to resolve mysteries surrounding the nature of the fragile magnetism in YbBiPt. We discovered collinear AFM ordering below $T_N = 0.4$ K at $\tau = (\frac{1}{2} \frac{1}{2} \frac{1}{2})$ with a moment of $\leq 0.8 \mu_B$ aligned along τ . [2] Previous studies of the crystalline-electric-field splitting suggest that the symmetry of the lattice is lower than cubic below $T = 6$ K. However, our high-energy x-ray scattering results find no structural phase transition occurring between $T = 1.8$ and 18 K, and that the low-temperature thermal expansion may be fit assuming either cubic or less-than-cubic point symmetry for the Yb sites. [P14]

Magnetic oxides: We have conducted neutron scattering experiments on single-crystals of LiMPO_4 ($M = \text{Fe, Ni, Co, Mn}$) to determine their intricate magnetic structures and exchange energies in relation to their magnetoelectric coupling [P13,30-32]. Measurements of spin waves and crystal field excitations reveal extra excitations below $T_N = 50$ K that are nearly dispersionless and are most intense around magnetic zone centers. We use a MF-RPA model to show that these excitations correspond to transitions between Fe^{2+} crystal field and spin-orbit split states. In addition, our other studies determine the H - T phase diagram [P13,29,30], and we are finalizing our project on magnetic frustration effects in SrHo_2O_4 and Fe_2VO_4 [P1,10].

Magnetic quasicrystals and related compounds: Our discovery [1] of a new family of local-moment bearing binary quasicrystals, i - R -Cd ($R = \text{Gd through Tm} + \text{Y}$) is particularly exciting because they represent the compositionally simplest system for the study of the magnetic interactions in aperiodic systems. The existence of a corresponding set of periodic approximants, RCd_6 , to the icosahedral phase allows for direct comparison between the low-temperature magnetic states of crystalline and quasicrystalline phases with fundamentally similar local atomic motifs. In collaboration with P. Canfield's group we have continued our investigations of the structure [P20] and properties [P2] of the i - R -Cd quasicrystals and RCd_6 approximants [P28]:

- We accomplished a full six-dimensional structural refinement of the i - R -Cd ($R = \text{Gd, Dy and Tm}$) that demonstrated the presence of chemical disorder on the nominal R sites in the quasicrystalline structure (Cd substitution for $\sim 20\%$ of the R ions), and established that the i - R -Cd quasicrystals represent a new sub-class of icosahedral structures [P20].
- We have performed inelastic neutron scattering measurements on powder samples of the quasicrystal approximant, TbCd_6 , grown using isotopically enriched ^{112}Cd . The inelastic excitations, and their evolution with temperature, are well described by the leading axial term of the crystalline electric field (CEF) Hamiltonian for local pentagonal symmetry for the rare-earth ions, so that the Tb moment is directed primarily along the unique local pseudo-five-fold axis of the icosahedral atomic clusters [P28].

Future Plans

Iron pnictides and chalcogenides: Several open questions remain in the study of iron-based superconductors under pressure. Due to the high pressures and small expected moment size, it is very challenging to determine magnetic structures in the high pressure phase diagram of FeSe using neutron diffraction. Part of our strategy is to explore chemical substitutions in FeSe that could make magnetic phases more accessible to neutron diffraction, or even make possible the study of spin fluctuations in different ground states at ambient pressure. In a similar vein, we plan to explore structural and magnetic phases under pressure in the new 1144 compounds. Finally, control of magnetic, structural and superconducting phases using strain and composition has been demonstrated in CaFe_2As_2 . This has opened up the possibility to study the spin

fluctuations in different phases of $\text{Ca}(\text{Fe}_{1-x}\text{Co}_x)_2\text{As}_2$ without resorting to high pressure sample environments.

Manganese and cobalt arsenides: We have discovered two new phenomena in the Mn- and Co-arsenides that warrant further study. For the Mn-arsenides, we will continue to study the evolution of itinerant FM order in the presence of local-moment Néel order, including study of the spin fluctuations and the possibility of coupling between the orders. We have preliminary XMCD data showing the same effect in $(\text{Ba}_{1-x}\text{Rb}_x)\text{Mn}_2\text{As}_2$ as in $(\text{Ba}_{1-x}\text{K}_x)\text{Mn}_2\text{As}_2$, and we also plan to explore the doped RMnPnO system. The lower values of T_N will make it easier to examine the relationship between coexisting AFM and FM states in hole-doped compositions. For the Co-arsenides, we will continue to study the evolution of extreme frustration in these itinerant magnets. This includes detailed INS work on A-type ordered CaCo_2As_2 and $\text{Ca}(\text{Co}_{0.85}\text{Fe}_{0.15})\text{Co}_2\text{As}_2$, where magnetic order is suppressed. These studies will be expanded to the RCoPnO compounds. LaCoAsO and LaCoPO are both 2D itinerant FM systems with low Curie temperatures where investigations of the spin fluctuations can reveal magnetic frustration.

Magnetic quasicrystals and related compounds: We have grown sizeable samples of both the Tb-Cd icosahedral quasicrystal and the Tb_6Cd periodic approximant phase using the ^{114}Cd isotope. Our INS measurements of the low-energy spin excitations on the quasicrystal show that there is significant static diffuse and inelastic magnetic scattering, with overall icosahedral symmetry, indicating short-range magnetic ordering on the clusters of Tb ions found in the structure. We are modeling the static magnetic short-range order via reverse Monte Carlo methods [P20]. The inelastic scattering, which most likely arises from the Tb^{3+} CEF excitations, will be compared with our previous measurements on the approximant phase [P28] to gain further insight into the local environment of the magnetic ions.

Heavy fermions: The quantum-critical point (QCP) in YbBiPt can be tuned through the application of magnetic fields or pressure. We have been investigating the evolution of AFM order and magnetic fluctuations upon approaching the QCP at $H_c \approx 0.4$ T. Neutron diffraction is being used to probe the anisotropic response of the AFM order by applying the field along different crystallographic directions. We are also performing high-resolution INS experiments to examine the evolution of the dynamic magnetic susceptibility through the QCP. Finally, we previously discovered that short-range magnetic correlations appear below $T^* = 0.7$ K that persist in the AFM ordered state,[2] and have taken neutron spin echo data down to $T = 0.1$ K in order to determine if the correlations are static or fluctuating.

High pressure: The iron pnictides and related compounds provide ample motivation to develop capabilities for performing single-crystal x-ray and neutron scattering measurements under applied pressure. We have had recent success at the APS using diamond anvil cells (DAC) to perform high pressure diffraction, XMCD and Mossbauer measurements. These experiments have led to unique insights into the phase stability of superconductors and other metals with large magnetoelastic interactions. Studies of FeSe , doped BaFe_2As_2 compositions and Co-based itinerant metals under pressure will continue at APS. Over the last two years, we have established a collaboration with ORNL in the area of high pressure neutron scattering. One notable opportunity is a concerted effort to develop a program focused on single-crystal investigations of quantum materials systems using DAC.

References (citations starting with "P" are from Publications list)

1. Alan I. Goldman, Tai Kong, Andreas Kreyssig, Anton Jesche, Mehmet Ramazanoglu, Kevin W. Dennis, Sergey L. Bud'ko, and Paul C. Canfield, *Nature Materials* **12**, 714 (2013).
2. B. G. Ueland et al., *Phys. Rev. B* **89**, 180403 (R) (2014).

Publications

1. "Magnetic Excitations and Anomalous Spin-Wave Broadening in Multiferroic FeV_2O_4 ", Q. Zhang, M. Ramazanoglu, S. Chi, Y. Liu, T. A. Lograsso, and D. Vaknin, *Phys. Rev. B* **89**, 224416 (2014).
2. "Magnetic and transport properties of i-R-Cd icosahedral quasicrystals (R=Y, Gd-Tm)", Tai Kong, Sergey L. Bud'ko, Anton Jesche, John McArthur, Andreas Kreyssig, Alan I. Goldman, and Paul C. Canfield, *Phys. Rev. B* **90**, 014424 (2014).
3. "Crystallography and physical properties of BaCo_2As_2 , $\text{Ba}_{0.94}\text{K}_{0.06}\text{Co}_2\text{As}_2$, and $\text{Ba}_{0.78}\text{K}_{0.22}\text{Co}_2\text{As}_2$ " V. K. Anand, D. G. Quirinale, Y. Lee, B. N. Harmon, Y. Furukawa, V. V. Ogloblichev, A. Huq, D. L. Abernathy, P. W. Stephens, R. J. McQueeney, A. Kreyssig, A. I. Goldman, and D. C. Johnston, *Phys. Rev. B* **90**, 064517 (2014).
4. "Lattice distortion and stripelike antiferromagnetic order in $\text{Ca}_{10}(\text{Pt}_3\text{As}_8)(\text{Fe}_2\text{As}_2)_5$ ", A. Sapkota, G. S. Tucker, M. Ramazanoglu, W. Tian, N. Ni, R. J. Cava, R. J. McQueeney, A. I. Goldman, and A. Kreyssig, *Phys. Rev. B* **90**, 100504(R) (2014).
5. "Complex magnetic ordering in $\text{CeGe}_{1.76}$ studied by neutron diffraction", W. T. Jayasekara, W. Tian, H. Hodovanets, P. C. Canfield, S. L. Bud'ko, A. Kreyssig, and A. I. Goldman, *Phys. Rev. B* **90**, 134423 (2014).
6. "Charge order and its connection with Fermi-liquid charge transport in a pristine high-Tc cuprate", W. Tabis, Y. Li, M. Le Tacon, L. Braicovich, A. Kreyssig, M. Minola, G. Dellea, E. Weschke, M. J. Veit, M. Ramazanoglu, A. I. Goldman, T. Schmitt, G. Ghiringhelli, N. Barišić, M. K. Chan, C. J. Dorow, G. Yu, X. Zhao, B. Keimer and M. Greven, *Nature Comm.* **5**:5875 doi:10.1038/ncomms6875 (2014).
7. "Neutron Scattering Measurements of Spin Excitations in LaFeAsO and $\text{Ba}(\text{Fe}_{0.953}\text{Co}_{0.047})_2\text{As}_2$: Evidence for a Sharp Enhancement of Spin Fluctuations by Nematic Order", Qiang Zhang, Rafael M. Fernandes, Jagat Lamsal, Jiaqiang Yan, Songxue Chi, Gregory S. Tucker, Daniel K. Pratt, Jeffrey W. Lynn, R. W. McCallum, Paul C. Canfield, Thomas A. Lograsso, Alan I. Goldman, David Vaknin, and Robert J. McQueeney, *Phys. Rev. Lett.* **114**, 057001 (2015).
8. "Itinerant ferromagnetism in the As 4p conduction band of $\text{Ba}_{0.6}\text{K}_{0.4}\text{Mn}_2\text{As}_2$ identified by x-ray magnetic circular dichroism", B. G. Ueland, Abhishek Pandey, Y. Lee, A. Sapkota,

- Y. Choi, D. Haskel, R. A. Rosenberg, J. C. Lang, B. N. Harmon, D. C. Johnston, A. Kreyssig, and A. I. Goldman, *Phys. Rev. Lett.* **114**, 217001 (2015).
9. “Structural and magnetic phase transitions near optimal superconductivity in $\text{BaFe}_2(\text{As}_{1-x}\text{P}_x)_2$ ”, Ding Hu, Xingye Lu, Wenliang Zhang, Huiqian Luo, Shiliang Li, Peipei Wang, Genfu Chen, Fei Han, Shree R. Banjara, A. Sapkota, A. Kreyssig, A. I. Goldman, Z. Yamani, Christof Niedermayer, Markos Skoulatos, Robert Georgii, T. Keller, Pengshuai Wang, Weiqiang Yu, and Pengcheng Dai, *Phys. Rev. Lett.* **114**, 157002 (2015).
 10. “Disorder from Order Among ANNNI Spin Chains in SrHo_2O_4 ” J.-J. Wen, W. Tian, V. O. Garlea, S. M. Koohpayeh, T. M. McQueen, H.-F. Li, J.-Q. Yan, D. Vaknin, C. L. Broholm, *Phys. Rev. B* **91**, 054424 (2015).
 11. “Spin Reorientation and Ce-Mn Coupling in Antiferromagnetic Oxypnictide CeMnAsO ”, Q. Zhang, W. Tian, S. G. Peterson, K. W. Dennis, and D. Vaknin, *Phys. Rev. B* **91**, 064418 (2015).
 12. “Jahn-Teller versus quantum effects in the spin-orbital material LuVO_3 ” M. Skoulatos, S. Toth, B. Roessli, M. Enderle, K. Habicht, D. Sheptyakov, A. Cervellino, P. G. Freeman, M. Reehuis, A. Stunault, G. J. McIntyre, L. D. Tung, C. Marjerrison, E. Pomjakushina, P. J. Brown, D. I. Khomskii, Ch. Rüegg, A. Kreyssig, A. I. Goldman, and J. P. Goff, *Phys. Rev. B* **91**, 161104(R) (2015).
 13. “Anomalous Magnetic Structure and Spin Dynamics in Magnetoelectric LiFePO_4 ”, R. Toft-Petersen, M. Reehuis, TBS. Jensen, N. H. Andersen, J. Li, M. D. Le, M. Laver, C. Niedermayer, B. Klemke, K. Lefmann, and D. Vaknin, *Phys. Rev. B* **92**, 024404 (2015).
 14. “High-resolution x-ray diffraction study of the heavy-fermion compound YbBiPt ,” B. G. Ueland, S. M. Saunders, S. L. Bud’ko, G. M. Schmiedeshoff, P. C. Canfield, A. Kreyssig, and A. I. Goldman, *Phys. Rev. B* **92**, 184111 (2015).
 15. “Pressure induced collapsed-tetragonal phase in SrCo_2As_2 ” W. T. Jayasekara, U. S. Kaluarachchi, B. G. Ueland, Abhishek Pandey, Y. B. Lee, V. Taufour, A. Sapkota, K. Kothapalli, N. S. Sangeetha, G. Fabbris, L. S. I. Veiga, Yejun Feng, A. M. dos Santos, S. L. Bud’ko, B. N. Harmon, P. C. Canfield, D. C. Johnston, A. Kreyssig, and A. I. Goldman, *Phys. Rev. B* **92**, 224103 (2015).
 16. “Spin dynamics near a putative antiferromagnetic quantum critical point in Cu-substituted BaFe_2As_2 and its relation to high-temperature superconductivity”, M. G. Kim, M. Wang, G. S. Tucker, P. N. Valdivia, D. L. Abernathy, Songxue Chi, A. D. Christianson, A. A. Aczel, T. Hong, T. W. Heitmann, S. Ran, P. C. Canfield, E. D. Bourret-Courchesne, A. Kreyssig, D. H. Lee, A. I. Goldman, R. J. McQueeney, and R. J. Birgeneau, *Phys. Rev. B* **92**, 214404 (2015).

17. “Structure and magnetic properties of $LnMnSbO$ ($Ln = La$ and Ce)”, Qiang Zhang, C. M. N. Kumar, Wei Tian, Kevin W. Dennis, Alan I. Goldman, and David Vaknin, *Phys. Rev. B* **93**, 094413 (2016).
18. “Discovery of an Unconventional Charge Density Wave at the Surface of $K_{0.9}Mo_6O_{17}$ ” Daixiang Mou, A. Sapkota, H.-H. Kung, Viktor Krapivin, Yun Wu, A. Kreyssig, Xingjiang Zhou, A. I. Goldman, G. Blumberg, Rebecca Flint, and Adam Kaminski, *Phys. Rev. Lett.* **116**, 196401 (2016).
19. “Anisotropic thermodynamic and transport properties of single-crystalline $CaKFe_4As_4$ ”, W. R. Meier, T. Kong, U. S. Kaluarachchi, V. Taufour, N. H. Jo, G. Drachuck, A. E. Böhmer, S. M. Saunders, A. Sapkota, A. Kreyssig, M. A. Tanatar, R. Prozorov, A. I. Goldman, Fedor F. Balakirev, Alex Gurevich, S. L. Bud’ko, and P. C. Canfield, *Phys. Rev. B* **94**, 064501 (2016).
20. “Atomic structure of the i - R -Cd quasicrystals and consequences for magnetism”, T. Yamada, H. Takakura, T. Kong, P. Das, W. T. Jayasekara, A. Kreyssig, G. Beutier, P. C. Canfield, M. de Boissieu, and A. I. Goldman, *Phys. Rev. B* **94**, 060103(R) (2016).
21. “Strong cooperative coupling of pressure-induced magnetic order and nematicity in $FeSe$ ”, K. Kothapalli, A.E. Böhmer, W.T. Jayasekara, B.G. Ueland, P. Das, A. Sapkota, V. Taufour, Y. Xiao, E. Alp, S.L. Bud’ko, P.C. Canfield, A. Kreyssig & A.I. Goldman, *Nature Commun.* **7**, 12728 (2016).
22. “An Icosahedral Quasicrystal and Its $1/0$ Crystalline Approximant in the Ca - Au - Al System”, Joyce Pham, Andreas Kreyssig, Alan I. Goldman, and Gordon J. Miller, *Inorg. Chem.* **55**, 10425 (2016).
23. “Magnetic Nematicity: A Debated Origin”, D. Vaknin, *Nature Materials* **15** (2), 131-132 (2016).
24. “X-Ray diffraction on large single crystals using a powder diffractometer”, A. Jesche, M. Fix, A. Kreyssig, W. R. Meier, P. C. Canfield, *Phil. Mag.* **96** 2115 (2016).
25. “Origin of the Resistivity Anisotropy in the Nematic Phase of $FeSe$ ”, M. A. Tanatar, A. E. Böhmer, E. I. Timmons, M. Schütt, G. Drachuck, V. Taufour, K. Kothapalli, A. Kreyssig, S. L. Bud’ko, P. C. Canfield, R. M. Fernandes, R. Prozorov, *Phys. Rev. Lett.* **117** 127001 (2016).
26. “Collinear antiferromagnetism in trigonal $SrMn_2As_2$ revealed by single crystal neutron diffraction”, Pinaki Das, N. S. Sangeetha, Z. A. Benson, T. W. Heitmann, D. C. Johnston, A. I. Goldman, and A. Kreyssig, *J. Phys. Condens. Matter* (in press).

27. “Suppression of magnetic order in CaCo_2As_2 by Fe substitution: Magnetization, neutron diffraction, and x-ray diffraction studies on single crystals of $\text{Ca}(\text{Co}_{1-x}\text{Fe}_x)_y\text{As}_2$ ”, W. T. Jayasekara, Abhishek Pandey, A. Kreyssig, N. S. Sangeetha, A. Sapkota, K. Kothapalli, V. K. Anand, W. Tian, D. Vaknin, D. C. Johnston, R. J. McQueeney, A. I. Goldman, and B. G. Ueland, submitted to *Phys. Rev. B*.
28. “Crystal electric field excitations in the quasicrystal approximant TbCd_6 studied by inelastic neutron scattering”, Pinaki Das, P. -F. Lory, R. Flint, T. Kong, T. Hiroto, S. L. Bud’ko, P. C. Canfield, M. de Boissieu, A. Kreyssig, and A. I. Goldman, submitted to *Phys. Rev. B*.
29. “Spin fluctuations with reduced dimensionality in the highly-frustrated metal $\text{CaCo}_{2-y}\text{As}_2$ ”, A. Sapkota, B. G. Ueland, V. K. Anand, D. L. Abernathy, M. B. Stone, J. L. Niedziela, D. C. Johnston, A. Kreyssig, A. I. Goldman and R. J. McQueeney, submitted to *Phys. Rev. Lett.*
30. “Hybrid excitations due to crystal-field, spin-orbit coupling and spin-waves in LiFePO_4 ”, Y. Yiu, M.- D. Le, R. Toft-Peterson, G. Ehlers, R. J. McQueeney, and D. Vaknin, *Phys. Rev. B* (submitted available online at [arXiv:1608.05761](https://arxiv.org/abs/1608.05761)).
31. “Field induced reentrant magnetoelectric phase in LiNiPO_4 ”, R. Toft-Petersen, Ellen Fogh, T. Kihara, J. Jensen, K. Fritsch, J. Lee, G. E. Granroth, M. B. Stone, D. Vaknin, H. Nojiri, and N. B. Christensen, submitted to *Phys. Rev. Lett.*
32. “Neutron study of the 1/3 magnetization plateau in quasi-Ising LiCoPO_4 ”, E. Fogh, R. Toft-Petersen, E. Ressouche, O. Zaharko, J. Schefer, C. Niedermayer, S. L. Holm, M. Korning-Sorensen, A. B. Kristensen, N. H. Andersen, D. Vaknin, and N. B. Christensen, (preprint available).

Measurement and Modeling of Structure and Dynamics in Doped Organic Semiconductors

Adam J. Moule – Chemical Engineering at the University of California, Davis

Program Scope

The ability to pattern materials using photolithography has been the key manufacturing advance that enabled the IT revolution and has driven Moore's Law. Photolithographic methods are routinely used to fabricate heterostructures of inorganic electronic materials with lateral features of <100 nm. By comparison, organic semiconductors (OSCs) have been largely limited to lateral features of >10 μm because non-chemically-destructive methods to pattern organic materials are limiting. During our first BES award, we developed a new patterning technology called dopant induced solubility control (DISC) for OSCs. *The key scientific principle is that molecular dopants can be used to reversibly control the solubility of OSCs.* Our published results show that DISC could revolutionize the solution fabrication of organic electronic materials.(refs 1,6) We demonstrated sub-diffraction limited optical patterning of organic features with a size of 250 nm. The patterning work resulted in funding of a new NSF center grant with Moule as PI. However, the interaction between the molecular dopants and conjugated polymers and also dopant transport within the polymer are poorly understood processes. There is a critical need to develop methods and supporting modeling that can measure and predict the relationship between structure, charge delocalization, and dopant transport in organic semiconducting materials. Our long term goal is to use neutron methods and multi-scale modeling to explain complex charging effects in heterogeneous organic materials and mixtures. To achieve this goal, we are working to improve interpretation of neutron scattering data of doped OSCs that display structural inhomogeneity, delocalized charged sites, and diffusive dopants using combined electronic (density functional theory (DFT)) and molecular dynamics (MD) modeling methods.

We will test the central hypothesis objectively by pursuing the following four specific aims:

- (1) **Measure dopant and polymer diffusion between DISC processed layers:** Our hypothesis is that entangled polymers do not mix with adjacent layers upon solvent swelling or dedoping but small molecule dopants diffuse and drift across interfaces.
- (2) **Develop model interpretation for the inelastic neutron scattering (INS) spectrum:** Our hypothesis is that the low energy portion of the INS spectrum, which measures delocalized phonon modes, contains information that governs fundamental aspects of the polymer mechanical stability, charge stabilization, and charge transport.
- (3) **Develop multi-scale models of charged polymers:** Our hypothesis is that an understanding of dopant site choice and the change in molecular structure upon doping can be achieved with combined DFT and MD modeling validated by INS data.
- (4) **Develop multi-scale models for interpretation of INS data in amorphous domains:** Our hypothesis is that INS data can be modeled using combined MD and DFT data also in amorphous domains using combined MD and DFT simulations.

The proposed research is a departure from our past research. We are highly focused on the using INS to measure and model the position of the dopant within the polymer and to understand how the dopant changes the structure of the polymer. This problem is difficult to solve because electronic levels of modeling accuracy are required for charged sites but the samples tend to be semicrystalline and the low energy portion of the INS spectrum (phonons) is poorly defined by short range interactions and in amorphous domains. To effectively model the full INS spectrum for OSC's, significant multi-scale modeling development is needed.

Recent Progress

- 1) We determined how neutral and ionic dopants differ in their effectiveness at p-type doping polythiophene polymers. This question of effectiveness is complicated because the dopant must be miscible with the polymer. The acidic dopant formed surface states and reacted with the OSC to form a doped interlayer. The process is generally seen in the preparation of organic photovoltaic devices. (**ref 4**) In **ref 7** we demonstrate that selective solvents can be used to dope either amorphous polymer or both amorphous and crystalline domains in semiconducting polymers. This is important because it gives us precise control over the doping mechanism and allowed us to measure the doping site density on the polymer.
- 2) We synthesized a family of p-type dopants for organic films with side groups that can be optimized for solubility, doping effectiveness, control of the diffusion rate, and neutron scattering contrast. Here we showed that a more miscible dopant is more effective at doping the crystalline domains of the polymer. This method to chemically tailor dopants for solubility control also gives us the ability to control the size and therefore diffusion rate of the dopant in the polymer matrix. (**ref. 3**)
- 3) We used the functionalized dopants to generate non-uniform doping profiles to study the doping effectiveness, thermal persistence of the dopant, and diffusion mechanism. In organic devices a dopant can diffuse or drift to a neighboring layer causing an electronic breakdown of the device. In **ref 2** we show that large dopants diffuse slower in small molecule samples. In **refs 8** and **9** we examine polyelectrolyte/polymer bilayers with external dopants. We show that the external dopants react with the polyelectrolyte and cause morphological changes to the polymer electrolyte. In **ref 13** we use QENS and fluorescence microscopy to determine the microscopic and macroscopic diffusion rate of the dopant synthesized in **ref 3**. We found that the dopant must de-charge to diffuse and that the jump-distance of the dopant depends on the undoped site density on the polymer. In **ref 15** we use this information to understand how dopant diffusion rates vary depending on the crystallinity of the polymer. More crystalline polymers have fewer doping sites because the dopants diffuse through the amorphous domains, thus the macroscopic diffusion rate is higher in highly crystalline films.
- 4) We used INS to measure the structure of crystalline packing in undoped and doped P3HT films and modeled the data using DFT methods. This paper is really groundbreaking because we show that multiple polymer configurations are necessary to describe the crystal structure of P3HT because a single structure is not capable of describing the INS data. As a result, the average crystal structure determined using XRD is in fact not represented in a real sample. (**ref 11**) **Ref. 14** is a critical review article of multi-scale simulation methods for polymers. Our main point is that modeling methods that simulate long range electronic interactions (particularly in complex or amorphous structures) are lacking.
- 5) We invented a new method to pattern semiconductor polymers (**ref 1**) and dopant density (**ref 6**) that is based on the data we gathered from the dopant diffusion studies. This new method called Dopant Induced Solubility Control (DISC) is the equivalent of photolithography for organic semiconductors and has already yielded patterning with sub-diffraction limited resolution. The key new finding is that a dopant molecule has a large effect on the solubility of the OSC. So doping significantly reduces the solubility. In order to use this new idea for patterning we invented methods to chemically (**ref 12**) and optically (**ref 5**) dedope the OSC by inducing reactions with dopant molecule. In **ref 15** we study how the crystallinity of the

polymer and solvent quality of the developing solution affects the sharpness of the resultant patterned structure. In this case, the diffusion rate of the dopant and number of undoped sites on the polymer (determined in **refs 7 and 13**) are critical parameters. This patterning work also led directly to a new small NSF funded center grant (\$1,125,000) with Moulé as PI.

- 6) In **ref 16** we use SANS and DSC to understand how the dopant affects the structure formation of the polymer in solution. Our assumption was that a co-crystal would form as we saw in sequentially doped films (**ref 4**). Instead we find that the charging of the polymer causes the formation of much more complex aggregates in solution. Here the processing parameters have a critical effect on the structure of polymer.

Future Plans – this grant will support 3 PhD theses

Thomas Harrelson will focus his studies on modeling the low energy part of the INS spectrum (long range phonons) in crystalline small molecule semiconductors and crystalline domains in semiconducting polymers. We are interested in the relationship between the phonon spectrum, dynamic disorder, and charge mobility. Recent experimental papers have shown that charge mobility is limited by large amplitude dynamic movement of the conjugated core in both small molecule and polymer OSCs. The motion is inferred from broadening of crystal spot patterns but cannot be tied to a specific dynamic mode or amplitude. Thomas will measure the phonon spectrum of several high mobility OSC's using INS at VISION and fit the spectrum using plane wave DFT to model the energy spectrum of the modes. We will then correlate the dynamic motion of the OSC backbone to the temperature dependent mobility.

To accurately simulate charge transport however, we need to envision charged sites in the organic lattice. Each charged site undergoes configurational reorganization due to the presence of an electron or hole state. These charged sites have different dynamics due to altered sigma and pi bond densities around backbone carbons (as shown in ref. 11). We will simulate charged sites by doping OSC's with molecular dopants and then measuring the change in dynamics using INS on VISION. However as already demonstrated with P3HT, organic dopants also induce significant increases in structural disorder that need to be accounted for. We anticipate the use of neutron diffraction on VISION and x-ray diffraction techniques to validate models of doped OSC's.

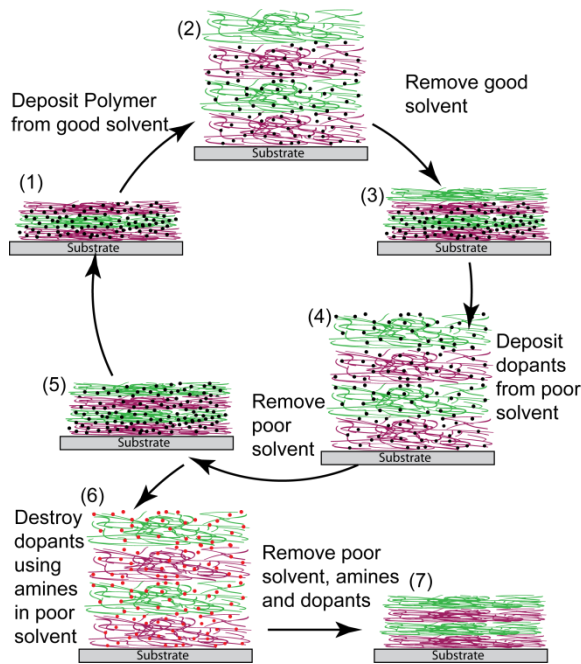
Varuni Dantanarayana will focus her studies on developing computational methods to model INS data of amorphous samples and domains. As we discovered in our studies of P3HT, plane-wave electronic modeling software does not allow the simulation of amorphous domains because this would require that a non-optimized geometry with non-repeating boundary conditions must be simulated. Alternatively, vacuum DFT techniques are also not suitable for simulation of either local vibrations or delocalized phonons because the molecular neighborhood of each proton has a huge effect on the motion spectrum. Finally we already tried to use molecular dynamics (MD) to simulate P3HT in multiple configurations. It was possible to construct a phonon spectrum from MD by sampling the position autocorrelation function and taking a Fourier transform to extract a frequency spectrum. However, since MD models are parameterized by a local DFT electronic model, the simulated phonon spectrum yields frequencies that are not even close to the measured INS spectrum.

Varuni will extract P3HT geometries from well validated MD structural models and then perform constrained DFT on these models to extract electronic vibrational and phonon spectra for amorphous polymer domains. Next the DFT models will be recursively used to develop

optimized force fields for improved MD models. The goal is to develop MD force fields that reproduce the vibrational dynamics of all of the hydrogens in a sample both at high energy loss (local vibrations) and low energy loss (phonons). This type of force field will self-assemble and form structure predictably over much larger length scales than the current best MD models. Finally we will apply the improved force fields to predict the INS spectra of other small molecule and polymer OSC's to determine how broadly applicable the long range classical models are. Our long term goal is to develop a robust method to model INS data in amorphous samples using combined classical/quantum methods. This would greatly extend the range of samples that could successfully be studied using INS.

This project will be in collaboration with Karl Kirschner from Bonn-Rhein-Sieg University in Germany who specializes in force field development for MD models and Roland Faller at UC Davis who specializes in multi-scale polymer modeling.

Tucker Murrey will focus on understanding how molecular dopants induce structure formation in OSC's both in film and solution samples using SANS and NR. He is scheduled for 9 days of measurement time at the Heinz Maier-Leibnitz Zentrum (Garching, Germany) in February to measure NR and GISANS. His samples will consist of P3HT and fully deuterated P3HT layer stacks that were coated using the DISC method invented in the previous grant period. Our goal is to determine whether the dopants are acting like tie-chains in a cross linked polymer or whether the dopants are affecting the enthalpy of dissolution of the polymer crystals. The neutron studies will be supported by a series of UV/vis and DSC experiments. These NR experiments will also allow us to quantify the amount of mixing between polymer layers. Normally mixing between polymer layers is controlled by the reptation rate and since the films are far below the melting temperature, no mixing is expected to occur. However, since the film is being swelled with solvent to 2-5x its original thickness, the tube diameter for a single polymer chain is, in principle greatly increased and so the mixing between films could occur at a much lower temperature. These NR experiments are being performed in both solvent swelled and post processed films to determine changes in mixing compared to thermally annealed samples. Also GISANS on solvent swelled films are expected to yield the average domain size and orientation of crystalline domains in doped solvent swelled films.



Fabrication of multiple layer structures using DISC fabrication steps. Here differently colored polymer layers represent the same polymer structure but fully hydrogenated or deuterated.

Publications^{1-9 10-13 14,15} (supported postdoc, graduate students, and undergraduate researchers)

1. Jacobs, I. E.; Li, J.; Berg, S. L.; Bilsky, D. J.; Rotondo, B. T.; Augustine, M. P.; Stroeve, P.; Moule, A. J., Reversible optical Control of Conductive Polymer Solubility with Sub-Micrometer Resolution. *ACS Nano* **2015**, 9, (2), 1905-1912.
2. Li, J.; Rochester, C. W.; Jacobs, I. E.; Friedrich, S.; Stroeve, P.; Riede, M.; Moule, A. J., Measurement of Small Molecular Dopant F4TCNQ and C60F36 Diffusion in Organic Bilayer Architectures. *ACS applied materials & interfaces* **2015**, 7, (51), 28420-8.
3. Li, J.; Zhang, G.; Holm, D. M.; Jacobs, I. E.; Yin, B.; Stroeve, P.; Mascal, M.; Moule, A. J., Introducing solubility control for improved organic p-type dopants. *Chemistry of Materials* **2015**, 27, (16), 5765-5774.
4. Moule, A. J.; Jung, M.-C.; Rochester, C. W.; Tress, W.; LaGrange, D.; Jacobs, I. E.; Li, J.; Mauger, S. A.; Rail, M. D.; Lin, O.; Bilski, D. J.; Qi, Y.; Stroeve, P.; Berben, L. A.; Reide, M., Mixed interlayers at the interface between PEDOT:PSS and conjugated polymers provide charge transport control. *Journal of Materials Chemistry C* **2015**, 3, 2664-2676.
5. Fuzell, J.; Jacobs, I. E.; Ackling, A.; Harrelson, T. F.; Huang, D. M.; Larsen, D. S.; Moule, A. J., Optical Dedoping Mechanism for P3HT/F4TCNQ Mixtures. *Journal of physical Chemistry Letters - published online* **2016**.
6. Jacobs, I. E.; Aasen, E. W.; Nowak, D.; Li, J.; Morrison, W.; Roehling, J. D.; Augustine, M. P.; Moule, A. J., Direct-write optical patterning of P3HT films beyond the diffraction limit. *Advanced Materials published online* **2016**.
7. Jacobs, I. E.; Li, J.; Aasen, E. W.; Lopez, J.; Fonseca, T.; Zhang, G.; Stroeve, P.; Augustine, M. P.; Mascal, M.; Moule, A. J., Comparison of solution-mixed and sequentially processed P3HT:F4TCNQ films: effect of doping-induced aggregation on film morphology. *Journal of Materials Chemistry C* **2016**, 4, 3454-3466.
8. Li, J.; Jacobs, I. E.; Friedrich, S.; Stroeve, P.; Moule, A. J., Solution aging and degradation of a transparent conducting polymer dispersion. *Organic Electronics* **2016**, 34, 172-178.
9. Li, J.; Rochester, C. W.; Jacobs, I. E.; Aasen, E. W.; Friedrich, S.; Stroeve, P.; Moule, A. J., The effect of thermal annealing on dopant site choice in conjugated polymers. *Organic Electronics* **2016**, 33, 23-31.

Submitted

10. Bilski, D. J.; Rotondo, B. T.; Lewis, R.; Jacobs, I. E.; Moule, A. J., DISC patterning of polymer microstructures using light interference. *submitted* **2016**.
11. Harrelson, T. F.; Cheng, Y. Q.; Li, J.; Jacobs, I. E.; Ramirez-Cuesta, A. J.; Faller, R.; Moule, A. J., Identifying Structural Motifs in Doped Polythiophenes using Inelastic Neutron Scattering. *Submitted* **2016**.
12. Jacobs, I. E.; Wang, F.; Hazefi, N.; Medina-Plaze, C.; Li, J.; Augustine, M. P.; Mascal, M.; Moule, A. J., Quantitative dedoping of conducting polymers. *submitted* **2016**.
13. Li, J.; Koshnick, C.; Diallo, S. O.; Hong, K.; Zhang, G.; Stroeve, P.; Mascal, M.; Moule, A. J., Quantitative Measurements of the Macro-scale and Micro-scale Dynamics of Molecular Dopants in a conjugated polymer. *Submitted* **2016**.
14. Harrelson, T. F.; Moule, A. J.; Faller, R., Modeling organic electronic materials: bridging length and time scales. *accepted in Molecular Simulations* **2016**.

In-Preparation

15. Li, J.; Holm, D. M.; Guda, S.; Jacobs, I. E.; Moule, A. J., Correlating polymer crystallinity and doping level to local solubility. *In Preparation* **2016**.
16. Murrey, T.; Li, J.; Moule, A. J., Small angle scattering study of dopant induced aggregation of P3HT. *In Preparation* **2016**.

Interactions Governing the Self-Assembly of Protein-Polymer Conjugates

Bradley D. Olsen

Department of Chemical Engineering, Massachusetts Institute of Technology
DOE-BES Award ER46824

Program Scope

Engineering enzymes and optically active proteins into bioelectronic devices for the production of H_2 ,^{1,2} the reduction of CO_2 ,^{3,4} or the production of biofuels^{5,6} allows the evolutionarily optimized performance of the protein to be exploited to produce high-performance biomolecular variants of catalysts. Engineering biocatalytic materials requires achieving a high protein activity and active site density, controlling substrate/product transport through the material, maintaining protein stability, and developing low-cost processes for material fabrication. Analogous to synthetic catalysts^{7,8} or organic electronics,^{9,10} this requires the arrangement and orientation of the protein at an interface between two phases that provide for the transport of each reagent or charge carrier.

The self-assembly of block copolymers containing an enzyme or optically active protein block provides a bottom-up method to produce nanostructures that simultaneously achieve control over transport through two phases and yield a high density of oriented protein at an interface. This project investigates the fundamental structure and thermodynamics of block copolymer systems containing a globular protein block, enabling the production of functional nanomaterials (Figure 1). Both the folded protein chain shape and the specific interactions between globular proteins differ significantly from the Gaussian coil block copolymers, adding significant complexity to the phase behavior of these systems. The goal of this project is to apply neutron scattering and clever biological design of materials to elucidate the fundamental forces that govern self-assembly in protein-polymer block copolymer systems. Over the past 2.5 years, we have addressed the following questions:

- (1) How can neutron scattering methods be used to measure the interactions between proteins and polymers relevant to their phase behavior and self-assembly?
- (2) What is the effect of charge on protein-polymer block copolymer self-assembly?
- (3) What is the effect of protein shape on self-assembly?

Recent Accomplishments

In collaboration with Wei-Ren Chen at Oak Ridge National Lab, we developed a novel approach to measure the interactions between protein and polymer using bioconjugates. Our lab synthesized a series of protein-polymer bioconjugates with the model protein mCherry and a series of water-soluble polymers selected due to differences in

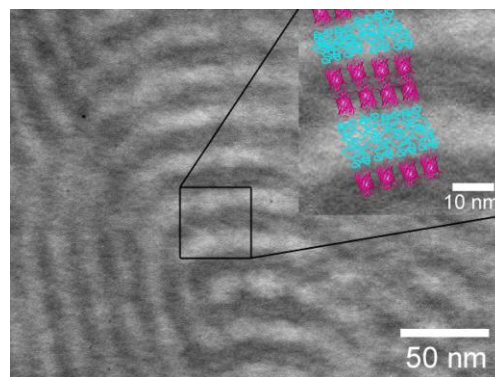


Figure 1. Transmission electron micrograph of mCherry-poly(N-isopropylacrylamide) block copolymer self-assembled into lamellar structures. Protein nanodomains appear dark due to staining.

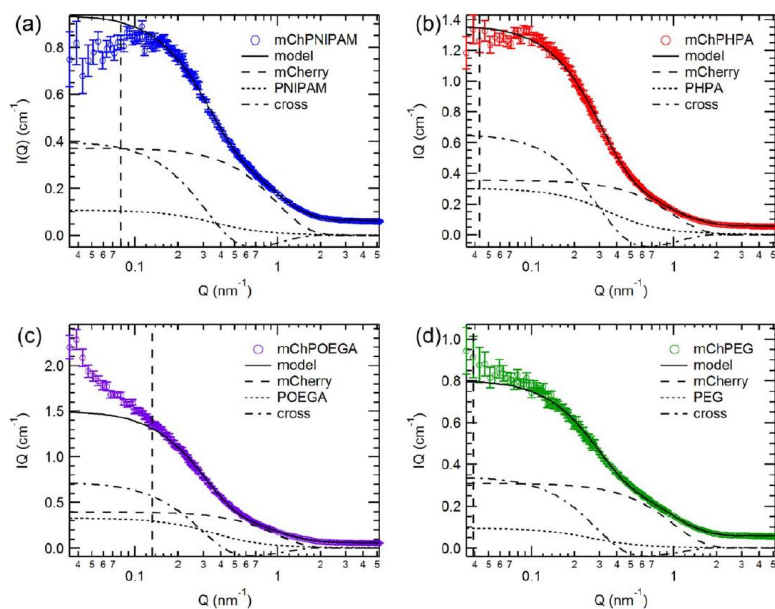


Figure 2. Nonlinear least-squares regression of coarse-grained cylinder-coil form factors (black lines) to experimental mCherry-polymer bioconjugate SANS data (open circles) for (a) mCherry-PNIPAM(26000) (b) mCherry-PHPA(30000) (c) mCherry-POEGA(26000), and (d) mCherry-PEG(28000). The dashed vertical lines denote data points at low Q that are omitted in the model fitting.

hydrogen bonding pattern and show large differences in the propensity for self-assembly. The form factor of each bioconjugate in solution was measured by small-angle neutron scattering, and the shape of the unconjugated protein and polymer were also measured to provide molecular shape measurements for each individual block. Wei-Ren’s group developed an analytical scattering function for the conjugates, assuming that the polymer follows a self-avoiding walk configuration, and this function was validated by fits to the experimental data (Figure 2). This result indicates that all protein/polymer pairs were strongly repulsive, but does not enable measurement of the strength of interaction.

Therefore, we also applied molecular dynamics simulation to model the protein-polymer form factor as a function of the strength of the interaction between protein and polymer, moving from the repulsive to the attractive regime. These simulations clearly show a transition from a “dumbbell” to a “wrapped” configuration of the polymer in moving from repulsive to attractive interactions, and this is readily apparent in the simulated scattering curves. However, in the purely repulsive regime (Figure 3), the scattering curve is largely insensitive to the strength of the repulsive interaction due to the large separation between the protein and polymer beads. Therefore, the method we developed is highly sensitive at quantifying repulsive to attractive transitions, but we find that all our polymers are in the strongly repulsive regime.

Building on previous work where we comprehensively mapped the phase diagram for a model protein-polymer block copolymer based on an mCherry protein block and various polymer blocks, we aim to understand which properties of these polymers and proteins affected the resulting self-assembly. We hypothesized that total charge in the protein would impact protein self-assembly, with increased total charge creating net repulsive interactions between proteins. To test the role of total charge, we prepared a series of green fluorescent protein mutants (EGFP) that were supercharged through genetic mutation of select lysine residues into glutamic acids, providing a series of three proteins with total charge of 0, -8, and -20. Self-assembly of otherwise identical bioconjugates from the three proteins illustrated that increasing magnitude of the total charge led to an increase in the concentration required for self-assembly. The addition of salt, which should screen electrostatic interactions, led to some decrease in this concentration for the highly charged proteins.

Second, we hypothesized that conjugation to a zwitterionic polymer, which is strongly antifouling and therefore protein repulsive, would lead to self-assembly across a wide range of concentrations. However, experiments indicated that the opposite was true. We observed that these protein-polymer conjugates only self-assembled over a very narrow range of concentration around 50%, the narrowest region of self-assembly for any polymer explored. This result indicates that charge pairing and other ionic interactions between proteins can promote self-assembly when the polymer block is uncharged. The addition of salt for the zwitterionic conjugates also strongly modulates order, leading to disordering at low salt when the polymer is “salted in,” but re-ordering at higher concentration when the protein is “salted out.”

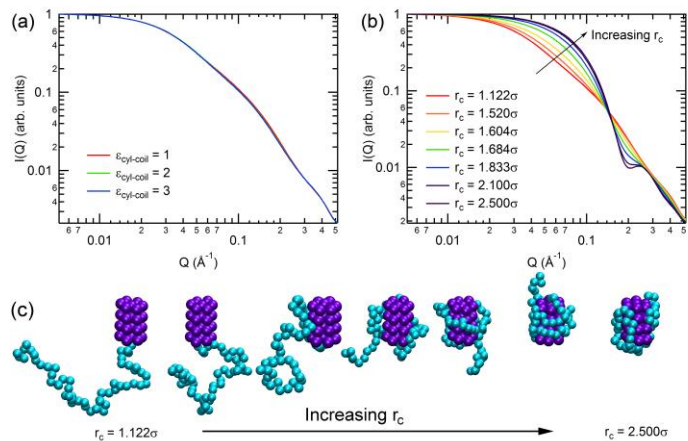


Figure 3. Simulations of a coarse-grained cyl-coil unit with 54 coil beads. (a) Purely repulsive WCA potentials are modeled between pairwise bead interactions. The form factor is not sensitive to the change in the interaction strength between cylinder and coil beads, $\epsilon_{\text{cyl-coil}}$. (b) The form factor is calculated as a function of the cutoff radius using a truncated and shifted Lennard-Jones interaction potential between cylinder and coil beads. Form factors show the qualitative shift from a dumbbell structure (coil extends away from the cylinder) to a shroud-like structure (coil wraps around the cylinder) as the cutoff radius increases. The SANS resolution function is taken into account, smearing the oscillations at high Q . (c) Snapshots of the coarse-grained cylinder-coil structure with increasing cutoff radius.

Finally, over the past years we have made attempts to understand the effect of protein shape by exploring self-assembly in a variety of different proteins. So far we have explored mCherry, EGFP, myoglobin, cytochrome P450, DFPase, BSA, IgG antibody, and SS011 nanobodies. While mCherry, EGFP, BSA, and IgG form well-ordered phases, SS011 and DFPase form less ordered structures and myoglobin and cytochrome P450 show a very low degree of order, although they remain microphase separated. We are working to expand this set of proteins out to about 12, enabling us to correlate the properties of the protein with the degree of ordering in an attempt to elucidate factors that may impact self-assembly in this extremely complex, discrete, and nonlinear parameter space. This will then enable systematic experiments using engineered proteins for hypothesis testing. As a side effect of exploring these proteins, we are also able to demonstrate efficacy in catalysis and sensing applications, having built model catalysts that are 5-10 times more active than other methods of enzyme immobilization and model biosensors that can improve sensitivity by 100-fold. These demonstrations, while beyond the scientific scope of the project, clearly illustrate the value of the fundamental science for eventual DOE-relevant technology development.

Future Plans

During the remaining period of our project, we will complete two key studies. First, we will complete our efforts to analyze neutron scattering data on cross structure factors of proteins and

polymers in concentrated solution, using coarse-grained molecular dynamics modeling in order to extract effective interaction potentials between the protein and polymer. This will provide a new method for quantifying protein-polymer interactions and hopefully provide insight into why changing polymer chemistry in a bioconjugate has such a large impact on its phase behavior. Second, we will complete the synthesis and study of bioconjugates from a large number of proteins to generate a large (approximately 12) set of proteins that are dramatically different in shape, structure, and charge. Using this set, we will attempt to correlate various parameters for quality of self-assembly with various coarse-grained parameters of the protein, with the aim of gaining insight into which properties of the protein might be most important for observed variations in the quality of ordering between well-ordering proteins like mCherry and poorly ordering proteins like myoglobin. Beyond these two studies, our work will start to lay the groundwork for understanding the role of water and hydration in moderating the interactions between proteins and polymers at high concentration, particularly where hydration shells overlap, using neutron scattering and spectroscopic methods. Current efforts in understanding self-assembly suggest that hydration is playing a key role in these materials. Finally, we will develop preliminary data demonstrating the feasibility of coarse-grained simulation approaches for modeling self-assembly of many-molecule systems using the LAMMPS platform.

References

- (1) Hambourger, M.; Gervaldo, M.; Svedruzic, D.; King, P. W.; Gust, D.; Ghirardi, M.; Moore, A. L.; Moore, T. A. *Journal of the American Chemical Society* **2008**, *130*, 2015.
- (2) Krassen, H.; Schwarze, A.; Friedrich, B.; Ataka, K.; Lenz, O.; Heberle, J. *Acs Nano* **2009**, *3*, 4055.
- (3) Reda, T.; Plugge, C. M.; Abram, N. J.; Hirst, J. *Proceedings of the National Academy of Sciences of the United States of America* **2008**, *105*, 10654.
- (4) Parkinson, B. A.; Weaver, P. F. *Nature* **1984**, *309*, 148.
- (5) Iso, M.; Chen, B. X.; Eguchi, M.; Kudo, T.; Shrestha, S. *Journal of Molecular Catalysis B-Enzymatic* **2001**, *16*, 53.
- (6) Velonia, K.; Rowan, A. E.; Nolte, R. J. M. *Journal of the American Chemical Society* **2002**, *124*, 4224.
- (7) Benson, E. E.; Kubiak, C. P.; Sathrum, A. J.; Smieja, J. M. *Chemical Society Reviews* **2009**, *38*, 89.
- (8) Mikkelsen, M.; Jorgensen, M.; Krebs, F. C. *Energy & Environmental Science*, *3*, 43.
- (9) Yang, X.; Loos, J. *Macromolecules* **2007**, *40*, 1353.
- (10) Boudouris, B. W.; Frisbie, C. D.; Hillmyer, M. A. *Macromolecules* **2008**, *41*, 67.

Publications Resulting from Work Supported by DOE-BES Neutron Program Since 2014 Review

1. "Scattering from Colloid-Polymer Conjugates with Excluded Volume Effect." X. Li, C.N. Lam, L.E. Sanchez-Diaz, G. Smith, B.D. Olsen, and W. Chen. *ACS Macro Letters* **2015**, *4*, 165-170.
2. "The Shape of Protein-Polymer Conjugates in Dilute Solution." C.N. Lam, D. Chang, M. Wang, W.-R. Chen, and B.D. Olsen. *J. Poly. Sci. A Polymer Chemistry* **2015**, *54*, 292-302.
3. "Highly Active Biocatalytic Coatings from Protein-Polymer Diblock Copolymers." A. Huang, G. Qin, and B.D. Olsen. *ACS Applied Materials and Interfaces* **2015**, *7*, 14660-14669.
4. "Self-Assembly of Protein-Zwitterionic Polymer Bioconjugates Into Nanostructured Biomaterials." D. Chang and B.D. Olsen. *Polymer Chemistry* **2016**, *7*, 2410-2418.
5. "Self-Assembly of Differently Shaped Protein-Polymer Conjugates Through Modification of the Bioconjugation Site." A. Huang and B.D. Olsen. *Macromolecular Rapid Communications* **2016**, *in press*.
6. "The Effect of Protein Electrostatic Interactions on Globular Protein-Polymer Block Copolymer Self-Assembly." C.N. Lam and B.D. Olsen. *Biomacromolecules* **2016**, *online*
7. "Self-Assembly of Protein-Polymer Conjugates." X. Dong, A. Huang, A.E. Obermeyer, and B.D. Olsen. Submitted as chapter in book edited by R. Nagarajan.
8. "Topological Effects on Globular Protein-ELP Fusion Block Copolymer Self-Assembly." G. Qin, M.J. Glassman, C.N. Lam, D. Chang, E. Schiabile, A. Hexemer, and B.D. Olsen. *Advanced Functional Materials* **2015**, *25*, 729-738.
9. "Effect of Polymer Chemistry on Globular Protein-Polymer Block Copolymer Self-Assembly." D. Chang, C.N. Lam, and B.D. Olsen. *Polymer Chemistry* **2014**, *5*, 4884-4895.
10. "Synthesis and Application of Protein-Containing Block Copolymers." A.C. Obermeyer and B.D. Olsen. *ACS Macro Letters* **2015**, *4*, 101-110.

Neutron Scattering Investigation of the Relationship between Molecular Structure, Morphology and Dynamics in Conjugated Polymers

Prof. Lilo D. Pozzo, Dept. of Chemical Engineering, University of Washington - Seattle

Program Scope

Conjugated polymer films, nanofibers, and networks are ideal materials for efficient photovoltaic devices, batteries, thermoelectric cells, light emitting diodes and bio-electronic technologies such as artificial skin and neural implants. Moreover, it is now recognized that the structure and dynamics of organic semiconductor materials correlates strongly with large changes in optical, electronic and mechanical properties so that their control and manipulation is essential to advancing this field. The principal objective of this project is to develop the fundamental understanding of the intermolecular interactions that are at play during self-assembly and during charge transport processes for conjugated polymers in solution and in the concentrated solid and glassy states where they are commonly utilized.

In order to address this, we use a comprehensive suite of elastic (neutron diffraction, SANS and USANS) and quasi-elastic (NSE and backscattering spectroscopy) neutron scattering techniques along with MD simulations and (*in-situ*) property evaluation via dielectric spectroscopy and rheology. The project objectives focus on: 1) evaluating the influence of chain architecture on solution conformation, 2) determination of the influence of molecular structure and external fields on CP self-assembly and 3) identifying the correlation between dynamic molecular relaxations and macroscopic properties of CPs in the solid state. In addition to experimental components, molecular simulation (e.g. atomistic molecular dynamics and density functional theory) are used to fully understand the relationship between chain structure, mesoscale morphology, dynamic relaxation processes and macroscopic properties for these materials. Through the completion of this fundamental investigation we help inform scientists and engineers actively working on the synthesis of novel polymer architectures so that they can achieve simple processing and optimized properties via rational molecular design.

Recent Progress

Here, we specifically highlight recent results in two important areas related to the broader objectives of this project: 1) Synergistic use of molecular simulation and neutron scattering to understand polymers in solution and in the solid-state and 2) Assessing the effect of external electric fields on the self-assembly and orientation of nano-fibers from conjugated polymers.

Combined MD simulation and neutron scattering for improved molecular design

Molecular simulations promise to enable *in-silico* design of new materials to allow us to more efficiently identify materials that will have optimum performance in specific uses. Unfortunately, the molecular simulation methods that are currently used for conjugated polymers

and molecules are crude and have not been validated to demonstrate the accurate representation of real systems. In this research, we use neutron and x-ray scattering data to guide the development of accurate force fields and molecular simulation parameters for conjugated polymer systems.(1) We demonstrate that the synergy between quasi-elastic neutron scattering (QENS) and efficient MD simulations is ideal to help us understand the nature of important nanoscale motions and relaxations (Figure 1). X-ray and polarized neutron diffraction are also used to correlate experimental data with simulated polymer structures. QENS validation of MD force fields presents a unique opportunity to increase the

accuracy of highly uncertain parameters that are essential to the simulation of conjugated polymers. In particular we find that the simulation results are especially sensitive to changes in partial charges and backbone torsion potentials. These parameters are currently estimated from quantum mechanical calculations including density functional theory (DFT) but, unlike many force fields for small molecules, they had not been parameterized with experimental data. High variability is observed in these parameters for the small number of force fields that have been proposed in the literature.(2-4) The optimum force field for P3HT has been identified (Moreno FF2) and procedures for future simulations of high accuracy are established.(4)

Controlled Alignment of Conductive Polymer Nanowires for Efficient Optoelectronic Devices

In this sub-project, alternating current (AC) and direct current (DC) electric fields have been applied to conjugated polymers dissolved in organic solvents during a controlled self-assembly and gelation process. Dielectric spectroscopy measurements of the gels, small angle neutron scattering (SANS) and *in-situ* rheology

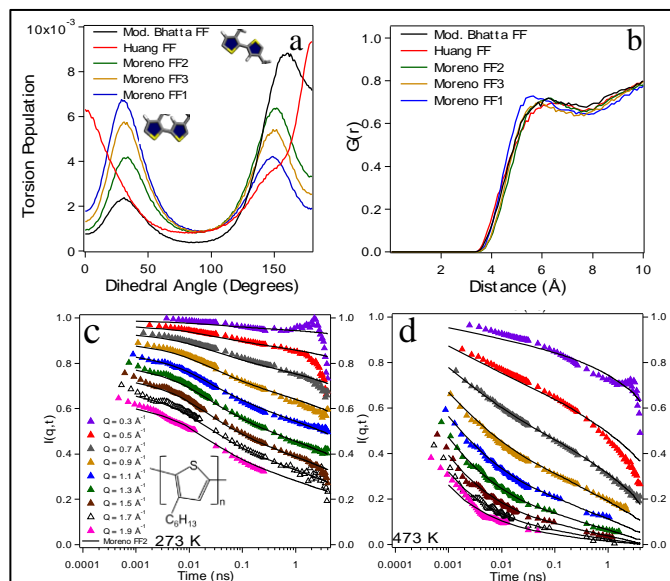


Figure 1: (a) Backbone torsion histogram for P3HT from different MD simulations (0° cis and 180° trans). (b) Ring-Ring radial distribution function for different simulations. (c),(d) Intermediate scattering function; QENS data (DCS and HFBS at NIST and BASIS at ORNL) compared to P3HT simulations utilizing Moreno FF2 force field.(4)

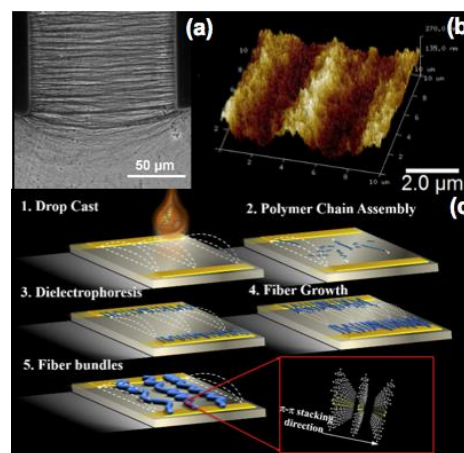


Figure 2: (a) Microscope image and (b) AFM surface profile for poly(3-hexylthiophene) grown and aligned under and AC electric field. (c) Mechanism of nanowire growth and alignment in electric fields.

measurements have been conducted under various electric field conditions. All of these measurements indicate that structural changes including nanofiber alignment are taking place under electric fields. In this application, neutron scattering is an excellent technique to probe the structure of self-assembled P3HT organogels. Time resolved small angle neutron scattering (TR-SANS) was used to evaluate structural changes during self-assembly as a function of time. Electrical properties of the organogels were also correlated to these structural differences. The application of electric fields during gelation provides an effective way to engineer the electrical and structural properties of conductive polymers for use in several electronic applications (e.g. OPVs, OLEDs and OFETs).

Future Plans

The next years of the project will focus on two areas of research. The first is to develop new processes for the manipulation of conductive polymer assembly through the use of ultrasound acoustic fields. It was recently found that acoustic radiation produces local stress fields that can lead to the formation of organized nanostructures and improved performance in organic electronic devices. Figure 3 shows representative SANS data for P3HT after increasing acoustic activation time. The changes that are observed in the profile are consistent with the formation of large nanofibers that are stable in solution. This effect is highly counterintuitive since ultrasound is typically used to break up aggregates. Here, it is demonstrated that acoustic fields can lead to the formation of organized polymer structures in solution that also have improved performance metrics.

The second area focuses on developing more efficient methods for running accurate molecular simulations of complex conductive polymer systems. These materials currently lack adequate molecular simulation frameworks due to large effects related to electronic conjugation. At this point, very few force fields are available to simulate conjugated polymers and most focus on poly-3-alkyl-thiophenes in spite of the great diversity of molecules that is now available. This is a huge impediment for achieving *in-silico* molecular design objectives. Moving forward, we will work to accelerate and improve the framework that we currently use to develop experimentally-validated force fields and parameters for complex conductive polymers. QENS and x-ray scattering will again be used to rigorously assess the quality of the simulations.

References

1. A Arbe, F. Alvarez, J. Colmenero, *Soft Matter*, 8, 8257, (2012)
2. R. S. Bhatta, Y. Y. Yimer, D. S. Perry, M. Tsige, *J. Phys. Chem. B*, 117, 10035 (2013)
3. D. M. Huang, R. Faller, K. Do and A. J. Moule, *J. Chem. Theory Comput.*, 1, (2010)

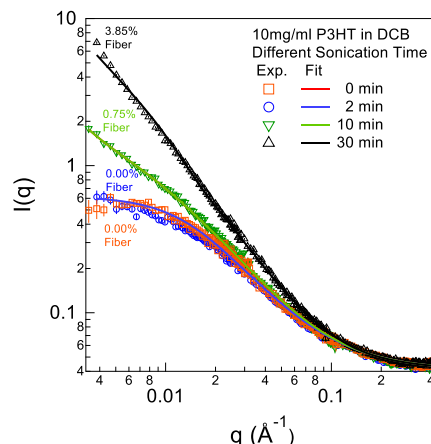


Figure 3: SANS profiles for P3HT solutions after ultrasound application. Fits are also included corresponding to a rigid nanofiber with a rectangular cross-section.

4. M. Moreno, M. Casalegno, G. Raos, S. V Meille, R. Po, *J. Phys. Chem. B*, 114, 1591 (2010)

Publications

1. “A Room-Temperature Processable PDI-Based Electron-Transporting Layer for Enhanced Performance in PDI-Based Non-Fullerene Solar Cells” J Yu, Y Xi, CC Chueh, D Zhao, F Lin, LD Pozzo, W Tang, AK Jen, *Advanced Materials Interfaces*, 3 (18), 1600476 (2016)
2. “Open-Circuit Voltage Losses in Selenium-Substituted Organic Photovoltaic Devices from Increased Density of Charge-Transfer States” Dana B Sulas, Kai Yao, Jeremy J Intemann, Spencer T Williams, Chang-Zhi Li, Chu-Chen Chueh, Jeffrey J Richards, Yuyin Xi, Lilo D Pozzo, Cody W Schlenker, Alex K-Y Jen, David S Ginger, *Chemistry of Materials*, 27, 19, 6583 (2015)
3. “Influence of Molecular Geometry of Perylene Diimide Dimers and Polymers on Bulk Heterojunction Morphology Toward High-Performance Nonfullerene Polymer Solar Cells” Chen, Hao Wu, Chu Chen Chueh, YuYin Xi, Hong Liang Zhong, Guang Peng Gao, Zhao Hui Wang, Lilo D Pozzo, Ten Chin Wen, Alex K Y Jen, *Advanced Functional Materials*, 25, 33, 5326 (2015)
4. “Structure Characterization and Properties of Metal Surfactant Complexes Dispersed in Organic Solvents” P de la Iglesia, V Jaeger, Y Xi, J Pfaendtner, LD Pozzo, *Langmuir*, 31, 33 (2015)
5. “Designing two-dimensional protein arrays through fusion of multimers and computational interface redesign” JF Matthaei, F DiMaio, JJ Richards, LD Pozzo, D Baker, F Baneyx, *Nano letters*, 15(8), 5235, (2015)
6. “A conductive liquid crystal via facile doping of an n-type benzodifurandione derivative” B Zhao, CZ Li, SQ Liu, JJ Richards, CC Chueh, F Ding, LD Pozzo, X Li, *Journal of Materials Chemistry A* 3 (13), 6929-6934 (2015)
7. “Solvatochromism and Conformational Changes in Fully Dissolved Poly (3-alkylthiophene)s” GM Newbloom, SM Hoffmann, AF West, MC Gile, P Sista, HKC Cheung, J. Pfaendtner, LD Pozzo *Langmuir*, 31 (1), 458 (2015)
8. “Correlating structure and photocurrent for composite semiconducting nanoparticles with contrast variation small-angle neutron scattering and photoconductive atomic force microscopy” JJ Richards, CL Whittle, G Shao, LD Pozzo, *ACS Nano* 8 (5), 4313 (2014)
9. “Controlled gelation of poly (3-alkylthiophene) s in bulk and in thin-films using low volatility solvent/poor-solvent mixtures” GM Newbloom, P de la Iglesia, DC Pozzo, *Soft matter* 10 (44), 8945 (2014)

Status and Future Plans on Analysis and Modeling Software capabilities for Neutron Scattering Research at the ORNL Neutron Scattering Facilities

Th. Proffen, Neutron Sciences Directorate, Oak Ridge National Laboratory, Oak Ridge, TN 37831

Introduction

Neutron scattering enables simultaneous measurement of structural and dynamic properties of materials from the atomic scale (0.1 nm, 0.1ps) to the mesoscale (1 μ m, 1 μ s). These ranges are remarkably complementary to current capabilities of computational modeling, and the simplicity of the scattering cross section allows the straight-forward prediction of neutron scattering data from computer models. Co-location of the Oak Ridge Leadership Computing Facility (OLCF) and the Spallation Neutron Source (SNS) and High Flux Isotope Reactor (HFIR) at Oak Ridge National Laboratory (ORNL) provides a unique opportunity to close the gap between advanced neutron scattering capabilities and advanced materials modeling enabled by high performance computing (HPC). The CAMM project was funded through the neutron scattering program as part of the Materials Sciences and Engineering Division Office of Basic Energy Sciences and jumpstarted the developments of methods and software. A refinement workflow for molecular dynamics (MD) simulations based on neutron scattering data developed as part of CAMM is now available to SNS users. The figure on the right shows the calculated and observed quasielastic neutron scattering from hydrated RNA on nano-diamond resulting from a refinement of an effecting interaction potential used in MD simulations of the system [1]. The Neutron Data Analysis and Visualization Division (NDAV) in the Neutron Sciences Directorate at ORNL is responsible for meeting user software and computing needs related to collection, reduction and analysis and modeling of neutron scattering data. NDAV deploys and maintains the relevant software

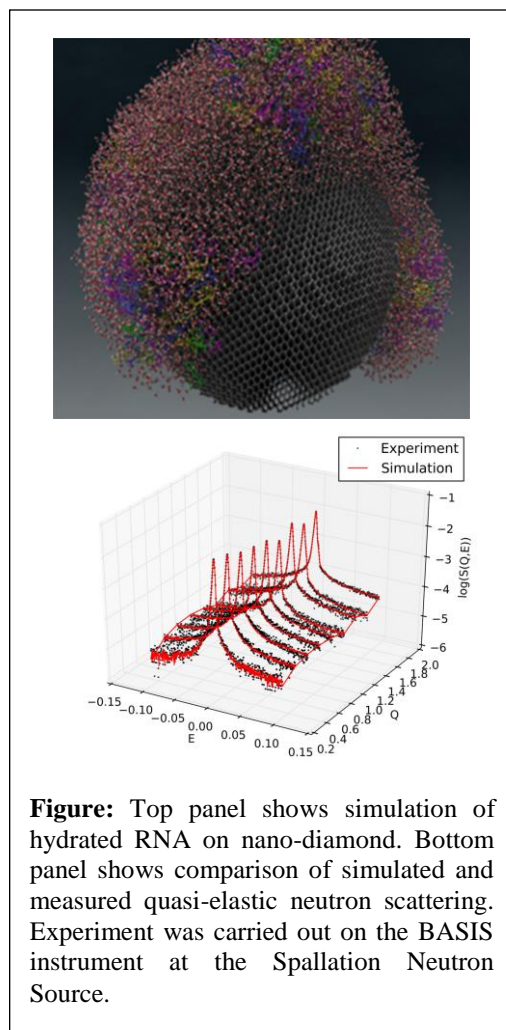


Figure: Top panel shows simulation of hydrated RNA on nano-diamond. Bottom panel shows comparison of simulated and measured quasi-elastic neutron scattering. Experiment was carried out on the BASIS instrument at the Spallation Neutron Source.

including tools created by CAMM. The future roadmap is developed in close collaboration with the user community. Recent community engagement included a comprehensive workshop on *Frontiers in Data, Modeling, and Simulation*¹, held as part of a series of Grand Challenge Workshops related to neutron science.

Current Capabilities

Users at the SNS and HFIR have access to computing resources ranging from local analysis clusters to HPC resources at NERSC and OLCF by request. Recently a dedicated 1000 node cluster was added to facilitate DFT calculations for users of the high throughput neutron vibrational spectrometer VISION at the SNS. **Standard analysis and modeling packages** are installed on these resources and accessible to users. The CAMM project was critical to developing the advanced capabilities in three main areas outlined below.

Phonon Modeling: A critical link between first principles calculations and neutron scattering is the ability to calculate the phonon dynamical structure factor, $S(Q,E)$, and the phonon density-of-states (DOS). The code *SimPhonies* provides this link and is currently in the final stages of documentation and deployment. Related hands-on workshop is planned this year and scientific publications using this code can be found in [5-6,10-12].

Force Field Refinement: Users have access to a workflow and tools allowing the refinement of potential parameters used in MD of a specific model based on neutron scattering data. The system was first demonstrated for LiCl in water [3] and later using simulations of nano-diamond + RNA + water [1]. The tools leverage the new Pegasus workflow system [7] to seamlessly run the required simulations on supercomputing resources without users needing to be ‘experts’.

Dynamic Pair Density Function (DPDF): DPDF provides a completely new approach to studying dynamics using neutron scattering and goes beyond simply focusing on the dispersion of excitations and utilizes all the data collected on the spectrometers at SNS. A first prototype for data reduction to a DPDF was implemented in the data reduction framework Mantid used at the Spallation Neutron Source (SNS). Initial science applications focused on understanding dynamics in super fluid helium and heavy water.

Future Plans

Current work is taking advantage of certain novel research efforts in computational sciences at ORNL, namely the Compute and Data Environment for Science (CADES) as well as the Bellerophon Environment for Analysis of Materials (BEAM). A workflow prototype for refinement of a single force-field parameter against QENS data has been implemented in these computing frameworks. The user can monitor from his/her laptop or workstation the progress of a refinement that is being carried out at a remote cluster. These efforts allow leveraging of

¹ Workshop Reports: <http://neutrons.ornl.gov/grand-challenge-workshops>

existing developments outside of Neutron Sciences and providing a more user friendly user interfaces. A critical element to future success is user engagement and promoting advanced tools to extract more detailed information about materials from complex neutron scattering experiments. As part of these efforts additional hands-on workshops will be offered and additional tutorials and documentation will be made available. A tutorial for the current MD force field refinement workflow can be found at <http://camm.ornl.gov>.

In addition to working with the user community to most effectively use the existing tools, NDAV is partnering with groups within and outside of ORNL to develop the next generation techniques, algorithms and tools. The ACUMEN project² is an example of a recent collaboration bringing applied mathematics methods to neutron scattering analysis and modeling.

Publications

1. G.K. Dhindsa, D. Bhowmik, M. Goswami, H. O'Neill, E. Mamontov, B.G. Sumpter, L. Hong, P. Ganesh and X. Chu, "Enhanced Dynamics of Hydrated tRNA on Nanodiamond Surfaces: A Combined Neutron Scattering and MD Simulation Study", *J. Phys. Chem. B*, **120** (38), 10059-10068 (2016) – DOI: 10.1021/acs.jpcc.6b07511
2. J-M Carrillo, Z. Seibers, R. Kumar, M.A. Matheson, J.F. Ankner, M. Goswami, K. Bhaskaran-Nair, W.A. Shelton, B.G. Sumpter, and S.M. Kilbey, "Petascale Simulations of the Morphology and the Molecular Interface of Bulk Heterojunctions", *ACS Nano*, **10** (7), 7008-7022 (2016) - 10.1021/acsnano.6b03009
3. J-M.Y. Carrillo, M.A. Sakwa-Novak, A. Holewinski, M.E. Potter, G. Rother, C.W. Jones and B.G. Sumpter, "Unraveling the Dynamics of Aminopolymer/Silica Composites", *Langmuir* **32**(11), 2617-2625 (2016) – DOI: 10.1021/acs.langmuir.5b04299
4. E. Mamontov, S. Veerendra, J.M. Borreguero, and T. Madhusudan, "Protein-Style Dynamical Transition in a non-Biological Polymer and a non-Aqueous Solvent", *Journal of Physical Chemistry B*, **120** (12) 3232-3239 (2016) – DOI: 10.1021/acs.jpcc.6b00866
5. J.M. Borreguero, and V.E. Lynch, "Molecular dynamics force-field refinement against quasi-elastic neutron scattering data", *J. Chem. Theory Comput.* **12**, 9-17 (2015) – DOI: 10.1021/acs.jctc.5b00878
6. M. Goswami, J.M. Borreguero, P.A. Pincus and B.G. Sumpter, "Surfactant-Mediated Polyelectrolyte Self-Assembly in a Polyelectrolyte–Surfactant Complex", *Macromolecules* **48**, 9050-9059 (2015) – DOI: 10.1021/acs.macromol.5b02145

² <http://cam.ornl.gov/acumen/>

7. D. Bansal, C.W. Li, A.H. Said, D.L. Abernathy, J. Yan, and O. Delaire, “Electron-phonon coupling and thermal transport in the thermoelectric compound $\text{Mo}_3\text{Sb}_{7-x}\text{Te}_x$ ”, *Phys. Rev. B* **92**, 214301 (2015) – DOI: 10.1103/PhysRevB.92.214301
8. C.W. Li, J. Hong, A. F. May, D. Bansal, S. Chi, T. Hong, G. Ehlers and O. Delaire, “Orbitally driven giant phonon anharmonicity in SnSe”, *Nature Physics* **11**, 1063-1069 (2015) – DOI: 10.1038/NPHYS3492
9. Ewa Deelman, Christopher Carothers, Anirban Mandal, Brian Tierney, Jeffrey S Vetter, Ilya Baldin, Claris Castillo, Gideon Juve, Dariusz Krol, Vickie Lynch, Ben Mayer, Jeremy Meredith, Thomas Proffen, Paul Ruth and Rafael Ferreira da Silva, “PANORAMA: An approach to performance modeling and diagnosis of extreme-scale workflows”, *The International Journal of High Performance Computing Applications*, 1-15 (2015) – DOI: 10.1177/1094342015594515
10. J. Carrillo, S. Cheng, R. Kumar, M. Goswami, A. Sokolov and B. Sumpter, “Unentangling the effects of chain rigidity on the structure and dynamics of strongly adsorbed polymer melts” *Macromolecules*, **48**, 4207-4219 (2015) – DOI: 10.1021/acs.macromol.5b00624
11. Monojoy Goswami, Jose M. Borreguero and Bobby G. Sumpter, “Self-assembly and structural relaxation in a model ionomer melt” *J. Chem. Phys.*, **142**, 084903, (2015) – DOI: 10.1063/1.4913517
12. O. Delaire, I. I. Al-Qasir, A. F. May, C. W. Li, B. C. Sales, J. L. Niedziela, J. Ma, M. Matsuda, D. L. Abernathy, and T. Berlijn, “Heavy-impurity resonance, hybridization, and phonon spectral functions in $\text{Fe}_{1-x}\text{M}_x\text{Si}$ ($M=\text{Ir}, \text{Os}$)”, *Phys. Rev. B* **91**, 094307 (2015) – DOI: 10.1103/PhysRevB.91.094307
13. C. W. Li, J. Ma, H. B. Cao, A. F. May, D. L. Abernathy, G. Ehlers, C. Hoffmann, X. Wang, T. Hong, A. Huq, O. Gourdon, and O. Delaire, “Anharmonicity and atomic distribution of SnTe and PbTe thermoelectrics”, *Phys. Rev. B* **90**, 214303 (2014) – DOI: 10.1103/PhysRevB.90.214303
14. John D. Budai, Jiawang Hong, Michael E. Manley, Eliot D. Specht, Chen W. Li, Jonathan Z. Tischler, Douglas L. Abernathy, Ayman H. Said, Bogdan M. Leu, Lynn A. Boatner, Robert J. McQueeney, Olivier Delaire, “Metallization of vanadium dioxide driven by large phonon entropy”, *Nature* **515**, 535–539 (2014) - DOI:10.1038/nature13865

Inelastic Neutron and X-ray Scattering Investigation of Electron-Phonon Effects in Quantum Materials

Dmitry Reznik

Program Scope

Current research investigates Cu and Fe-based high temperature superconductors and related materials such as stripe-ordered nickelates and CMR manganites. Inelastic neutron scattering studies of electron-lattice effects in these materials aim to uncover different types of excitations of the atomic lattice that shed light on properties of electrons to which the atomic lattice is coupled. Phonons, dynamic charge stripes, and polatonic distortions have been discovered and investigated.

Recent Progress

1. Systematic investigation of $|\mathbf{q}|>0$ nematic fluctuations in Fe-based superconductors

Parent compounds of Fe-based superconductors undergo a structural phase transition from a tetragonal to an orthorhombic structure. We measured the temperature dependence of the frequencies of transverse acoustic (TA) phonons that extrapolate to the shear vibrational mode associated with this transition. It is typically detected by resonant ultrasound (RUS), which corresponds to the orthorhombic deformation of the structure at low temperatures in BaFe_2As_2 and SrFe_2As_2 . We found that acoustic phonons at small wavevectors soften gradually towards the transition from high temperatures, tracking the increase of the size of slowly fluctuating magnetic domains. On cooling below the transition the phonons harden following the square of the magnetic moment (which we find is proportional to the anisotropy gap).¹

Next we performed the same measurement as a function of Co doping with the emphasis on nematic fluctuations. Nematic order is ubiquitous in liquid crystals and is characterized by a preferred direction in an otherwise uniform liquid. Recently a similar symmetry breaking has been observed in some electronic phases in quantum materials related to high temperature superconductors.² We investigated the prototypical Fe-based high-temperature superconductor $\text{Ba}(\text{Fe}_{1-x}\text{Co}_x)_2\text{As}_2$ where the interplay of electronic nematic order and superconductivity is well established.³ Previous measurements found a strong suppression of nematic fluctuations at zero momentum in the superconducting state, but what happens at nonzero momentum is unknown. We found that fluctuations at small momenta, which correspond to wavelengths of as much as 25 unit cells, do not compete with superconductivity. Instead they continue to grow below

superconducting T_c . Our results imply the existence of a length scale larger than 25 unit cells that is important for understanding of the interplay between nematicity and superconductivity.

We also investigated long-wavelength nematic fluctuations in an Fe-based superconductor LiFeAs near $\mathbf{q}=(0.05,0,0)$ by measuring temperature-dependent renormalization of acoustic phonons. We found that the phonons have conventional behavior, expected in the absence of electronic nematic fluctuations. This observation implies that either electron-phonon coupling is too weak to see any effect or that nematic fluctuations are not there.⁴

2 Polaronic metal phases in $\text{La}_{0.7}\text{Sr}_{0.3}\text{MnO}_3$ uncovered by inelastic neutron and x-ray scattering

Among colossal magnetoresistive manganites the prototypical ferromagnetic manganite $\text{La}_{0.7}\text{Sr}_{0.3}\text{MnO}_3$ has a relatively small magnetoresistance, and has been long assumed to have only weak electron-lattice coupling. We found that $\text{La}_{0.7}\text{Sr}_{0.3}\text{MnO}_3$ has strong electron-phonon coupling: Our neutron and x-ray scattering experiments show strong softening and broadening of transverse acoustic phonons on heating through

the Curie temperature $T_C=350\text{K}$. Simultaneously, we observed two phases where metallic resistivity and polarons coexist. The ferromagnetic polaronic metal phase between 200K and T_C is characterized by quasielastic scattering from dynamic CE-type polarons with the relatively short lifetime of $\tau \approx 1\text{ps}$. This scattering is greatly enhanced above T_C in the paramagnetic polaronic metal phase. Our results suggest that the strength of magnetoresistance in manganites scales with the inverse of the polaron lifetime, not the strength of electron-phonon coupling.⁵

3. Phonons possibly related to the 10 meV ARPES kink in copper oxide superconductor $\text{Bi}_2\text{Sr}_2\text{CaCu}_2\text{O}_{8+\delta}$.

One of the possible mechanisms of high T_c superconductivity is Cooper pairing with the help of bosons responsible for kinks in electronic dispersion observed by angle-resolved photoemission

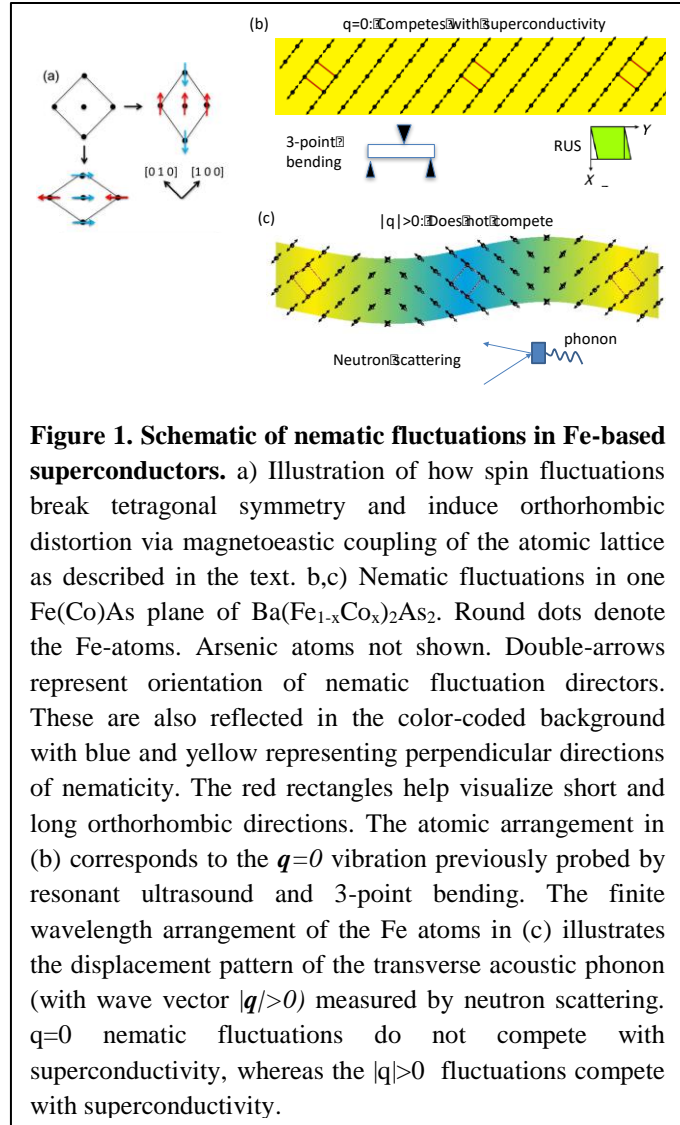


Figure 1. Schematic of nematic fluctuations in Fe-based superconductors. a) Illustration of how spin fluctuations break tetragonal symmetry and induce orthorhombic distortion via magnetoelastic coupling of the atomic lattice as described in the text. b,c) Nematic fluctuations in one $\text{Fe}(\text{Co})\text{As}$ plane of $\text{Ba}(\text{Fe}_{1-x}\text{Co}_x)_2\text{As}_2$. Round dots denote the Fe-atoms. Arsenic atoms not shown. Double-arrows represent orientation of nematic fluctuation directors. These are also reflected in the color-coded background with blue and yellow representing perpendicular directions of nematicity. The red rectangles help visualize short and long orthorhombic directions. The atomic arrangement in (b) corresponds to the $\mathbf{q}=0$ vibration previously probed by resonant ultrasound and 3-point bending. The finite wavelength arrangement of the Fe atoms in (c) illustrates the displacement pattern of the transverse acoustic phonon (with wave vector $|\mathbf{q}|>0$) measured by neutron scattering. $\mathbf{q}=0$ nematic fluctuations do not compete with superconductivity, whereas the $|\mathbf{q}|>0$ fluctuations compete with superconductivity.

(ARPES). Up to now most effort has been devoted to the kinks near 70 meV. More recent ARPES experiments revealed an additional energy scale near 10 meV.^{6,7} Since no magnetic excitations peaked at these energies have been identified, the likeliest candidates appear to be phonons. We recently measured all phonons below 15 meV in a large single crystal sample of optimally-doped $\text{Bi}_2\text{Sr}_2\text{CaCu}_2\text{O}_{8+\delta}$ (BSCCO). The high quality dataset covered several Brillouin zones and neutron final energies, despite the widespread belief that phonon measurements on BSCCO are too difficult. We measured all phonons below 15 meV. There are many branches, in particular, an optic branch disperses from 7 meV from the zone center as well as another optic branch dispersing from 4 meV. In addition, a low energy longitudinal acoustic phonon branch has been uncovered (See figure 1). We propose a new mechanism for the 10 meV kink based on interaction with optic phonons dispersing in the L-direction that is consistent with these results. Manuscript is in preparation.

4. Development of a new method to measure phonons in materials with large unit cells at the SNS: Multizone phonon refinement. We have been developing software for extracting phonon dispersions from TOF datasets obtained on materials with large unit cells. A prototype version of the software has been written in the previous cycle and was successfully used on SrFe_2As_2 .⁸ The particular focus is on adapting the algorithm to work with data obtained on small samples, which have challenges of poor statistics with relatively large background. We measured a copper oxide superconductor, $\text{HgBa}_2\text{CuO}_4$, on ARCS and used this dataset to test the new code. The Matlab/Horace version of the software has been by now completed and tested.

Now the software consists of two separate modules: The background subtraction module and the multizone fitting module. They can be used separately: Background subtraction module can be used if only background subtraction needs to be done. Multizone fitting alone can be used if background-subtracted data are available. Multizone fitting module can be used also for triple-axis data. Manuscript is in preparation.

Future Plans

We plan to shift emphasis to new investigations of electron-phonon effects in select materials with orbital degrees of freedom: Fe-based superconductors, manganite perovskites and 4d/5d transition metal oxides. Scientific questions to be addressed are as follows:

What is the interplay between nematicity, orbital order, and superconductivity in both FeAs and FeSe-based superconductors with the emphasis on the latter? We will measure transverse acoustic phonons coupled to nematic fluctuations as the materials go through nematic/orbital ordering and superconducting transitions. This work will address arguably the most important question in the field of Fe-based superconductors.

How does short-range orbital order affect the lattice dynamical spectrum in quasicubic ferromagnetic manganites such as $\text{La}_{1-x}\text{Sr}_x\text{MnO}_3$? Preliminary experiments on optic phonons showed radical effects of short-range orbital order and we now plan to understand these effects. This work will lead to a complete picture of the relationship between orbital ordering, lattice dynamics, and electrical transport.

What is the role of electron-phonon coupling in 4d and 5d transition metal oxides (TMOs) such as ruthenates and iridates? They received a lot of attention lately, because strong spin-orbit coupling is responsible for a rich and enigmatic phase diagram.⁹ It is generally recognized that spin-phonon coupling plays a big role, because orbital degrees of freedom entangled into magnetic moments couple them to the atomic lattice.^{10,11} We plan a comprehensive study of phonons in these compounds with the emphasis on rotational modes of the MO₆ (M-Ru, Ir) octahedra.

Methods: We will use IXS for measurements of phonons in Fe-based superconductors and iridates, INS for manganites, and both INS and IXS for ruthenates. A large Ca₃Ru₂O₇ sample will be coaligned so that magnetic excitations as well as phonons could be measured by the time-of-flight method. Multizone phonon refinement (MPR) developed during the current cycle will be used for data analysis.

Methods development: The current Matlab version of MPR now works very well for in-house purposes. Here we propose to adapt MPR to the standards of the software group at the SNS, which requires all software to be written in Python and to work on top of Mantid.

References

- ¹ D. Parshall et al., *Physical Review B* **91**, 134426 (2015).
- ² E. Fradkin, S. A. Kivelson, M. J. Lawler, J. P. Eisenstein, A. P. Mackenzie, *Annual Review of Condensed Matter Physics* **1**, 153-178 (2010).
- ³ F. Weber et al., arXiv:1610.00099.
- ⁴ A. Merritt, J. Rodriguez-Rivera, Yu Li, Weiyi Wang, C. Zhang, P. Dai, D. Reznik, *Supercond. Nov. Magn.* (2016). doi:10.1007/s10948-016-3810-x.
- ⁵ M. Maschek, D. Lamago, J.P. Castellán, A. Bosak, D. Reznik, F. Weber, *Phys. Rev. B* **93**, 045112 (2016).
- ⁶ N.C. Plumb, T. J. Reber, J. D. Koralek, Z. Sun, J. F. Douglas, Y. Aiura, K. Oka, H. Eisaki, and D. S. Dessau, *Phys. Rev. Lett.* **105**, 046402 (2010)
- ⁷ I. M. Vishik, W. S. Lee, F. Schmitt, B. Moritz, T. Sasagawa, S. Uchida, K. Fujita, S. Ishida, C. Zhang, T. P. Devereaux, and Z. X. Shen, *Phys. Rev. Lett.* **104**, 207002 (2010).
- ⁸ D. Parshall, R. Heid, J. L. Niedziela, Th. Wolf, M. B. Stone, D. L. Abernathy, and D. Reznik, *Phys. Rev. B* **89**, 064310 (2014).
- ⁹ Jeffrey G. Rau, Eric Kin-Ho Lee, and Hae-Young Kee, *Annual Review of Condensed Matter Physics* **7**, 195 (2016).
- ¹⁰ J. C. Wang, J. Terzic, T. F. Qi, Feng Ye, J. Yuan, S. Aswartham, S. V. Streltsov, D. I. Khomskii, R. K. Kaul, and G. Cao, *Phys. Rev. B* **90**, 161110(R) (2014).
- ¹¹ M. Ge, T. F. Qi, O. B. Korneta, D. E. De Long, P. Schlottmann, W. P. Crummett, and G. Cao, *Phys. Rev. B* **84**, 100402(R) (2011).

Publications

F. Weber, D. Parshall, L. Pintschovius, J.-P. Castellan, M. Merz, Th. Wolf, and D. Reznik, “Enhancement of finite wavevector nematic fluctuations in the superconducting state of $\text{Ba}(\text{Fe}_{1-x}\text{Co}_x)_2\text{As}_2$ ”, arXiv:1610.00099. (2016) Submitted to Science Advances.

R. Zhong, B.L. Winn, G. Gu, D. Reznik, and J. M. Tranquada, “Evidence for a nematic phase in $\text{La}_{1.75}\text{Sr}_{0.25}\text{NiO}_4$ ” arXiv:1608.04799 (2016). Submitted to PRL.

D. Parshall, L. Pintschovius, J. L. Niedziela, J.-P. Castellan, D. Lamago, R. Mittal, Th. Wolf, and D. Reznik, “Close correlation between magnetic properties and the soft phonon mode of the structural transition in BaFe_2As_2 and SrFe_2As_2 ”, Phys. Rev. B, Phys. Rev. B **91**, 134426 (2015).

D Reznik, D Parshall, SR Park, JW Lynn, T Wolf, “Absence of magnetic field dependence of the anomalous bond-stretching phonon in $\text{YBa}_2\text{Cu}_3\text{O}_{6.6}$ ” Journal of Superconductivity and Novel Magnetism, 1-2, (2015).

M. Maschek, D. Lamago, J.-P. Castellan, A. Bosak, D. Reznik, and F. Weber, “Polaronic metal phases in $\text{La}_{0.7}\text{Sr}_{0.3}\text{MnO}_3$ uncovered by inelastic neutron and x-ray scattering,” Physical Review B **93** (4), 045112 (2016).

L. Pintschovius, D. Reznik, F. Weber, P. Bourges, D. Parshall, R. Mittal, Samrath Lal Chaplot, R. Heid, T. Wolf, D. Lamago, J.W. Lynn, “Spurious peaks arising from multiple scattering events involving the sample environment in inelastic neutron scattering” Applied Crystallography, **47** 1472 (2014).

C. Stock, P. M. Gehring, G. Xu, D. Lamago, D. Reznik, M. Russina, J. Wen, and L. A. Boatner, “Fluctuating defects in the incipient relaxor $\text{K}_{1-x}\text{Li}_x\text{TaO}_3$ ($x=0.02$), ” Phys. Rev. B **90**, 224302 (2014).

A. Merritt, J. Rodriguez-Rivera, Yu Li, Weiyi Wang, C. Zhang, P. Dai, D. Reznik, “Absence of long wavelength nematic fluctuations in LiFeAs , ” Supercond Nov Magn (2016). doi:10.1007/s10948-016-3810-x.

The Next Ferroic Order: Synthesis and Neutron Scattering of Ferrotoroidic Materials

Efrain E. Rodriguez

Chemistry and Biochemistry, University of Maryland, College Park, MD 20742

Program Scope

Our research activities focus on studying the fourth of the known primary ferroics in condensed matter systems through an experimental program on ferrotoroidic materials. Three of the primary ferroics are well understood and include ferromagnets, ferroelectrics, and ferroelastics (see Figure 1). A common characteristic of these materials is a spontaneous symmetry breaking with respect to an order parameter such as magnetization. For example, in a ferromagnet, time-reversal symmetry is broken when the spins in the crystal lattice align in one direction. The ferrotoroidic order, which breaks both types of symmetry, is more difficult to observe than the others, and we plan to reveal it through our combined program consisting of materials synthesis and neutron scattering experiments.

Our central hypothesis is that ferrotoroidic materials exist as their own separate category from the known primary ferroic orders and that spherical neutron polarimetry (SNP) will be one of the definitive techniques to prove this thesis.

Studying the change in domain population through (SNP) and manipulation by an applied toroidal field will therefore be critical to proving this new ferroic order. This behavior is possible in a material where the magnetic moments are arranged in a vortex-like configuration, which gives rise to a toroidal moment (Figure 1).[1-3] Another property of a ferrotoroidic material is that it expresses the magnetoelectric effect, whereby an applied magnetic field affects the electric polarization and, conversely, application of an electric field affects the magnetization. The relationship between the combined toroidal field and the order parameter are given by the magnetoelectric tensor. What is special about a ferrotoroidic material is that it must contain only off-diagonal terms in this tensor. By performing diffraction with SNP, we can directly probe the off-diagonal terms of the magnetoelectric tensor, and thereby establish whether the material is ferrotoroidic.

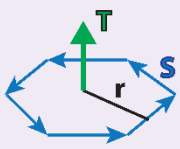
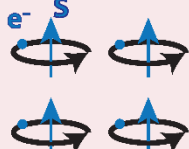
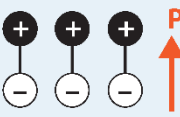
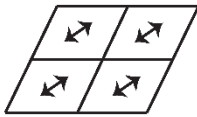
SPACE \ TIME	CHANGE	INVARIANT
CHANGE	a.) Ferrotoroidic 	b.) Ferromagnetic 
INVARIANT	c.) Ferroelectric 	d.) Ferroelastic 

Figure 1. Table of the four primary ferroic orders with respect to time-reversal and space-inversion symmetries. In a.) a vortex of spin vectors S leads to a toroidal moment T , which breaks both time and space symmetries below the antiferromagnetic ordering temperature. In b.) magnetic moments align for ferromagnetism and in c.) electric dipoles align for ferroelectric polarization. In d.) a ferroelastic material does not break either time- or space inversion symmetries.

Recent Progress

1. Materials synthesis: For the materials design portion, we have both crystal chemistry and symmetry considerations in pursuing new ferrotoroidic materials. From symmetry considerations, there are strict requirements on the type of magnetic point groups that allow a spontaneous toroidal moment to develop. From a crystal chemistry perspective, we have focused on finding toroidal arrangement of moments in cluster inorganic-organic materials and two-dimensional (2D) inorganic sheets. In the 2D case, we have synthesized the series of phosphates LiMPO_4 for $M = \text{Mn, Fe, Co, and Ni}$, which crystallize in the olivine structure, to complete our hypothesis on ferrotoroidic materials. We are pursuing this system since one of the most well-known materials to develop a toroidal moment is the magnetoelectric LiCoPO_4 , which adopts the so-called olivine structure with space group $Pnma$, [4,5] In this oxide, CoO_6 octahedra share edges to form layers that are in turn linked by phosphate tetrahedra. The local symmetry of the Co cations is key to achieving the ferrotoroidicity as it allows small displacements of the Co cations from a special position in the crystal structure. Below the Neel temperature the magnetic moments align antiferromagnetically, and due to a small canting of the spins,[5] the material expresses a net toroidal moment. Van Aken et al established for the first time that LiCoPO_4 was a ferrotoroidic material based on second harmonic generation (SHG) optical measurements,[3] and one initial SNP study on LiCoPO_4 has found some promising results on the presence of ferrotoroidicity.[6]

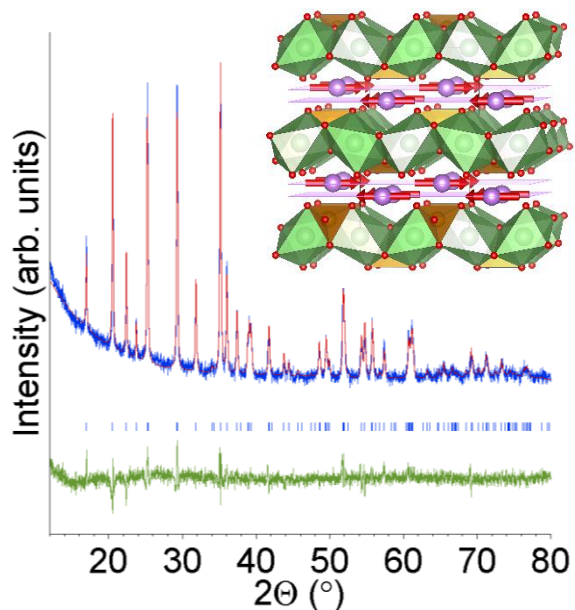


Figure 2. The XRD powder pattern of phase pure LiMnPO_4 prepared in our lab. The Rietveld refinement to the structure shows calculated in red, observed in blue, and difference in green. The inset shows the crystal structure of LiMPO_4 for the series where $M = \text{Mn, Fe, Co, and Ni}$.

Since the Mn analogue is thought to not have ferrotoroidicity based on the magnetic space group, this compound will be an important control for understanding the SNP results. Figure 2 shows the powder pattern of LiMnPO_4 , which we have prepared phase pure through hydrothermal synthesis. We have also prepared the other transition metal analogues.

2. Spherical polarized neutron scattering (SNP): We have started the design stage for the construction of an apparatus based on the MuPAD apparatus built at European neutron sources.[7] We have chosen to design the apparatus for the BT-7 triple axis spectrometer at the NIST Center for Neutron Scattering (NCNR). The wavelength of choice is 3.35416 \AA with the PG(002) monochromator.

We have commenced modeling how the applied magnetic field gradient experienced by a polarized neutron beam preserves the beam's polarization to within the detection limit. Such a specification is important to determine the geometry and operation of both shields and coils used for beam manipulation at the BT-7 instrument. For the magnetic shielding, high saturation/permeability metals will act to distort the magnetic field in such a way that the field in one region of space while increasing another region. While mu-metal will comprise the majority of shielding, we are also considering high- T_c superconducting materials for certain shielding. Increasing field or "flux focusing", which occurs within the high saturation/permeability metals, can potentially depolarize the neutron beam. Therefore, field gradients are needed to both align and orient the beam for a given experiment. Figure 3 depicts the relationship between the rotating magnetic field and the polarization vector of the neutron beam. We are interested in the quantity α , which is analogous to the opening angle of Larmor frequency, ω_L with the rotation rate of the magnetic field in the neutron frame of reference, ω . The angle α now defines the opening angle of the spin precession about an off axis, \mathbf{W} , from the magnetic field axis.

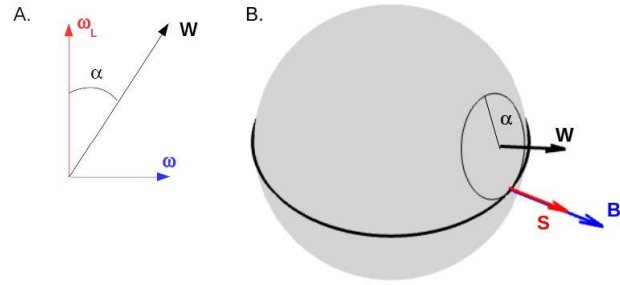


Figure 3. a.) Depiction of the relationship between the field rotation rate and the Larmor precession rate. b) Diagram illustrating the geometry of the off axis precession, field B and spin S.

Three regimes of Figure 4 can be identified for the behavior of the polarization under a rotating magnetic field. At BT-7, beam polarization with the highest intensity is achieved with polarized ^3He cells. Since the flipping ratio, R , is the standard measure of polarization, it is the error in the measure of R that will determine the truly adiabatic and field flipping regimes. For polarization alignment on BT-7, the error in a typical measurement is on the order of ± 4 cnt/s. Thus, the error in the flipping ratio has been estimated to be on the order of ± 0.006 , which leads to a misalignment of nearly 0.6° . For a beam of energy 14.7 meV in a 200 G magnetic field, the 0.6° misalignment leads to an adiabatic limit of 2.2 G/cm, which can be easily measured with a Gaussmeter. Our goal now is to understand the maximum allowable reduction in flipping ratio for a successful magnetic diffracton experiment on our proposed ferrotoroidic materials.

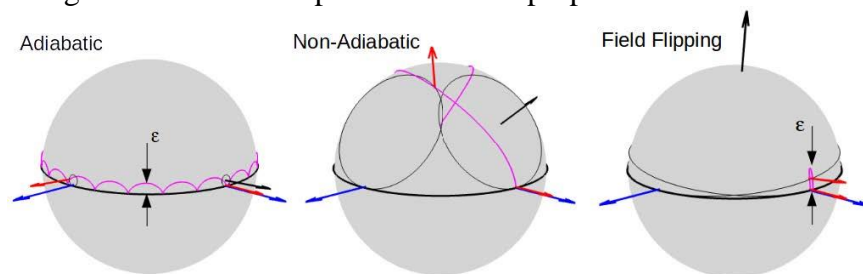


Figure 4. (Left) Adiabatic Regime: The magnetic field rotates slowly enough for the polarization to follow it to within ϵ . (Center) Non-Adiabatic Regime: The dynamic precession results in potentially large misalignment. (Right) Field Flipping Regime: The magnetic field rotates so fast that the polarization is only perturbed to within ϵ .

Future Plans

1. Materials synthesis: Our next goal is to optimize the hydrothermal conditions by raising the temperature of reaction and applying temperature gradients to grow single crystals of sufficient size for neutron diffraction studies. For this purpose we have rebuilt a hydrothermal furnace in our lab that can reach temperatures up to 800 °C and higher pressures than available with autoclaves. Once single crystals have been isolated, we will perform SNP measurements at international neutron sources while we continue construction of the SNP apparatus locally. Finally, we are continuing our synthesis of the molecular clusters Dy-6 and Dy-3,[8,9] on which we plan to perform some preliminary neutron powder diffraction experiments to establish whether they order below 3 K, and if so to solve the long-range magnetic ordering.

2. SNP development: Once we calculate the distances required on BT-7 for the adiabatic and spin flipping regimes of the neutron polarization, we will start designing components with drafting software. These include designs of the zero-field chamber and Larmor precession devices that will allow us to polarize the neutron beam and perform the polarization analysis in any direction. In the coming year, we aim to machine the parts and build the apparatus. Ultimately, our goal is to make our technique available to the wider North American neutron scattering community, including DOE user facilities, where it can be extended to other types of measurements such as inelastic and small angle neutron scattering.

References

1. Y. V. Kopaev, "Toroidal ordering in crystals," *Physics-Uspekhi*, vol. 52, no. 11, p. 1111, 2009.
2. K. M. Rabe, "Solid-state physics: Response with a twist," *Nature*, vol. 449, no. 7163, pp. 674–675, 2007.
3. B. B. Van Aken, J.-P. Rivera, H. Schmid, and M. Fiebig, "Observation of ferrotoroidic domains," *Nature*, vol. 449, pp. 702–705, 2007.
4. D. Vaknin, J. L. Zarestky, L. L. Miller, J.-P. Rivera, and H. Schmid, "Weakly coupled antiferromagnetic planes in single-crystal LiCoPO_4 ," *Physical Review B*, vol. 65, p. 224414, 2002.
5. P. J. Baker, I. Franke, F. L. Pratt, T. Lancaster, D. Prabhakaran, W. Hayes, and S. J. Blundell, "Probing magnetic order in LiMPO_4 ($M = \text{Ni, Co, Fe}$) and lithium diffusion in Li_xFePO_4 ," *Physical Review B*, vol. 84, p. 174403, 2011.
6. P. J. Brown, J. B. Forsyth, and F. Tasset, "Studies of magneto-electric crystals using spherical neutron polarimetry," *Solid State Sciences*, vol. 7, no. 6, pp. 682 – 689, 2005.
7. M. Janoschek, S. Klimko, R. Gahler, B. Roessli, and P. Boni, "Spherical neutron polarimetry with MuPAD," *Physica B: Condensed Matter*, vol. 397, pp. 125 –130, 2007.
8. L. Ungur, W. Van den Heuvel, and L. F. Chibotaru, "Ab initio investigation of the non-collinear magnetic structure and the lowest magnetic excitations in dysprosium triangles," *New Journal of Chemistry*, vol. 33, pp. 1224–1230, 2009.
9. S. K. Langley, B. Moubaraki, C. M. Forsyth, I. A. Gass, and K. S. Murray, "Structure and magnetism of new lanthanide 6-wheel compounds utilizing triethanolamine as a stabilizing ligand," *Dalton Transactions*, vol. 39, pp. 1705–1708, 2010.

Complex Electronic Materials

Filip Ronning, Eric Bauer, Marc Janoschek, John Joyce, Roman Movshovich, Priscila Rosa, Joe Thompson (Los Alamos National Lab)

Program Scope

Complex and collective states that emerge in strongly correlated electron materials pose significant scientific challenges, solutions to which define the frontier of science and enable the energy and defense security of the nation. Research in this project focuses on developing a fundamental understanding of complex electronic materials, with strongly correlated *f*-electron systems serving as prototypes of classes of problems found broadly in *d*- and *f*-electron materials. Slight changes in sample composition, temperature, pressure or magnetic field tune the delicate balance among competing interactions and induce transitions between states of matter. These complex behaviors are most pronounced near magnetic/non-magnetic and metal/insulator boundaries and become particularly poorly understood as these boundaries are tuned to absolute zero temperature, i.e., to a quantum-critical point. A successful program of discovering new physics through new materials requires integration of materials preparation, preferably as single crystals, with complementary programs of materials characterization and in-depth investigations leading to microscopic understanding for which new techniques are developed as necessary. A broad suite of tools, ranging from structural, thermodynamic, magnetic, and transport measurements to spin and charge spectroscopies, in most cases at extremes of temperature (to 20 mK), pressure (to 3 GPa) and field (to 100 T), and aided by theoretical calculations, is employed to discover and understand new science that emerges on multiple length and time scales. Our pursuit of new science in complex electronic materials makes extensive use of DOE national facilities and special facilities at Los Alamos and is leveraged through an extensive network of collaborators.

Recent Progress

CeRhIn₅ is an antiferromagnet at 4 K. With the application of pressure, CeRhIn₅ can be tuned to a so-called “unconventional” quantum-critical point (QCP) where the *f*-electron becomes delocalized at the same pressure where the magnetic order parameter is tuned to zero and gives rise to a dome of superconductivity. Our thermopower measurements show that the *f*-electron localization/delocalization boundary and the magnetic QCP are separated in Ir-doped CeRhIn₅ [1]. This is possibly a consequence of reduced magnetic frustration, which we have found to be surprisingly strong in this family. By measuring the spin-wave dispersion in CeRhIn₅ we determined the magnetic exchange interactions in the parent compound CeRhIn₅ (see Fig. 1) [2]. However, these interactions fail to reproduce the magnetic field (H-T) phase diagram. Our

theory collaborators suggested that a field-induced anisotropy is required to generate the observed phase diagram, and we have confirmed this prediction with neutron-scattering measurements in magnetic fields up to 9 T [3]. The presence of a temperature-dependent ordering wavevector in applied magnetic fields is similar to the ANNNI model that is well-known to the frustrated magnetism community. At even higher magnetic fields of ~ 30 T, a field-induced Fermi-surface transformation takes place in CeRhIn_5 [4]. At similar fields, the system undergoes a density-wave instability [5] that also breaks C4 symmetry akin to what is found in the nematic phase in $\text{Sr}_3\text{Ru}_2\text{O}_7$. Large magnetic fields, among other effects, modify crystal fields and hence the orbital component of the $4f$ wavefunctions. In CeIn_3 , the structural building block of CeRhIn_5 , we have shown that this change modifies the magnetic exchange interaction away from a simple spherically symmetric interaction [6]. This has relevance also for CeRhIn_5 at ambient pressure, where we showed in collaboration with Andrea Severing that the ground state of CeMIn_5 ($M=\text{Co}, \text{Rh}, \text{Ir}$) is correlated with the orbital character of the $4f$ crystal field [7].

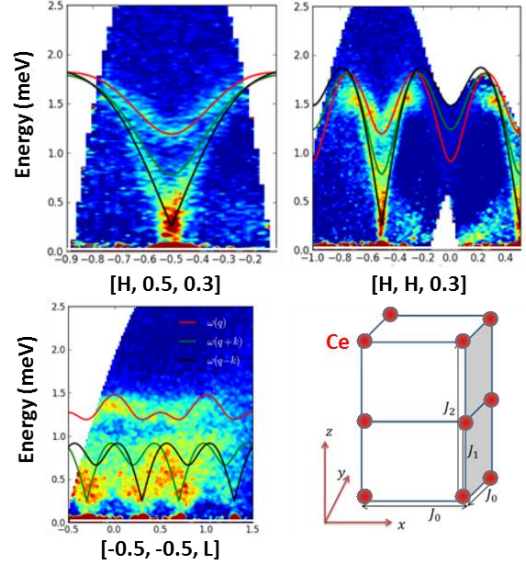


Fig. 1 Images show the spin-wave dispersion of CeRhIn_5 taken along three momentum directions. Solid curves are model fits that capture the three dispersing branches. The lower right figure illustrates exchange paths of the model that reproduce the data.

Plutonium is a strongly correlated metal as we have demonstrated through inelastic neutron-scattering measurements that revealed the presence of valence fluctuations [8]. Such fluctuations also appear to be present in PuCoGa_5 , in which we have used resonant ultrasound spectroscopy to discover an anomalous softening of its bulk modulus that is associated with the presence of superconductivity and suggesting that superconductivity is mediated by valence fluctuations [9]. The $5f$ elements provide an instructive bridge between the physics of $4f$'s and the $3d$'s. In general, relatively strong hybridization in $3d$ metals is expected to quench the Kondo physics. However, in dilute concentrations of Fe doped SrNi_2As_2 we discovered an orbitally selective single-ion Kondo effect that is caused by anomalously weak hybridization of the Fe $d_{x^2-y^2}$ orbitals [10]. In our search for new physics, we also have discovered a new class of layered intermetallics: CeMA_4X_2 and $\text{Ce}_2\text{MA}_7\text{X}_4$ (where M = transition metal, and X = Ga, Si) [11]. These new systems have strongly quasi 2-dimensional electronic structures and large effective masses in the ordered state. Finally, separate work on CeNi_2As_2 has revealed that a low carrier density may be a new route to discovering unconventional QCPs [12].

Future Plans

Our approach to revealing and understanding complex and collective states of strongly correlated materials in the next three years takes a multipronged approach, building on the

success and insights provided by our past work. Our neutron measurements quantitatively determined the magnetic exchange interactions in CeRhIn₅ but also revealed the presence of an unexplained spin gap, which may provide insight into the interplay between Kondo and RKKY interactions. We will investigate the Kondo scale in CeRhIn₅ and related compounds. As these systems approach the quantum-critical point, we will use thermopower as well as measurements of the Gruneisen ratio to determine how magnetic frustration leads to differences in the nature of quantum criticality. Additionally, with large applied magnetic fields, we have opened a new window into investigating the competing interactions in the CeRhIn₅ family of materials, and we will explore the effects of dimensionality and crystal fields on this interesting new physics.

In our search for new physics, we will expand our phase space. Importantly, we will explore dimensionality through the synthesis of heavy-fermion thin films, the effects of non-collinear spin textures in rare-earth systems, and the relation to 3d transition-metal systems in intermetallic compounds such as ThCo₂Sn₂ [13]. Additionally, we will investigate the interplay of topology and strong correlations, which will provide new and interesting boundaries with novel properties between systems with different topologies. Our prior work on SmB₆ revealed a heavy-surface state in contradiction to ARPES and dHvA results [14]. We will investigate this further by studying the 5f analog PuB₆, which has larger energy scales relative to SmB₆. We will utilize the high magnetic fields available at Los Alamos to induce correlations in otherwise uncorrelated topological materials. Finally, we will extend our measurement capabilities in extreme environments. For example, with the small energy scales in 4f materials, uniaxial strain devices will be an efficient symmetry-breaking tuning capability that can be utilized with numerous probes, ranging from transport to NMR and neutron scattering.

References

- [1] Y. Luo, X. Lu, A.P. Dioguardi, P.F.S. Rosa, E.D. Bauer, Q. Si, and J.D. Thompson, "Quantum criticality in CeRh_{0.58}Ir_{0.42}In₅: Kondo-breakdown and spin-density critical points," Submitted to *Phys. Rev. Lett.*; ArXiv:1606.07848
- [2] P. Das, S.-Z. Lin, N.J. Ghimire, K. Huang, F. Ronning, E.D. Bauer, J.D. Thompson, C.D. Batista, G. Ehlers, and M. Janoschek, "The magnitude of the magnetic exchange interaction in the heavy fermion antiferromagnet CeRhIn₅," *Phys. Rev. Lett.* **113**, 246403 (2014).
- [3] D. Fobes, et al., unpublished.
- [4] L. Jiao, Y. Chen, Y. Kohama, D. Graf, E.D. Bauer, J. Singleton, J.-X. Zhu, Z. Weng, G. Pang, T. Shang, J. Zhang, H.-O. Lee, T. Park, M. Jaime, J.D. Thompson, F. Steglich, Q. Si, and H.Q. Yuan, "Fermi surface reconstruction and multiple quantum phase transitions in the antiferromagnet CeRhIn₅," *Proc. Nat. Acad. Sci.* **112**, 673 (2015).

- [5] P.J.W. Moll, B. Zeng, L. Balicas, S. Galeski, F.F. Balakirev, E.D. Bauer, and F. Ronning, “Field induced density wave in the heavy fermion compound CeRhIn₅,” *Nature Comm.* **6**, 6663 (2015); P.J.W. Moll, et al., unpublished
- [6] P.J.W. Moll, et al., unpublished
- [7] T. Willers, F. Strigari, Z. Hu, V. Sessi, N. B. Brookes, E. D. Bauer, J. L. Sarrao, J. D. Thompson, A. Tanaka, S. Wirth, L. H. Tjeng, and A. Severing, “Correlation between ground state and orbital anisotropy in heavy fermion materials,” *Proc. Nat. Acad. Sci.* **112**, 2384 (2015).
- [8] M. Janoschek, Pinaki Das, B. Chakrabarti, D. L. Abernathy, M. D. Lumsden, J. M. Lawrence, J. D. Thompson, G. H. Lander, J. N. Mitchell, S. Richmond, M. Ramos, F. Trouw, J.-X. Zhu, K. Haule, G. Kotliar, E. D. Bauer, “The valence-fluctuating ground state of plutonium,” *Science Advances* **1**, e1500188 (2015).
- [9] B. J. Ramshaw, A. Shekhter, R. D. McDonald, J. B. Betts, J. N. Mitchell, P. H. Tobash, C. H. Mielke, E. D. Bauer, and A. Migliori, “Avoided valence transition in a plutonium superconductor,” *Proc. Nat. Acad. Sci.* **112**, 3285 (2015).
- [10] N. Wakeham, Ni Ni, J.-X. Zhu, E.D. Bauer, J.D. Thompson, and F. Ronning, “Observation of an orbitally selective Kondo effect.,” submitted to *Nat. Comm.*
- [11] N. J. Ghimire, F. Ronning, D. Williams, B.L. Scott, Y. Luo, J.D. Thompson, and E.D. Bauer, “Investigation of the physical properties of the tetragonal CeMAI₄Si₂ (M = Rh, Ir, Pt) compounds,” *J. Phys.: Condens. Matter*, **27**, 025601 (2015); N. J. Ghimire, S.K. Cary, S. Eley, N. Wakeham, P.F.S. Rosa, T. Albrecht-Schmitt, Y. Lee, M. Janoschek, C.M. Brown, L. Civale, J.D. Thompson, F. Ronning, and E.D. Bauer, “Investigation of the physical properties of the Ce₂MAI₇Ge₄ (M = Co, Ir, Ni, Pd) heavy fermion compounds” *Phys. Rev. B*, **93**, 205141 (2016); N. J. Ghimire, S. Calder, M. Janoschek, and E. D. Bauer, “Magnetic structure of the antiferromagnetic Kondo lattice compounds CeRhAl₄Si₂ and CeIrAl₄Si₂,” *J. Phys.: Condens. Matter* **27**, 245603 (2015); H. Sakai, T. Hattori, Y. Tokunaga, S. Kambe, N.J. Ghimire, F. Ronning, E.D. Bauer, and J.D. Thompson, “Incommensurate to commensurate antiferromagnetism in CeRhAl₄Si₂: An ²⁷Al NMR Study” *Phys. Rev. B*, **93**, 014402 (2016)
- [12] Y. Luo, F. Ronning, N. Wakeham, X. Lu, T. Park, Zhu-an Xu, and J. D. Thompson, “Pressure- and field-tuned quantum criticality in the antiferromagnetic Kondo semi-metal CeNi₂As₂,” *Proc. Nat. Acad. Sci.* **112**, 13520 (2015).
- [13] P.F.S. Rosa, T.M Garitezi, Z. Fisk and P.G. Pagliuso, “3d magnetism in ThCo₂Sn₂ single crystals,” *J. Phys. Conf. Ser.* **592**, 012053 (2015).
- [14] Y. Luo, H. Chen, J. Dai, Z. A. Xu and J. D. Thompson, “Heavy surface state in a possible topological Kondo insulator: magneto-thermoelectric transport on the [011]-plane of SmB₆,” *Phys. Rev. B* **91**, 075130 (2015).

Publications

Put the 2-year list of publications SUPPORTED BY BES here using this font (Times New Roman 12 pt)

(Led by this FWP)

Y. Luo, F. Ronning, N. Wakeham, X. Lu, T. Park, Zhu-an Xu, and J. D. Thompson, "Pressure- and field-tuned quantum criticality in the antiferromagnetic Kondo semi-metal CeNi_2As_2 ," *Proc. Nat. Acad. Sci.* **112**, 13520 (2015).

L. Jiao, Y. Chen, Y. Kohama, D. Graf, E.D. Bauer, J. Singleton, J.-X. Zhu, Z. Weng, G. Pang, T. Shang, J. Zhang, H.-O. Lee, T. Park, M. Jaime, J.D. Thompson, F. Steglich, Q. Si, and H.Q. Yuan, "Fermi surface reconstruction and multiple quantum phase transitions in the antiferromagnet CeRhIn_5 ," *Proc. Nat. Acad. Sci.* **112**, 673 (2015).

B. J. Ramshaw, A. Shekhter, R. D. McDonald, J. B. Betts, J. N. Mitchell, P. H. Tobash, C. H. Mielke, E. D. Bauer, and A. Migliori, "Avoided valence transition in a plutonium superconductor," *Proc. Nat. Acad. Sci.* **112**, 3285 (2015).

T. Willers, F. Strigari, Z. Hu, V. Sessi, N. B. Brookes, E. D. Bauer, J. L. Sarrao, J. D. Thompson, A. Tanaka, S. Wirth, L. H. Tjeng, and A. Severing, "Correlation between ground state and orbital anisotropy in heavy fermion materials," *Proc. Nat. Acad. Sci.* **112**, 2384 (2015).

H. H. Kung, R. E. Baumbach, E. D. Bauer, V. K. Thorsmølle, W. L. Zhang, K. Haule, J. A. Mydosh, and G. Blumberg, "Chirality density wave of the 'hidden order' phase in URu_2Si_2 ," *Science* **347**, 1339 (2015).

P.J.W. Moll, A. Potter, N. Nair, B. Ramshaw, K. Modic, S. Riggs, B. Zeng, N. Ghimire, E.D. Bauer, R. Kealhofer, F. Ronning, and J. Analytis, "Magnetic torque anomaly in the quantum limit of Weyl semi-metals," *Nat. Comm.* **7**, 12492 (2016).

S. Seo, E. Park, E. D. Bauer, F. Ronning, J. N. Kim, J.-H. Shim, J. D. Thompson, and T. Park, "Controlling superconductivity by tunable quantum critical points," *Nature Comm.* **6**, 6433 (2015).

S. C. Riggs, M.C. Shapiro, A. V. Maharaj, S. Raghu, E. D. Bauer, R. E. Baumbach, P. Giraldo-Gallo, M. Wartenbe, and I. R. Fisher, "Evidence for a nematic component to the hidden-order parameter in URu_2Si_2 from differential elastoresistance measurements," *Nature Comm.* **6**, 6425 (2015).

P.J.W. Moll, B. Zeng, L. Balicas, S. Galeski, F.F. Balakirev, E.D. Bauer, and F. Ronning, "Field induced density wave in the heavy fermion compound CeRhIn_5 ," *Nature Comm.* **6**, 6663 (2015).

P. S. Riseborough and J. M. Lawrence, “Mixed valent metals,” *Rep. Prog. Phys.* **79**, 084501 (2016)

D.Y. Kim, S.-Z. Lin, F. Weickert, M. Kenzelmann, E.D. Bauer, F. Ronning, J.D. Thompson and R. Movshovich, “Intertwined orders in heavy-fermion superconductor CeCoIn₅” *Accepted in Phys. Rev. X*; ArXiv:1606.05015

Y. Luo, X. Lu, A.P. Dioguardi, P.F.S. Rosa, E.D. Bauer, Q. Si, and J.D. Thompson, “Quantum criticality in CeRh_{0.58}Ir_{0.42}In₅: Kondo-breakdown and spin-density critical points” Submitted to *Phys. Rev. Lett.*; ArXiv:1606.07848

P. Das, S.-Z. Lin, N.J. Ghimire, K. Huang, F. Ronning, E.D. Bauer, J.D. Thompson, C.D. Batista, G. Ehlers, and M. Janoschek, “The magnitude of the magnetic exchange interaction in the heavy fermion antiferromagnet CeRhIn₅,” *Phys. Rev. Lett.* **113**, 246403 (2014).

Y. Chen, W.B. Jiang, C.Y. Guo, F. Ronning, E.D. Bauer, T. Park, H.Q. Yuan, Z. Fisk, J.D. Thompson, and Xin Lu, “Reemergent superconductivity and avoided quantum criticality in Cd-doped CeIrIn₅ under pressure,” *Phys. Rev. Lett.* **114**, 146403 (2015).

A.M. Mounce, H. Yasuoka, G. Koutroulakis, N. Ni, E.D. Bauer, F. Ronning, and J.D. Thompson, “Evidence for spin-triplet superconductivity in U₂PtC₂ from ¹⁹⁵Pt NMR,” *Phys. Rev. Lett.* **114**, 127001 (2015).

G. Koutroulakis, H. Yasuoka, P. H. Tobash, J. N. Mitchell, E. D. Bauer, and J. D. Thompson, “Extended nuclear quadrupole resonance study of the heavy-fermion superconductor PuCoGa₅,” *Phys. Rev. B*, **94**, 165115 (2016)

K. Chen, F. Strigari, M. Sundermann, S. Agrestini, N. J. Ghimire, S.-Z. Lin, C. D. Batista, E. D. Bauer, J. D. Thompson, E. Otero, A. Tanaka and A. Severing, “Exchange field effect in the crystal-field ground state of CeMAl₄Si₂,” *Phys. Rev. B* **94**, 115111 (2016).

P. F. S. Rosa, A. Oostra, J. D. Thompson, P. G. Pagliuso, and Z. Fisk, “Unusual Kondo-hole effect and crystal-field frustration in Nd-doped CeRhIn₅,” *Phys. Rev. B* **94**, 045101 (2016).

R. Y. Chen, S.J. Zhang, E.D. Bauer, J.D. Thompson, and N.L. Wang, “Optical spectroscopy and ultrafast pump-probe studies on the heavy fermion compound CePt₂In₇,” *Phys. Rev. B* **94**, 035161 (2016).

N. Wakeham, E.D. Bauer, M. Neupane, and F. Ronning, “Large magnetoresistance in the antiferromagnetic semi-metal NdSb,” *Phys. Rev. B* **93**, 205152 (2016).

Y. Luo, P.F.S. Rosa, E.D. Bauer, and J.D. Thompson, “Vortexlike excitations in the heavy-fermion superconductor CeIrIn₅,” *Phys. Rev. B* **93**, 201102(R) (2016).

- C. H. Booth, S. A. Medling, J.G. Tobin, R.E. Baumbach, E.D. Bauer, D. Sokaras, D. Nordlund, and T.-C. Weng, “Probing 5f-state configurations in URu₂Si₂ with U LIII-edge resonant x-ray emission spectroscopy,” *Phys. Rev. B* **94**, 045121 (2016) (Editor’s suggestion)
- N. J. Ghimire, S.K. Cary, S. Eley, N. Wakeham, P.F.S. Rosa, T. Albrecht-Schmitt, Y. Lee, M. Janoschek, C.M. Brown, L. Civale, J.D. Thompson, F. Ronning, and E.D. Bauer, “Investigation of the physical properties of the Ce₂MAI₇Ge₄ (M = Co, Ir, Ni, Pd) heavy fermion compounds,” *Phys. Rev. B* **93**, 205141 (2016).
- H. Sakai, T. Hattori, Y. Tokunaga, S. Kambe, N.J. Ghimire, F. Ronning, E.D. Bauer, and J.D. Thompson, “Incommensurate to commensurate antiferromagnetism in CeRhAl₄Si₂: an ²⁷Al NMR study” *Phys. Rev. B* **93**, 014402 (2016).
- Y. Luo, N. J. Ghimire, M. Wartenbe, H. Choi, M. Neupane, R. D. McDonald, E. D. Bauer, J.-X. Zhu, J. D. Thompson, and F. Ronning, “Electron-hole compensation effect between topologically trivial electrons and non-trivial holes in NbAs,” *Phys. Rev. B* **92**, 205134 (2015).
- M. Janoschek, D. Haskel, J. Fernandez-Rodriguez, M. van Veenendaal, J. Rebizant, G.H. Lander, J.X. Zhu, J.D. Thompson, and E.D. Bauer, “Ground-state wave function of plutonium in PuSb as determined via x-ray magnetic circular dichroism,” *Phys. Rev. B* **91**, 035117 (2015).
- N. Wakeham, Ni Ni, E.D. Bauer, J.D. Thompson, E. Tegtmeier, and F. Ronning, “Magnetism and superconductivity in U₂Pt_xRh_{1-x}C₂,” *Phys. Rev. B* **91**, 024408 (2015).
- P. Das, N. Kanchanavatee, J. S. Helton, K. Huang, R. E. Baumbach, E. D. Bauer, B. D. White, V. W. Burnett, M. B. Maple, J. W. Lynn, and M. Janoschek, “Chemical pressure tuning of URu₂Si₂ via isoelectronic substitution of Ru with Fe,” *Phys. Rev. B* **91**, 085122 (2015).
- Y. Luo, H. Chen, J. Dai, Z. A. Xu and J. D. Thompson, “Heavy surface state in a possible topological Kondo insulator: magneto-thermoelectric transport on the [011]-plane of SmB₆,” *Phys. Rev. B* **91**, 075130 (2015).
- E.R. Schemm, R.E. Baumbach, P.H. Tobash, F. Ronning, E.D. Bauer, and A. Kapitulnik, “Evidence for broken time-reversal symmetry in the superconducting phase of URu₂Si₂,” *Phys. Rev. B* **91**, 140506(R) (2015).
- R.E. Baumbach, A. Gallagher, T. Besara, J. Sun, T. Siegrist, D.J. Singh, J.D. Thompson, F. Ronning, and E.D. Bauer, “Complex magnetism and strong electronic correlations in Ce₂PdGe₃,” *Phys. Rev. B* **91**, 035102 (2015).
- H. Sakai, F. Ronning, J.-X. Zhu, N. Wakeham, H. Yasuoka, Y. Tokunaga, S. Kambe, E. D. Bauer, and J. D. Thompson, “Microscopic investigation of electronic inhomogeneity induced by substitutions in a quantum critical metal CeCoIn₅,” *Phys. Rev. B* **92**, 121105(R) (2015).

M. Neupane, M.M. Hosen, I. Belopolski, N. Wakeham, K. Dimitri, N. Dhakal, J.-X. Zhu, M.Z. Hasan, E.D. Bauer, and F. Ronning, "Observation of a Dirac-like semi-metallic phase in NdSb," *J. Phys.: Condens Matter* **28**, 23LT02 (2016).

Y. Luo, N. Ghimire, E.D. Bauer, J.D. Thompson, and F. Ronning, "'Hard" crystalline lattice in the Weyl semimetal NbAs," *J. Phys.: Condens Matter* **28**, 055502 (2016).

C.H. Wang, L. Poudel, A.E. Taylor, J.M. Lawrence, A.D. Christianson, S. Chang, J.A. Rodriguez-Rivera, J.W. Lynn, A.A. Podlesnyak, G. Ehlers, R.E. Baumbach, E.D. Bauer, K. Gofryk, F. Ronning, K.J. McClellan, and J.D. Thompson, "Quantum critical fluctuations in the heavy fermion compound $\text{Ce}(\text{Ni}_{0.935}\text{Pd}_{0.065})_2\text{Ge}_2$," *J. Phys.: Condens. Matter*, **27**, 015602 (2015).

N. Ghimire, F. Ronning, D. Williams, B.L. Scott, Y. Luo, J.D. Thompson, and E.D. Bauer, "Investigation of the physical properties of the tetragonal $\text{CeMAl}_4\text{Si}_2$ (M = Rh, Ir, Pt) compounds," *J. Phys.: Condens. Matter*, **27**, 025601 (2015). Highlighted on Cover.

N.J. Ghimire, Y. Luo, M. Neupane, D. Williams, E.D. Bauer, and F. Ronning, "Magnetotransport of single crystalline NbAs," *J. Phys.: Condens. Matter* **27**, 152201 (2015).

N. J. Ghimire, S. Calder, M. Janoschek, and E. D. Bauer, "Magnetic structure of the antiferromagnetic Kondo lattice compounds $\text{CeRhAl}_4\text{Si}_2$ and $\text{CeIrAl}_4\text{Si}_2$," *J. Phys.: Condens. Matter* **27**, 245603 (2015).

M. Kang, N. Wakeham, N. Ni, E.D. Bauer, J.H. Kim, and F. Ronning, "Thermal and transport properties of $\text{U}_2\text{Pt}_{1-x}\text{Ir}_x\text{C}_2$," *J. Phys.: Condens. Matter* **27**, 365702 (2015). Highlighted on cover.

Y. Luo, H. Li, Y. M. Dai, H. Miao, Y. G. Shi, H. Ding, A. J. Taylor, D. A. Yarotski, R. P. Prasankumar and J. D. Thompson "Hall effect in the extremely large magnetoresistance semimetal WTe_2 " *Appl. Phys. Lett.* **107**, 182411 (2015)

J.L. Sarrao, F. Ronning, E.D. Bauer, C.D. Batista, J.-X. Zhu, and J.D. Thompson, "Building blocks for correlated superconductors and magnets," *APL Materials* **3**, 041512 (2015). (invited)

E.D. Bauer and J.D. Thompson, "Plutonium-based heavy-fermion systems," *Ann. Rev. Condensed Matt. Phys.* **6**, 137 (2015). (invited)

Y. Luo, R.D. McDonald, P.F.S Rosa, B.L. Scott, N. Wakeham, N.J. Ghimire, E.D. Bauer, J.D. Thompson, and F. Ronning, "Anomalous electronic structure and magnetoresistance in TaAs_2 ," *Scientific Reports* **6**, 27294 (2016).

J. D. Thompson, "SCES2016 Summary: experiment", *Phil. Mag.* DOI: 10.1080/14786435.2016.1216196 (invited)

T. Durakiewicz, "Photoemission investigations of URu_2Si_2 ," *Phil. Mag.* **94**, 3723 (2014). (invited)

J. L. Sarrao, E. D. Bauer, J. N. Mitchell, P. H. Tobash, and J. D. Thompson, “Superconductivity in plutonium compounds,” *Physica C* **514**, 184 (2015). (invited)

B. D. White, J. D. Thompson and M. B. Maple, “Unconventional superconductivity in heavy-fermion compounds,” *Physica C* **514**, 246 (2015). (invited)

W. Lee, K.-Y. Choi, S. Yoon, B. J. Suh, Z. Jang, P. K. Biswas, R. E. Baumbach, and E. D. Bauer, “Anomalous local magnetism in the 4f-localized ferromagnets CeRu₂X₂B (X = Al, Ga) revealed by using ZF- μ SR,” *J. Korean Phys. Soc.* **68**, 1200 (2016).

F. Ronning and J.-X. Zhu, “Electronic structure of U₂PtC₂ and U₂RhC₂,” *J. of Phys.: Conf. Series* **592**, 012037 (2015).

Collaborator-driven publications

A. Gyenis, E. H. da Silva Neto, R. Sutarto, E. Schierle, F. He, E. Weschke, M. Kawai, R. E. Baumbach, J. D. Thompson, E. D. Bauer, Z. Fisk, A. Damascelli, A. Yazdani, and P. Aynajian, “Quasiparticle interference of heavy fermions in resonant elastic x-ray scattering,” *Science Advances* **2**, e1601086 (2016).

M. Janoschek, Pinaki Das, B. Chakrabarti, D. L. Abernathy, M. D. Lumsden, J. M. Lawrence, J. D. Thompson, G. H. Lander, J. N. Mitchell, S. Richmond, M. Ramos, F. Trouw, J.-X. Zhu, K. Haule, G. Kotliar, E. D. Bauer, “The valence-fluctuating ground state of plutonium,” *Science Advances* **1**, e1500188 (2015).

X. Lü, A. Chen, Y. Luo, P. Lu, Y. Dai, E. Enriquez, P. Dowden, H. Xu, P.G. Kotula, A.K. Azad, D.A. Yarotski, R.P. Prasankumar, A.J. Taylor, J.D. Thompson, and Q. Jia, “Conducting interface in titania homojunction: origin of superior properties in black TiO₂,” *Nano Lett.* **16**, 5751 (2016)

Y. Zhou, Q. Wu, P.F.S. Rosa, R. Yu, J. Guo, W. Yi, S. Zhang, Z. Wang, H. Wang, S. Cai, K. Yang, A. Li, Z. Jiang, S. Zhang, X. Wei, Y. Huang, Y.-F. Yang, Z. Fisk, Q. Si, L. Sun and Z. Zhao “Quantum phase transition and destruction of Kondo effect in pressurized SmB₆,”
Submitted to Nat. Phys. Arxiv:1603.05607

Madhab Neupane, Su-Yang Xu, Nasser Alidoust, Guang Bian, D. J. Kim, Chang Liu, I. Belopolski, T.-R. Chang, H.-T. Jeng, T. Durakiewicz, H. Lin, A. Bansil, Z. Fisk, and M. Z. Hasan, “Non-Kondo-like electronic structure in the correlated rare-earth hexaboride YbB₆,” *Phys. Rev. Lett.* **114**, 016403 (2015).

M. Falmbigl, D. Putzky, J. Ditto, M. Esters, S.R. Bauers, F. Ronning, and D. C. Johnson, “Influence of defects on the charge density wave of ([SnSe]_{1+ δ})₁(VSe₂)₁ ferecrystals,” *ACS Nano* **9**, 8440 (2015).

N. Wakeham, P.F.S. Rosa, Y.Q. Wang, M. Kang, Z. Fisk, F. Ronning, and J.D. Thompson, "Investigation of the low temperature conducting state in two candidate topological Kondo insulators, SmB_6 and $\text{Ce}_3\text{Bi}_4\text{Pt}_3$," *Phys. Rev. B* **94**, 035127 (2016); Editor's suggestion.

N. J. Laurita, C. M. Morris, S. M. Koohpayeh, P. F. S. Rosa, W. A. Phelan, Z. Fisk, T. M. McQueen, and N. P. Armitage, "Anomalous 3D bulk AC conduction within the Kondo gap of SmB_6 single crystals," *Phys. Rev. B*, **94**, 165154 (2016)

J. Stankiewicz, P. F. S. Rosa, P. Schlottmann, and Z. Fisk. "Electrical transport properties of single-crystal CaB_6 , SrB_6 , and BaB_6 ," *Phys. Rev. B*, **94**, 125141 (2016).

P.F.S. Rosa, Y. Luo, E.D. Bauer, J.D. Thompson, P.G. Pagliuso, and Z. Fisk, "Ferromagnetic Kondo behavior in UAuBi_2 single crystals," *Phys. Rev. B* **92**, 104425 (2015).

N. Wakeham, Y. Wang, Z. Fisk, F. Ronning, and J. D. Thompson, "Surface state reconstruction in ion-damaged SmB_6 ," *Phys. Rev. B* **91**, 085107 (2015).

T. Shang, Y. H. Chen, F. Ronning, N. Cornell, J. D. Thompson, A. Zakhidov, M.B. Salamon, and H.Q. Yuan, "Magnetocrystalline anisotropic effect in $\text{GdCo}_{1-x}\text{Fe}_x\text{AsO}$ ($x = 0; 0:05$)," *Phys. Rev. B* **91**, 125106 (2015).

Y. Luo, H.-F. Zhai, P. Zhang, Z.-A. Xu, G.-H. Cao, and J. D. Thompson, "Pressure-enhanced superconductivity in $\text{Eu}_3\text{Bi}_2\text{S}_4\text{F}_4$," *Phys. Rev. B* **90**, 220510(R) (2014).

M. W. Butchers, J. A. Duffy, J. W. Taylor, S. R. Giblin, S. B. Dugdale, C. Stock, P. H. Tobash, E. D. Bauer, and C. Paulsen, "Determination of spin and orbital magnetization in the ferromagnetic superconductor UCoGe ," *Phys. Rev. B* **92**, 121107 (R) (2015).

D. S. Parker, N. Ghimire, J. Singleton, J. D. Thompson, E. D. Bauer, R. Baumbach, D. Mandrus, L. Li and D. J. Singh, "Magnetocrystalline anisotropy in UMn_2Ge_2 and related Mn-based actinide ferromagnets," *Phys. Rev. B* **91**, 174401 (2015).

A.A. Aczel, L. Li, V.O. Garlea, J.-Q. Yan, F. Weickert, V.S. Zapf, R. Movshovich, M. Jaime, P.J. Baker, V. Keppens, and D. Mandrus, "Spin-liquid ground state in the frustrated J_1 - J_2 zigzag chain system BaTb_2O_4 ," *Phys. Rev. B* **92**, 041110 (2015).

A.A. Aczel, L. Li, V.O. Garlea, J.-Q. Yan, F. Weickert, M. Jaime, B. Maiorov, R. Movshovich, L. Civale, V. Keppens, and D. Mandrus, "Magnetic ordering in the frustrated J_1 - J_2 Ising chain candidate BaNd_2O_4 ," *Phys. Rev. B* **90**, 134403 (2014).

A. M. Mounce, H. Yasuoka, G. Koutroulakis, J. A. Lee, H. Cho, F. Gendron, E. Zurek, B. L. Scott, J. A. Trujillo, A. K. Slemmons, J. N. Cross, J. D. Thompson, S. A. Kozimor, E. D. Bauer, J. Autschbach, and D. L. Clark, "Nuclear magnetic resonance measurements and electronic structure of Pu(IV) in $[(\text{Me})_4\text{N}]_2\text{PuCl}_6$," *Inorg. Chem.* **55**, 8371 (2016).

- R. S. Kumar, A. Svane, G. Vaitheeswaran, V. Kanchana, D. Antonio, A. L. Cornelius, E. D. Bauer, Y. Xiao, and P. Chow, “Effect of pressure on valence and structural properties of YbFe₂Ge₂ heavy fermion compound—A combined inelastic X-ray spectroscopy, X-ray diffraction, and theoretical investigation,” *Inorg. Chem.* **54**, 10250 (2015).
- S. Conradson, S.M. Gilbertson, S. Daifuku, J. Kehl, T. Durakiewicz, D. Andersson, A. Bishop, D. Byler, P. Oppeneer, J. Valdez, M. Neidig, and G. Rodriguez, “Possible demonstration of a polaronic Bose-Einstein(-Mott) condensate in UO_{2(+x)} by ultrafast THz spectroscopy and microwave dissipation,” *Scientific Reports* **5**, 15278 (2015).
- F. Nasreen, D. Antonio, D. VanGennep, C. H. Booth, K. Kothapalli, E. D. Bauer, J. L. Sarrao, B. Lavina, V. Iota-Herbei, S. Sinogeikin, P. Chow, Y. Xiao, Y. Zhao, and A. L. Cornelius, “High pressure effects on U L₃ x-ray absorption in partial fluorescence yield mode and single crystal x-ray diffraction in the heavy fermion compound UCd₁₁,” *J. Phys.: Condens. Matter* **28**, 105601 (2016).
- M.J. Winiarski, B. Wiendlocha, S. Gołąb, S. K. Kushwaha, P. Wisniewski, D. Kaczorowski, J. D. Thompson, R. J. Cava, and T. Klimczuk, “Superconductivity in CaBi₂,” *Phys. Chem. Chem. Phys.* **18**, 21737 (2016).
- N. Wakeham, J. Wen, Y.Q. Wang, Z. Fisk, F. Ronning, and J.D. Thompson, “The effect of magnetic and non-magnetic ion damage on the surface state in SmB₆,” *J. Mag. Mag. Mater* **400**, 62 (2016).
- N. Haberkorn, J. Kim, K. Gofryk, F. Ronning, A.S. Sefat, W. Ulrich, L. Fang, W.K. Kwok, and L. Civale, “Enhancement of the critical current density by increasing the collective pinning energy in heavy ion irradiated Co-doped BaFe₂As₂ single crystals,” *Supercond. Sci. Techn.* **28**, 055011 (2015).
- J. Kim, N. Haberkorn, E. Nazaretski, R. de Paula, T. Tan, X.X. Xi, T. Tajima, R. Movshovich, L. Civale, “Strong magnetic field dependence of critical current densities and vortex activation energies in an anisotropic clean MgB₂ thin film”, *Solid State Comm.* **204**, 56 (2015).
- J. Kim, N. Haberkorn, K. Gofryk, M. J. Graf, F. Ronning, A. S. Sefat, R. Movshovich, and L. Civale, “Superconducting properties in heavily overdoped Ba(Fe_{0.86}Co_{0.14})₂As₂ single crystals,” *Solid State Comm.* **201**, 20 (2015).
- P. Söderlind, A. Landa, J. G. Tobin, P. Allen, S. Medling, C. H. Booth, E. D. Bauer, J. C. Cooley, D. Sokaras, T.-C. Weng, and D. Nordlund, “On the valence fluctuation in the early actinide metals,” *J. Electr. Spectr. Related Phenom.* **207**, 14 (2016).
- E. Park, X. Lu, F. Ronning, J. D. Thompson, Q. Zhang, L. Balicas and T. Park, “Spectroscopic evidence for two-gap superconductivity in the quasi-one dimensional chalcogenide Nb₂Pd_{0.81}S₅,” *submitted to Sci. Rep.*; ArXiv:1505.01258

- J. Strychalska, J. D. Thompson, R. J. Cava and T. Klimczuk, “Superconductivity and ferromagnetism in Pd-doped Y_9Co_7 ,”s *Intermetallics* **71**, 73 (2016).
- N. Kanchanavatee, M. Janoschek, K. Huang, B. D. White, P. S. Riseborough, A.V. Balatsky, and M. B. Maple, “Emergence of higher order rotational symmetry in the hidden order phase of URu_2Si_2 ,” *Phil. Mag.* DOI: 10.1080/14786435.2016.1235294 (2016)
- J. Strychalska, M. Roman, Z. Sobczak, B. Wiendlocha, M.J. Winiarski, F. Ronning, and T. Klimczuk, “Physical properties and electronic structure of La_3Co and La_3Ni intermetallic superconductors,” *Physica C* **528**, 73 (2016)
- O. Janka, T. Shang, R. E. Baumbach, E. D. Bauer, J. D. Thompson, and S. M. Kauzlarich, “Structure and magnetic properties of Ce-3(Ni/Al/Ga)(11)-a new phase with the La_3Al_{11} structure type,” *Crystals* **5**, 1 (2015).
- D. Lee, D.J. Williams, S.C. Vogel, Th. Proffen, J.D. Thompson, L.L. Daemen, and Sungkyun Park, “Tailoring structure and magnetic properties of $Ni_xCo_{1-x}(N(CN)_2)_2$ molecular magnets,” *Curr. Appl. Phys.* **16**, 1100 (2016)

Complex Electronic Materials: New Physics Through New Materials

Priscila Rosa and Eric Bauer (Los Alamos National Lab)

Program Scope

Quantum materials are a powerful avenue for the discovery and investigation of new states of matter. From high-temperature superconductors to topological insulators, promising applications arise from emergent phenomena that can only be explained by quantum mechanics. Despite the myriad of functionalities that emerge in different quantum materials, there is a strong correlation between crystal structure and physical properties. The search for new materials is crucial not only to further understand the relationship between structure and materials' properties, but also to discover new states of matter that may emerge from novel atomic arrangements. Consequently, crystal growth is a critical component of this FWP, both for discovering new materials with novel phenomena and for synthesizing high-quality samples for in-depth exploration.

Recent Progress

In our search for new physics through new materials, we discovered two new families of layered, tetragonal CeMAI_4X_2 and $\text{Ce}_2\text{MAI}_7\text{X}_4$ (where M = transition metal, and X = Si, Ge) compounds [1, 2]. Our neutron diffraction and NMR measurements reveal a complex magnetic field-temperature (H-T) phase diagram in the $\text{CeMAI}_4\text{Si}_2$ compounds [3, 4]. Three of the $\text{Ce}_2\text{MAI}_7\text{Ge}_4$ (M=Co, Ni, Ir) order magnetically below 2 K and have a large Sommerfeld specific heat coefficient below T_{mag} . These materials are predicted to have a 2D Fermi surface from density functional theory (DFT) calculations, in agreement with significant electronic anisotropy ($\rho_c / \rho_a \sim 10 - 20$) observed for $\text{Ce}_2\text{PdAl}_7\text{Ge}_4$. Similar to CeCoIn_5 , $\text{Ce}_2\text{PdAl}_7\text{Ge}_4$ appears to be close to a quantum critical point at ambient pressure [2].

It is well known that superconductivity tends to live in families. In the case of the Fe-based intermetallic compounds, layered tetragonal structures containing FeAs_4 planes is a common structural feature. One of our routes for the search of new materials comprises the synthesis of similar crystal structures that contain different transition metal elements. ThCo_2Sn_2 is an example of a novel Co-based tetragonal compound that can be grown in single crystalline form [5]. ThCo_2Sn_2 is also magnetic with a transition temperature of $T_N = 76$ K and applied pressure to 25 kbar suppresses the magnetic transition to about 50 K [5]. Higher hydrostatic pressures are key to reaching the magnetic/non-magnetic

boundary, and a modified Bridgman pressure cell is being developed to achieve this goal. CaCo_5As_3 is another example of Co-based material containing CoAs_4 tetrahedra with a magnetically ordered ground state ($T_N = 16$ K) [6]. CaCo_5As_3 , however, crystallizes in a novel three-dimensional orthorhombic structure that provides a unique platform for the study of magnetic frustration in correlated itinerant systems. Linking the physics of 3d-systems to 4f-materials, we have found an unexpected orbitally selective Kondo effect in dilute concentrations of Fe substituted into the non-magnetic compound SrNi_2As_2 [7].

As a consequence of our investment to purifying single crystals of URu_2Si_2 , in collaboration with our network of internationally renown collaborators we have made significant progress on understanding the enigmatic “hidden order” and unconventional superconducting states [8-10]. Briefly, the hidden order is consistent with a chirality density wave, which possesses nematic fluctuations above the hidden order state, while the superconducting state breaks time reversal symmetry.

Future Plans

Our approach to discovering and understanding emergent states in quantum matter in the next three years will integrate several fronts as a result of the success and insights provided by our past work.

Motivated by our NMR results suggesting even-parity unconventional superconductivity in nearly ferromagnetic U_2PtC_2 [11]. However, detailed questions about the superconducting order remain, including whether or not a chiral order parameter exists, which could be consistent with topological superconductivity. All work to date has been done on aligned powders. As in the case of URu_2Si_2 , an investment in synthesis will have enormous dividends. We will explore the phase stability with our differential scanning calorimeter (DSC), which will allow us to identify a new flux growth procedure. We will also grow thin films of U_2PtC_2 via polymer assisted deposition, reproducing the success of growing epitaxial UC_2 films. Complementing these studies, we will also investigate the superconducting order parameter in ferromagnetic superconductors such as UCoGe and URhGe by performing field-angle thermal conductivity and specific heat measurements down to 50 mK and in high magnetic fields.

Following our neutron scattering results, which found an unexplained spin gap in zero magnetic field in CeRhIn_5 , we will perform neutron scattering measurements on related family members CePt_2In_7 , Ce_2RhIn_8 and CeIn_3 , which will enable us to investigate the influence of dimensionality and the Kondo scale on this spin gap. For this, we will need to develop a protocol for synthesizing larger single crystals of CePt_2In_7 , which we will use with our DSC. To further explore the effects of dimensionality on heavy fermions, in general,

we will synthesize heterostructures of CeFeOP and LaFeOP using pulsed laser deposition (PLD) in collaboration with CINT at LANL.

We will also explore non-collinear/non-coplanar spin textures in $3d$ transition metal as well as in rare-earth systems. EuPtIn₄ is a promising candidate that provides large single crystals [12] and has been shown recently to have a non-collinear magnetic structure at zero-field. Co-based materials also provide a fruitful platform for the study of non-collinear spin textures. We have synthesized high-quality single crystals of CaCo₂As₂ ($T_N = 76$ K) that allowed us to identify the materials' intrinsic low-temperature magnetic properties, which were controversial in the literature. Our results point to the presence of a non-collinear spin structure and further microscopic measurements (e.g. neutron diffraction) will determine the magnetic structure in this material. Further, to drive $3d$ magnetic systems to their magnetic/non-magnetic boundary, we will develop a Bridgman pressure cell modified for the use of liquid pressure media, which ensure hydrostaticity.

Another important direction of our project is the investigation of the interplay between topology and strong correlations. To this end, we will synthesize and investigate PuTe and PuB₆, the latter of which is a $5f$ analog of the topological Kondo insulator SmB₆, which are also predicted to be topological. The larger energy scales of plutonium's $5f$ electrons should make the identification of effects due to electronic correlations more easy to observe than in SmB₆ using our unique transuranic ARPES capability.

References

- [1] N. J. Ghimire, F. Ronning, D. Williams, B.L. Scott, Y. Luo, J.D. Thompson, and E.D. Bauer, "Investigation of the physical properties of the tetragonal CeMAI₄Si₂ (M = Rh, Ir, Pt) compounds," *J. Phys.: Condens. Matter*, **27**, 025601 (2015).
- [2] N. J. Ghimire, S.K. Cary, S. Eley, N. Wakeham, P.F.S. Rosa, T. Albrecht-Schmitt, Y. Lee, M. Janoschek, C.M. Brown, L. Civale, J.D. Thompson, F. Ronning, and E.D. Bauer, "Investigation of the physical properties of the Ce₂MAI₇Ge₄ (M = Co, Ir, Ni, Pd) heavy fermion compounds" *Phys. Rev. B*, **93**, 205141 (2016).
- [3] N. J. Ghimire, S. Calder, M. Janoschek, and E. D. Bauer, "Magnetic structure of the antiferromagnetic Kondo lattice compounds CeRhAl₄Si₂ and CeIrAl₄Si₂," *J. Phys.: Condens. Matter* **27**, 245603 (2015).
- [4] H. Sakai, T. Hattori, Y. Tokunaga, S. Kambe, N.J. Ghimire, F. Ronning, E.D. Bauer, and J.D. Thompson, "Incommensurate to commensurate antiferromagnetism in CeRhAl₄Si₂: An ²⁷Al NMR Study" *Phys. Rev. B*, **93**, 014402 (2016).

- [5] P.F.S. Rosa, T.M Garitezi, Z. Fisk and P.G. Pagliuso, “3d magnetism in ThCo₂Sn₂ single crystals,” *J. Phys. Conf. Ser.* **592**, 012053 (2015).
- [6] P. F. S. Rosa, B. L. Scott, F. Ronning, E. D. Bauer, and J. D. Thompson. “Filling the holes in the CaFe₄As₃ structure: synthesis and magnetism of CaCo₅As₃,” *in preparation*.
- [7] N. Wakeham, Ni Ni, J.-X. Zhu, E.D. Bauer, J.D. Thompson, and F. Ronning, “Observation of an orbitally selective Kondo effect,” submitted.
- [8] H. H. Kung, R. E. Baumbach, E. D. Bauer, V. K. Thorsmølle, W. L. Zhang, K. Haule, J. A. Mydosh, and G. Blumberg, “Chirality density wave of the ‘hidden order’ phase in URu₂Si₂,” *Science* **347**, 1339 (2015).
- [9] S. C. Riggs, M.C. Shapiro, A. V. Maharaj, S. Raghu, E. D. Bauer, R. E. Baumbach, P. Giraldo-Gallo, M. Wartenbe, and I. R. Fisher, “Evidence for a nematic component to the hidden-order parameter in URu₂Si₂ from differential elastoresistance measurements,” *Nature Comm.* **6**, 6425 (2015).
- [10] E.R. Schemm, R.E. Baumbach, P.H. Tobash, F. Ronning, E.D. Bauer, and A. Kapitulnik, “Evidence for broken time-reversal symmetry in the superconducting phase of URu₂Si₂,” *Phys. Rev. B* **91**, 140506(R) (2015).
- [11] A.M. Mounce, H. Yasuoka, G. Koutroulakis, N. Ni, E.D. Bauer, F. Ronning, and J.D. Thompson, “Evidence for spin-triplet superconductivity in U₂PtC₂ from ¹⁹⁵Pt NMR,” *Phys. Rev. Lett.* **114**, 127001 (2015).
- [12] P.F.S. Rosa, C.B.R. Jesus, Z. Fisk, P.G. Pagliuso “Physical properties of EuPtIn₄ intermetallic antiferromagnet”. *J. Magn. Magn. Mater.* **371**, 5 (2014).

Neutron and x-ray scattering studies of complex phenomena in bulk materials and heterostructures of strongly correlated systems

**S. Rosenkranz, O. Chmaissem*, R. Osborn, D. Phelan, S.G.E. te Velthuis
Argonne National Laboratory; *and Northern Illinois University**

Program Scope

The assumption of a long-range-ordered crystalline lattice has provided a very successful foundation for describing a diverse range of properties of condensed matter for over a century. Many phenomena of recent interest are, however, associated with the presence of complex disorder and short-range correlations that emerge from the influence of multiple ground-states with incompatible order, which are poorly described with the old paradigm. Materials with complex short-range correlations generally exhibit unusual and often strongly enhanced responses to external stimuli such as magnetic or electric fields and are of considerable technological potential for future applications. We utilize, and develop when necessary to advance our scientific program, the latest advances in neutron and synchrotron x-ray instrumentation to study complex disorder and short-range correlations in bulk and heterostructures of strongly correlated systems on a range of length and time scales. Our goal is to utilize efficient techniques that we have been developing to characterize nanoscale fluctuations in the competing order, both static and dynamic, in order to make a major impact on our progress towards understanding how complex disorder affects material functionality of interest including superconductivity, magnetism, thermoelectricity, ionic conduction, *etc.* Our programs focus on the origin of charge density wave correlations and their connection to unusual electronic and physical properties, studies of charge and spin correlations at interfaces of heterostructures and how they drive emergent phenomena, studies of the influence of spin, charge, and orbital correlations in strongly correlated electron systems, particularly in iron-based superconductors, and studies of complex structural disorder and their influence on bulk properties, particularly in relaxors and strongly correlated battery electrode materials. A secondary focus of our program is to develop novel methods to enable and advance research utilizing neutron and synchrotron x-ray diffraction.

Recent Progress

Charge density wave correlations: Our studies combining X-ray scattering, STM, ARPES, and transport measurements reveal the presence of a pseudogap over a large region of temperature and doping in the strong-coupling CDW compound $2H\text{-NbSe}_2$. We find that the gap in the electronic spectra in the absence of long-range order is due to the presence of a well-defined amplitude of the underlying CDW order parameter, whose phase however is strongly disordered. Our observations emphasize the importance of phase fluctuations in strongly coupled CDW systems and provide new insights into the significance of phase incoherence in the realization of pseudogap states, a poorly understood phenomenon observed in a variety of materials ranging

from cold atoms to high temperature superconductors. Our investigation of the soft CDW phonon mode upon entering the superconducting state furthermore provides novel insight into the interplay between these competing states. From the observed changes in the phonon lineshape, we demonstrate that the superconducting gap exhibits an out-of-plane dependence. Conversely, our data imply that the CDW energy gap is strongly localized along k_z , a result that could not be obtained with surface techniques, such as ARPES or STM. This confinement of the CDW gap to a very small momentum region explains the coexistence of CDW order and superconductivity in $2H$ -NbSe₂. Our results further provide a microscopic explanation of the decrease/increase of T_c / T_{CDW} in single-layer NbSe₂ as compared to the bulk system. In the trilayer nickelates, which have recently been successfully synthesized for the first time in single crystal form at ANL, our synchrotron x-ray diffraction studies reveal the presence of charge stripes, providing a novel route to investigate the stripe physics surrounding the closely related cuprate superconductors.

Thin films and heterostructures: Using polarized neutron reflectometry and XMCD we have explored modifications of the interfacial magnetic properties in ferromagnetic La_{1-x}Sr_xMnO₃ (LSMO) based heterostructures. We demonstrate that inserting a single La_{0.33}Sr_{0.67}O layer at the interface between LSMO and SrTiO₃ increases the interfacial magnetization. We conclude that with this engineered interface a polar discontinuity is prevented and local atomic reconstruction is eliminated, improving the macroscopic magnetization and electrical conductivity. In LSMO/cuprate bilayers we show that the observed strong memristive behavior is due to a subtle electric field induced displacement of the Mn ions, which switch an interfacial magnetic “dead layer” on or off. In a synthetic multiferroic, LSMO/BaTiO₃, we observe an unexpected net Ti moment, which decays faster than the Mn moment with increasing temperature. This behavior is explained by a weak Ti-Mn exchange coupling that is insufficient to overcome the thermal energy at high temperatures. Furthermore, we show that the interfacial magnetism of highly ordered Sr₂CrReO₆ (SCRO) ferrimagnetic films can be tuned by inclusion of a buffer layer between the film and substrate, irrespective of the strain induced by the substrate. Interestingly, the magnetization suppression region is wider than the Cr/Re anti-site disorder region at the interface between SCRO and the buffer layer.

External electric fields were successfully used to directly manipulate the magnetic properties of ultra-thin Co films adjacent to Gd₂O₃ gate oxides. Our XMCD experiments show that the Co films can be reversibly changed from an optimally-oxidized state with a strong perpendicular magnetic anisotropy to a metallic state with an in-plane magnetic anisotropy, or to a fully-oxidized state with nearly zero magnetization.

Finally, we discovered how magnetic skyrmions can be created and stabilized at room temperature in Ta/CoFeB/TaOx trilayers. Experiments and micromagnetic simulations show that sending a current through a constriction wire results in spatially divergent spin-orbit torques leading to the formation of magnetic skyrmion bubbles. This further enabled us to provide the first experimental observation of a transverse motion of magnetic skyrmions due to topological charge – the skyrmion Hall effect, in analogy to the Hall effect of electrical charges.

Cuprates and iron-based superconductors: Following our discovery of a novel tetragonal magnetic phase (C_4 phase) in Na-doped $BaFe_2As_2$, we have combined high-resolution neutron and synchrotron x-ray powder diffraction and transport measurements to show that the C_4 phase is universally present in hole-doped 122 iron arsenides $(A_{1-x}A'_x)Fe_2As_2$ with $A=Ba, Sr, Ca$, and $A'=Na, K$. The C_4 phase is found to be particularly stable over a wide range of doping in $Sr_{1-x}Na_xFe_2As_2$. This allowed us to perform detailed neutron diffraction and Mössbauer spectroscopy investigations of the magnetic order. We find that 50% of the Fe-sites in the C_4 state are non-magnetic whereas the other 50% have double the moment as compared to the orthorhombic magnetic phase, proving that the magnetic order in the C_4 phase is in the form of a double-Q spin-density-wave. This redistribution of spin density can only occur as a Fermi surface-induced instability in an itinerant system, hence ruling out local moment models for iron superconductors. Furthermore, the tetragonal symmetry of the double-Q state rules out orbital symmetry-breaking showing that nematic order in the iron arsenide superconductors is driven by magnetic interactions. Our results therefore conclusively settle two of the most important questions in the iron-based superconductors, *i.e.*, the nature of the magnetism and the origin of the nematicity.

Other systems and technique developments: Following our preliminary design, the novel single crystal diffuse scattering instrument *Corelli* was built at SNS. We performed commissioning experiments to verify that the instrument performs according to specification. These first experiments proved that the cross-correlation successfully eliminates inelastic scattering processes and further revealed that it also drastically reduces background from large sample environments, therefore enabling novel research to investigate superstructures and short-range correlations in extreme environments. We then performed extensive diffuse scattering measurements of relaxor materials over a large range of temperature, doping, and different materials families. These measurements provided surprising new results, revealing strong anisotropies in some of the diffuse scattering features and enabled us to separate various major contributions to the diffuse scattering and to identify which features are related to their unusual physical properties. We also developed synchrotron x-ray methods for efficient measurements of large volumes of diffuse scattering utilizing fast area detectors combined with continuous sample rotation. To handle the “big data” produced by this technique, we worked with computational scientists to develop novel ways of interfacing with data streamed to remote servers that facilitate both interactive data analysis and automated workflows over the network. The availability of high quality diffuse scattering data over large volumes enabled us to develop novel analysis tools, such as generating 3D Pair Distribution Functions to directly extract real-space correlation in disordered crystalline materials. Utilizing these new methods, we observed a sublattice melting in $Na_xV_2O_5$, a strongly correlated oxide of great interest for battery electrodes.

Future Plans

CDW correlations. We will extend our studies of the interplay between CDW order and other ground-states to other strong-coupling systems, such as RTe_3 , which exhibit magnetic order

coexisting with, and superconductivity competing with CDW order. TaSe₂ is a CDW system very similar to 2H-NbSe₂, which however locks into a commensurate CDW at low temperature. While previous neutron scattering investigations reported unusual behavior with incomplete softening and possibly a central peak, the behavior of this system and how it compares to other strong-coupling compounds remains unclear. We also plan to investigate the evolution of the CDW correlations in Cu_xTiSe₂ as CDW order is suppressed with pressure and doping. The CDW order in TiSe₂ is believed to be boosted by excitonic correlations. Suppressing the CDW could therefore lead to the elusive excitonic superconducting state.

Thin films and heterostructures: We plan to investigate the novel interfacial phenomena and modified magnetic properties that are expected to emerge in heterostructures in which ferromagnetic manganites are exposed to oxides with strong spin orbit coupling, such as SrIrO₃. New ground states are expected to arise as a result of the interplay between the double or super exchange interaction in the manganite, and symmetry breaking and/or spin orbit interactions in the iridate. We will probe changes in anisotropy and interfacial magnetism, and look for chiral magnetic states. We will also investigate how applied magnetic fields affect the competition between ferromagnetic and charge-orbital ordered states and in particular, how the applied magnetic field overcomes the phase separation in zero field and leads to a predominantly FM-metallic phase. Investigations will include measurements of the magnetic states on a multilayer of ferromagnetic La_{0.5}Sr_{0.5}MnO₃ and charge ordered Pr_{0.5}Ca_{0.5}MnO₃ on *Corelli*.

Superconductors: We plan detailed investigations, utilizing high-resolution powder neutron and synchrotron x-ray diffraction, of the ternary iron arsenides (Ba_{1-y}Sr_y)_{1-x}Na_xFe₂As₂ and (Sr_{1-y}Cy)_{1-x}Na_xFe₂As₂ in order to determine the underlying structural parameters that stabilize the C₄ phase. We further plan to determine whether the C₄ state occurs in other families of iron based superconductors, such as the ‘1111’ compounds. In order to obtain a better understanding of stripe phases and their influence on superconductivity, we will perform various elastic and inelastic neutron and synchrotron x-ray scattering experiments to investigate the novel trilayer nickelates La₄Ni₃O₈ and La₄Ni₃O₁₀, which are closely related to cuprate superconductors.

Other systems and technique development: We will perform further tests on the feasibility of utilizing various sample environments for diffuse scattering studies on *Corelli*. For example, we plan to extend our measurements on relaxors performed in the standard displax setup to a furnace, which will provide both a benchmark for high temperature measurements as well as allow us to investigate the evolution of the diffuse scattering upon crossing the Burns temperature. We plan to then utilize this setup to investigate alleged sublattice melting, and its relation to low thermal conductivity, in a copper chalcogenide, through detailed temperature dependent studies of the diffuse scattering. We will also investigate the feasibility of performing magnetic diffuse scattering studies in high applied magnetic fields, by measuring ErSb, a rare-earth monopnictide with indications of topological band properties, antiferromagnetic ordering, and unusual longitudinal magnetoresistance.

Publications

1. F. Weber, S. Rosenkranz, R. Heid, A.H. Said, [Superconducting energy gap of 2H-NbSe₂ in phonon spectroscopy](#), *Phys. Rev. B* **94**, 140504(R) (2016).
2. S. Rosenkranz, [Status and Future of Neutron Scattering in North America](#), *Neutron News* **27**, 2-3 (2016).
3. Wanjun Jiang, Xichao Zhang, Guoqiang Yu, Wei Zhang, Xiao Wang, M. Benjamin Jungfleisch, John E. Pearson, Xuemei Cheng, Olle Heinonen, Kang L. Wang, Yan Zhou, Axel Hoffmann, Suzanne G. E. te Velthuis, [Direct Observation of the Skyrmion Hall Effect](#), *Nat. Phys.* doi: 10.1038/nphys3883 (2016).
4. A. Kaminski, S. Rosenkranz, M.R. Norman, H. Raffy, Z.Z. Li, M. Randeria, J.C. Campuzano, [Destroying coherence in high-temperature superconductors with current flow](#), *Phys. Rev. X* **6**, 031040 (2016).
5. Junjie Zhang, Yu-Sheng Chen, D. Phelan, Hong Zheng, M.R. Norman, and J.F. Mitchell, [Stacked charge stripes in the quasi-2D trilayer nickelate La₄Ni₃O₈](#), *Proc. Natl. Acad. Sci. U.S.A.* **113**, 8945 (2016).
6. Xiao Shen, T. J. Pennycook, D. Hernandez-Martin, Ana Pérez, Y. S. Puzyrev, Yaohua Liu, S. G. E. te Velthuis, J.W. Freeland, P. Shafer, Chenhui Zhu, M. Varela, C. Leon, Z. Sefrioui, J. Santamaria, S.T. Pantelides, [High on/off Ratio Memristive Switching of Manganite-Cuprate Bilayer by Interfacial Magnetoelectricity](#), *Adv. Mater. Interfaces* **3**, 1600086 (2016).
7. K.M. Taddei, J.M. Allred, D.E. Bugaris, S. Lapidus, M.J. Krogstad, R. Stadel, H. Claus, D.Y. Chung, M.G. Kanatzidis, S. Rosenkranz, R. Osborn, O. Chmaissem, [Detailed magnetic and structural analysis mapping a robust magnetic C₄ dome in Sr_{1-x}Na_xFe₂As₂](#), *Phys. Rev. B* **93**, 134510 (2016).
8. Yaohua Liu, J. Tornos, S.G.E. te Velthuis, J.W. Freeland, H. Zhou, P. Steadman, P. Bencok, C. Leon, J. Santamaria, [Induced Ti-Magnetization at La_{0.7}Sr_{0.3}MnO₃ and BaTiO₃ Interfaces](#), *APL Mater.* **4**, 046105 (2016).
9. M.P. Smylie, M. Leroux, V. Mishra, L. Fang, K. Taddei, O. Chmaissem, H. Claus, A. Kayani, A. Snezhko, U. Welp, W.-K. Kwok, [Effect of proton irradiation on superconductivity in optimally doped BaFe₂\(As_{1-x}P_x\)₂ single crystals](#), *Phys. Rev. B* **93**, 115119 (2016).
10. Olle Heinonen, Wanjun Jiang, Hamoud Soumaily, Suzanne G.E. te Velthuis, Axel Hoffmann, [Generation of magnetic skyrmion bubbles by inhomogeneous spin-Hall currents](#), *Phys. Rev. B* **93**, 094407 (2016).
11. Wanjun Jiang, Wei Zhang, Guoqiang Yu, M. Benjamin Jungfleisch, Pramey Upadhyaya, Hamoud Soumaily, John E. Pearson, Yaroslav Tserkovnyak, Kang L. Wang, Olle Heinonen, Suzanne G.E. te Velthuis, Axel Hoffmann, [Mobile Néel skyrmions at room temperature: status and future](#), *AIP Advances* **6**, 055602 (2016).
12. Shan Jiang, Chang Liu, Huibo Cao, Turan Birol, Jared M. Allred, Wei Tian, Lian Liu, Kyuil Cho, Matthew J. Krogstad, Jie Ma, Keith M. Taddei, Makariy A. Tanatar, Moritz Hoesch, Ruslan Prozorov, Stephan Rosenkranz, Yasutomo J. Uemura, Gabriel Kotliar, Ni Ni, [Structural and magnetic phase transitions in Ca_{0.73}La_{0.27}FeAs₂ with electron-overdoped FeAs layers](#), *Phys. Rev. B* **93**, 054522 (2016).
13. J.M. Allred, K.M. Taddei, D.E. Bugaris, M.J. Krogstad, S.H. Lapidus, D.Y. Chung, H. Claus, M.G. Kanatzidis, D.E. Brown, J. Kang, R.M. Fernandes, I. Eremin, S. Rosenkranz, O. Chmaissem, R. Osborn, [Double-Q spin-density wave in hole-doped iron arsenides](#), *Nat. Phys.* **12**, 493 (2016).

14. C. Phatak, A. K. Petford-Long, H. Zheng, J. F. Mitchell, S. Rosenkranz, M. R. Norman, [Ferromagnetic domain behavior and phase transition in bilayer manganites investigated at the nanoscale](#), *Phys. Rev. B* **92**, 224418 (2015).
15. J.M. Wozniak, K. Chard, B. Blaiszik, R. Osborn, M. Wilde, I. Foster, [Big Data Remote Access Interfaces for Light Source Science](#), *2015 IEEE/ACM 2nd International Symposium on Big Data computing (BDC)* **0**, 51-60 (2015).
16. Yuelin Li, Donald A. Walko, Qing'an Li, Yaohua Liu, Stephan Rosenkranz, Hong Zheng, John F. Mitchell, [Evidence of photo-induced dynamic competition of metallic and insulating phases in a layered manganite](#), *J. Phys. Condens. Matter* **27**, 495602 (2015).
17. I. Foster, R. Ananthkrishnan, B. Blaiszik, K. Chard, R. Osborn, S. Tuecke, M. Wilde, J. Wozniak, [Networking Materials Data: Accelerating Discovery at Experimental Facilities](#), *Advances in Parallel Computing, Vol 26: Big Data and High Performance Computing*, (Ed. L. Grandinetti, G.R. Joubert, M. Kunze, V. Pascucci, IOS Press 2015) p 117 – 132.
18. J.M. Allred, S. Avci, D.Y. Chung, H. Claus, D.D. Khalyavin, P. Manuel, K.M. Taddei, M.G. Kanatzidis, S. Rosenkranz, R. Osborn, O. Chmaissem, [Tetragonal magnetic phase in \$Ba_{1-x}K_xFe_2As_2\$ from x-ray and neutron diffraction](#), *Phys. Rev. B* **92**, 094515 (2015).
19. K.M. Taddei, M. Sturza, D.Y. Chung, H.B. Cao, H. Claus, M.G. Kanatzidis, R. Osborn, S. Rosenkranz, O. Chmaissem, [Cesium vacancy ordering in phase-separated \$Cs_xFe_{2-y}Se_2\$](#) , *Phys. Rev. B* **92**, 094505 (2015).
20. C. Abughayada, B. Dabrowski, S. Kolesnik, D. Brown, O. Chmaissem, [Characterization of oxygen storage, structural and magnetic properties of oxygen-loaded hexagonal \$RMnO_{3+\delta}\$ \(\$R = Ho, Er, \text{ and } Y\$ \)](#), *Chem. Mat.* **27**, 6259 (2015).
21. B.J. Campbell, S. Rosenkranz, H.J. Kang, H.T. Stokes, P.J. Chupas, S. Komiya, Y. Ando, Shiliang Li, Pengcheng Dai, [Long-range two-dimensional superstructure in the superconducting electron-doped cuprate \$Pr_{0.88}LaCe_{0.12}CuO_4\$](#) , *Phys. Rev. B* **92**, 014118 (2015).
22. Wanjun Jiang, Pramey Upadhyaya, Wei Zhang, Guoqiang Yu, M. Benjamin Jungfleisch, Frank Y. Fradin, John E. Pearson, Yaroslav Tserkovnyak, Kang L. Wang, Olle Heinonen, Suzanne G.E. te Velthuis, Axel Hoffmann, [Blowing magnetic skyrmion bubbles](#), *Science* **349**, 283(2015).
23. M. Maschek, S. Rosenkranz, R. Heid, A.H. Said, D. Young, P. Giraldo-Gallo, I. R. Fisher, F. Weber, [Wave vector dependent electron-phonon coupling and the charge-density-wave transition in \$TbTe_3\$](#) , *Phys. Rev. B* **91**, 235146 (2015).
24. Wei Zhang, M.B. Jungfleisch, Wanjun Jiang, Yaohua Liu, J.E. Pearson, S.G.E te Velthuis, A. Hoffmann, F. Freimuth, Y. Mokrousov, [Reduced spin-Hall effects from magnetic proximity](#), *Phys. Rev. B* **91**, 115316 (2015).
25. X. Luo, V. Stanev, B. Shen, L. Fang, X.S. Ling, R. Osborn, S. Rosenkranz, T.M. Benseman, R. Divan, W.K. Kwok, U. Welp, [Antiferromagnetic and nematic phase transitions in \$BaFe_2\(As_{1-x}P_x\)_2\$ studied by AC microcalorimetry and SQUID magnetometry](#), *Phys. Rev. B* **91**, 094512 (2015).
26. J.M. Lucy, A.J. Hauser, Y. Liu, H. Zhou, Y. Choi, D. Haskel, Suzanne G.E. te Velthuis, F. Y. Yang, [Depth-resolved magnetic and structural analysis of relaxing epitaxial \$Sr_2CrReO_6\$](#) , *Phys. Rev. B* **91**, 094413 (2015).
27. U. Chatterjee, J. Zhao, M. Iavarone, R.Di Capua, J.P. Castellan, G. Karapetrov, C.D. Malliakas, M.G. Kanatzidis, H. Claus, J.P.C. Ruff, F. Weber, J. van Wezel, J.C. Campuzano, R. Osborn, M. Randeria, N. Trivedi, M.R. Norman, and S. Rosenkranz, [Emergence of Coherence in the Charge Density Wave State of \$2H-NbSe_2\$](#) , *Nature Comm.* **6**:6313 (2015).

28. M. Könnecke, F.A. Akeroyd, H.J. Bernstein, A.S. Brewster, S.I. Campbell, B. Clausen, S. Cottrell, J.U. Hoffmann, P.R. Jemian, D. Männicke, R. Osborn, P.F. Peterson, T. Richter, J. Suzuki, B. Watts, E. Wintersberger, J. Wuttke, [the NeXus data format](#), *J. Appl. Cryst.* **48**, 301-305 (2015).
29. D. Phelan, E. E. Rodriguez, J. Gao, Y. Bing, Z.-G. Ye, Q. Huang, Jinsheng Wen, Guangyong Xu, C. Stock, M. Matsuura, P.M. Gehring, [Phase diagram of the relaxor ferroelectric \(1-x\)Pb\(Mg_{1/3}Nb_{2/3}\)O₃ + xPbTiO₃ revisited: a neutron powder diffraction study of the relaxor skin effect](#), *Phase Transitions* 88, 283 (2015).
30. M. Huijben, Y. Liu, H. Boschker, V. Lauter, R. Egoavil, J. Verbeeck, S.G.E. te Velthuis, G. Rijnders, G. Koster, [Enhanced Local Magnetization by Interface Engineering in Perovskite-Type Correlated Oxide Heterostructures](#), *Adv. Mater. Interfaces* **2**, 1400416 (2015).
31. Chong Bi, Yaohua Liu, T. Newhouse-Illige, M. Xu, M. Rosales, J.W. Freeland, O. Mryasov, Shufeng Zhang, S.G.E te Velthuis, W.G. Wang, [Reversible Control of Co Magnetism by Voltage-Induced Oxidation](#), *Phys. Rev. Lett.* **113**, 267202 (2014).
32. Sami Vasala, Maxim Avdeev, Sergey Danilkin, Omar Chmaissem, and Maarit Karppinen, [Magnetic structure of Sr₂CuWO₆](#), *J. Phys.: Condens. Matter* **26**, 496001(2014).
33. D.D. Khalyavin, S.W. Lovesey, P. Manuel, F. Krüger, S. Rosenkranz, J.M. Allred, O. Chmaissem, R. Osborn, [Symmetry of re-entrant tetragonal phase in Ba_{1-x}Na_xFe₂As₂: Magnetic versus orbital ordering mechanism](#) *Phys. Rev. B* **90**, 174511(2014).
34. D.K. Pratt, J.W. Lynn, J. Mais, O. Chamissem, D.E. Brown, S. Kolesnik, B. Dabrowski, [Neutron scattering studies of the ferroelectric distortion and spin dynamics in the type-1 multiferroic perovskite Sr_{0.56}Ba_{0.44}MnO₃](#), *Phys. Rev. B* **90**, 140401(R) (2014).
35. Yaohua Liu, J.M. Lucy, A. Glavic, H. Ambaye, V. Lauter, F.Y. Yang, S.G.E. te Velthuis, [Effects of strain and buffer layer on interfacial magnetization in Sr₂CrFeO₆ films determined by polarized neutron reflectometry](#) *Phys. Rev. B* **90**, 104416 (2014).
36. J.M. Allred, K.M. Taddei, D.E. Bugaris, S. Avci, D.Y. Chung, H. Claus, C. dela Cruz, M.G. Kanatzidis, S. Rosenkranz, R. Osborn, O. Chmaissem, [Coincident structural and magnetic order in BaFe₂\(As_{1-x}P_x\)₂ revealed by high-resolution neutron diffraction](#) *Phys. Rev. B* **90**, 104513 (2014).
37. Qing'an Li, K.E. Gray, S.B. Wilkins, M. Garcia Fernandez, S. Rosenkranz, H. Zheng, J.F. Mitchell, [Prediction and Experimental Evidence for Thermodynamically Stable Charged Orbital Domain Walls](#), *Phys. Rev. X* **4**, 031028 (2014).
38. C. Abughayada, B. Dabrowski, M. Avdeev, S. Kolesnik, S. Remsen, O. Chmaissem, [Structural, magnetic, and oxygen storage properties of hexagonal Dy_{1-x}Y_xMnO_{3-δ}](#), *J. Solid State Chem.* **217**, 127 (2014).
39. V.R. Fanelli, J.M. Lawrence, E.A. Goremychkin, R. Osborn, E.D. Bauer, K.J. McClellan, J.D. Thompson, C.H. Booth, A.D. Christianson, P.S. Riseborough, [O-dependence of the spin fluctuations in the intermediate valence compound CePd₃](#), *J. Phys.: Condens. Matter* **26**, 225602 (2014).
40. M. Marezio, O. Chmaissem, C. Bougerol, M. Karppinen, H. Yamauchi, T. H. Geballe, [High-T_c Superconducting Cuprates, \(Ce,Y\)₈O_{2s-2}Sr₂\(Cu_{2.75}Mo_{0.25}\)O_{6+δ}: T_c-increase with apical Cu-O decrease at constant Cu-O planar distance](#), *J. Phys.: Conf. Series* **507**, 012031 (2014).
41. Yuelin Li, D. Walko, Qing'an Li, Yaohua Liu, S. Rosenkranz, H. Zheng, J.F. Mitchell, H. Wen, E. Dufresne, B. Adams, [Photo-modulated dynamic competition between metallic and insulating phases in a layered manganite](#), *MRS Online Proceedings Library* **1636**, mrsf13-1636-u6.09 (2014).

Exploration of Novel Magnetic Phenomena in Two Dimensional Nanoengineered Materials

Deepak K. Singh, University of Missouri, Columbia, MO

Program Scope

The PI's research is focused on understanding some of the most fundamental problems of magnetism by creating unique two-dimensional artificial honeycomb lattices. Recent theoretical calculations have shown that an artificial magnetic honeycomb lattice can undergo through a variety of novel ordered regimes of correlated spins and magnetic charges of both fundamental and practical importance as a function of temperature. [1,2] It includes long-range spin ice, entropy-driven magnetic charge-ordered state and spin-order due to the spin chirality as a function of reducing temperature. At low enough temperature, the spin correlation is expected to develop into a spin solid state density where the magnetization profile assumes a chiral vortex configuration involving six vertexes of the honeycomb lattice. The spin solid state, manifested by the distribution of the pairs of vortex states of opposite chirality across the lattice, provides a unique opportunity to realize a magnetic material with net zero entropy and magnetization for an ordered ensemble of magnetic moments. The experimental efforts to realize the temperature dependent magnetic correlations in the artificial honeycomb lattice is limited due to the employment of the present nanofabrication method of the electron-beam lithography. [3-5]

We have devised a new nanofabrication scheme, which allows the creation of the macroscopic size artificial honeycomb lattice with ultra-small dimension of the connecting bond, 12 nm. 5 nm. 5 nm. Detail experimental investigations, combined with numerical simulation, on the newly fabricated honeycomb lattice demonstrate the temperature dependent evolution of magnetic correlation, ultimately tending to attain the spin solid state at low temperature. The most interesting behavior, however, is found in the differential conductivity measurements on the permalloy honeycomb lattice where an asymmetric current bias, analogous to the properties of a semiconductor diode, is found to develop at higher temperature ($T \rightarrow 225$ K). The one-to-one correspondence between the temperature dependent current bias and the development of magnetic correlation indicates the role of the underlying magnetism in the anomalous observation. Consequently, this new discovery can be exploited to design a magnetic transistor for practical applications, thus replacing conventional electronics with spintronics devices.

In a related research on the exploration of new spintronics properties in this system, we have found that an artificial honeycomb lattice made of hybrid material (made of Sn and Nd thin films, ~ 3 nm) exhibit colossal change in conductivity on a moderate current application (~ 5 μ A) in zero magnetic field. The current driven colossal conductance persists all the way to $T = 300$ K, albeit weakly. The property of achieving colossal conductance by a moderate current application is a major research enterprise in spintronics at present times. Moreover, the persistence of effect to room temperature makes it employable in the design of next generation computing devices. This is another research avenue where we plan to invest significantly in near future and where neutron scattering, especially polarized reflectometry and SANS measurements, is expected to play key role in developing a thorough understanding of the underlying mechanism.

In addition to the study of the artificial honeycomb lattice, I have also pursued two other projects within the ambit of the DOE-BES research support. One of the projects involves the exploration of quantum magnetism in the disorder induced artificial spin-1/2 in simple perovskite and that has important implication to the study of the novel magnetism in artificial honeycomb

lattice. We have discovered that the dimers, due to artificial spin-1/2, exhibit singlet-to-triplet excitation at low temperature ($T \sim 80$ mK) without any ordered spin correlation. The localized gapped excitation evolves into a gapless quasi-continuum. The quasi-continuum spectrum in energy and momentum persists to an unusual high temperature of $T = 250$ K, thus extending the exploration to the semi-classical regime—a new frontier in the study of quantum magnetism. Second project involves the exploration of unconventional superconductivity in binary antiferromagnetic materials. The PI's research team has made considerable progress in this endeavor also, as evidenced by the recent finding of minority superconducting phase in NiSi.

Recent Progress

Artificial magnetic honeycomb lattice: One of the major accomplishments of this project is to successfully create macroscopic size artificial honeycomb lattice of magnetic material. We have also extended our fabrication technique to create artificial honeycomb lattice of hybrid structure as well. The atomic force micrographs of the newly fabricated honeycomb lattice of ultra-small bonds, with lateral size of the order of ~ 12 nm.5 nm.5 nm, are shown below.

Experimental investigations on the newly fabricated artificial honeycomb lattice of ultra-small bond indeed reveal multiple magnetic regimes, suggestive of varying magnetic correlation, as a function of reducing temperature. The most remarkable transition occurs at low temperature, $T < 30$ K, where the overall net magnetization tends to attend a zero value. This discernible effect is most conspicuous in applied magnetic field of $H = 500$ Oe, where the near-zero magnetic moment at low temperature in the zero field cool state rapidly jumps to the field-aligned saturated magnetic moment value as temperature increases. The experimental results are verified by the micromagnetic simulations. The micromagnetic simulations show that the magnetization profile near zero field value is dominated by the distribution of the pairs of circular vortex configurations, involving six vertexes of the honeycomb lattice, of opposite chirality. This is further complemented by detail electrical measurements of resistance versus temperature in applied field where temperature dependent magnetic correlations are identified by the change in the electrical transport properties. A much more dramatic effect, however, is observed in the differential conductivity measurements in zero field. It is found that the differential conductivity is asymmetric with respect to the current direction as temperature increases above $T = 30$ K. This process becomes much more drastic as the measurement temperature increases towards $T \sim 225$ K. Above $T > 225$ K, the differential conductivity gradually decreases and tends to become symmetric again at $T \rightarrow 300$ K; also reflected in the electric power measurement as a function of the applied current (**Summers et al., 2016**)

We have also made strong efforts in determining the spin correlation in the spin solid state in permalloy honeycomb by performing polarized reflectometry and small angle neutron scattering measurements on magnetic reflectometer (beam line BL-4A, SNS) and GPSANS

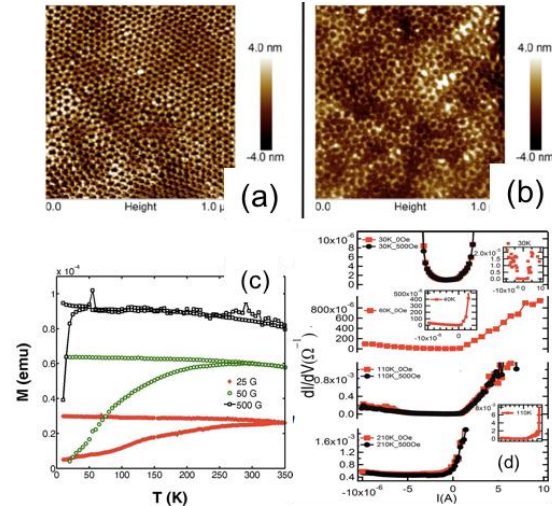


Fig. (a-b) AFM micrograph of honeycomb lattice and metallic honeycomb. (c) M vs. T data. (d) Asymmetric current biasing in permalloy honeycomb lattice.

(HIFR), respectively. The polarized Reflectometry data at $T \sim 5$ K clearly manifest a significant change in the scattering pattern in the spin flip channel of the polarized data, compared to the non-spin flip data. Therefore, the scattering pattern is magnetic in origin. At present, we are still trying to understand this by performing numerical modeling of possible magnetic configuration in the artificial honeycomb lattice. Precise determination of the background is key to this effort.

Artificial hybrid honeycomb lattice: In a related, yet separate, research on the hybrid honeycomb lattice, with similar connecting bond size but made of Sn and Nd thin film layers of the order of ~ 3 nm, we have found that the system exhibits strong diamagnetic tendency in zero field cool magnetization data. The diamagnetic behavior reverses to the paramagnetic upon magnetic field application. As the applied field increases, the diamagnetic characteristics significantly weakens and eventually the system exhibits the ferromagnetic behavior in the field cool magnetization data. An important aspect of the newly designed hybrid honeycomb is manifested in the electronic measurements. It is found that the differential conductivity increases by at least two orders of magnitude as the applied current increases from 0 to 5 μ A. This enormous current-driven enhancement in dI/dV persists all the way to the room temperature, albeit weakly. We also note that the current-induced enhancement in dI/dV is symmetric with respect to the current application direction, which is different from the permalloy honeycomb lattice. In the latter case, the gain in differential conductivity was found to be asymmetrically biased. Although detail research works are needed to fully understand the role of underlying magnetism in the current driven colossal conductance in the newly fabricated hybrid honeycomb system, the new finding can be exploited to design new spintronics-based computing devices.

Quantum magnetism in artificial spin-1/2 system: The quantum spin liquid type state and the associated spin fractionalization in spin-1/2 systems are evolving as the novel paradigm to study exotic, yet, the fundamental properties of matter, in general. [6-7] A lot of studies, in this regard, have focused on the exploration of spin-1/2 system in the chemically ordered lattice. Taking an altogether different route, we have demonstrated the feasibility of observing the quantum mechanical properties of spin-1/2 system in a disorder induced tailored frustrated system (Gunasekera et al., 2016). Using synergistic theoretical and experimental investigations, we have showed that the chemical disorder, due to Co-substitution of Ru as a control parameter in a simple perovskite CaRuO_3 , creates artificial spin-1/2's that not only causes a similar effect but also provides flexibility in extending the exploration to the semi-classical regime. A quenched disorder prohibits the propagation of the long-range order, hence automatically creates frustration. At the same time, the random distribution of spin-1/2 generates multiple partitioning effects between the nearest neighbors and further separated moments with varying exchange energy, J , in the dimer formation; also reminiscent of the liquid-like superposition between spin-1/2's in frustrated lattice. We have discovered that the dimers, due to artificial spin-1/2, exhibit singlet-to-triplet excitation at low temperature ($T \sim 80$ mK) without any ordered spin correlation. The localized gapped excitation evolves into a gapless quasi-continuum as dimer pairs break and create freely fluctuating fractionalized spins at high temperature, $T = 80$ K. This behavior is also complemented by the observation of strong Q-independent dynamic susceptibility (χ'') at high temperature in the ac susceptibility measurements. Together these properties hint of a new quantum magnetic state with strong resemblance to the resonance valence bond system.

Future Plans

One of the priorities is to perform detail neutron scattering measurements (polarized reflectometry and SANS) on both magnetic and hybrid artificial honeycomb lattice samples.

While there are strong evidences of the development of the spin solid state at low temperature in permalloy honeycomb, neutron scattering measurements can be used to deduce the spin correlation in the spin solid state. Similarly, a detail neutron scattering measurements on the hybrid honeycomb lattice will allow us to understand the role of the underlying magnetism in the current driven colossal conductance in this system. My group is also working on developing a new device to estimate the heat capacity and entropy of the newly designed artificial honeycomb lattice. It can be achieved by utilizing the thermal differential scanning calorimetry technique.

Both endeavors-- the study intended to develop a fundamental understanding and exploring the possibilities for practical application of electronic properties (in magnetic and hybrid honeycomb lattice systems) -- are equally important. Therefore, we will develop a robust new platform to create honeycomb lattice systems of varying size and thicknesses. This will not only help us in tuning the electronic properties but also allow us to develop a systematic understanding of the evolution of the underlying physics.

Similarly, the new finding of resonant valence bond-type state in disorder induced artificial spin-1/2 in simple perovskite needs to be investigated in great detail. I will continue to explore the implications of the microscopic mechanism (behind the quantum fluctuations of artificial spin-1/2 moments in Co-doped CaRuO_3) to the physics of the RVB-type state using both polycrystalline and single crystal samples. The research will also be extended to other perovskite with different lattice structure, for example Ca_2IrO_4 . The diversity in the lattice configurations will allow us to understand the physics of the RVB state independent of the underlying crystal structure.

References

- [1] G. Moller and R. Moessner, *Phys. Rev. B* **80**, 140409 (R) (2009)
- [2] G. W. Chern, P. Mellado, and O. Tchernyshyov, *Phys. Rev. Lett.* **106**, 207202 (2011)
- [3] C. Nisoli, R. Moessner and P. Schiffer, *Rev. Mod. Phys.* **85**, 1473 (2013).
- [4] C. Nisoli, J. Li, D. Garand, P. Schiffer and V. H. Crespi, *Phys. Rev. Lett.* **105**, 047205 (2010)
- [5] Y. Qi, T. Brintlinger, and J. Cumings, *Phys. Rev. B* **77**, 094418 (2008)
- [6] T. Han, J. Helton, S. Chu, D. Nocera, J. Rodriguez, C. Broholm and Y. S. Lee, *Nature* **492**, 406 (2012)
- [7] S. T. Bramwell, *Nature* **439**, 273 (2006)

Publications

- [1] B. Summers, L. Debeer-Schmitt, A. Dahal, P. Kampschroeder, J. Gunasekera and D. K. Singh, "Temperature dependent magnetism and asymmetric current biasing in artificial honeycomb lattice", (Under review in *Advanced Materials*, 2016)
- [2] L. Harriger, S. Disseler, J. Gunasekera, J. Rodriguez-Rivera, J. Pixley, P. Manfrinetti, S. K. Dhar and D. K. Singh, "Gapped excitation in dense Kondo lattice CePtZn ", (Under review in *Phys. Rev. B (Rapid Communication)*, 2016)
- [3] J. Gunasekera, A. Dahal, J. Rodriguez, L. Harriger, S. Thomas, A. Ernst and D. K. Singh, "Quantum magnetic properties in perovskite with artificial spin-1/2", (Under review in *Nature Communications*, submitted in 2016)
- [4] A. Dahal, J. Gunasekera, L. Harriger, S. H. Lee, Y. S. Hor, D. J. Singh and D. K. Singh, "Intermediate regime between metal and superconductor below $T = 100$ K in NiSi ", (Accepted in *Phys. Rev. B*, 2016)

National School on Neutron and X-ray Scattering

Suzanne G.E. te Velthuis, Materials Science Division, Argonne National Laboratory
Bryan C. Chakoumakos, Quantum Condensed Matter Division, Oak Ridge National Laboratory

Jonathan C. Lang, Brian H. Toby, Advanced Photon Source, Argonne National Laboratory

John D. Budai, Materials Science and Technology Division, Oak Ridge National Laboratory

Program Scope

Since 1999, the National School on Neutron and X-ray Scattering has provided a comprehensive introduction to the underlying theory of neutron and x-ray scattering and related experimental techniques that are available. The school plays an important strategic role in educating the United States scientific community in the capabilities of its national neutron and x-ray user facilities. While the two-week school was initially held at Argonne National Laboratory, in 2008 ANL partnered with Oak Ridge National Laboratory, and now participants spend equal time at both sites. The program includes both classroom lectures from experts in the field and hands-on experiments.



Recent Progress

The 17th and 18th National School on Neutron and X-ray Scattering were held June 13th - 27th, 2015 and July 20th – August 13th, 2016, respectively. Interest from the scientific community in the school is strong as the school has been consistently oversubscribed, by a factor of 3 or more. During the school, the participants (61 in 2015, 60 in 2016) each performed a total of four neutron scattering experiments using Oak Ridge National Laboratory's Spallation Neutron Source and High Flux Isotope Reactor beamlines. They also performed three to four x-ray experiments at Argonne National Laboratory's

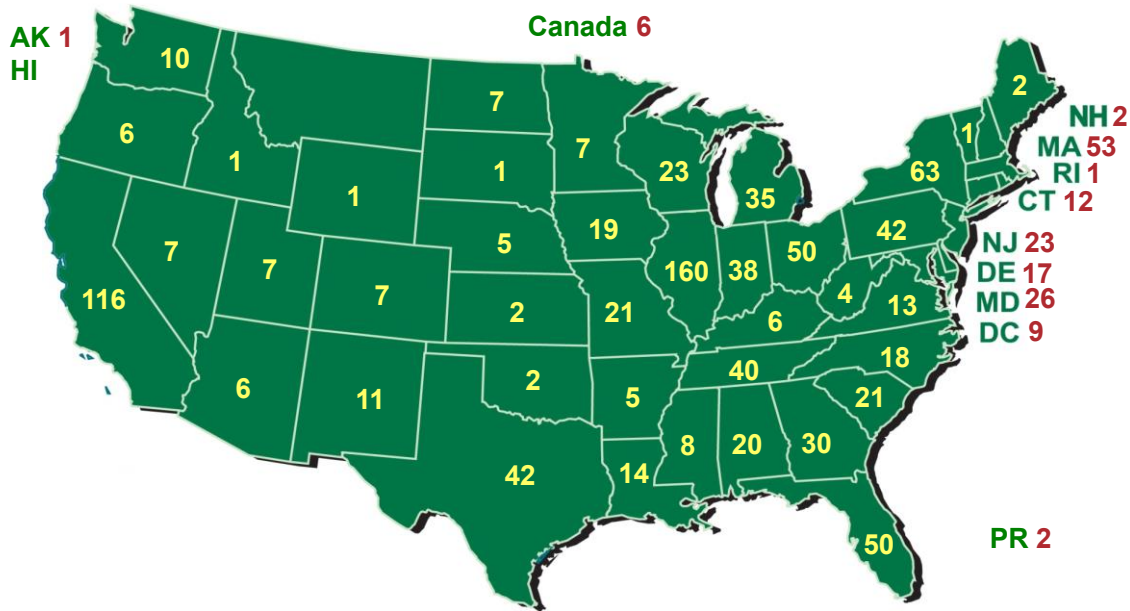


Figure 1: Geographic distribution of school participants from North America, 1999-2016.

Advanced Photon Source. On the last day of the school as small groups the students give a short presentation on one of the experiments they participated in. The feedback from the students is positive each year, and many of the students subsequently apply for postdoctoral positions at Argonne and other neutron and X-ray scattering facilities, or continue to use the facilities for their research.

To date, 1082 participants have attended the school. The national character of the school is reflected in the wide geographic distribution of the participants that have attended as is shown in Fig. 1. Participating students have represented over 165 unique North American colleges and universities, spread over 48 different states, Washington DC, Puerto Rico, and Canada. About 18% of the participants attended schools in EPSCoR states. The

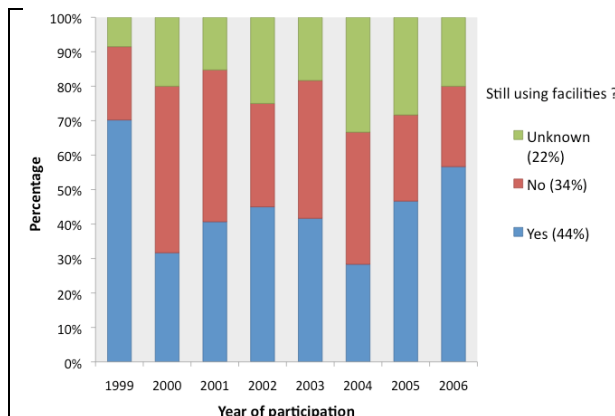


Figure 2: Percentages of 1999-2006 participants that are still using Neutron and/or X-ray facilities¹.

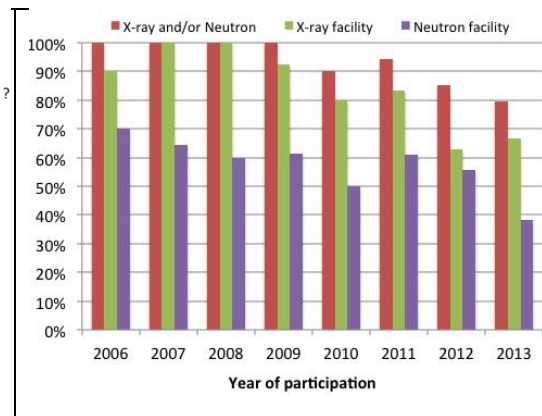


Figure 3: Percentages of 2006-2013 participants that used Neutron and/or X-ray facilities after attending the school².

¹As determined by searches of the internet and facility user records between 2009-2011.

²Derived from a 2014 survey sent to participants from 2006-2013.

distribution of the participants over the different states or territories generally tracks the distribution of the applicants.

Most participants perform a neutron and/or X-ray experiment at a facility in the years directly following their attendance at the school (Figure 3). Additionally, many of the participants continued to utilize these sources well past their graduate studies in their post-doctoral research positions and beyond. In fact, 70% of the participants who attended the school in the first year (1999) are currently active facility users, while averaged over 1999-2006 this percentage is at least 44% (see Figure 2). To date, four of the school's alumni have been invited to return to the school as lecturers, as they have become recognized experts in the field.

Future Plans

The purpose of the school is to give the participants the opportunity to learn the fundamentals of the interaction of x-rays and neutrons with matter, as well as the methods of producing synchrotron radiation and neutrons. The school will dwell on the applications of these techniques to various scientific or technological areas, providing hands-on experience with instruments at neutron (HFIR, SNS) and x-ray (APS) facilities. The course, which will deal with all details of the interactions of x-rays and neutrons with matter, will be taught by leading experts in the field working at national facilities and universities and will represent a unique educational opportunity. The continuing participation of lecturers from outside the two organizing national laboratories is considered essential to preserving the national character of the school.

The school's directors will select at least 60 participants each year, consisting of graduate students from North American universities, postdoctoral researchers, investigators from U.S. universities, national laboratories and industries. The primary audience for the school is graduate students from U.S. institutions near the beginning of their thesis studies; therefore this group will make up at least 75% of each class. Due to capacity limitations, we expect no more than 70 students a year.

The National School on Neutron and X-ray Scattering will continue to be held for a period of two weeks, with dates chosen to minimize overlap with the academic year, other schools, and conferences, yet coinciding with the operation of the three facilities involved. The students will spend approximately one week at Argonne National Laboratory and one week at Oak Ridge National Laboratory, and if possible, the site at which the school starts is alternated each year. The 19th National School on Neutron and X-ray Scattering will be held August 5-19, 2017.

Neutron Scattering Studies of High-Temperature Superconductors

J. M. Tranquada (jtran@bnl.gov), G. D. Gu, and I. A. Zaliznyak
Condensed Matter Physics & Materials Science Department
Brookhaven National Laboratory, Upton, NY 11973-5000

Program Scope

This program is organized around the challenge of understanding the antiferromagnetic spin correlations characteristic of high-temperature superconductors, with particular focus on systems such as copper oxides and the iron-based superconductors. The main experimental tool is neutron scattering, with experiments performed at the best facilities in the U.S. and abroad. Problems addressed include: doping of correlated insulators, self-organized spin and charge inhomogeneities (such as stripes), electron-phonon coupling, spin dynamics, quantum magnetism in low-dimensional systems, and the impact of disorder. Growth of suitable single-crystal samples is an essential part of the program, with complementary characterizations performed in collaboration with other Brookhaven groups, especially at the National Synchrotron Light Source II; this includes synthesis of new topological insulators. There are also close interactions with the Center for Emergent Superconductivity, an Energy Frontier Research Center. This program leads the Instrument Development Team for HYSPEC, an inelastic spectrometer with polarization analysis, now operating at the Spallation Neutron Source; it also participates in the US-Japan Cooperative Program on Neutron Scattering, which has partial access to the cold-neutron triple-axis spectrometer at the High Flux Isotope Reactor.

Recent Progress

Intertwined order in cuprates: The concept of intertwined order has been developed [with Kivelson (Stanford) and Fradkin (Illinois)] as a counterpoint to the idea of competing order. In the latter, density wave orders compete with superconductivity. In the new concept, the strong interactions that lead to pairing may also result in intertwined charge and/or spin orders. As a physical example of this, we have observed the coexistence of incommensurate spin fluctuations with superconductivity in $\text{La}_{2-x}\text{Ba}_x\text{CuO}_4$ (LBCO) with $x = 0.095$ ($T_c = 32$ K); in particular, there is no spin gap or resonance in the superconducting state, contrary to the behavior in optimally doped cuprates. More recently, we have demonstrated similar behavior in $\text{La}_{2-x}\text{Sr}_x\text{CuO}_4$ (LSCO) with $x = 0.07$ ($T_c = 20$ K), including weak spin-stripe order.

LBCO exhibits charge and spin stripe order in a low-temperature crystal structure with inequivalent Cu-O bonds in the planes. This anisotropy is associated with a particular tilt pattern of the CuO_6 octahedra. We have now measured the tilt dynamics associated with this pattern as

a function of temperature. Unlike soft-mode behavior, the tilt fluctuations remain gapless at higher temperatures. The presence of these low-energy fluctuations in the higher-temperature phases reconciles the lack of temperature dependent changes found in pair-distribution-function (PDF) analyses, due to energy integration in the scattering measurements used in the PDF studies. We have also found that these gapless tilt fluctuations, as well as weak superlattice peaks, are present in LSCO with $x = 0.07$. These results indicate that the lattice symmetry of LSCO is lower than commonly assumed, and provides an explanation for observations of weak charge and spin stripe order in LSCO.

Superconducting iron chalcogenides: Our neutron scattering measurements on superconducting $\text{FeTe}_{1-x}\text{S}_x$ (from BNL collaborator Petrovic) and $\text{FeTe}_{1-x}\text{Se}_x$ reveal low-energy spin fluctuations with a momentum dependence that changes with temperature. We have found that we can model the Q dependence of the scattering with simple models of four-spin plaquettes that are antiferromagnetic with respect to neighboring plaquettes. The plaquette local symmetry changes with doping, from C_4 for FeTe parent system to C_2 for superconducting material compositions. In superconducting compositions near optimal doping, the changes with temperature correspond to a change in the effective modulation wave vector. Concomitantly, we have detected a thermal variation in the tetrahedral bond angle, which is known to impact orbital occupancy and hybridization.

We have also detected a surprising phonon mode. First observed as an acoustic mode near the allowed (100) peak of the low-temperature monoclinic phase of $\text{Fe}_{1.1}\text{Te}$, it survives at higher temperatures as a “forbidden” mode in the tetragonal phase, and is also detected in superconducting $\text{FeTe}_{1-x}\text{Se}_x$. Investigations are continuing in an attempt to explain this unexpected feature.

Orbital-exchange magnetism: One of us (I.Z.) collaborated with M. Aronson (formerly BNL/SBU, now Texas A&M) on a study of magnetism in the metallic compound $\text{Yb}_2\text{Pt}_2\text{Pb}$. This system was initially of interest as a potential example of the Shastry-Sutherland lattice, containing two-dimensional layers of Yb dimers with frustrated inter-dimer couplings and large Yb moments ($J = 7/2$) [1]. It was surprising, then, when inelastic neutron scattering measurements revealed a spectrum corresponding to a system of $S = 1/2$ chains, with dispersion perpendicular to the dimer layers. The structure actually contains 2-leg ladders of antiferromagnetically-ordered Yb ions; however, the orbital configuration only allows interactions along the ladder’s legs. Theoretical analysis shows that, because of strong-spin orbit coupling, the exchange of a pair of electrons between neighboring electrons along a ladder leg causes both moments to flip, which is analogous to an excitation of a pair of spinons in an $S = 1/2$ chain, despite the large Yb moments. Given that the orbital exchange is charge neutral, the result is 1D behavior with separation of the orbital and charge degrees of freedom.

Topological crystalline insulators and chiral magnetic effect: Given the excitement about topological quantum materials, we have explored a few systems through synthesis and

transport measurements. In particular, we have studied the impact of In substitution in $\text{Pb}_{1-x}\text{Sn}_x\text{Te}$. This system is of interest as a potential topological crystalline insulator; however, defects tend to render the bulk metallic. Substitution of In can tune the carrier concentration. For $x = 0.5$, we found that the system becomes superconducting for an In concentration of 10%, with T_c reaching a maximum of 4.7 K with 30% In. In contrast, for $x = 0.3$, 6% In tunes the bulk to an insulating state but leaves metallic surface states.

One of us (G.G.) has grown high quality crystals of ZrTe_5 , which was predicted to be a large-gap quantum spin Hall insulator [2]. Instead, measurements and theory by BNL collaborators Q. Li and D. Kharzeev, respectively, revealed that this compound is a Dirac semimetal that exhibits the chiral magnetic effect, a negative magneto-resistance that occurs when the current flows parallel to the applied magnetic field. This effect has the potential to yield a dissipationless current.

Future Plans

Charge stripe fluctuations in nickelates: In collaboration with D. Reznik (U. Colorado), we will continue to investigate charge-stripe fluctuations in $\text{La}_{2-x}\text{Sr}_x\text{NiO}_4$. Recent measurements at HYSPEC (SNS) on a crystal with $x = 0.25$ provide evidence for a nematic phase and demonstrate that the charge-stripped excitations have an anisotropic dispersion, with a lower velocity along the modulation direction [3]. New measurements on an $x = 0.33$ crystal obtained at ARCS (SNS) are presently being analyzed.

Polarized-beam studies of $\text{FeTe}_{1-x}\text{Se}_x$: The polarized-beam option is now fully functional at HYSPEC [4]. We have begun to use it to separate magnetic and lattice excitations in superconducting $\text{FeTe}_{1-x}\text{Se}_x$. For more on this, see the abstract by I. A. Zaliznyak.

Spin dynamics of superconducting $\text{La}_{1.9}\text{Ca}_{1.1}\text{Cu}_2\text{O}_{6+\delta}$: We have begun an investigation of spin fluctuations in $\text{La}_{1.9}\text{Ca}_{1.1}\text{Cu}_2\text{O}_{6+\delta}$. Large crystals have been grown and then annealed in our high-pressure oxygen furnace, yielding the first superconducting crystals. Neutron scattering measurements have been performed at SEQUOIA (SNS) on crystals with $T_c = 45$ K and 55 K. (A recent post-annealing study has demonstrated that T_c can be raised to 62 K [5].) The rotating crystal measurements make it straightforward to identify the bilayer structure factor of the magnetic excitations. An initial survey of the data indicates an absence of spin gap or resonance features in the superconducting state, similar to what we have observed in underdoped LBCO and LSCO. Data analysis is continuing.

References

1. M. S. Kim and M. C. Aronson, Phys. Rev. Lett. **110**, 017201 (2013).
2. H. M. Weng, X. Dai, and Z. Fang, Phys. Rev. X **4**, 011002 (2014).
3. R. D. Zhong, B. L. Winn, G. D. Gu, D. Reznik, and J. M. Tranquada, “Evidence for a nematic phase in $\text{La}_{1.75}\text{Sr}_{0.25}\text{NiO}_4$,” arXiv:1608.04799. ^[1]_[SEP]

4. I. A. Zaliznyak, A. T. Savici, V. O. Garlea, B. Winn, J. Schneeloch, J. M. Tranquada, G. D. Gu, A. F. Wang, and C. Petrovic, “Polarized neutron scattering on HYSPEC: the HYbrid SPECtrometer at SNS,” arXiv:1610.06018.
5. J. Schneeloch and G. D. Gu (unpublished).

Publications

1. M. Hücker, N. B. Christensen, A. T. Holmes, E. Blackburn, E. M. Forgan, R. Liang, D. A. Bonn, W. N. Hardy, O. Gutowski, M. v. Zimmermann, S. M. Hayden, and J. Chang, “Competing charge, spin, and superconducting orders in underdoped YBa₂Cu₃O_y,” *Phys. Rev. B* **90**, 054514 (2014). ^[1]_{SEP}
2. R. D. Zhong, J. A. Schneeloch, T. S. Liu, F. E. Camino, J. M. Tranquada, and G. D. Gu, “Superconductivity induced by In substitution into the topological crystalline insulator Pb_{0.5}Sn_{0.5}Te,” *Phys. Rev. B* **90**, 020505(R) (2014). ^[1]_{SEP} ^[1]_{SEP}
3. Y. M. Dai, A. Akrap, J. Schneeloch, R. D. Zhong, T. S. Liu, G. D. Gu, Q. Li, and C. C. Homes, “Spectral weight transfer in strongly correlated Fe_{1.03}Te,” *Phys. Rev. B* **90**, 121114 (2014). ^[1]_{SEP}
4. Nicoletti, E. Casandruc, Y. Laplace, V. Khanna, C. R. Hunt, S. Kaiser, S. S. Dhesi, G. D. Gu, J. P. Hill, and A. Cavalleri, “Optically induced superconductivity in striped La_{2-x}Ba_xCuO₄ by polarization-selective excitation in the near infrared,” *Phys. Rev. B* **90**, 100503 (2014). ^[1]_{SEP}
5. L. J. Sandilands, A. A. Reijnders, A. H. Su, V. Baydina, Z. Xu, A. Yang, G. Gu, T. Pedersen, F. Borondics, and K. S. Burch, “Origin of the insulating state in exfoliated high-T_c two-dimensional atomic crystals,” *Phys. Rev. B* **90**, 081402 (2014). ^[1]_{SEP}
6. M. B. Stone, Y. Chen, D. H. Reich, C. Broholm, G. Xu, J. R. D. Copley, and J. C. Cook, “Magnons and continua in a magnetized and dimerized spin-1 chain,” *Phys. Rev. B* **90**, 094419 (2014). ^[1]_{SEP}
7. X. Xi, X.-G. He, F. Guan, Z. Liu, R. D. Zhong, J. A. Schneeloch, T. S. Liu, G. D. Gu, X. Du, Z. Chen, X. G. Hong, W. Ku, and G. L. Carr, “Bulk Signatures of Pressure-Induced Band Inversion and Topological Phase Transitions in Pb_{1-x}Sn_xSe,” *Phys. Rev. Lett.* **113**, 096401 (2014).
8. T. Yilmaz, I. Pletikosić, A. P. Weber, J. T. Sadowski, G. D. Gu, A. N. Caruso, B. Sinkovic, and T. Valla, “Absence of a Proximity Effect for a Thin-Films of a Bi₂Se₃ Topological Insulator Grown on Top of a Bi₂Sr₂CaCu₂O_{8+δ} Cuprate Superconductor,” *Phys. Rev. Lett.* **113**, 067003 (2014). ^[1]_{SEP}
9. Z. Xu, C. Stock, S. Chi, A. I. Kolesnikov, G. Xu, G. Gu, and J. M. Tranquada, “Neutron-Scattering Evidence for a Periodically Modulated Superconducting Phase in the Underdoped Cuprate La_{1.905}Ba_{0.095}CuO₄,” *Phys. Rev. Lett.* **113**, 177002 (2014).

10. H. Hu, Y. Zhu, X. Shi, Q. Li, R. Zhong, J. A. Schneeloch, G. Gu, J. M. Tranquada, and S. J. L. Billinge, “Nanoscale coherent intergrowthlike defects in a crystal of $\text{La}_{1.9}\text{Ca}_{1.1}\text{Cu}_2\text{O}_{6+d}$ made superconducting by high-pressure oxygen annealing,” *Phys. Rev. B* **90**, 134518 (2014).
11. P. Zhang, P. Richard, N. Xu, Y.-M. Xu, J. Ma, T. Qian, A. V. Fedorov, J. D. Denlinger, G. D. Gu, and H. Ding, “Observation of an electron band above the Fermi level in $\text{FeTe}_{0.55}\text{Se}_{0.45}$ from in-situ surface doping,” *Appl. Phys. Lett.* **105**, 172601 (2014). [SEP]
12. P. M. Dean, A. J. A. James, A. C. Walters, V. Bisogni, I. Jarrige, M. Hücker, E. Giannini, M. Fujita, J. Pelliciani, Y. B. Huang, R. M. Konik, T. Schmitt, and J. P. Hill, “Itinerant effects and enhanced magnetic interactions in Bi-based multilayer cuprates,” *Phys. Rev. B* **90**, 220506 (2014). [SEP]
13. Anand, S. Buvaev, A. F. Hebard, D. B. Tanner, Z. Chen, Z. Li, K. Choudhary, S. B. Sinnott, G. Gu, and C. Martin, “Temperature-driven band inversion in $\text{Pb}_{0.77}\text{Sn}_{0.23}\text{Se}$: Optical and Hall effect studies,” *Phys. Rev. B* **90**, 235143 (2014). [SEP]
14. S. Frank, A. Huber, U. Ammerahl, M. Hücker, and C. A. Kuntscher, “Polarization-dependent infrared reflectivity study of $\text{Sr}_{2.5}\text{Ca}_{1.5}\text{Cu}_{24}\text{O}_{41}$ under pressure: Charge dynamics, charge distribution, and anisotropy,” *Phys. Rev. B* **90**, 224516 (2014). [SEP]
15. J. D. Rameau, T. J. Reber, H.-B. Yang, S. Akhanjee, G. D. Gu, P. D. Johnson, and S. Campbell, “Nearly perfect fluidity in a high-temperature superconductor,” *Phys. Rev. B* **90**, 134509 (2014). [SEP]
16. P. Zareapour, A. Hayat, S. Y. F. Zhao, M. Kreshchuk, Y. K. Lee, A. A. Reijnders, A. Jain, Z. Xu, T. S. Liu, G. D. Gu, S. Jia, R. J. Cava, and K. S. Burch, “Evidence for a new excitation at the interface between a high- T_c superconductor and a topological insulator,” *Phys. Rev. B* **90**, 241106 (2014). [SEP]
17. Zeljkovic, J. Nieminen, D. Huang, T.-R. Chang, Y. He, H.-T. Jeng, Z. Xu, J. Wen, G. Gu, H. Lin, R. S. Markiewicz, A. Bansil, and J. E. Hoffman, “Nanoscale Interplay of Strain and Doping in a High-Temperature Superconductor,” *Nano Lett.* **14**, 6749 (2014). [SEP]
18. J. A. Schneeloch, Z. Xu, J. Wen, P. M. Gehring, C. Stock, M. Matsuda, B. Winn, G. Gu, S. M. Shapiro, R. J. Birgeneau, T. Ushiyama, Y. Yanagisawa, Y. Tomioka, T. Ito, and G. Xu, “Neutron inelastic scattering measurements of low-energy phonons in the multiferroic BiFeO_3 ,” *Phys. Rev. B* **91**, 064301 (2015).
19. J. M. Tranquada, “Exploring intertwined orders in cuprate superconductors,” *Physica B* **460**, 136 (2015).

20. Z. Xu, J. A. Schneeloch, R. D. Zhong, J. A. Rodriguez-Rivera, L. W. Harriger, R. J. Birgeneau, G. D. Gu, J. M. Tranquada, and G. Xu, “Low-energy phonons and superconductivity in Sn_{0.8}In_{0.2}Te,” *Phys. Rev. B* **91**, 054522 (2015).
21. A. Zaliznyak and J. M. Tranquada, “Neutron Scattering and Its Application to Strongly Correlated Systems,” in *Strongly Correlated Systems*, Springer Series in Solid-State Sciences, Vol. 180, edited by A. Avella and F. Mancini (Springer Berlin Heidelberg, 2015) pp. 205–235. ^[1]_[SEP]
22. E. Fradkin, S. A. Kivelson, and J. M. Tranquada, “Colloquium : Theory of intertwined orders in high temperature superconductors,” *Rev. Mod. Phys.* **87**, 457 (2015). ^[1]_[SEP]
23. R. Zhong, X. He, J. A. Schneeloch, C. Zhang, T. Liu, I. Pletikosic, T. Yilmaz, B. Sinkovic, Q. Li, W. Ku, T. Valla, J. M. Tranquada, and G. Gu, “Surface-state-dominated transport in crystals of the topological crystalline insulator In-doped Pb_{1-x}Sn_xTe,” *Phys. Rev. B* **91**, 195321 (2015).
24. Zaliznyak, A. T. Savici, M. Lumsden, A. Tsvelik, R. Hu, and C. Petrovic, “Spin-liquid polymorphism in a correlated electron system on the threshold of superconductivity,” *Proc. Nat. Acad. Sci.* **112**, 10316 (2015).
25. E. S. Bozin, R. Zhong, K. R. Knox, G. Gu, J. P. Hill, J. M. Tranquada, and S. J. L. Billinge, “Reconciliation of local and long-range tilt correlations in underdoped La_{2-x}Ba_xCuO₄ ($0 \leq x \leq 0.155$),” *Phys. Rev. B* **91**, 054521 (2015).
26. Lee, C. K. Kim, J. Lee, S. J. L. Billinge, R. Zhong, J. A. Schneeloch, T. Liu, T. Valla, J. M. Tranquada, G. Gu, and J. C. S. Davis, “Imaging Dirac-mass disorder from magnetic dopant atoms in the ferromagnetic topological insulator Cr_x(Bi_{0.1}Sb_{0.9})_{2-x}Te₃,” *Proc. Natl. Acad. Sci. USA* **112**, 1316 (2015).
27. Q. Meng, M.-G. Han, J. Tao, G. Xu, D. O. Welch, and Y. Zhu, “Velocity of domain- wall motion during polarization reversal in ferroelectric thin films: Beyond Merz’s Law,” *Phys. Rev. B* **91**, 054104 (2015).
28. J. Wang, R. Zhong, S. Li, Y. Gan, Z. Xu, C. Zhang, T. Ozaki, M. Matsuda, Y. Zhao, Q. Li, G. Xu, G. Gu, J. M. Tranquada, R. J. Birgeneau, and J. Wen, “Substitution of Ni for Fe in superconducting Fe_{0.98}Te_{0.5}Se_{0.5} depresses the normal-state conductivity but not the magnetic spectral weight,” *Phys. Rev. B* **91**, 014501 (2015).
29. Winn, Barry, Filges, Uwe, Garlea, V. Ovidiu, Graves-Brook, Melissa, Hagen, Mark, Jiang, Chenyang, Kenzelmann, Michel, Passell, Larry, Shapiro, Stephen M., Tong, Xin, and Zaliznyak, Igor, “Recent progress on HYSPEC, and its polarization analysis capabilities,” *EPJ Web of Conferences* **83**, 03017 (2015).
30. S. Benhabib, A. Sacuto, M. Civelli, I. Paul, M. Cazayous, Y. Gallais, M.-A. Measson, R. D. Zhong, J. Schneeloch, G. D. Gu, D. Colson, and A. Forget, “Collapse of the Normal-

State Pseudogap at a Lifshitz Transition in the $\text{Bi}_2\text{Sr}_2\text{CaCu}_2\text{O}_{8+\delta}$ Cuprate Superconductor,” *Phys. Rev. Lett.* **114**, 147001 (2015). ^[L]_[SEP]

31. E. Casandruc, D. Nicoletti, S. Rajasekaran, Y. Laplace, V. Khanna, G. D. Gu, J. P. Hill, and A. Cavalleri, “Wavelength-dependent optical enhancement of superconducting interlayer coupling in $\text{La}_{1.885}\text{Ba}_{0.115}\text{CuO}_4$,” *Phys. Rev. B* **91**, 174502 (2015). ^[L]_[SEP]
32. Z.-Y. Du, D.-L. Fang, Z.-Y. Wang, D. Guan, X. Yang, H. Yang, G.-D. Gu, and H.-H. Wen, “Investigation of scanning tunneling spectra on iron-based superconductor $\text{FeSe}_{0.5}\text{Te}_{0.5}$,” *Acta Phys. Sinica* **64**, 97401 (2015). ^[L]_[SEP]
33. C. C. Homes, Y. M. Dai, J. S. Wen, Z. J. Xu, and G. D. Gu, “ $\text{FeTe}_{0.55}\text{Se}_{0.45}$: A multiband superconductor in the clean and dirty limit,” *Phys. Rev. B* **91**, 144503 (2015). ^[L]_[SEP]
34. P. D. Johnson, H.-B. Yang, J. D. Rameau, G. D. Gu, Z.-H. Pan, T. Valla, M. Weinert, and A. V. Fedorov, “Spin-Orbit Interactions and the Nematicity Observed in the Fe- Based Superconductors,” *Phys. Rev. Lett.* **114**, 167001 (2015). ^[L]_[SEP]
35. D. E. McNally, J. W. Simonson, J. J. Kistner-Morris, G. J. Smith, J. E. Hassinger, L. DeBeer-Schmidt, A. I. Kolesnikov, I. A. Zaliznyak, and M. C. Aronson, “ CaMn_2Sb_2 : Spin waves on a frustrated antiferromagnetic honeycomb lattice,” *Phys. Rev. B* **91**, 180407 (2015).
36. D. Mou, R. Jiang, V. Taufour, R. Flint, S. L. Bud’ko, P. C. Canfield, J. S. Wen, Z. J. Xu, G. Gu, and A. Kaminski, “Strong interaction between electrons and collective excitations in the multiband superconductor MgB_2 ,” *Phys. Rev. B* **91**, 140502 (2015). ^[L]_[SEP]
37. M. Naamneh, Y. Lubashevsky, E. Lahoud, G. D. Gu, and A. Kanigel, “Anisotropic scattering rate in Fe-substituted $\text{Bi}_2\text{Sr}_2\text{Ca}(\text{Cu}_{1-x}\text{Fe}_x)_2\text{O}_{8+\delta}$,” *Phys. Rev. B* **91**, 205138 (2015). ^[L]_[SEP]
38. D. Phelan, E. Rodriguez, J. Gao, Y. Bing, Z.-G. Ye, Q. Huang, J. Wen, G. Xu, C. Stock, M. Matsuura, and P. Gehring, “Phase diagram of the relaxor ferroelectric $(1-x)\text{Pb}(\text{Mg}_{1/3}\text{Nb}_{2/3})\text{O}_3+x\text{PbTiO}_3$ revisited: a neutron powder diffraction study of the relaxor skin effect,” *Phase Transitions* **88**, 283 (2015). ^[L]_[SEP]
39. R. Y. Chen, S. J. Zhang, J. A. Schneeloch, C. Zhang, Q. Li, G. D. Gu, and N. L. Wang, “Optical spectroscopy study of the three-dimensional Dirac semimetal ZrTe_5 ,” *Phys. Rev. B* **92**, 075107 (2015). ^[L]_[SEP]
40. S. Cho, B. Dellabetta, R. Zhong, J. Schneeloch, T. Liu, G. Gu, M. J. Gilbert, and N. Mason, “Aharonov-Bohm oscillations in a quasi-ballistic three-dimensional topological insulator nanowire,” *Nat. Commun.* **6** (2015); <http://dx.doi.org/10.1038/ncomms8634>. ^[L]_[SEP]

41. G. Du, Z. Du, D. Fang, H. Yang, R. D. Zhong, J. Schneeloch, G. D. Gu, and H.-H. Wen, “Fully gapped superconductivity in In-doped topological crystalline insulator $\text{Pb}_{0.5}\text{Sn}_{0.5}\text{Te}$,” *Phys. Rev. B* **92**, 020512 (2015). ^[1]_{SEP}
42. W. Si, C. Zhang, L. Wu, T. Ozaki, G. Gu, and Q. Li, “Superconducting thin films of (100) and (111) oriented indium doped topological crystalline insulator SnTe ,” *Appl. Phys. Lett.* **107**, 092601 (2015).
43. A. Kaminski, T. Kondo, T. Takeuchi, and G. Gu, “Pairing, pseudogap and Fermi arcs in cuprates,” *Phil. Mag.* **95**, 453 (2015).
44. A. J. Stollenwerk, N. Hurley, B. Beck, K. Spurgeon, T. E. Kidd, and G. Gu, “Manipulation of subsurface carbon nanoparticles in $\text{Bi}_2\text{Sr}_2\text{CaCu}_2\text{O}_{8+\delta}$ using a scanning tunneling microscope,” *Phys. Rev. B* **91**, 125425 (2015).
45. W. Wang, F. Yang, C. Gao, J. Jia, G. D. Gu, and W. Wu, “Visualizing ferromagnetic domains in magnetic topological insulators,” *APL Materials* **3**, 083301 (2015). ^[1]_{SEP}
46. H.-M. Yi, C.-Y. Chen, X. Sun, Z.-J. Xie, Y. Feng, A.-J. Liang, Y.-Y. Peng, S.-L. He, L. Zhao, G.-D. Liu, X.-L. Dong, J. Zhang, C.-T. Chen, Z.-Y. Xu, G.-D. Gu, and X.-J. Zhou, “Electronic Structure, Irreversibility Line and Magnetoresistance of $\text{Cu}_{0.3}\text{Bi}_2\text{Se}_3$ Superconductor,” *Chinese Phys. Lett.* **32**, 067401 (2015). ^[1]_{SEP}
47. H. Jacobsen, I. A. Zaliznyak, A. T. Savici, B. L. Winn, S. Chang, M. Hücker, G. D. Gu, and J. M. Tranquada, “Neutron scattering study of spin ordering and stripe pinning in superconducting $\text{La}_{1.93}\text{Sr}_{0.07}\text{CuO}_4$,” *Phys. Rev. B* **92**, 174525 (2015). ^[1]_{SEP}
48. J. A. Schneeloch, Z. Xu, B. Winn, C. Stock, P. M. Gehring, R. J. Birgeneau, and G. Xu, “Phonon coupling to dynamic short-range polar order in a relaxor ferroelectric near the morphotropic phase boundary,” *Phys. Rev. B* **92**, 214302 (2015). ^[1]_{SEP}
49. S.-H. Baek, Y. Utz, M. Hücker, G. D. Gu, B. Büchner, and H.-J. Grafe, “Magnetic field induced anisotropy of ^{139}La spin-lattice relaxation rates in stripe ordered $\text{La}_{1.875}\text{Ba}_{0.125}\text{CuO}_4$,” *Phys. Rev. B* **92**, 155144 (2015). ^[1]_{SEP}
50. S. Benhabib, Y. Gallais, M. Cazayous, M.-A. Méasson, R. D. Zhong, J. Schneeloch, A. Forget, G. D. Gu, D. Colson, and A. Sacuto, “Three energy scales in the superconducting state of hole-doped cuprates detected by electronic Raman scattering,” *Phys. Rev. B* **92**, 134502 (2015). ^[1]_{SEP}
51. R. Y. Chen, Z. G. Chen, X.-Y. Song, J. A. Schneeloch, G. D. Gu, F. Wang, and N. L. Wang, “Magnetoinfrared Spectroscopy of Landau Levels and Zeeman Splitting of Three-Dimensional Massless Dirac Fermions in ZrTe_5 ,” *Phys. Rev. Lett.* **115**, 176404 (2015).
52. E. M. Forgan, E. Blackburn, A. T. Holmes, A. K. R. Briffa, J. Chang, L. Bouchenoire, S. D. Brown, R. Liang, D. Bonn, W. N. Hardy, N. B. Christensen, M. V. Zimmermann, M.

- Hucker, and S. M. Hayden, “The microscopic structure of charge density waves in underdoped YBa₂Cu₃O_{6.54} revealed by X-ray diffraction,” *Nat. Commun.* **6**, 10064 (2015). ^[1]_[SEP]
53. A. Kogar, S. Vig, A. Thaler, M. H. Wong, Y. Xiao, D. Reig-i-Plessis, G. Y. Cho, T. Valla, Z. Pan, J. Schneeloch, R. Zhong, G. D. Gu, T. L. Hughes, G. J. MacDougall, T.-C. Chiang, and P. Abbamonte, “Surface Collective Modes in the Topological Insulators Bi₂Se₃ and Bi_{0.5}Sb_{1.5}Te_{3-x}Sex,” *Phys. Rev. Lett.* **115**, 257402 (2015). ^[1]_[SEP]
54. A. Pramanick, A. Glavic, G. Samolyuk, A. A. Aczel, V. Lauter, H. Ambaye, Z. Gai, J. Ma, A. D. Stoica, G. M. Stocks, S. Wimmer, S. M. Shapiro, and X.-L. Wang, “Direct in situ measurement of coupled magnetostructural evolution in a ferromagnetic shape memory alloy and its theoretical modeling,” *Phys. Rev. B* **92**, 134109 (2015). ^[1]_[SEP]
55. Z. Yu, L. Wang, Q. Hu, J. Zhao, S. Yan, K. Yang, S. Sinogeikin, G. Gu, and H.-K. Mao, “Structural phase transitions in Bi₂Se₃ under high pressure,” *Scientific Reports* **5**, 15939 (2015). ^[1]_[SEP]
56. G. L. Dakovski, T. Durakiewicz, J.-X. Zhu, P. S. Riseborough, G. Gu, S. M. Gilbertson, A. Taylor, and G. Rodriguez, “Quasiparticle dynamics across the full Brillouin zone of Bi₂Sr₂CaCu₂O_{8+δ} traced with ultrafast time and angle-resolved photoemission spectroscopy,” *Structural Dynamics* **2**, 054501 (2015). ^[1]_[SEP]
57. Y.-F. Lv, W.-L. Wang, J.-P. Peng, H. Ding, Y. Wang, L. Wang, K. He, S.-H. Ji, R. Zhong, J. Schneeloch, G.-D. Gu, C.-L. Song, X.-C. Ma, and Q.-K. Xue, “Mapping the Electronic Structure of Each Ingredient Oxide Layer of High-T_c Cuprate Superconductor Bi₂Sr₂CaCu₂O_{8+δ},” *Phys. Rev. Lett.* **115**, 237002 (2015). ^[1]_[SEP]
58. Z. Xu, J. A. Schneeloch, J. Wen, E. S. Božin, G. E. Granroth, B. L. Winn, M. Feyngenson, R. J. Birgeneau, G. Gu, I. A. Zaliznyak, J. M. Tranquada, and G. Xu, “Thermal evolution of antiferromagnetic correlations and tetrahedral bond angles in superconducting FeTe_{1-x}Sex,” *Phys. Rev. B* **93**, 104517 (2016). ^[1]_[SEP]
59. L. S. Wu, W. J. Gannon, I. A. Zaliznyak, A. M. Tsvelik, M. Brockmann, J.-S. Caux, M. S. Kim, Y. Qiu, J. R. D. Copley, G. Ehlers, A. Podlesnyak, and M. C. Aronson, “Orbital-exchange and fractional quantum number excitations in an f-electron metal, Yb₂Pt₂Pb,” *Science* **352**, 1206 (2016). ^[1]_[SEP]
60. D. M. Fobes, I. A. Zaliznyak, J. M. Tranquada, Z. Xu, G. Gu, X.-G. He, W. Ku, Y. Zhao, M. Matsuda, V. O. Garlea, and B. Winn, “Forbidden phonon: Dynamical signature of bond symmetry breaking in the iron chalcogenides,” *Phys. Rev. B* **94**, 121103 (2016). ^[1]_[SEP]
61. J. Achkar, M. Zwiebler, C. McMahan, F. He, R. Sutarto, I. Djianto, Z. Hao, M. J. P. Gingras, M. Hücker, G. D. Gu, A. Revcolevschi, H. Zhang, Y.-J. Kim, J. Geck, and D. G. Hawthorn, “Nematicity in stripe-ordered cuprates probed via resonant x-ray scattering,” *Science* **351**, 576 (2016). ^[1]_[SEP]

62. S. Alraddadi, W. Hines, T. Yilmaz, G. D. Gu, and B. Sinkovic, “Structural phase diagram for ultra-thin epitaxial Fe₃O₄/MgO(001) films: thickness and oxygen pressure dependence,” *J. Phys.: Condens. Matter* **28**, 115402 (2016). ^[1]_[SEP]
63. S. Cho, R. Zhong, J. A. Schneeloch, G. Gu, and N. Mason, “Kondo-like zero-bias conductance anomaly in a three-dimensional topological insulator nanowire,” *Sci. Rep.* **6**, 21767 (2016). ^[1]_[SEP]
64. C. Homes, Y. M. Dai, J. Schneeloch, R. D. Zhong, and G. D. Gu, “Phonon anomalies in some iron telluride materials,” *Phys. Rev. B* **93**, 125135 (2016). ^[1]_[SEP]
65. W. Müller, L. S. Wu, M. S. Kim, T. Orvis, J. W. Simonson, M. Gamza, D. M. McNally, C. S. Nelson, G. Ehlers, A. Podlesnyak, J. S. Helton, Y. Zhao, Y. Qiu, J. R. D. Copley, J. W. Lynn, I. Zaliznyak, and M. C. Aronson, “Magnetic structure of Yb₂Pt₂Pb: Ising moments on the Shastry-Sutherland lattice,” *Phys. Rev. B* **93**, 104419 (2016). ^[1]_[SEP]
66. J. Achkar, F. He, R. Sutarto, C. McMahan, M. Zwiebler, M. Hucker, G. D. Gu, R. Liang, D. A. Bonn, W. N. Hardy, J. Geck, and D. G. Hawthorn, “Orbital symmetry of charge-density-wave order in La_{1.875}Ba_{0.125}CuO₄ and YBa₂Cu₃O_{6.67},” *Nat. Mater.* **15**, 616 (2016). ^[1]_[SEP]
67. J. Chang, E. Blackburn, O. Ivashko, A. T. Holmes, N. B. Christensen, M. Hucker, R. Liang, D. A. Bonn, W. N. Hardy, U. Rutt, M. v. Zimmermann, E. M. Forgan, and S. M. Hayden, “Magnetic field controlled charge density wave coupling in underdoped YBa₂Cu₃O_{6+x},” *Nat. Commun.* **7**, 11494 (2016). ^[1]_[SEP]
68. V. Khanna, R. Mankowsky, M. Petrich, H. Bromberger, S. A. Cavill, E. Möhr-Vorobeva, D. Nicoletti, Y. Laplace, G. D. Gu, J. P. Hill, M. Först, A. Cavalleri, and S. S. Dhesi, “Restoring interlayer Josephson coupling in La_{1.885}Ba_{0.115}CuO₄ by charge transfer melting of stripe order,” *Phys. Rev. B* **93**, 224522 (2016). ^[1]_[SEP]
69. Q. Li, D. E. Kharzeev, C. Zhang, Y. Huang, I. Pletikosic, A. V. Fedorov, R. D. Zhong, J. A. Schneeloch, G. D. Gu, and T. Valla, “Chiral magnetic effect in ZrTe₅,” *Nat. Phys.* **12**, 550 (2016).
70. Y.-F. Lv, W.-L. Wang, H. Ding, Y. Wang, Y. Ding, R. Zhong, J. Schneeloch, G. D. Gu, L. Wang, K. He, S.-H. Ji, L. Zhao, X.-J. Zhou, C.-L. Song, X.-C. Ma, and Q.-K. Xue, “Electronic structure of the ingredient planes of the cuprate superconductor Bi₂Sr₂CuO_{6+δ}: A comparison study with Bi₂Sr₂CaCu₂O_{8+δ},” *Phys. Rev. B* **93**, 140504 (2016). ^[1]_[SEP]
71. Y.-X. Zhang, L. Zhao, G.-D. Gu, and X.-J. Zhou, “A Reproducible Approach of Preparing High-Quality Overdoped Bi₂Sr₂CaCu₂O_{8+δ} Single Crystals by Oxygen Annealing and Quenching Method,” *Chin. Phys. Lett.* **33**, 067403 (2016).
72. G. Fabbris, M. Hücker, G. D. Gu, J. M. Tranquada, and D. Haskel, “Combined single

crystal polarized XAFS and XRD at high pressure: probing the interplay between lattice distortions and electronic order at multiple length scales in high T_c cuprates,” *High Pressure Res.* **36**, 348 (2016).

73. J. Levallois, M. K. Tran, D. Pouliot, C. N. Presura, L. H. Greene, J. N. Eckstein, J. Uccelli, E. Giannini, G. D. Gu, A. J. Leggett, and D. van der Marel, “Temperature-Dependent Ellipsometry Measurements of Partial Coulomb Energy in Superconducting Cuprates,” *Phys. Rev. X* **6**, 031027 (2016). ^[1]_{SEP}
74. M. Tsvetlik and I. A. Zaliznyak, “Heisenberg necklace model in a magnetic field,” *Phys. Rev. B* **94**, 075152 (2016).
75. Y. Tian, A. A. Reijnders, G. B. Osterhoudt, I. Valmianski, J. G. Ramirez, C. Urban, R. Zhong, J. Schneeloch, G. Gu, I. Henslee, and K. S. Burch, “Low vibration high numerical aperture automated variable temperature raman microscope,” *Rev. Sci. Instrum.* **87**, 043105 (2016).
76. Y. Zhang, C. Hu, Y. Hu, L. Zhao, Y. Ding, X. Sun, A. Liang, Y. Zhang, S. He, D. Liu, L. Yu, G. Liu, X. Dong, G. Gu, C. Chen, Z. Xu, and X. Zhou, “In situ carrier tuning in high temperature superconductor $\text{Bi}_2\text{Sr}_2\text{CaCu}_2\text{O}_{8+\delta}$ by potassium deposition,” *Sci. Bull.* **61**, 1037 (2016). ^[1]_{SEP}
77. Y. Zhong, Y. Wang, S. Han, Y.-F. Lv, W.-L. Wang, D. Zhang, H. Ding, Y.-M. Zhang, L. Wang, K. He, R. Zhong, J. A. Schneeloch, G.-D. Gu, C.-L. Song, X.-C. Ma, and Q.-K. Xue, “Nodeless pairing in superconducting copper-oxide monolayer films on $\text{Bi}_2\text{Sr}_2\text{CaCu}_2\text{O}_{8+\delta}$,” *Sci. Bull.* **61**, 1239 (2016). ^[1]_{SEP}
78. X. M. Chen, V. Thampy, C. Mazzoli, A. M. Barbour, H. Miao, G. D. Gu, Y. Cao, J. M. Tranquada, M. P. M. Dean, and S. B. Wilkins, “Remarkable Stability of Charge Density Wave Order in $\text{La}_{1.875}\text{Ba}_{0.125}\text{CuO}_4$,” *Phys. Rev. Lett.* **117**, 167001 (2016).
79. Aifeng Wang, I. Zaliznyak, Weijun Ren, Lijun Wu, D. Graf, V. O. Garlea, J. B. Warren, E. Bozin, Yimei Zhu, and C. Petrovic, “Magnetotransport study of Dirac fermions in YbMnBi_2 antiferromagnet,” *Phys. Rev. B* **94**, 165161 (2016).

Polymer Conformations and Chain Dynamics under 1D and 2D Rigid Confinement

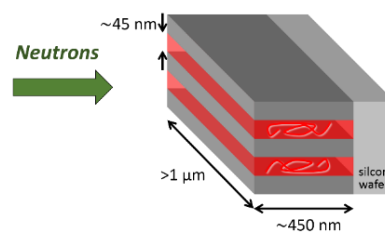
Karen I. Winey, Materials Science and Engineering, University of Pennsylvania

Robert A. Riggleman, Chemical and Biomolecular Engineering, University of Pennsylvania

Program Scope

Polymers are often employed in applications where they are highly confined *and* the polymer motions play a critical role. Examples include pressure-sensitive adhesives, semiconductor fabrication, thin films and coatings, polymer-filled nanoporous materials, and highly filled polymer nanocomposites. A fundamental attribute of polymers under confinement is the shape of the polymer conformation, particularly when the confining dimension is less than 100 nanometers. Simulations and theories have predicted anisotropic polymer conformations when the polymer is confined in one or two dimensions, corresponding to thin films and cylindrical pores. The characteristic size of the polymer is expected to increase parallel to the confining wall and significantly decrease perpendicular to the wall. To date, this prediction has not been experimentally verified. Without knowing the shape of the polymer conformation as a function of confinement dimension, polymer molecular weight, polymer stiffness, and interactions between the polymer and the confining wall, progress towards understanding how confinement affects the motion of polymers will be hampered and largely qualitative.

Small angle neutron scattering (SANS) is the most valuable experimental method for probing the shape and size of polymer conformations. This project employs SANS along with a novel set of rigid templates that enable for the first time the use of SANS to simultaneously measure the polymer conformation parallel and perpendicular to the confining wall. These experiments will directly probe anisotropy in the shape of the polymer conformations under confinement. The impact of confinement in thin films and cylindrical pores will be studied as a function of the confinement dimension relative to the polymer end-to-end distance, as well as the nature of the interactions between the polymer and the confining walls. Molecular dynamics simulations will be performed using confinement parameters that match our template shapes, sizes and polymer-wall interactions to enable quantitative comparisons to our SANS results.



Anisotropic changes in the polymer conformations modify the packing of the chains relative to each other, which alters the density of interchain entanglements and thereby the chain-scale motions. Thus, the impact of polymer confinement will be explored by measuring the center-of-mass motion of the polymer and correlating these results to the changes in polymer conformations detected by SANS. Again, molecular dynamics simulations will provide complimentary insights about the impact of confinement on polymer dynamics from the segmental to the chain scale.

Achieving these goals will impact a broad spectrum of topics within polymer science and engineering from adhesives to thin films to polymer nanocomposites. Our SANS experiments will resolve many of the longstanding controversial issues pertaining to polymers under confinement.

Recent Progress – Polymer Conformation in 1D Confinement

Figure 1a uses earlier theoretical and molecular dynamics simulation work to estimate the polymer conformations under 1D confinement (between parallel walls [1]). The degree of confinement (h/R_{ee}) is defined by the distance between the walls (h) normalized by the polymer end-to-end distance (R_{ee}). The arrows indicate the planned experiments using a deep channel template (see schematic above) by varying the polymer molecular weight (100, 200, 400 and 1000 kg/mol). For the specific confinement parameter of $h/R_{ee} = 1.18$, **Figure 1b** shows the expected SANS profiles for the confined polymer parallel (green) and perpendicular (red) to the confining walls relative to the bulk polymer. These profiles demonstrate that if the confined and unconfined directions could be simultaneously measured, the differences in $R_{ee,parallel}$ and $R_{ee,perpendicular}$ would be measurable.

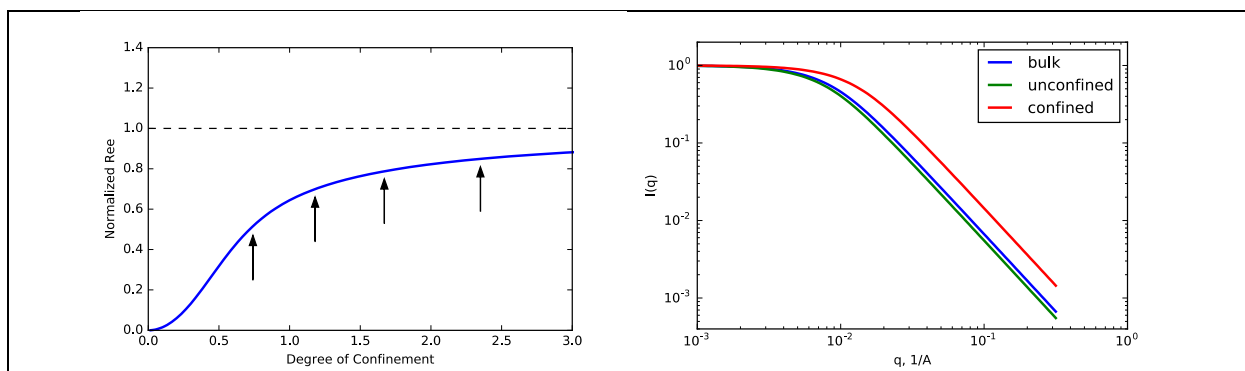


Figure 1. Left: Normalized R_{ee} ($R_{ee}/R_{ee,bulk}$) vs. degree of confinement (h/R_{ee}) in 1D confinement [1]. Arrows indicate planned experiments using channel templates of $\langle h \rangle \approx 50$ nm and polymers of various molecular weights. Right: Calculated SANS scattering profiles for 400 kg/mol polystyrene ($h/R_{ee} \approx 1.18$) in the bulk (blue) compared with polymer confined to a channel (red – perpendicular to channel wall; green – parallel to channel wall).

A novel attribute of our project is the design of a rigid template that allows for the simultaneous detection of polymer conformations parallel and perpendicular to the confining walls; see schematic above. This direct comparison is not possible in a thin film (supported or free standing). Rather, we have designed deep, narrow channel templates in collaboration with Dr. Dan Sanders of IBM Research – Almaden; see schematic above. The channels are first etched into silica and then further narrowed by coating with alumina using atomic layer deposition. The first version of the channel templates was small with slight discontinuities between the channels (**Figure 2**) and gave modest SANS results in May 2016, **Figure 3**. Using a larger mask and a single exposure, the second version of the templates improved channel perfection and increased sample area by 16x, which allows for a larger beam. The channels are

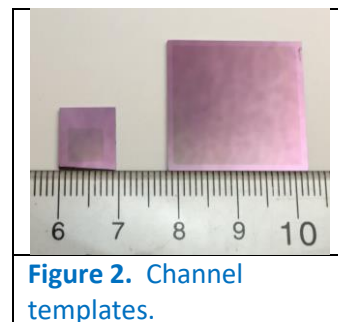


Figure 2. Channel templates.

50 nm wide and 300 nm deep with a pitch of 400 nm. **Figure 3** shows the SANS results from these larger templates from October 2016 with significantly better signal to noise, such that the periodic scattering peaks from the channels is evident in the direction perpendicular to the channels.

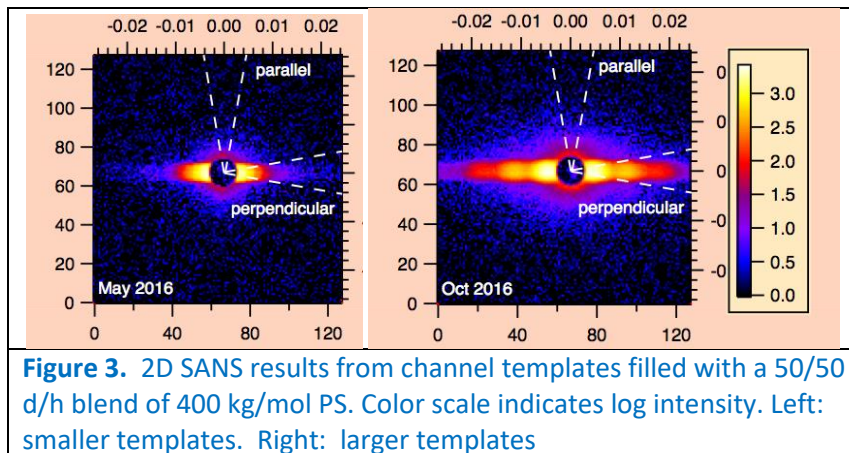


Figure 3. 2D SANS results from channel templates filled with a 50/50 d/h blend of 400 kg/mol PS. Color scale indicates log intensity. Left: smaller templates. Right: larger templates

Analysis of these data (October 2016) are now underway. **Figure 4** shows excellent agreement between the SANS profile from an isotropic thick film of polystyrene (PS) (100 kg/mol) and the expected SANS profile for a Gaussian chain, $R_{g,bulk}$. To capture the anisotropy of the SANS data, the scattering data parallel and perpendicular to the confining wall are extracted from the 2D scattering data by integrating 20° sectors, see **Figure 3b**. The results are shown in **Figure 4** along with the polymer chain scattering according to Sussman *et al.*, wherein $R_{g,parallel} > R_{g,bulk} > R_{g,perpendicular}$. Perpendicular to the confining walls (blue) the scattering profile has distinct oscillations, which are absent in the data parallel to the confining walls (green). We are currently developing a model by which to remove the contribution from the channel templates, which will be aided by critical dimension SAXS (CD-SAXS) to quantitatively measure the shape and evaluate the uniformity of the channel templates.

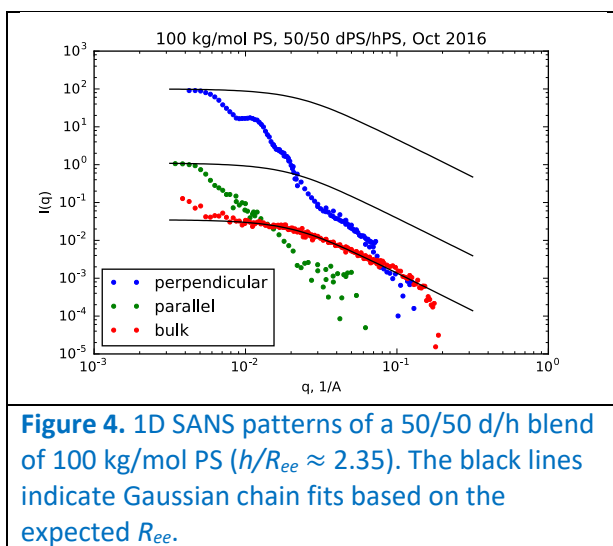


Figure 4. 1D SANS patterns of a 50/50 d/h blend of 100 kg/mol PS ($h/R_{ee} \approx 2.35$). The black lines indicate Gaussian chain fits based on the expected R_{ee} .

Additional SANS on Channel Templates: To facilitate extracting the anisotropic polymer conformations from SANS measurements we are planning additional experiments, particularly the use of a random copolymer and tilting the template relative to the incident beam. A random copolymer with deuterated and non-deuterated styrene units will not exhibit the characteristic Gaussian coil scattering, thus the scattering will originate from the template alone. By subtracting the scattering from a copolymer-filled template from that of a homopolymer-filled (PS:dPS) template will isolate the signal arising from the polymer chains and greatly facilitate analysis of the polymer conformations. Another approach to reducing the scattering contribution of the templates is to tilt the template to align the incident beam relative along the tapered wall. As the

sample is tilted the scattering features from the template will strengthen and weaken and change q positions, while the scattering from the polymer will be relatively unaffected. Analyzing how the SANS patterns change as a function of tilt angle will facilitate separating the template and polymer scattering.

Future Plans

We will establish the role of rigid confinement on the polymer conformations, segmental dynamics and chain dynamics wherein the interaction between the polymer and the confining wall is weak. 1D (deep channels) and 2D (cylindrical pores) rigid confinement will be accomplished using templates functionalization with phenyl groups to provide a weak interaction with polystyrene and deuterated polystyrene. In addition to SANS to determine polymer conformations, neutron spin echo (NSE) will provide segmental relaxation times, potentially distinguishing the relaxation times parallel and perpendicular to the confining walls. ERD at the University of Pennsylvania will measure the center-of-mass tracer diffusion coefficients. Simulations will probe the polymer conformations, segmental dynamics, and chain diffusion for direct comparison with experiments, as well as finding the entanglement density, and the surface energy between the polymer and the confining walls will be matched by matching the contact angle in the simulations and experiments.

By changing the surface treatment of the 1D and 2D templates, we will establish the role of rigid confinement on the polymer conformations, segmental dynamics and chain dynamics wherein the interaction between the polymer and the confining wall is strong. The simulations will explore a range of polymer-wall interaction strengths to identify an interesting and experimentally accessible system, and connections to the experimental interactions will be made by comparing the contact angle in both simulations and experiments. A possible system would involve poly(2-vinyl pyridine) and hydroxyl-terminated templates. Relative to weakly interacting systems, the impact of confinement might be much greater in strongly attractive systems due to the presence of trapped loops that will be thoroughly explored using simulations.

We will investigate the impact of confinement at multiple length scales. The deep channels and cylindrical pores discussed above provide rigid 1D and 2D confinement, respectively, with one characteristic length scale. We will also employ rigid templates of random nanoscale pores with two characteristic lengths, namely the pore diameter (~ 7 nm) and average pore length (~ 15 nm). In contrast to the simpler 1D and 2D templates wherein polymers are confined to one cavity, polymers infiltrated into these random templates are likely to inhabit multiple interconnected and neighboring pores. Simulations will capture this type of confinement using a periodic template (e.g. plumber's nightmare).

1. D. M. Sussman^{†*}, W.-S. Tung[†], K. I. Winey, K. S. Schweizer, R. A. Riggleman^{*}, *Macromolecules*, **47**, 6462-6472, 2014. ([†]indicates joint first authorship)

Publications: None. Project began 8/1/2016.

Unpolarized and Polarized Neutron Scattering Studies of Fe-based Superconductors: Magnetism, Electron Itinerancy and Orbital Hybridization

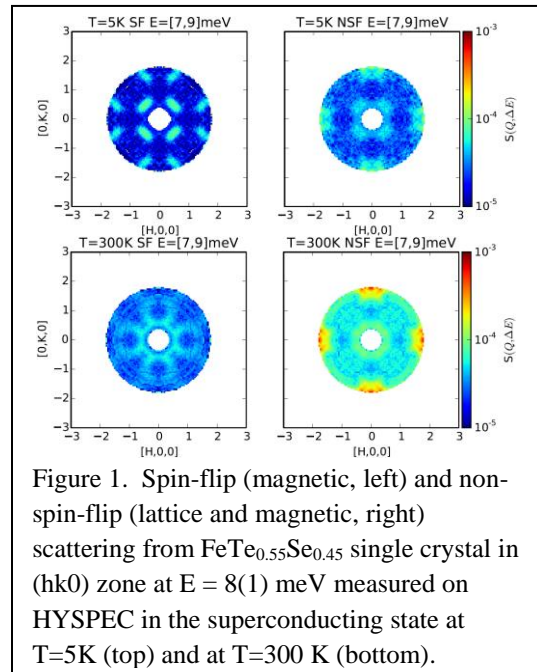
I. A. Zaliznyak (zaliznyak@bnl.gov), G. D. Gu, and J. M. Tranquada

Condensed Matter Physics & Materials Science Department, Brookhaven National Laboratory, Upton, NY 11973-5000

Program Scope

The microscopic physical mechanisms of unconventional high-temperature superconductivity (HTSC) in both iron pnictide and chalcogenide materials and in longer-studied cupric oxide superconductors are still poorly understood. Such understanding is desirable because HTSC provides attractive technological opportunities for energy applications and because fundamental physical phenomena in these materials are common to a number of other functionalities. A competition between strong correlation, which favors local-moment magnetism, and electron hopping (itinerancy), which depends on orbital hybridization and is sensitive to orbital degrees of freedom and spin-orbit interaction, leads to the formation of new electronic and structural phases and to non-trivial topological electronic states and spin textures. In addition to HTSC, these phases exhibit thermoelectric, multiferroic and magnetoresistive responses, all with potential technological functionalities. Their electronic nature is revealed by studying static and dynamical magnetism and its correlation with the atomic structure and lattice dynamics, for which neutron scattering is an ideal probe.

In this program, we use unpolarized and polarized neutron scattering to investigate the nature of static and dynamical magnetism and the character of magnetic correlations in the HTSC materials family, focusing primarily on the $\text{Fe}_{1+y}\text{Te}_{1-x}(\text{Se},\text{S})_x$ system. We address the relative role of magnetic moments from localized electrons, which do not participate in charge transport, and the conduction electrons near the Fermi energy. We investigate the interaction between these two species, the role of the degenerate 3d orbitals, orbital ordering, and an orbital-selective Mott transition. We also look at the role of frustrated interactions and competing magnetic phases. Using polarized neutron spectroscopy, which allows clearly distinguishing magnetic and lattice scattering, we also explore the temperature-dependent hybridization



of the electronic wave functions revealed by the magnetic form factor. Neutron polarization analysis (NPA) is a new advance in time-of-flight neutron spectroscopy. Developing this method and its applications to spectroscopy of strongly correlated electronic materials is a major technical thrust of this program.

Recent Progress

Temperature and doping dependence of plaquette liquid correlations in $Fe_{1+y}Te_{1-x}(Se,S)_x$. Our neutron scattering studies revealed the coexistence and competition as a function of temperature and Se, or S, doping of different types of short-range, liquid-like dynamical magnetic correlations (a spin-liquid polymorphism) in an “11” iron chalcogenide superconductor family [1]. A non-superconducting, magnetic and poorly-metallic $Fe_{1+y}Te$ reveals ferromagnetic (FM) four-iron square plaquettes with antiferromagnetic inter-plaquette correlations. In a filamentary superconductor, $FeTe_{0.87}S_{0.13}$, magnetic response is described by the coexistence of the FM plaquette phase observed in $Fe_{1+y}Te$, which preserves the C_4 symmetry of the underlying square lattice and is favored at high temperatures, and the antiferromagnetic (AFM) plaquette phase with broken C_4 symmetry, which emerges with doping and is predominant at low temperatures. Applying plaquette models to low-temperature magnetic scattering in optimally superconducting crystals of $FeTe_{1-x}Se_x$, we find that it is dominated by these new, C_2 -symmetric AFM plaquettes, but the characteristic wave vector describing the antiferromagnetic inter-plaquette correlations changes with temperature, from that of the bicollinear structure found in $Fe_{1+y}Te$ (at high temperature) to that associated with the stripe structure of antiferromagnetic iron arsenides (at low temperature) [2]. The phase with lower, C_2 local symmetry whose emergence precedes superconductivity, naturally accounts for the propensity for forming electronic nematic states, which have been observed experimentally in cuprate and iron-based superconductors alike.

The experimentally observed extent of magnetic scattering in the wave vector space is suggestive of marked covalent compression of magnetic form factor, supporting strong d-p hybridization of the magnetic 3d electrons. The change of magnetic form factor with temperature provides a direct indication of the temperature-dependent hybridization of the electronic wave functions, a possible driving mechanism for electron pairing and orbital-selective Mott, or Kondo physics. The quantitative measurement of this type requires discrimination between magnetic and structural scattering, as the strength of the latter increases with temperature. Such studies are now possible using the polarized beam option on Hybrid Spectrometer (HYSPEC) at the SNS [3,4] (Figures 1 and 2).

Unusual lattice dynamics in $Fe_{1+y}Te_{1-x}(Se,S)_x$. The magnetism and the lattice in iron chalcogenides are closely coupled. Our recent studies show that the

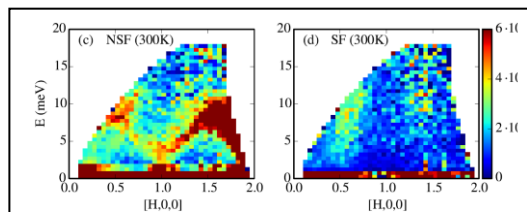


Figure 2. Non-spin-flip scattering revealing an acoustic mode near the forbidden (1,0,0) Bragg position (left) and spin-flip (magnetic, right) scattering from $FeTe_{0.55}Se_{0.45}$ single crystal measured on HYSPEC at $T=300$ K.

bicollinear antiferromagnetism in the ground state of parent compound Fe_{1+y}Te is stabilized by a bond-order wave (BOW) transition, implying a ferro-orbital order associated with the formation of zigzag Fe-Fe chains [5]. This transition entails lowering of the unit cell symmetry, so that the (1,0,0) lattice Bragg reflection, which is forbidden at high T, becomes allowed. Surprisingly, an acoustic-phonon-like dispersion centered at (1,0,0) is observed in the inelastic spectra in all structural phases [6]. This mode is unexpected because although in the monoclinic low-temperature phase of Fe_{1+y}Te the phonon mode is accompanied by a Bragg peak at $Q = (1,0,0)$, in the tetragonal phase elastic Bragg scattering at this Q is forbidden by unit cell symmetry and no accompanying Bragg peak was observed despite the continued observation of an acoustic phonon mode. Notably, this mode is also observed in superconducting $\text{FeTe}_{0.55}\text{Se}_{0.45}$, where structural and magnetic transitions are suppressed, and no BOW has been observed. The predominantly structural character of the observed excitation has been confirmed using neutron polarization analysis (Fig. 2). The presence of this “forbidden” phonon indicates that the lattice symmetry is dynamically or locally broken by magneto-orbital BOW fluctuations, which are strongly coupled to the lattice in these materials.

Future Plans

We will further develop the polarization analysis on HYSPEC and use new opportunities to investigate the evolution of dynamical magnetism in $\text{Fe}_{1+y}\text{Te}_{1-x}(\text{Se},\text{S})_x$ chalcogenides and other HTSCs with temperature and doping. We plan to quantify the changes in magnetic form factor by comparing the measured magnetic scattering patterns with the calculated magnetic form factors for different Fe 3d orbitals, thus pinpointing magnetically active orbitals. Such studies will provide a direct indication of the temperature-dependent hybridization of the electronic wave functions, uncovering possible driving mechanisms for electron pairing and the orbital-selective Mott, or Kondo physics. Secondly, we plan to undertake polarized neutron studies of lattice and magnetic dynamics near the structurally forbidden Bragg peaks in materials of the chalcogenide family and in cuprates, aiming to uncover possible commonalities in behavior.

References

1. I. A. Zaliznyak, A. T. Savici, M. Lumsden, A. Tsvelik, R. W. Hu, C. Petrovic. Spin-liquid polymorphism in a correlated electron system on the threshold of superconductivity. [Proc. Natl. Acad. Sci. **112**, 10316 \(2015\).](#)
2. Zhijun Xu, J. A. Schneeloch, Jinsheng Wen, E. S. Bozin, G. E. Granroth, B. L. Winn, M. Feyngenson, R. J. Birgeneau, Genda Gu, I. A. Zaliznyak, J. M. Tranquada, Guangyong Xu. Thermal evolution of antiferromagnetic correlations and tetrahedral bond angles in superconducting $\text{FeTe}_{1-x}\text{Se}_x$. [Phys. Rev. B **93**, 104517 \(2016\).](#)
3. B. Winn, U. Filges, V. O. Garlea, M. Graves-Brook, M. Hagen, C. Jiang, M. Kenzelmann, L. Passell, S. M. Shapiro, X. Tong, I. A. Zaliznyak. Recent progress on HYSPEC, and its polarization analysis capabilities. WINS-2014 Conference Proceedings, [EPJ Web of Conferences **83**, 03017 \(2015\).](#)

4. I. A. Zaliznyak, A. T. Savici, V. O. Garlea, B. Winn, J. Schneeloch, J. M. Tranquada, G. Gu, A. Wang, C. Petrovic. Polarized neutron scattering on HYSPEC: the HYbrid SPECTrometer at SNS. PNCMI-2016 Conference Proceedings, to appear in EPJ Web of Conferences; [arXiv:1610.06018](https://arxiv.org/abs/1610.06018) (2016).
5. D. Fobes, I. A. Zaliznyak, Zhijun Xu, Ruidan Zhong, Genda Gu, J. M. Tranquada, L. Harriger, D. Singh, V. O. Garlea, M. Lumsden, B. Winn. Ferro-orbital ordering transition in iron telluride Fe_{1+y}Te . [Phys. Rev. Lett. **112**, 187202](https://doi.org/10.1103/PhysRevLett.112.187202) (2014).
6. D. M. Fobes, I. A. Zaliznyak, Zhijun Xu, Genda Gu, Xu-Gang He, Wei Ku, J. M. Tranquada, Yang Zhao, M. Matsuda, V. O. Garlea, B. Winn. “Forbidden” phonon: dynamical signature of bond symmetry breaking in the iron chalcogenides. [Phys. Rev. B **94**, 121103\(R\)](https://doi.org/10.1103/PhysRevB.94.121103) (2016).

Searching for the Universality of Liquid Dynamics At and Out of Equilibrium

Yang Zhang, Department of Nuclear, Plasma, and Radiological Engineering, Department of Materials Science and Engineering, Program of Computational Science and Engineering, Beckman Institute for Advanced Science and Technology, University of Illinois at Urbana-Champaign

Program Scope

Liquids, ubiquitous on earth, are prototypical disordered condensed matter. However, the physics of liquids is far from being completely understood. Furthermore, when liquids approach critical points or are driven out of equilibrium, their dynamics becomes strongly correlated and heterogeneous. As a result, the phase behaviors of liquids and metastable liquids are exceptionally rich, and in-depth understanding of them requires the development of new theoretical concepts and new experimental techniques. In addition, numerous soft and biological materials of amazing far-from-equilibrium complexity seem to share many intriguing features of liquids. Therefore, quantitative descriptions of the structure and dynamics of liquids at and out of equilibrium will likely impact a wide range of disciplines in physics, chemistry, and materials science and engineering. Our research activities center around the searching for the universality of liquid dynamics (including metallic, molecular, and network liquids), both at and out of equilibrium, using integrated quasi-elastic and inelastic neutron scattering experimental probes and atomistic theory, computation, and simulation.

Recent Progress

1. We detected the onset of correlated dynamics of a model glass-forming metallic liquids by quasi-elastic neutron scattering (QENS) measurements [3,5,6].

Onset of correlated dynamics has been observed in many molecular liquids, colloids, and granular materials in the metastable regime on approaching their respective glass or jamming transition points, and is considered to play a

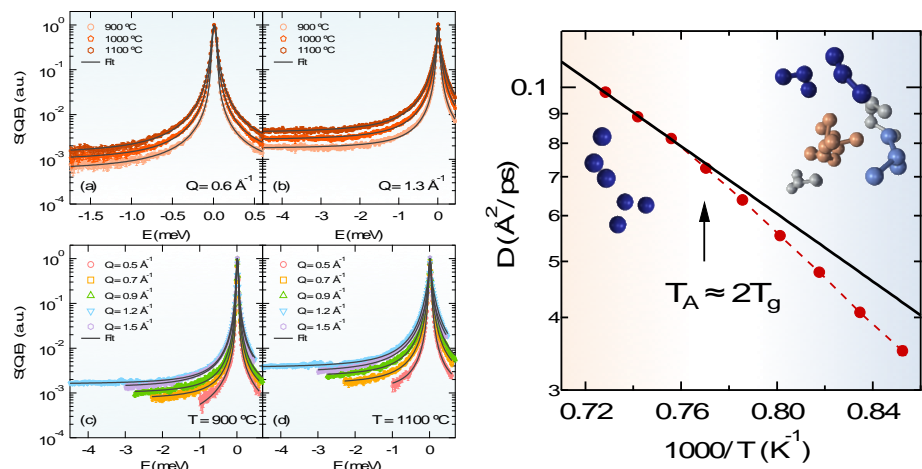


Figure 1. (A) Measured QENS spectra of glass-forming metallic liquid LM601 ($\text{Zr}_{51}\text{Cu}_{36}\text{Ni}_4\text{Al}_9$) at two wave-vector transfer values and two temperatures. Solid lines denote the fittings using the KWW model. (B) Temperature dependence of mean effective diffusion coefficient obtained from QENS measurements in the generalized hydrodynamic regime of melted LM601 in the temperature range 900–1100 °C. Solid line is Arrhenius fit at high temperatures. Deviations from the fit is observed at low temperatures which marks the dynamical onset temperature T_A .

significant role in the emergence of the slow dynamics. However, the nature of such dynamical cooperativity remains elusive in multicomponent metallic liquids characterized by complex many-body interactions and high mixing entropy. We performed extensive QENS measurements of the relaxational dynamics of a model glass-forming metallic liquid (LM601 $Zr_{51}Cu_{36}Ni_4Al_9$) – one of the best bulk metallic glass (BMG) formers. We found an evidence of its onset point of correlated dynamics. This is revealed by deviation of the mean effective diffusion coefficient from its high-temperature Arrhenius behavior below $T_A \approx 1300$ K, i.e., a Arrhenius crossover from uncorrelated dynamics above T_A to landscape-influenced correlated dynamics below T_A . Furthermore, the Arrhenius crossover temperature T_A in such a multicomponent bulk metallic glass-forming liquid is observed at approximately twice of its calorimetric glass transition temperature ($T_g \approx 697$ K) and in its stable liquid phase, unlike many molecular liquids.

2. We used molecular dynamics (MD) and machine learning (ML) analysis to reveal that growing dynamic correlation length underpins the onset of correlated dynamics in glass-forming metallic liquids [3,4,6].

We performed systematic studies of a model ternary metallic liquid $Cu_{40}Zr_{51}Al_9$ using MD simulations with embedded atom method (EAM). We confirmed the Arrhenius crossover phenomena observed by QENS. Below T_A , we found the elemental dynamics decoupled and the Stokes-Einstein relation broke down, indicating the onset of heterogeneous spatially correlated dynamics in the system mediated by dynamic communications among local configurational excitations. To directly characterize and visualize the correlated dynamics, we employed a non-parametric, unsupervised machine learning technique and identified dynamical clusters of atoms with similar atomic mobility. The revealed average dynamical cluster size shows an accelerated increase below T_A and mimics the trend observed in other ensemble averaged quantities that are commonly used to quantify the spatially heterogeneous dynamics such as the non-Gaussian parameter and the four-point correlation function.

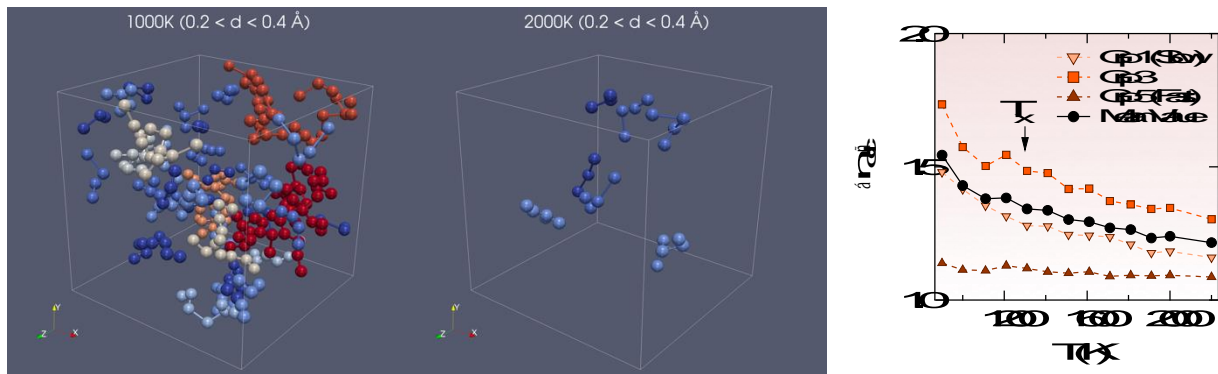


Figure 2. (A) Dynamic clusters of atoms with similar mobility identified using unsupervised machine learning techniques. The average size of such dynamic clusters (larger at 1000K than 2000K) could be a candidate “order parameter” characterizing the dynamic slowing down of the liquid upon cooling. (B) Mean number of atoms in dynamical clusters $\langle n_{dc} \rangle$ classified into 5 major groups. Clearly, cluster size increases with decreasing temperature, but it increases sharply below the dynamical onset temperature (T_A or T_x in this figure).

3. We discovered of a universal correlation between fragility and the Arrhenius crossover phenomenon in metallic, molecular, and network Liquids [1].

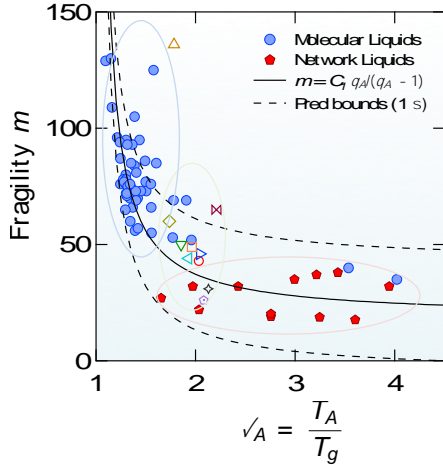


Figure 3. Correlations of the fragility index m with the reduced Arrhenius crossover temperature $\theta_A = T_A/T_g$ for various glass-formers. An roughly-inverse relation is observed between the two quantities.

We discovered a distinct correlation between the kinetic fragility index m and the reduced Arrhenius crossover temperature $\theta_A = T_A/T_g$ in various glass-forming liquids, identifying three distinguishable groups. In particular, for 11 glass-forming metallic liquids, we universally observe a crossover in the mean diffusion coefficient from high-temperature Arrhenius to low-temperature super-Arrhenius behavior at approximately $\theta_A \approx 2$ which is in the stable liquid phases. In contrast, for fragile molecular liquids, this crossover occurs at much lower $\theta_A \approx 1.4$ and usually in their supercooled states. The θ_A values for strong network liquids spans a wide range higher than 2. Intriguingly, the high-temperature activation barrier E_∞ is universally found to be $\sim 11 k_B T_g$ and uncorrelated with the fragility or the reduced crossover temperature θ_A for metallic and molecular liquids. These

observations provide a way to estimate the low-temperature glassy characteristics (T_g and m) from the high-temperature liquid quantities (E_∞ and θ_A).

4. We found that Ioffe-Regel localization of longitudinal acoustic excitations (LAE) determines the Arrhenius crossover regime in liquids [to be published].

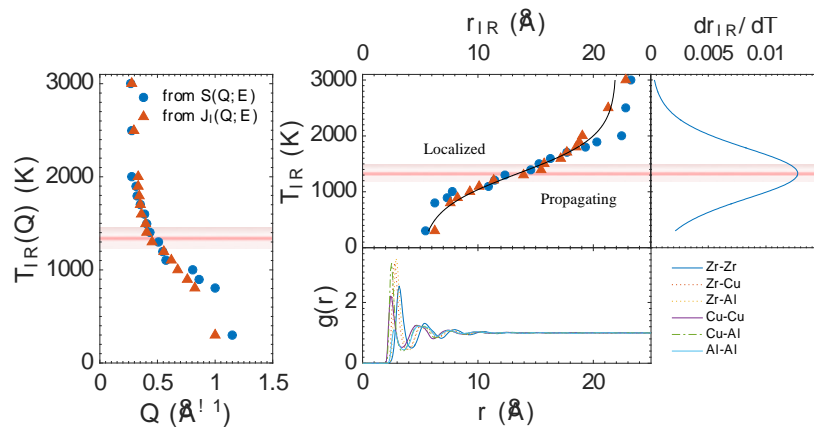


Figure 4. (A) Q -dependent Ioffe-Regel localization temperature of longitudinal acoustic excitation in a model glass-forming metallic liquid. (B) The distribution of the Ioffe-Regel localization temperatures determines the Arrhenius crossover regime.

We performed inelastic neutron scattering measurements of the “phonon” dispersion relations and the collective diffusions of metallic liquids from liquids to glass states. We also performed MD simulations and computed both the density and current correlation functions. We found that the LAEs in the high temperature liquids are very short lived – localized in the Ioffe-Regel sense. They only propagate

below the Ioffe-Regel temperature. The Q -dependent Ioffe-Regel localization temperature of LAEs reveals the nature and the range of the Arrhenius crossover regime.

5. We developed a parallel and extendable C++ numerical library – *LiquidLib* <http://zhang-group.github.io/LiquidLib/> for computing the statistical quantities of liquids and liquid-like systems from classical and *ab initio* molecular dynamics trajectories, which can be directly compared with neutron scattering experiments.

Often to understand the results of neutron scattering experiments, computer simulations, including classical and *ab initio* molecular dynamics (MD), are used to compare to the experiments. *LiquidLib* is a post-processing package for computing the statistical quantities of liquids and liquid-like systems from classical and *ab initio* MD trajectories. *LiquidLib* allows computation of various statistical quantities relevant to neutron scattering measurements. New quantities can easily be integrated into the library. *LiquidLib* can read MD trajectories of LAMMPS, GROMACS, and VASP. *LiquidLib* also offers an easy platform to extend the program to be able to read simulation trajectories organized in other file formats not included or from other packages. Incorporation of materials' neutron scattering lengths to weight the quantities' computations provides results comparable to neutron scattering measurements. Lastly, *LiquidLib* is dimensionally independent, which allows for trajectories in higher dimensions to be analyzed.

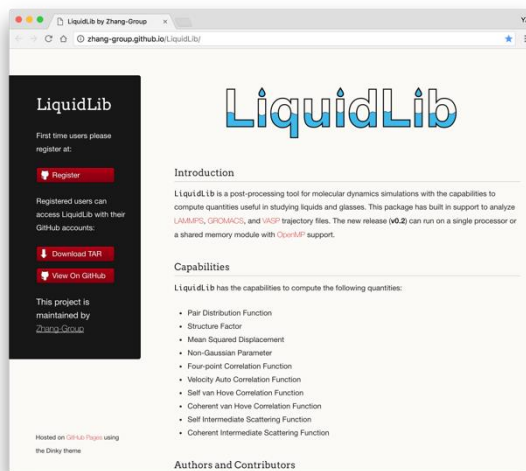


Figure 5. A snapshot of the *LiquidLib* website.

Future Plans

Our previous studies provide fairly good understandings of the role of longitudinal acoustic excitation as the carrier of the growing dynamic correlation length in glass-forming metallic liquids. We will further investigate the following questions using neutron scattering experiments and atomistic simulations. Some of them will use the newly-built containerless sample environment, the Neutron Electro-Static Levitator (NESL), to avoid any surface effect.

1. Are there any transverse acoustic excitations (TAE) in liquids? Are they localized in the Ioffe-Regel sense? Can TAE be “frozen” in the glassy state? How are they related to the notorious Boson peak in glasses and many disordered soft materials and proteins?
2. Are there any structural orderings, i.e. features in the two-point density correlation function, $S(Q)$ or $g(r)$, which can reflect the growing dynamic correlation length in glass-forming liquids?
3. How are these dynamical quantities related to the glass-forming abilities of the liquids? In other words, what are the genomes of glasses and crystals?
4. Further develop the functions and usability of *LiquidLib*.

Publications (2015.05 – 2016.11)

Journal Articles:

- [1] A. Jaiswal, T. Egami, K. F. Kelton, K. S. Schweizer, **Y. Zhang***, “Correlation between fragility and Arrhenius crossover phenomenon in metallic, molecular, and network liquids”, *Phys. Rev. Lett.* 117, 205701 (2016)
- [2] K. Yang, Z. Cai, M. Tyagi, M. Feygenson, J. C. Neuefeind, J. S. Moore, **Y. Zhang***, “Odd-even Structural Sensitivity on Dynamics in Network-forming Ionic Liquids”, *Chem. Mater.* 28(9), 3227 (2016).
- [3] A. Jaiswal, S. O’Keefe, R. Mills, A. Podlesynak, G. Ehlers, W. Dmowski, K. Lokshin, T. Egami, **Y. Zhang***, “Onset of cooperative dynamics in an equilibrium glass-forming metallic liquid”, *J. Phys. Chem. B* 120(6), 1142 (2016).
- [4] A. Jaiswal, **Y. Zhang***, “Robustness of dynamical cluster analysis in a glass-forming metallic liquid using an unsupervised machine learning algorithm”, *MRS Adv.* 1(26), 1929 (2016).
- [5] A. Jaiswal, A. Podlesynak, G. Ehlers, R. Mills, S. O’Keefe, J. Stevick, J. Kempton, G. Jelbert, W. Dmowski, K. Lokshin, T. Egami, **Y. Zhang***, “Coincidence of collective relaxation anomaly and specific heat peak in a bulk metallic glass-forming liquid”, *Phys. Rev. B* 92, 024202 (2015).
- [6] A. Jaiswal, T. Egami, **Y. Zhang***, “Atomic-scale dynamics of a model glass-forming metallic liquid: dynamical crossover, dynamical decoupling, and dynamical clustering”, *Phys. Rev. B* 91, 134204 (2015).
 - **Featured on the front page of *Phys. Rev. B* web site.**

Ph.D. and M.S. Theses:

1. A. Jaiswal, “Atomic Scale Dynamics of Glass-Forming Metallic Liquids: Atomistic Simulations and Neutron Scattering Experiments”, Ph.D. thesis, December 2016.
2. Z. Cai, “Energy Landscape Statistics and Coarsening in Liquids: A Relaxation Mode Analysis”, M.S. thesis, August 2016.
3. N. P. Walter, “Direct Energy Landscape Sampling of the Homogeneous Nucleation and Crystal Growth of a Model Liquid”, M.S. thesis, August 2016.
4. K. Yang, “Synthesis and Application of Ionic Molecular and Polymeric Materials”, Ph.D. thesis, May 2016.

Author Index

Agrawal, Harish K.	109
Armitage, N. P.	3
Bauer, Eric.....	147, 159
Broholm, Collin	3, 13
Budai, John D.....	14, 174
Butler, L. G.	51
Cava, R. J.	3
Chakoumakos, Bryan C.	174
Chandran, K. S. Ravi	21
Chen, Wei-Ren.....	26
Cheong, S.-W.....	31
Chmaissem, O.	163
Choi, Joshua	95
Dai, Pengcheng	38
Delaire, Olivier.....	14, 44
Dimeo, Robert.....	50
DiTusa, J. F.	51
Eskildsen, Morten R.....	59
Fobes, David	92
Fullerton, Eric E.....	64
Fultz, Brent.....	69
Garno, J. C.	51
Goldman, A. I.....	111
Greven, Martin	75
Gu, G. D.	79, 177, 192
Hayward, Jason P.	83
Helgeson, Matthew E.	88
Hermann, R. P.....	14
Janoschek, Marc.....	92, 147
Jiang, Hongchen.....	97
Jin, R.	51
John, V. T.....	51
Joyce, John	147
Khonsari, M.	51
Kiryukhin, V.	31
Kreyssig, A.....	111
Kumar, R.....	51
Lang, Jonathan C.....	174
Langan, Paul.....	94
Lee, Seung-Hun.....	95
Lee, Young.....	97
Leighton, Chris.....	100
Loguillo, Mark J.....	109
Louca, Despina.....	105
Lvov, Y. M.....	51
Lynn, Gary W.....	109
Manley, M. E.	14
Mao, Z.	51
Maranas, Janna.....	110
McQueen, T. M.....	3
McQueeney, R. J.....	111
Moule, Adam J.....	119
Movshovich, Roman.....	147
Nesterov, E.....	51
Olsen, Bradley D.....	125
Osborn, R.	163
Phelan, D.	163
Plummer, E. W.....	51
Pozzo, Lilo D.	130
Proffen, Thomas.....	134
Redmon, Chris M.....	109
Reznik, Dmitry	138
Rick, S. W.	51
Riggleman, Robert A.	188
Rodriguez, Efrain E.....	143
Ronning, Filip	147
Rosa, Priscila.....	147, 159
Rosenkranz, S.....	163
Schneider, G. J.	51
Shelton, W. A.....	51
Singh, Deepak K.	170
Sinha, Sunil	64
Sirenko, A.	31
Sprunger, P. T.	51
Tchernyshyov, O.....	3
te Velthuis, Suzanne G. E.	163, 174
Thompson, Joe	147
Toby, Brian H.	174
Tranquada, J. M.....	79, 177, 192
Turner, A.	3
Vaknin, D.	111
Winey, Karen I.....	188
Young, D. P.....	51
Zaliznyak, Igor A.	79, 177, 192
Zhang, D.....	51
Zhang, J.....	51
Zhang, Yang.....	196

Participant List

Name	Organization	Email
Armitage, Peter	The Johns Hopkins University	npa@jhu.edu
Bauer, Eric	Los Alamos National Laboratory	edbauer@lanl.gov
Bras, Wim	Oak Ridge National Laboratory	brasw@ornl.gov
Broholm, Collin	The Johns Hopkins University	broholm@jhu.edu
Budai, John	Oak Ridge National Laboratory	budajd@ornl.gov
Cava, Robert	Princeton University	rcava@princeton.edu
Chen, Wei-Ren	Oak Ridge National Laboratory	chenw@ornl.gov
Cheong, Sang-Wook	Rutgers University	sangc@physics.rutgers.edu
Choi, Joshua	University of Virginia	jjc6z@virginia.edu
Dai, Pengcheng	Rice University	pdai@rice.edu
Delaire, Olivier	Duke University	olivier.delaire@duke.edu
Dimeo, Robert	National Institute of Standards and Technology	robert.dimeo@nist.gov
DiTusa, John	Louisiana State University	ditusa@phys.lsu.edu
Eskildsen, Morten	University of Notre Dame	eskildsen@nd.edu
Fernandes, Rafael	University of Minnesota	rfernand@umn.edu
Ferrari S. Rosa, Priscila	Los Alamos National Laboratory	pfsrosa@lanl.gov
Fullerton, Eric	University of California, San Diego	efullerton@ucsd.edu
Fultz, Brent	California Institute of Technology	btf@caltech.edu
Greven, Martin	University of Minnesota	greven@umn.edu
Gu, Genda	Brookhaven National laboratory	ggu@bnl.gov
Hayward, Jason	University of Tennessee, Knoxville	jhayward@utk.edu
Helgeson, Matthew	University of California, Santa Barbara	helgeson@engineering.ucsb.edu
Hermann, Raphael	Oak Ridge National Laboratory	hermannrp@ornl.gov
Jalan, Bharat	University of Minnesota	bjalan@umn.edu
Janoschek, Marc	Los Alamos National Laboratry	mjanoschek@lanl.gov
Jiang, Hong-Chen	SLAC National Accelerator Lab/Stanford Univ.	hongchen777@gmail.com
Kiryukhin, Valery	Rutgers University	vkir@physics.rutgers.edu
Koohpayeh, Seyed	Johns Hopkins University	koohpayeh@jhu.ed
Kreyszig, Andreas	Ames Laboratory	kreyszig@ameslab.gov
Langan, Paul	Oak Ridge National Laboratory	langanpa@ornl.gov
Lee, Young	Stanford Univ./SLAC National Accelerator Lab	youngsl@stanford.edu
Lee, Seung-Hun	University of Virginia	shlee@virginia.edu
Leighton, Chris	University of Minnesota	leighton@umn.edu
Lynn, Gary	Oak Ridge National Laboratory	lynngw@ornl.gov
Manley, Michael	Oak Ridge National Laboratory	manleyme@ornl.gov
Maracas, George	U.S. Department of Energy	george.maracas@science.doe.gov
McQueen, Tyrel	The Johns Hopkins University	mcqueen@jhu.edu
Moule, Adam	University of California, Davis	amoule@ucdavis.edu
Movshovich, Roman	Los Alamos National Laboratory	roman@lanl.gov
Olsen, Bradley	Massachusetts Institute of Technology	bdolsen@mit.edu
Osborn, Raymond	Argonne National Laboratory	ROsborn@anl.gov
Phelan, Daniel	Argonne National Laboratory	dphelan@anl.gov
Pozzo, Lilo	University of Washington	dpozzo@uw.edu
Proffen, Thomas	Oak Ridge National Laboratory	tproffen@ornl.gov
Reznik, Dmitry	University of Colorado, Boulder	dmitry.reznik@colorado.edu
Rhyne, James	U.S. Department of Energy	james.rhyne@science.doe.gov
Riggleman, Robert	University of Pennsylvania	rrig@seas.upenn.edu
Rodriguez, Efrain	University of Maryland	efrain@umd.edu
Ronning, Filip	Los Alamos National Laboratory	fronning@lanl.gov

Singh, Deepak	University of Missouri	singhdk@missouri.edu
Sinha, Sunil	University of California, San Diego	ssinha@physics.ucsd.edu
Sirenko, Andrei	New Jersey Institute of Technology	sirenko@njit.edu
Tchernyshyov, Oleg	The Johns Hopkins University	olegt@jhu.edu
te Velthuis, Suzanne	Argonne National Laboratory	tevelthuis@anl.gov
Thiyagarajan, Thiyaga	U.S. Department of Energy	p.thiyagarajan@science.doe.gov
Thompson, Joe	Los Alamos National Laboratory	jdt@lanl.gov
Tranquada, John	Brookhaven National Laboratory	jtran@bnl.gov
Ueland, Benjamin	Ames Laboratory	bgueland@ameslab.gov
Vadlamani, Bhaskar	University of Utah	b.vadlamani@utah.edu
Vaknin, David	Ames Laboratory/Iowa State University	vaknin@ameslab.gov
Vetrno, John	U.S. Department of Energy	john.vetrano@science.doe.gov
Winey, Karen	University of Pennsylvania	winey@seas.upenn.edu
Yang, Junjie	University of Virginia	jy6p@virginia.edu
Zaliznyak, Igor	Brookhaven National Laboratory	zaliznyak@bnl.gov
Zhang, Yang	University of Illinois at Urbana-Champaign	zhyang@illinois.edu